

NAT'L INST. OF STAND & TECH R.I.C.



A11105 652501

NIST
PUBLICATIONS

NIST CENTER FOR NEUTRON RESEARCH

TECHNOLOGY DEVELOPMENTS

**MATERIALS
SCIENCE AND
ENGINEERING
LABORATORY**

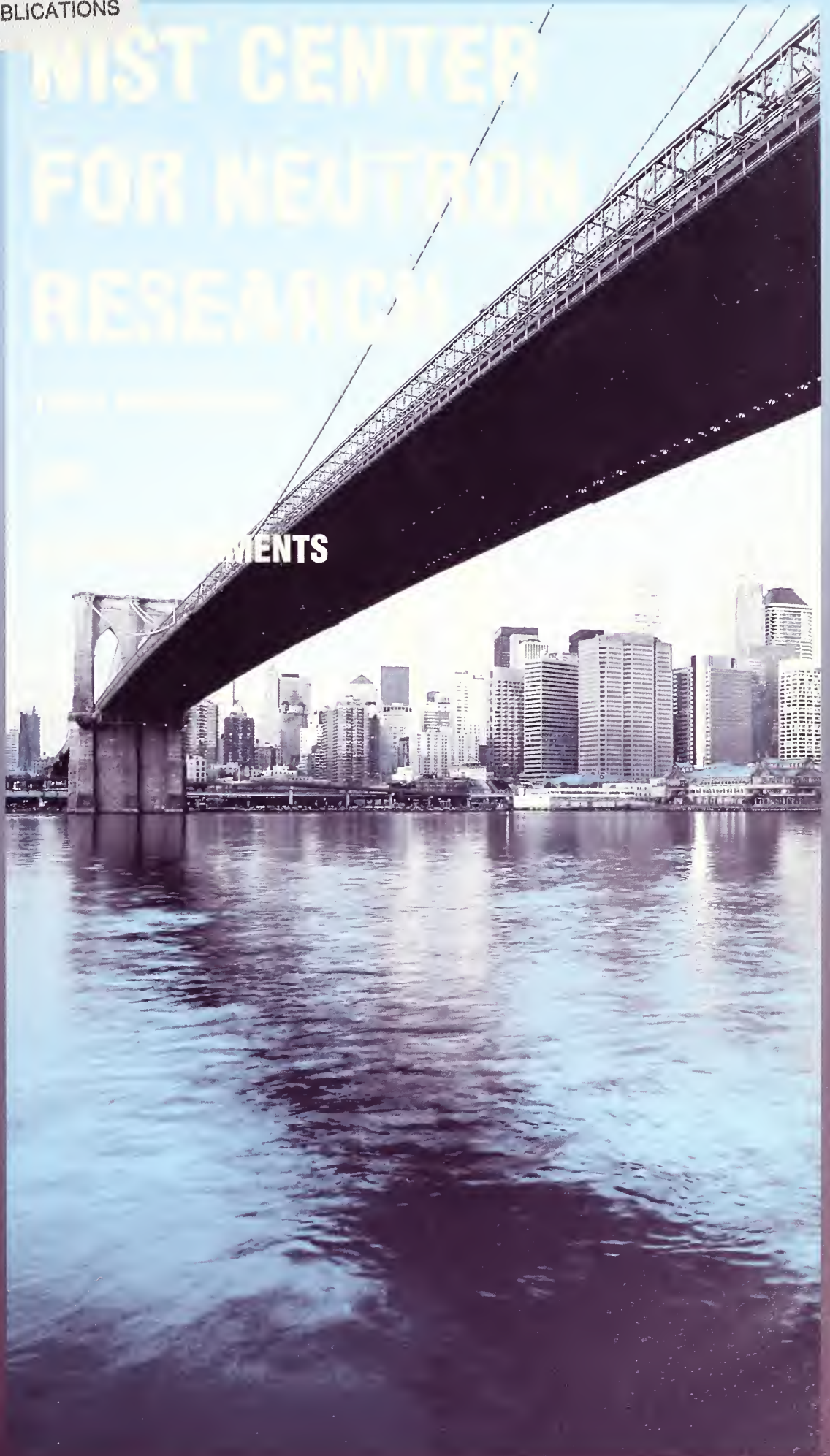
NISTIR 6251

**UNITED STATES
DEPARTMENT OF
COMMERCE**

**TECHNOLOGY
ADMINISTRATION**

**NATIONAL
INSTITUTE OF
STANDARDS AND
TECHNOLOGY**

C
00
56
0. 6251
999



Unique Capabilities Provide Critical Data

The NIST Center for Neutron Research (NCNR) offers a bridge between the world of atoms, molecules and sub-microscopic structures and the macroscopic world of buildings, automobiles, efficient energy utilization, and the environment. Over 1500 researchers from 34 countries made use of the NCNR's world-class capabilities in the area of neutron-based research in 1998.

**UNITED STATES
DEPARTMENT OF
COMMERCE**

William M. Daley,
Secretary

**TECHNOLOGY
ADMINISTRATION**

Gary R. Bachula,
Under Secretary for Technology

**NATIONAL
INSTITUTE OF
STANDARDS AND
TECHNOLOGY**

Raymond G. Kammer,
Director



MATERIALS SCIENCE AND ENGINEERING LABORATORY

NIST CENTER FOR NEUTRON RESEARCH

1998 PROGRAMS

AND

ACCOMPLISHMENTS

J. Michael Rowe, Director

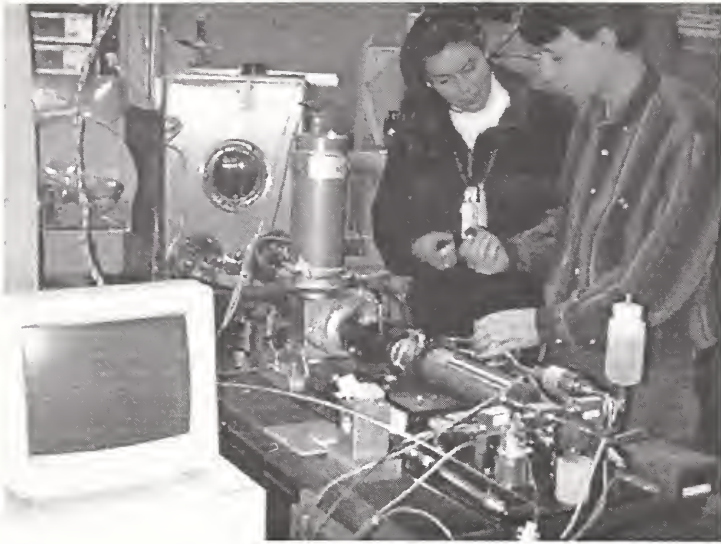
Tawfik M. Raby, Deputy

NISTIR 6251

January 1999

Contents

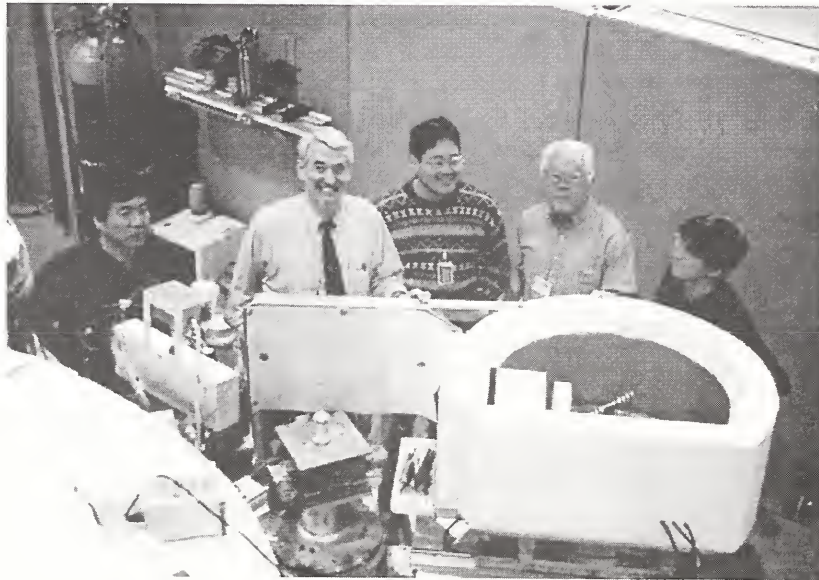
Foreword	4
Introduction to the NIST Center for Neutron Research (NCNR)	5
Research Highlights	
Solids that Shrink when Heated	8
Spin Correlations and Impurities in a One-Dimensional Quantum Spin Liquid	10
Deposition of Toxic Trace Elements and Heavy Metals to Lake Michigan	12
Magnetic Domains in Co-SiO ₂ Multilayer Tunnel Junctions	14
Mechanism of Thermal Barrier Coating Failure at High Temperature	16
A New Method to Determine Single Crystal Elastic Behavior from Polycrystals	18
Development of Three New Standard Reference Materials	20
Dimensions of Polyelectrolyte Chains with Multivalent Counterions	22
Characterization of New Biomimetic Materials Using Neutron Reflectivity	24
The Dynamics of Hydrogen in Solid C ₆₀	26
Polarons in Colossal Magnetoresistive Materials	28
Neutron Interferometry and Optics Facility (NIOF)	30
Protein Conformations and Interactions in Biochemical Regulation	32
Microstructure Transformation During Microemulsion and Micellar Polymerizations	34
Arborescent Graft Polymers	36
The Vibrational Isocoordinate Rule in Se-As-Ge Glasses	38
Membrane Mediated Polymer Interdiffusion	40
Interactions	42
Reactor Operations and Engineering	46
Instrumentation Developments	47
Research Topics	51
Materials Science	51
Polymers	52
Complex Fluids	53
Condensed Matter Physics	54
Biomolecular Science	56
Chemical Physics of Materials	56
Instrumentation	57
Neutron Physics	58
Materials Analysis	59
NCNR Staff Publications	62
Independent Publications	69
Organizational Charts	75
Roster of NCNR Resident Staff and Visiting Scientists	77
Roster of Other NIST Groups	78
Research and Engineering Staff	79



Steve Kline (NCNR) helping Anne-Valerie Ruzette, MIT, to set up the pressure cell for a SANS experiment.



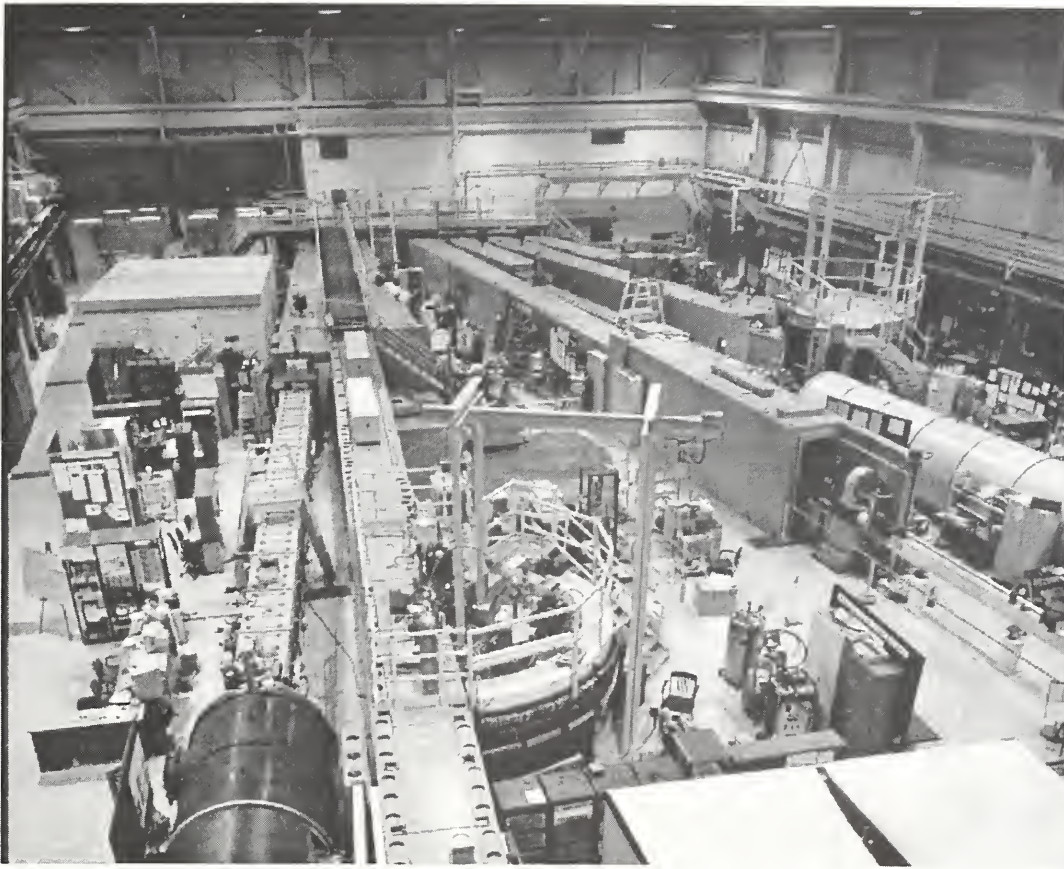
Joe Dura inspecting molecular beam epitaxy chamber.



Kazu Yamada (Kyoto University), Bob Birgeneau (MIT), Suichi Wakimoto (Tohoku University), Gen Shirane (BNL), and Seung Hun Lee (NCNR) at the SPINS spectrometer.



Steve Kline and Paul Butler (NCNR) working with Lee Magid, University of Tennessee to set up a SANS experiment.



Guide hall at the NCNR, as of late 1997.



Heather Chen (NIST) aligning focusing capillary array.



Nobel Laureate Clifford Shull, inspecting NIST interferometer.

Foreword



This has been a productive and exciting year for the NIST Center for Neutron Research (NCNR), with many achievements in operation, instrumentation, and science. The reactor operated well through September, when an unscheduled shutdown was required to investigate a small leak in the vicinity of the thermal column. As a result of an excellent effort by the Reactor Operations and Engineering staff, this shutdown lasted no more than one complete cycle (14 % of availability). The reactor is now once again operating on our normal seven week schedule. We apologize to all those who were inconvenienced, and will work to make up as much of the time as possible. The next long scheduled shutdown, for replacement of shim control arms, is scheduled to begin in February, 2000 and will last 3-6 months.

During this year, commissioning of the high intensity back scattering spectrometer was begun, with very favorable results (see section later in this report), and the instrument should be available for user scheduling at the next program proposal period. Great progress was also made on the Spin Echo and Disc Chopper Spectrometers, with commissioning expected in the coming year. The reliability of operating instruments continues to be better than 95 %, with the average over all instruments being 98 %. The final engineering design of the second generation liquid hydrogen cold source is nearing completion, and fabrication and testing will begin in 1999. This source is calculated to provide approximately a factor of two gain over the present source.

This year we have changed the format of our report, and are featuring science highlights, chosen from the experiments done during the year. Thus, I will refrain from discussing science accomplishments here, except to say that productivity and quality remain exceptionally high. One of the great parts of my job is to be able to walk around the facility talking to experimenters, and I continue to be impressed by the breadth of the research and the enthusiasm of the researchers.

Finally, we continue to make good progress on preparing a request for a license renewal for the reactor for 20 years beyond 2004. Many different activities are underway towards this end, and we are fully confident that we will be successful. Neutron science as a whole is in a very exciting period, with the funding of the Spallation Neutron Source at Oak Ridge National Laboratory, and plans for new sources in several parts of the world. The NIST Center for Neutron Research is and will remain at the center of a renewed U.S. neutron research effort, working to provide the neutron measurement capabilities that are becoming ever more important.

A handwritten signature in cursive script that reads "Mike Rowe". The signature is written in dark ink on a light background.

Introduction to the NIST Center for Neutron Research (NCNR)

The modern technological society is dependent upon increasingly more sophisticated use of materials, many of whose properties are dictated by their sub-microscopic structural and dynamical properties. Our knowledge of these properties is provided by a wide range of scientific techniques, of which the many types of scattering (X-rays, light, electrons, neutrons, ...) are arguably the most important. Of these scattering probes, neutrons are perhaps least known, but they provide important advantages for many types of measurements.

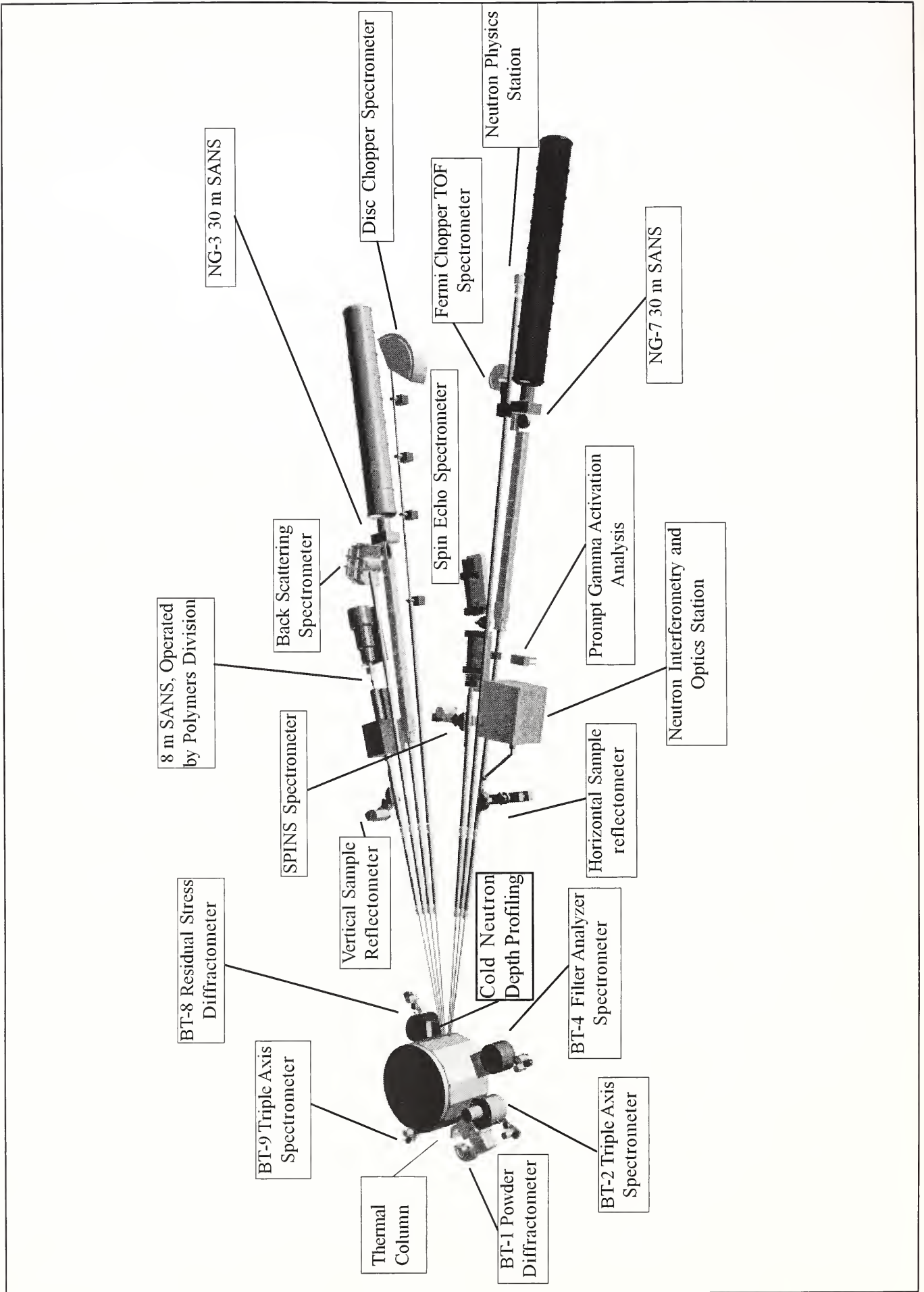
Neutrons, as prepared for use at modern sources, are moving at speeds comparable to those of atoms moving at room temperature, thus providing the ability to probe dynamical behavior. At the same time, neutrons are well matched to measurements at length scales ranging from the distances between atoms to the size of biological or polymer macromolecules. Neutrons are sensitive to the magnetic properties of atoms and molecules, allowing study of the underlying magnetic properties of materials. They also scatter quite differently from normal hydrogen atoms than they do from heavy hydrogen (deuterium), allowing selective study of individual regions of molecular systems. Finally, neutrons interact only weakly with materials, providing the opportunity to study samples in different environments more easily (high pressures, in shear, in reaction vessels, etc.), and making them a non-destructive probe. These favorable properties are offset by the relative weakness of the best neutron sources, when compared to X-ray or electron sources, and by the relatively large facilities required to produce neutrons. As a result, neutron sources are operated as national user facilities, to which researchers come from all over the U.S. (and abroad), to perform small scale science using the special measurement capabilities provided.

In addition to scattering measurements, neutrons can be used to probe the atomic composition of materials, by means of capture and resultant radioactive decay. The characteristics of the decay act as "fingerprints" for particular atomic nuclei, allowing studies of environmental samples for pollutants (e.g. heavy metals), characterization of Standard Reference Materials, and many other essential measurements. While the scattering and capture users of neutrons are little concerned with the innate nature of neutrons, there are important areas in physics that can be well studied by observing the behavior of the neutron. Examples include the lifetime of the free neutron, an important ele-

ment in the theory of astrophysics; the beta decay process of the neutron, the details of which are stringent tests of nuclear theory; and the effects of various external influences such as gravity or magnetic fields on neutrons.

The NCNR utilizes neutrons produced by the 20 MW NIST Research Reactor to provide facilities for all of the above types of measurements to a national user community. There are approximately 35 positions in the reactor and its associated beams which can provide neutrons for experiments. At the present time, there are 26 stations in active use, of which 6 provide high neutron flux positions in the reactor for irradiations, and 20 are beam facilities. A schematic layout of the beam facilities and brief descriptions of available instrumentation are given below. More complete descriptions can be found at <http://rrdjazz.nist.gov>.

These facilities are operated both to serve NIST mission needs and as a national user facility, with many different modes of access. Some of the instrumentation was built several years ago, and is not suited to general user access; however, user time is available for collaborative research. In some cases, NIST built new instrumentation, and reserves 1/3 of available time for mission needs, with the balance available to general users. In other cases, instrumentation was built and is operated by Participating Research Teams (PRT); in such cases, the PRT members have access to 75 % of available time, with the balance available to general users. In a special case, NIST and the National Science Foundation established the Center for High Resolution Neutron Scattering at the NCNR, with a 30-m Small Angle Scattering (SANS) instrument, a cold neutron triple axis spectrometer, and a perfect crystal SANS under construction. For these facilities, most time is available for general users. While most access is for work which is freely available to the general public, proprietary research can be performed under full cost recovery. Each year, 1400 research participants (persons who participated in experiments at the facility, but did not necessarily come here) from all areas of the country, from industry, academe, and government use the facility to perform measurements not otherwise possible. The research covers a broad spectrum of disciplines, including chemistry, physics, biology, materials science, and engineering.



Horizontal Sample Reflectometer

Horizontal surface of sample allows reflectivity measurements of free surfaces, liquid vapor interfaces, as well as polymer coatings.

Neutron Interferometry & Optics Station

Includes perfect silicon interferometer; vibration isolation system provides exceptional phase stability and fringe visibility.

Prompt Gamma Activation Analysis

Cold neutron fluxes allow detection limit for H of 1-10 microgram. Focused beams available for profiling.

NG-7 30m SANS

Small Angle Neutron Scattering instrument for microstructure measurement sponsored by NIST, the Exxon Research and Engineering Co., the University of Minnesota, and Texaco R&D.

Neutron Physics Station

A cold neutron beam 150 x 60 mm², available for fundamental neutron physics experiments.

Fermi Chopper TOF Spectrometer

A hybrid time-of-flight spectrometer for inelastic scattering, with wavelengths between 0.23 and 0.61 nm. The wavelength is chosen by focusing pyrolytic graphite crystal, while the beam is pulsed by a simple Fermi chopper.

Spin Echo Spectrometer

A neutron spin echo spectrometer offering neV energy resolution, based upon Julich design, sponsored by NIST, Julich and Exxon.

SPINS Spectrometer

Spin Polarized Inelastic Scattering, a cold neutron triple axis spectrometer with spin polarization capabilities for high resolution studies, and position sensitive detector capability, sponsored by the National Science Foundation and NIST; part of Center for High Resolution Neutron Scattering (CHRNS).

Disc Chopper TOF Spectrometer

Versatile time-of-flight spectrometer, with beam pulsing and monochromatization effected by 7 disk choppers. Used for studies of dynamics in condensed matter, including macromolecular systems.

NG-3 30m SANS

Instrument for microstructure measurement sponsored by the National Science Foundation and NIST; part of CHRNS.

Back Scattering Spectrometer

High intensity, very high resolution back scattering spectrometer, with many innovative features, and energy resolution of approximately 1 μ eV.

8M SANS

Instrument for polymer characterization, sponsored by Polymers Division.

Vertical Sample Reflectometer

Instrument for measuring subsurface structure with polarization analysis capability. Capable of measuring reflectivities down to 10⁻⁸.

BT-8 Residual Stress Diffractometer

Diffractometer optimized for depth profiling of residual stress in large components.

BT-9 Triple Axis Spectrometer

Triple axis crystal spectrometer for measurements of excitations and structure.

BT-1 Powder Diffractometer

Powder diffractometer with 32 detectors; incident wavelengths of 0.208, 0.154, and 0.159 nm, with highest resolution of $\delta d/d = 8 \times 10^{-4}$.

BT-2 Triple Axis Spectrometer

Triple axis crystal spectrometer with polarized beam capability for measurement of magnetic dynamics and structure.

BT-4 Filter Spectrometer

A triple axis crystal spectrometer with a Be or Be/Graphite filter analyzer option for chemical spectroscopy.

Cold Neutron Depth Profiling

A station for quantitative profiling of subsurface impurities and coatings, based on neutron capture and emission of a charged particle.

Thermal Column

A very well-thermalized beam of neutrons used for radiography, tomography, dosimetry, and other experiments.

Solids that Shrink when Heated

G. Ernst¹, C. Broholm^{2,3}, A. P. Ramirez¹, and G. Kowach¹

¹*Bell Laboratories, Lucent Technologies, 600 Mountain Ave, Murray Hill, NJ 07974*

²*Department of Physics and Astronomy, Johns Hopkins University, Baltimore, MD 21218*

³*NIST Center for Neutron Research, Gaithersburg, MD 20899*

Thermal expansion is the reason that cracks between railroad tracks are largest in the winter and that the Sears tower grows by 15 cm in the summer. The reason that solids generally expand when heated is that atoms move apart to make room for each other when the amplitude of their thermal motion increases. There are however exceptions to this rule; i.e. solids that *contract* when heated. Such materials can be of great technological significance because they allow engineers to create composites that retain their dimensions irrespective of temperature. One example of a solid that contracts as temperature increases is ZrW_2O_8 . Discovered by Martinek and Hummel in 1968[1] this cubic material shrinks by 9 ppm/K from cryogenic temperatures until its decomposition temperature of 1050°C (see Fig. 1). Because the material is a transparent dielectric Lucent Technologies is using ZrW_2O_8 to compensate for thermal expansion of standard dielectrics in fiber optic gratings that must maintain their optical dimensions over a large range of temperatures. Before ZrW_2O_8 arrives at a telephone exchange near you we wanted to understand its unusual behavior through a series of neutron scattering experiments[2].

Figure 1 shows the reduction of the lattice

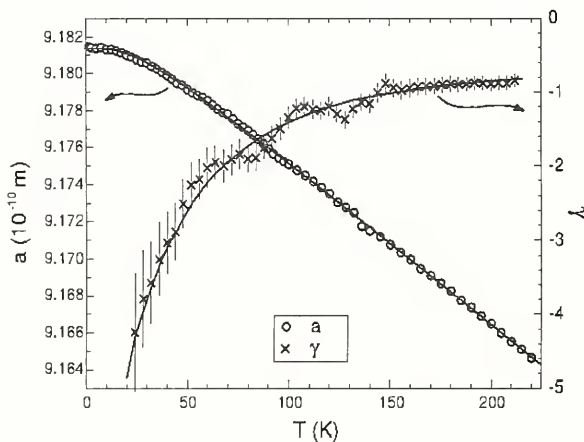


Figure 1. Temperature dependence of the cubic lattice parameter, a , and Grüneisen parameter $\gamma(T)$ for ZrW_2O_8 . Solid lines are based on a model described in the text.

parameter of ZrW_2O_8 with increasing temperature as measured with cold neutron diffraction on SPINS. The

Grüneisen theory of thermal expansion relates the thermal expansion coefficient $\alpha = d \ln a / dT$, to the specific heat as follows:

$$\alpha = \frac{1}{3B} \sum_i \gamma_i c_i \quad (1)$$

The summation is over normal modes, $B = -dP/d \ln V$ is the bulk modulus ($B = 4.8 \times 10^{10} \text{ Nm}^{-2}$ for ZrW_2O_8), c_i is the specific heat of a single mode, and $\gamma_i = -(\partial \ln \omega_i / \partial \ln V)$ is the Grüneisen parameter which modulates the contribution of each mode to thermal expansion. The overall Grüneisen parameter is defined as $\gamma(T) = 3B\alpha / C$ where $C = \sum_i c_i$ is the total specific heat. Clearly $\gamma(T)$ is temperature independent if all modes of vibration contribute equally to thermal expansion (or contraction). Fig. 1 shows $\gamma(T)$ for ZrW_2O_8 , which we determined by dividing the thermal contraction data in Fig. 1 with specific heat data[3]. $\gamma(T)$ is of course negative at all T and its absolute value increases down to the lowest temperature probed. This indicates that low energy modes drive thermal contraction in ZrW_2O_8 .

To quantify this statement we measured the phonon density of states (DOS) using inelastic neutron scattering and the result is shown in Fig. 2. The high energy modes correspond to librations of oxygen atoms. The top of the band at 140 meV lies higher than in Al_2O_3 by approximately 30 meV and this reflects the strong covalent bonding of oxygen in WO_4 tetrahedra and ZrO_6 octahedra (See inset to Fig. 2).

The low energy part of the spectrum is shown in Fig. 3. A large density of states remains down to 2.5 meV with a pronounced peak at 4 meV, which reveals low energy optical modes. Subsequent single crystal inelastic experiments have also identified several nearly dispersion-less modes around this energy.

To determine whether this DOS Peak could be important for thermal contraction we make the assumption that $\gamma(\hbar\omega) = \gamma_0 < 0$ for $E_0 < \hbar\omega < E_1$ and zero elsewhere as shown in the inset to Fig. 3. With $\gamma_0 = -14(2)$, $E_0 = 1.5(4)$ meV, and

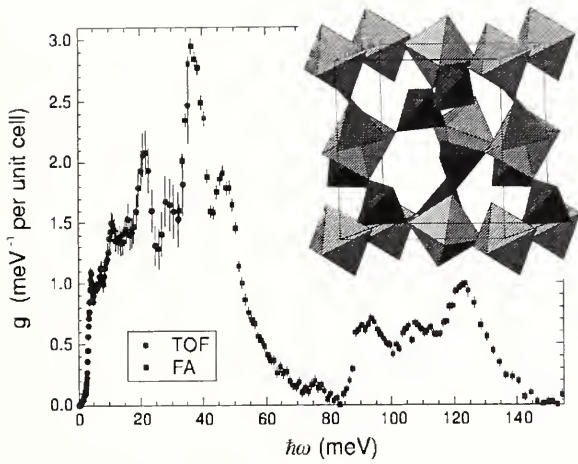


Figure 2. Density of states for ZrW_2O_8 at $T=300$ K measured using inelastic neutron scattering. For $0 < |\hbar\omega| < 40$ meV we used the TOF spectrometer with $E_i=5$ meV. For $\hbar\omega > 40$ meV we used BT4 with a polycrystalline Be filter analyser. Inset shows the structure with WO_4 tetrahedra in red and ZrO_6 octahedra in blue.

$E_1 = 9.5(2)$ meV and using the measured DOS, we obtain excellent fits to the data in Fig. 1 (solid lines). While the model is certainly not unique it establishes a range of energies for vibrations contributing to thermal contraction in ZrW_2O_8 .

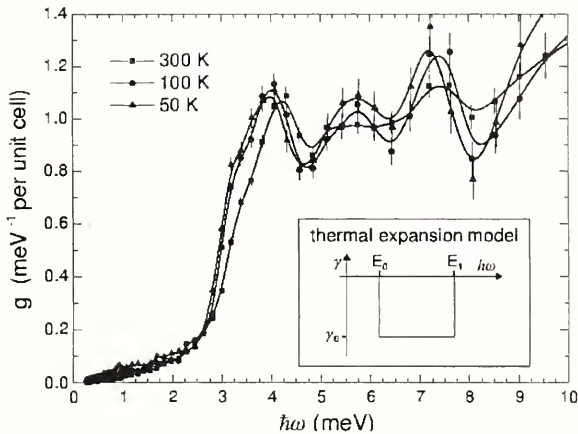


Figure 3. Low energy part of the phonon spectrum for ZrW_2O_8 and its temperature dependence. Inset shows our model for the energy dependence of the Grüneisen parameter.

An interesting aspect of these low energy modes is their temperature dependence shown in Fig. 3. There is a decrease in the frequency of the 4 meV optic mode as the temperature decreases and the unit cell volume increases. Naively this would appear to be in contradiction with a negative Grüneisen parameter because $(\partial\omega/\partial T)_p = -3\omega\gamma\alpha$ must be negative. But for an anharmonic vibration the mode frequency also depends on the amplitude and we propose that this non-linear effect which is not taken into account in the Grüneisen theory is responsible for the softening of the 4 meV optical mode.

What remains is to identify the microscopic nature of these modes. Single crystal phonon data will be required to accomplish this in earnest. Nonetheless inspection of the structure shown in Fig. 2 does provide important clues. ZrW_2O_8 consists of corner-sharing WO_4 tetrahedra and ZrO_6 octahedra. The unusual low energy optic modes are likely to correspond to twisting of these units with respect to one another and this twisting leads to contraction just as a vibrating guitar string tugs on its supports. What makes ZrW_2O_8 special is the unusually low energy of these twist modes which allows them to become highly excited and pull the structure together at temperatures far below those required to excite bond-stretching modes.

References

- [1] C. Martinek and F. A. Hummel, *J. Am. Ceram. Soc.* **51**, 227 (1968)
- [2] G. Ernst, C. Broholm, G. R. Kowach, and A. P. Ramirez, *Nature* **396**, 147 (1998)
- [3] A. P. Ramirez and G. Kowach. *Phys. Rev. Lett.* **80**, 4903 (1998)

Spin Correlations and Impurities in a One-Dimensional Quantum Spin Liquid

Guangyong Xu¹, G. Aeppli², P. Bischer², C. Broholm^{1,3}, J. F. DiTusa⁴, C. D. Frost⁵,
T. Ito⁶, K. Oka⁶, H. Takagi⁷, and M. Treacy²

¹Department of Physics and Astronomy, Johns Hopkins University, Baltimore, MD 21218

²NEC Research Institute, 4 Independence Way, Princeton, NJ 08540

³NIST Center for Neutron Research, Gaithersburg, MD 20899

⁴Department of Physics, Louisiana State University, Baton Rouge, Louisiana 70803

⁵ISIS Facility, Rutherford Appleton Laboratory, Chilton, Didcot, Oxon OX11 0QX, UK

⁶Electrotechnical Laboratory, Tsukuba 305, Japan

⁷The Institute of Solid State Physics, University of Tokyo, Roppongi, Tokyo 106 Japan

Though all solids contain electrons with spin-induced magnetic moments few materials will actually cling to your refrigerator door. The quantum theory of atoms explains that matter is generally non-magnetic because electron spins form non-magnetic (singlet-) states in the filled electronic shells of individual atoms. Here we discuss a new class of materials wherein singlet formation takes place *between* rather than *within* atoms to yield a macroscopic spin-less “molecule”. We explore the magnetism of Y_2BaNiO_5 , in which magnetic Ni^{2+} atoms interact antiferromagnetically (AFM) through intervening O^{2-} atoms to form spin chains.

Inelastic magnetic neutron scattering is a powerful probe of spin chains. The open circles in Fig. 1 show the low temperature equal time spin correlation function versus wave-vector transfer along the chain. In contrast to Néel AFM's that develop Bragg peaks when long range order develops at a second order phase

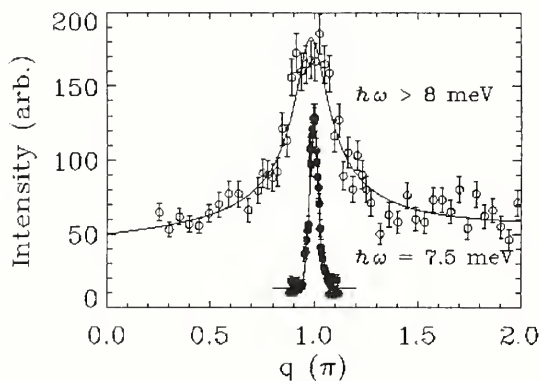


Figure 1. Neutron scattering from Y_2BaNiO_5 at $T=10$ K. Open symbols show energy-integrated data probing equal-time correlations. Solid symbols show a constant- $\hbar\omega$ scan at the gap energy.

transition, Y_2BaNiO_5 has no magnetic phase transition and our snap-shot of the spin configuration reveals short-range AFM order with a dynamic correlation length $\xi=4.3(6)$. Still this is not a thermally disordered paramagnet. The solid symbols in Fig. 1 show that at *fixed* energy transfer there are sharp peaks in the wave-vector dependence of the dynamic correlation function that allows us to put a lower limit of 50 lattice spacings on the coherence length for magnetic excitations.

Fig. 2 (a) shows another important feature of

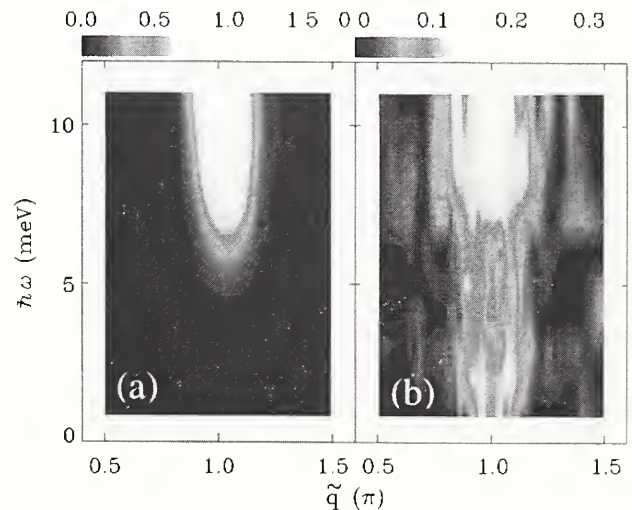


Figure 2. Contour map of low energy magnetic neutron scattering at $T=10$ K from (a) pure Y_2BaNiO_5 and (b) $\text{Y}_{1.905}\text{Ca}_{0.095}\text{BaNiO}_5$. The MARI spectrometer at the ISIS facility in the UK was used for (a) while BT2 and SPINS at the NIST were used for (b).

the AFM spin-1 chain: There is a gap in the excitation spectrum separating the ground state from excited states. The energy gap is the cost of creating a magnetic wave packet on the spin chain.

There are interesting effects of substituting Ca^{2+} for Y^{3+} . The extra hole occupies the π -orbital on the super-exchange mediating oxygen site and leads to a ferromagnetic (FM) impurity bond in the otherwise AFM spin chain. Fig. 2 (b) shows that such doping yields new sub-gap excitations. The extra magnetic scattering takes the form of a double ridge versus energy, which indicates that we are dealing with slow fluctuations of a rigid composite object. The wave-vector dependence provides valuable but ambiguous information about the real space structure of this object. A natural first interpretation would be that the holes have ordered to yield a new incommensurate periodicity. To explore this possibility Fig. 3 shows a comparison of high statistics -integrated data for samples with Ca concentrations differing by almost 50 %. The absence of a significant shift in the peak positions rules out hole ordering.

We propose instead that the double peak in Fig. 3 is the magnetic form factor of a hole in a quantum spin liquid. Consider first the dilute and static hole

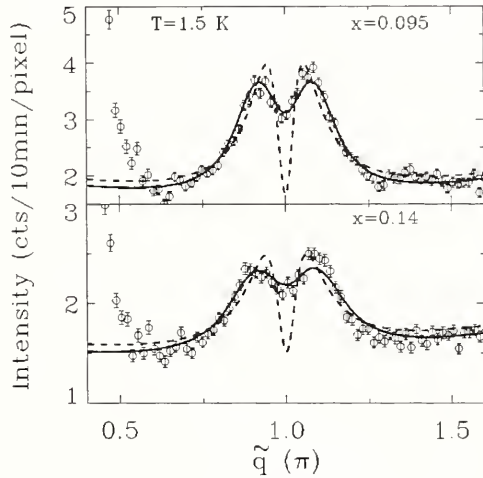


Figure 3. Q-dependence of energy integrated intensity from $\text{Y}_{2-x}\text{Ca}_x\text{BaNiO}_5$ with $x=0.095(5)$ and $x=0.14(1)$. The dashed line is a single impurity model. The solid line is a random impurity model.

limit of a single FM impurity bond on the spin chain. The energy of the macroscopic spin singlet has increased and a degenerate magnetizable state is now the ground state. If we assume that the spin disturbance associated with the impurity bond decays away from the impurity then we can show that the corresponding form-factor has the general features observed in the scattering data. Denote by $M(q)$ the form factor for the spin density which develops to the right of an impurity bond.

The corresponding form-factor for the disturbance to the left of the impurity is the complex conjugate, $M^*(q)$. The form factor for the combined object becomes $F(q)=M(q)e^{iq/2}M^*(q)e^{-iq/2}$. When the chain end spin degrees of freedom are antiferromagnetically combined, corresponding to the negative sign in this equation, $|F(q)|^2$ becomes the conventional structure factor for the quantum spin liquid in Fig. 1. However when the chain ends are stitched together ferromagnetically as we should expect for FM impurity bonds we have $F(q)=2\text{Re}\{M(q)e^{iq/2}\}$. This function vanishes for $q=(2n+1)\pi$ because $M(q)$ is real for $q=n\pi$ and the result is a notch at $q=n\pi$ as shown by the dashed lines in Fig. 3. To account for the finite intensity between the peaks we need to consider the finite density of impurity bonds. Neighboring holes arranged at random break inversion symmetry about individual holes and this brings back intensity at $q=\pi$. The solid lines in Fig. 3 correspond to an analytical expression for the scattering from a distribution of uncorrelated asymmetric impurities with exponentially decaying spin densities. The fact that the impurity scattering is distributed over a range of energies in Fig. 2 (b) indicates that the holes are moving or more likely that neighboring bound states interact.

The significance of all this is that we have directly measured the spin wave function associated with a bond reversing hole impurity in a quantum spin liquid. Because our raw data are so similar to the scattering data from doped copper oxide superconductors our results suggest that hole form-factor effects may also be important for interpreting those data.

References

- [1] Guangyong Xu *et al.*, Phys. Rev. B **54**, R6827 (1996)
- [2] J. F. DiTusa *et al.*, Phys. Rev. Lett. **73**, 1857 (1994)

Deposition of Toxic Trace Elements and Heavy Metals to Lake Michigan by Size and by Source

J. M. Ondov and P. F. Caffrey

Department of Chemistry, University of Maryland, College Park, MD 20742

Atmospheric deposition by wet and dry processes is known to be an important source of several anthropogenic, particulate-bound metals in critically important waters such as the north Atlantic Ocean, the coastal mid-Atlantic waters, and the Great Lakes. Lake Michigan is especially subject to deposition of anthropogenic air pollutants as it lies in close proximity to the heavily polluted urban and industrial areas stretching from Chicago to Gary, Indiana, i.e., an area containing 20% of the US steel production.

The University of Maryland (at College Park, UMCP) aerosol chemistry group has used the NBSR reactor for instrumental neutron activation analysis to characterize atmospheric aerosol particles and gases for more than 20 years. Detailed and accurate multielement analyses are routinely achieved, nondestructively, for up to 40 elements in samples collected for periods of several hours to a few days on various types of filters and in cascade impactors which size fractionate the aerosol into as many as 10 size domains. As many as 30 elements can be determined in as little as 100 μg of a size-segregated particulate fraction, allowing the application of receptor modeling techniques to determine the sources of size segregated aerosol particles. This is extremely important in assessing dry deposition of aerosol particles and their constituents because deposition velocity is highly sensitive to particle diameter (see Figure 1). Some of the elements measured, e.g., As, Cd, and Hg, are highly toxic and are, therefore, of epidemiological interest, especially in the Chesapeake Bay, Lake Michigan, and Coastal Marine environments. Equally important is that information on elemental constituents remains a powerful, fundamental tool with which atmospheric sources, transport, and processes may be elucidated.

As a part of EPA's Great Water's project, Atmospheric Exchange Over Lakes and Oceans (AEOLOS), size segregated aerosol particulate samples were collected, simultaneously, with 10-stage cascade impactors sited in south Chicago, aboard ship at sites 20 km east of Chicago, and on the Eastern shore, about 90 km down wind (Figure 2). Sampling campaigns were

conducted in spring, summer, and winter periods to observe seasonal differences in the concentrations and size distributions of inorganic elemental constituents. Several hundred size-segregated fractions were collected and analyzed by X-ray fluorescence (XRF)

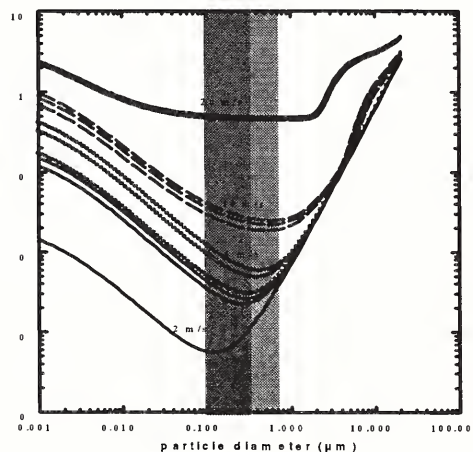


Figure 1. Deposition velocity vs. aerodynamic particle diameter.

and Instrumental Neutron Activation Analysis (INAA).

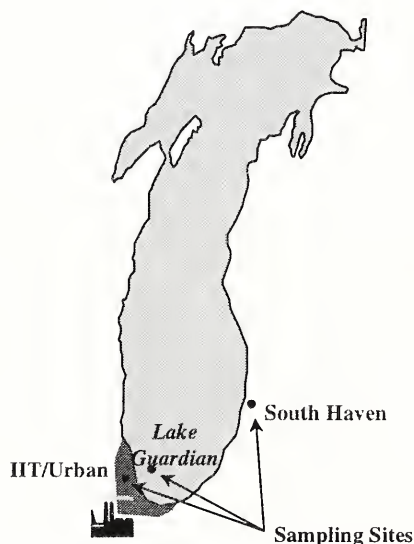


Figure 2. Location of sampling sites

A great deal of useful information about the sources of aerosol particles can be obtained from size spectra of constituent "marker" elements. In Figure 3, V, a marker of particles emitted from fuel oil combustion, is bimodal. Vanadium on

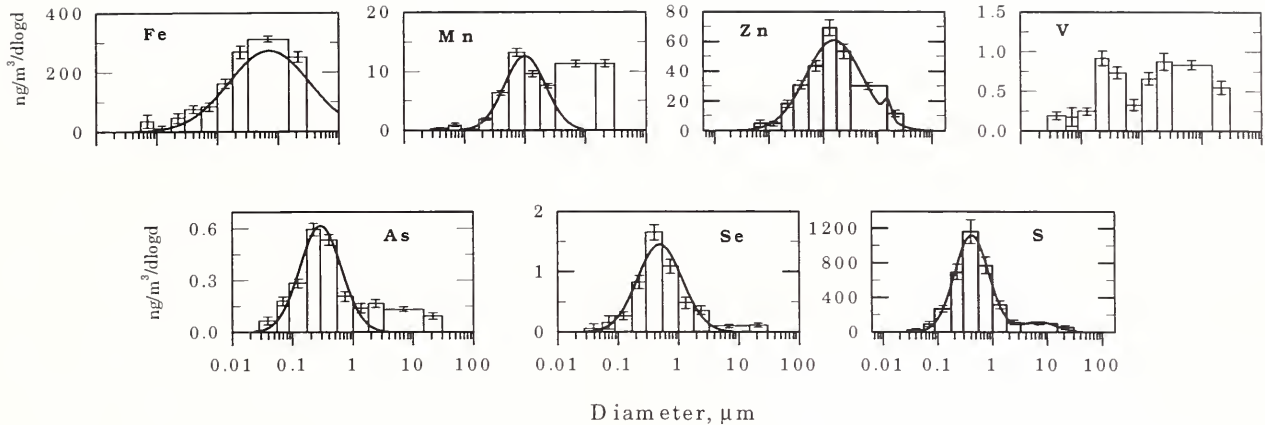


Figure 3. Concentration vs aerodynamic particle size distributions for several important “marker” elements determined from samples collected on Lake Michigan.

large (coarse) particles (i.e., those $>1 \mu\text{m}$) is associated with urban and rural dust particles. Vanadium on submicrometer (i.e., “fine”) particles was emitted from oil-fired power plants. Likewise, selenium is a marker of coal combustion particles; Zn, incineration; and As, steel mill emissions. Iron- and Mn-containing particles were also emitted from steel mills, but have substantial large particle components from this source. Manganese clearly has both a fine and coarse particle component.

Often, the size distributions of particles emitted from different sources overlap, and must be resolved by, for example, a chemical mass balance (CMB) method. The CMB involves solving a system of equations, constructed to explain the concentration of an elemental aerosol constituent at a sampling (receptor) site as a linear sum of the concentrations of elements from N number of sources for which the composition of particulate emissions is well characterized. Results for As and Zn are shown in Figure 4. This is the first successful resolution of the contributions of toxic constituents of aerosol particles by size and source. These data, and much more like it, have been used to provide the policy makers with far more accurate estimates of the deposition fluxes of toxic substances to Lake Michigan. Similar analyses are being performed by our group for the Chesapeake Bay.

References

[1] Peter Caffrey, Ph.D. Measurement of fine-particle dry particle deposition to Lake Michigan. December, 1997.

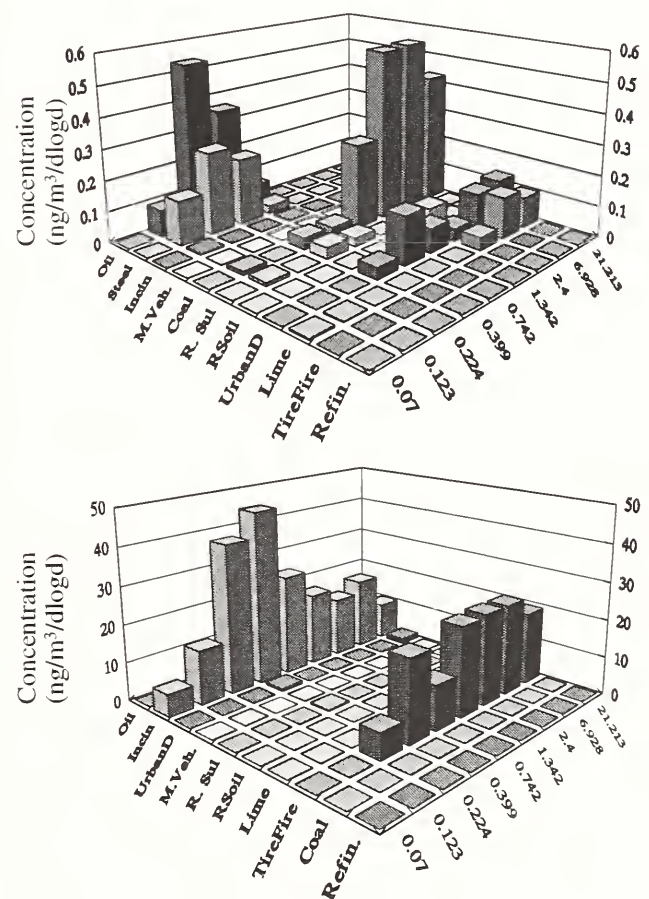


Figure 4. Distributions of As (upper) and Zn (lower) in particles sampled over Lake Michigan, by size and source.

Magnetic Domains in Co-SiO₂ Multilayer Tunnel Junctions

Daniel C. Dender¹, Julie A. Borchers¹, Ross W. Erwin¹, Steve Kline¹, Sandra Sankar,² and Ami E. Berkowitz²

¹NIST Center for Neutron Research
NIST, Gaithersburg, MD 20899

²Center for Magnetic Recording Research (CMRR)
University of California at San Diego, La Jolla, CA

In the ongoing search for sensors for magnetic recording applications, recent research has focussed on materials that exhibit spin-dependent tunneling. These systems are comprised of metallic, ferromagnetic particles or of layers that are well separated from each other by an insulating material. Magnetoresistance (MR) from spin-dependent tunneling was first reported for granular metal/insulator films in 1972 and for Co/Ge/Fe trilayer junctions in 1975. The effect arises because the tunnel conductance is minimum when the particle or layer moments are aligned antiparallel.

From a magnetic recording perspective, the objective is to maximize the change in the resistance while minimizing the active field range. Multilayer tunnel junctions exhibit pronounced field sensitivity, but the insulating barrier layers are susceptible to pinholes that connect the ferromagnetic layers. In contrast, granular films with small ferromagnetic particles are easy to fabricate by co-deposition of a metal with an immiscible insulator. However, the saturation fields for the MR are large and the approach to saturation is gradual because the particles are magnetically isolated.

Desirable characteristics of both magnetic tunnel junctions and the granular films are combined in discontinuous metal/insulator multilayers, which represent a new class of spin tunneling devices. These hybrid systems are prepared by alternately sputtering two immiscible materials, such as Co and SiO₂, onto a substrate. Since the metal does not wet the insulator, the ferromagnet breaks up into nanoparticles during growth. Transmission electron microscope images and x-ray diffraction data of Co/SiO₂ multilayers reveal that the Co forms either individual particles with diameters of 2.5 nm or chains composed of touching particles. In contrast to granular films, the MR of these hybrid structures is maximum at a smaller magnetic field, which is useful for applications. However, the dependence of the MR on small magnetic fields is not consistent with a simple picture of the magnetic moments of individual particles changing independently. Instead it is believed that the smaller particles are magnetically

coupled to form larger magnetic domains. Neutron scattering experiments characterize the magnetic structure (i.e., the magnetic correlation length) associated with the MR maximum. This correlation length is required to model the MR mechanism.

Initial neutron reflectivity studies of a [SiO₂(3.0 nm)|Co(2.0 nm)]_{24.5} multilayer with the sharpest MR showed that the Co spins are randomly oriented along the growth direction at fields near the coercive field, H_C, where the magnetic hysteresis loop crosses the field axis (i.e., zero net moment). However, the average size of the magnetic domains across the sample plane is substantially larger (1 – 5 μm) than the average size of the Co particles. A multilayer with a smaller nominal Co thickness, [SiO₂(3.0 nm)|Co(1.6 nm)]_{60.5}, showed no in-plane magnetic ordering within the sensitivity of the reflectivity experiments. Small angle neutron scattering (SANS) measurements of this multilayer and a 0.5 μm thick Co(0.4)/SiO₂(0.6) granular

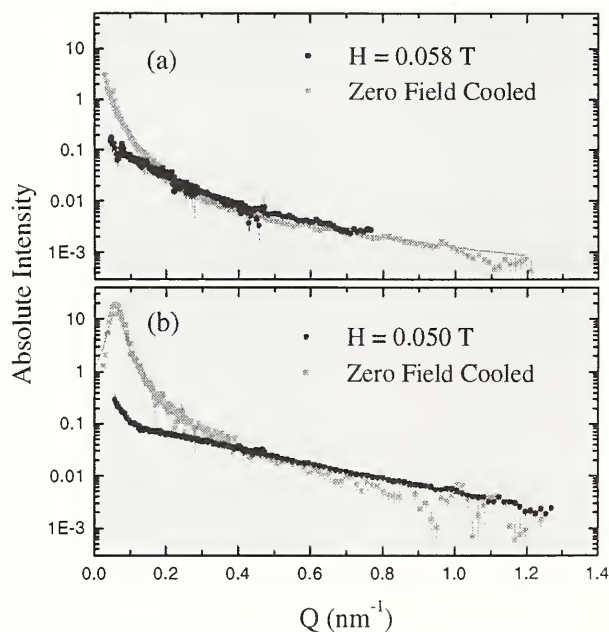


Figure 1. Circular average of SANS data for [SiO₂(3.0 nm)|Co(1.6 nm)]_{60.5} multilayer (a) and Co(0.4)/SiO₂(0.6) granular film (b) at 15 K. The ZFC data for the film is a sector average at 45°. Data fits are shown as lines.

film were thus undertaken to probe smaller lengthscales. These experiments indicate that the correlation lengths at H_C are larger for the discontinuous multilayer than for the granular film. In addition, data obtained for both samples after cooling in zero field (ZFC) indicate that the Co particles have an intrinsic magnetic interaction.

With the exception of the ZFC data for the granular film (Fig. 2), all of the data were circularly symmetric and could be averaged about the center of the detector. Figure 1 (a) shows the average magnetic intensity at 15 K plotted as a function of the wavevector Q for the discontinuous multilayer at $H_C = 0.058$ T (purple circles) after saturation in a 0.5 T field. The Lorentzian fit to these data gives a magnetic correlation length of 10 ± 2 nm, which is of the order of the size of the Co nanoparticle chains.

For comparison, the coercive field data (purple circles) for the granular film are shown in Fig. 1 (b). These data fit to a linear combination of two squared Lorentzians, which is a functional form often found for scattering from disordered magnets. The dominant term gives a short correlation length of approximately 1.7 ± 0.5 nm, which is *smaller* than the 4 nm spherical particle size in the granular film. For both the granular film and the discontinuous multilayer, the static and/or dynamic magnetic domains at the coercive field appear to be limited to the individual Co particles. The dramatic contrast in the MR curves for the discontinuous multilayer and the granular film could be a consequence of the difference in the electron-scattering surface area (i.e., the granular film has smaller particles and domains and thus has more scattering surfaces).

The demagnetization process for both the film and the multilayer, however, is very sensitive to field preparation conditions. Figure 1 (a) also shows the average magnetic intensity of the discontinuous multilayer at 15 K after cooling in zero field from room temperature (green squares). These data yield a correlation length of 30 ± 1.5 nm. The act of cooling the multilayer apparently induces interparticle interactions that stabilize domains larger than a single Co nanoparticle.

Figure 2 shows the scattering pattern for the granular film after cooling to 15 K in zero field from room temperature. The intensity is asymmetric with maximum intensity along the vertical axis. These data suggest that the Co moments are preferentially aligned along the horizontal axis. However, this spin anisotropy axis is not evident from magnetization and resistivity data.

The sector average in Fig. 1 (b) further reveals that the ZFC data have a sharp peak at $Q = 0.0605$ nm⁻¹. The data fits suggest that the ZFC structure for the granular

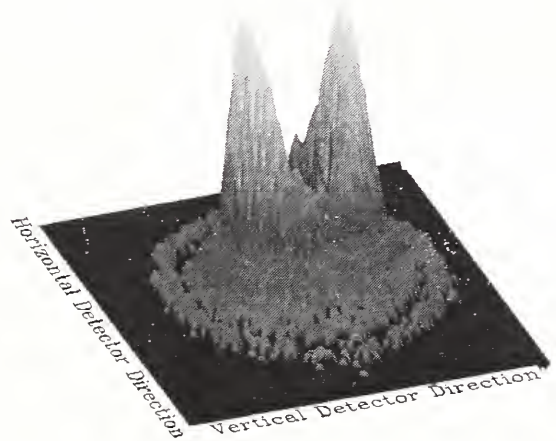


Figure 2. SANS image from a Co(0.4)/SiO₄(0.6) granular film after cooling from room temperature to 15 K in zero field.

film is comprised of magnetic domains separated by an average distance of 104 ± 1 nm in the film plane. Despite their small size, the Co particles interact with each other upon cooling in zero field to form a well-ordered magnetic state.

The observed difference between the magnetic domain formation in discontinuous spin-tunneling multilayers and granular films is essential to the understanding of their contrasting MR properties. Future studies will focus on the temperature and field evolution of the domains to optimize their performance as magnetic sensors.

Mechanism of Thermal Barrier Coating Failure at High Temperature

J. K. Stalick¹ and J. Ilavsky²

¹NIST Center for Neutron Research, Gaithersburg, MD 20899

²Institute of Plasma Physics, Prague, Czech Republic

Ceramic thermal barrier coatings (TBCs) are used in gas turbine engines and other combustion components to allow operation at increased temperatures, which increases efficiency, reduces cooling requirements, and extends component life. They are currently used in aircraft engines and are expected to be adopted for energy-generating gas turbines and diesel engines in the near future. It has been estimated that for the US power generation sector alone, a one percent increase in efficiency would lead to a savings of \$140M per year.

The most common industrial TBC is yttria stabilized zirconia (YSZ), which consists of zirconia, ZrO_2 , with about 8 wt % yttria, Y_2O_3 (equivalent to 8.7 mol % $YO_{1.5}$). Many factors contribute to the stability of YSZ coatings, including particle size and homogeneity of feedstock powders, coating deposition techniques, and metallic bond coat characteristics. We have been investigating the inherent stability of the crystallographic phases present in plasma-sprayed YSZ using neutron Rietveld refinement for quantitative phase analysis.

YSZ consists of three crystallographic phases: monoclinic, tetragonal, and cubic. According to the phase diagram, the tetragonal phase is predominant at about 8 wt % yttria. However, plasma spraying is a rapid solidification process that results in metastable phase mixtures of the monoclinic phase (0–6 wt % yttria), tetragonal phase (4–13 wt % yttria), and cubic phase (11–20 wt % yttria). It is thought that the coexistence of the tetragonal and cubic phases toughens the TBC through inhibition of crack propagation; however a presence of 5% or greater of the monoclinic phase results in coating instability because the monoclinic phase transforms to the tetragonal phase upon heating. Since this transformation is accompanied by a large volume change, thermal cycling generates stresses in the coatings leading to premature failure.

In order to simulate high-temperature operating conditions, we annealed plasma-sprayed YSZ coatings for periods of one to 100 hours at temperatures of 1000, 1200, and 1400 °C. These coatings were prepared from two feedstock powders with differing characteristics; feedstock 1 was prepared by a

spheroidization process and feedstock 2 by fusing and crushing. High-resolution neutron powder diffraction patterns were obtained on the NCNR 32-detector powder diffractometer at BT-1 and the data were analyzed using the Rietveld refinement technique. Results of the phase analysis of the feedstock powders, as-sprayed coatings, and annealed coatings are given in Fig. 1.

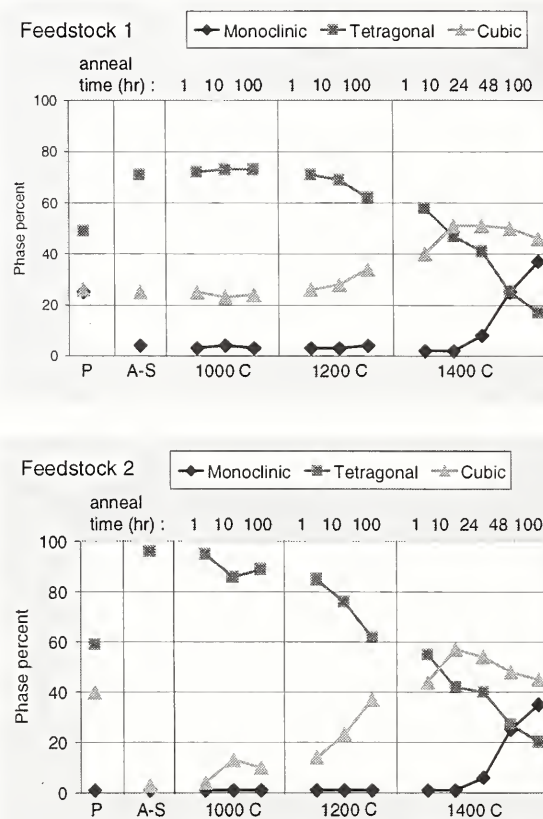


Figure 1. Change in phase composition of YSZ coatings upon annealing. P = starting feedstock powder; A-S is the as-sprayed coating.

The two feedstock powders, 1 and 2, have quite different initial phase compositions: 1 has about 25 % of the monoclinic phase, whereas 2 has virtually none. The plasma-sprayed coatings are initially different as well, with coating 1 having 25 % cubic phase content

and coating **2** being almost totally tetragonal. The phase content of both coatings changes gradually with annealing for longer times or at higher temperature (see Fig. 1), showing a general increase in the cubic phase content and decrease in the tetragonal phase content. However, with longer annealing times at 1400 °C a significant increase in the monoclinic phase content is seen; both **1** and **2** have nearly identical phase compositions after annealing for 24, 48, and 100 hours and sufficient monoclinic phase is present to cause coating failure.

While the general phase behavior upon annealing has been known for some time from x-ray studies, the use of the neutron Rietveld technique permits us to extract more information based upon the unit cell parameters of the tetragonal and cubic phases. It is known that the lattice parameter a of the cubic phase increases linearly with yttria content, and that the c/a ratio for the tetragonal phase decreases with increasing yttria content. Earlier studies, however, either underestimated the cubic phase content or assumed equal yttria content for the tetragonal and cubic phases. We were able to use the unit cell parameters obtained from the neutron data to extract the distribution of yttria in these phases assuming that the total yttria content is constant. Results are given in Table 1. Note that the nominal composition for both samples is 8.7 mol % $YO_{1.5}$, but that sample **2** appears to be low in total yttria content.

The data given in Table 1 give an indication as to why the phase changes on annealing occur. It can be seen that even at the lower annealing temperatures the yttria is leaving the tetragonal phase and entering the cubic phase, resulting in higher yttria content of the cubic phase (coating **2**) and increased cubic phase fraction (coatings **1** and **2**). As the samples are annealed for longer periods at higher temperatures, the yttria content of the tetragonal phase drops below 3-4 mol % $YO_{1.5}$, and destructive transformation to the monoclinic phase occurs.

These results indicate that there is an inherent limit to the temperature and time of YSZ component operation. While technological improvements to YSZ coatings are possible, new materials will be needed to achieve significantly higher operating temperatures.

Table 1. Yttria content of tetragonal (T) and cubic (C) phases given in mol % $YO_{1.5}$; estimated accuracy is ± 0.2 mol % for the tetragonal phase in the annealed coatings and ± 1 mol % for all other values. Yttria content of the monoclinic phase is assumed to be 3 mol % for the calculation of total yttria content.

Sample	Feedstock 1			Feedstock 2		
	T	C	total	T	C	total
Powder	7	14	8	6	7	6
As sprayed	8	15	9	8	--	8
1000 C/ 1h	6.6	14	9	7.4	--	7
10h	6.4	15	8	7.1	3	7
100h	6.2	15	8	6.9	4	7
1200 C/ 1h	6.2	15	9	7.1	5	7
10h	5.8	16	9	6.8	7	7
100h	5.0	17	9	5.3	11	7
1400 C/ 1h	5.2	14	9	5.7	8	7
10h	4.2	14	9	4.0	9	7
24h	3.8	12	8	3.5	8	6
48h	4.3	14	9	4.6	11	7
100h	6.7	14	9	7.0	10	7

A New Method to Determine Single Crystal Elastic Behavior from Polycrystals

Thomas Gnäupel-Herold^{1,2}, Paul C. Brand,¹ and Henry J. Prask¹

¹NIST Center for Neutron Research

NIST, Gaithersburg, MD 20899

²University of Maryland

College Park, MD

Modern engineering analysis techniques, used to ensure that parts in e.g. bridges, airplanes, or automobiles will survive the stresses of use, rely on understanding the proportionality between stress and strain. For many applications the description of the proportionality between stress and strain in terms of isotropic, i.e. independent of direction, elastic constants is still sufficient, the knowledge of these constants for anisotropic cases becomes increasingly important for manufacturing processes, for micromechanical modeling of materials behavior, as well as for custom tailoring new composite materials. For materials which are crystalline on some length scale, anisotropy begins at the grain size level (single crystal elastic constants) and extends as far as anisotropy can be introduced into the material.

This macroscopic anisotropy is induced by two basic effects - a preferred orientation of the crystal lattice of the constituent grains and/or a preferred grain shape distribution. A preferred grain shape distribution means that grains or inclusions have a non-spherical shape on average and they are aligned to some common axis as well. This effect is not necessarily connected to the first one.

The anisotropy of elastic properties on a macroscopic scale (≈ 1 mm) can be readily measured by straining the specimen or by ultrasonic resonance. However, these methods fail in cases in which the microscopic scale is of interest. Examples are precipitations or inhomogeneities of other phases whose elastic constants are unknown but determine nonetheless the strength of the composite or alloy as a whole. The goal can therefore be formulated as the determination of the anisotropic or single crystal elastic constants on the microscopic scale. This can be achieved by diffraction which provides information about the strain and the elastic response of the crystal lattice for a particular direction [hkl].

These so called diffraction elastic constants (DEC) describe the elastic response of a particular family of lattice planes in a certain group of grains

with the appropriate orientation to an applied load. Although the DEC are a feature of the polycrystal they can be readily compared to the directional dependence of the elastic constants in a single crystal (Fig. 1).

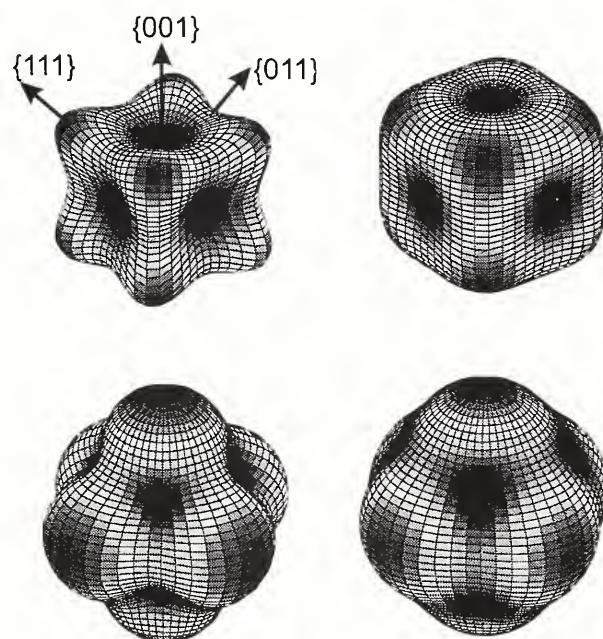


Figure 1: Dependence of Young's modulus E (top) and Poisson's ratio ν (bottom) on the direction hkl in the cubic crystal lattice for Ni. The left hand side represents the case of the single crystal, whereas the right hand side shows $E(hkl)$ and $\nu(hkl)$ as they would be obtained from a set of crystallites which have been selected out of an aggregate of randomly oriented grains. The selected crystallites have in common that for a certain hkl their lattice vectors are parallel.

The smoothing effect for the 'aggregate' constant is a result of the fact that each of the grains in the polycrystal is surrounded by other, not necessarily randomly oriented grains. The elastic response of the selected grains is therefore somewhat obstructed in comparison to the single crystal.

Thus, probing the DEC can provide a wealth of information about the average local conditions on the grain size level.

Since its commissioning the residual stress diffractometer at the thermal beamline BT8 has been used for a variety of engineering-applications-related measurements as well as for basic studies of the elas-

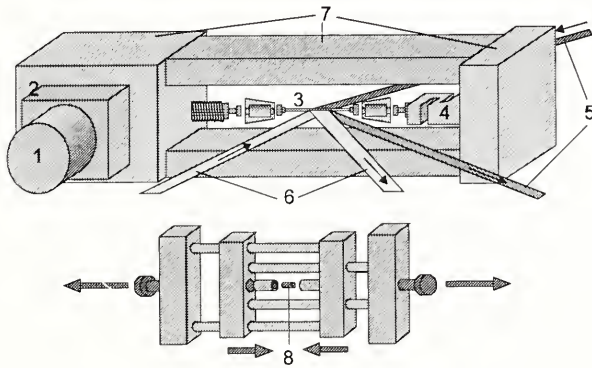


Figure 2 : Schematic of the stress rig.

tic behavior of materials. In the course of these experiments a method has been developed which allows the determination of single crystal elastic constants from measurements on polycrystals. This is done experimentally by loading a specimen in a stress rig and measuring the lattice response normal and parallel to the load direction (Fig.2 and Fig. 3).

- 1- stepping motor, resolution 1:360
- 2- gear, reduction 1:2500
- 3- tensile bar
- 4- 10 kN load cell
- 5- beam in transmission (Young's modulus)
- 6- beam in reflection (Poisson's ratio)
- 7- stainless steel frame
- 8- compression sample in compression adapter

These experimental results can be compared to models which calculate the DEC from the single crystal constants [1]. These models can be reversed in a way which considers the single crystal elastic constants as unknown parameters [2,3]. This way the problem can be expressed as a least square loop in which the single crystal elastic constants are refinable parameters.

Possible applications of the method are materials which cannot or can only under great difficulties be synthesized as sufficiently large single crystals. Examples are γ' precipitations in γ/γ' hardened superalloys or metastable phases as plasma sprayed γ -Al₂O₃.

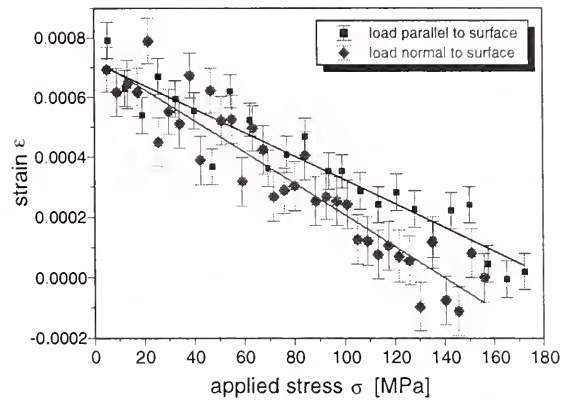


Fig. 3: Lattice strain response in a transmission-compression setup for a γ -Al₂O₃ plasma sprayed thermal barrier coating. Load experiments have been carried out normal and parallel to the coating surface. The difference in the slopes is due to the anisotropy of the sample.

γ' precipitates exist, strictly speaking, only within the equilibrium of the two phase compound, which therefore also requires the determination of their elastic constants from the composite. Thus, in these cases the method may provide the only available tool for determining their single crystal elastic constants.

References

- [1] Bollenrath, F.,Hauk, V. & Müller, E. H. (1967), *Z. Metallk* .58, 1, 76-82
- [2] T. Gnäupel-Herold, P.C. Brand, H.J. Prask, *J. Appl. Cryst* (1998), in press
- [3] T. Gnäupel-Herold, P.C. Brand, H.J. Prask, *Ann. X-ray Anal.* (1998), in press

Development of Three New Standard Reference Materials

G. P. Lamaze, R. M. Lindstrom, R. L. Paul, and R. Zeisler
Nuclear Methods Group, Analytical Chemistry Division
NIST, Gaithersburg, MD 20899

The chemical composition of materials critically determines their uses in commerce. Chemical analysis is a large endeavor in industry, and depends on the availability of materials with well-known composition to develop and validate analytical procedures and laboratories. NIST Standard Reference Materials (SRMs) are the most important such materials in the marketplace. Nuclear analytical methods have been a crucial contributor to the certification of SRMs for thirty years, because of their high sensitivity and specificity, and their freedom from chemical interferences. In addition to the continuing production and characterization of traditional Standard Reference Materials, three new approaches are underway to satisfy critical measurement needs, using the Analytical Chemistry facilities at the NCNR.

Air particulate matter. Investigations into the amounts and composition of particulate material in air are currently carried out in virtually every country. The investigations in the United States are pointing at particularly high risk factors associated with the fine fraction ($PM_{2.5}$, which is smaller than $2.5 \mu\text{m}$ aerodynamic diameter) of aerosols. The primary techniques for trace element analysis are based on nuclear physics principles (PIXE, XRF, NAA, etc.), due to their suitability for multicomponent determinations on the small sample sizes that are represented. However, few appropriate quality assurance materials are available to support this work. To assist in effective measurement and control of $PM_{2.5}$ aerosols in an economically sustainable way, NIST is developing this new class of SRMs.

We have collected air particulate matter corresponding to the $PM_{2.5}$ fraction in Baltimore, Maryland at an established EPA monitoring site. The aerosol is removed by ultrasonication from the Teflon membrane filters and suspended in water. Individual filters are prepared by filtering aliquots of the suspension through 47 mm diameter polycarbonate filter membranes with $0.4 \mu\text{m}$ pore size to form the SRM units. Elemental concentrations in this SRM will be certified using a variety of nuclear- and non-nuclear- based analytical techniques.

Hydrogen in titanium alloy. Hydrogen causes embrittlement of many metals, and the industry-standard analytical methods need same-matrix standards to calibrate their instruments. To meet this need we are

currently preparing a new SRM by direct reaction of a titanium alloy with measured amounts of hydrogen and using cold-neutron Prompt Gamma Activation Analysis to verify the doping level.

A procedure has been demonstrated for producing certified reference materials of titanium alloy (6% Al + 4% V) with a known concentration of hydrogen. In the reversible reaction $\text{Ti} + \text{H}_2 = \text{TiH}_2$ the equilibrium pressure is less than 10^{-13} atmospheres at room temperature, and 150 atmospheres at $900 \text{ }^\circ\text{C}$. Reaction is rapid at $300 \text{ }^\circ\text{C}$. This gettering reaction with hot titanium is in common use in geochemistry for separating hydrogen from oxygen and nitrogen (which react irreversibly) and from noble gases. Massive hydrides are prepared industrially by the same direct reaction process for hydrogen-based energy storage and nuclear applications.

Batches of a few grams of titanium alloy specimens have been doped with hydrogen using a simple closed gas handling system. Means are provided for pumping away air and hydrogen from samples at high temperature and for admitting a known pressure of hydrogen in a calibrated volume at room temperature, then raising the temperature of the system to carry out the reaction. The accuracy of the doping is limited by that of the pressure measurement, better than 0.5%. The amount of H in the metal samples was measured in 100-mg specimens by cold-neutron prompt-gamma activation analysis. The quantity measured by this technique and by gravimetry agreed with the volume of gas added. Eighty-gram cylinders of Ti alloy have been loaded by the same procedure, and the uniformity of doping verified elsewhere by quantitative neutron tomography.

These measurements indicate that Standard Reference Materials of hydrogen in titanium alloy can be made and certified by quantitative preparation and analysis as two independent methods, as is done with chemical solution standards at NIST. An apparatus has been constructed to dope 1-kg quantities of metal for Standard Reference Materials.

Titanium nitride films. Reference materials are a critical part of semiconductor metrology since they establish a means of comparison of data taken by different methods or between model and experiment. SEMATECH has requested a titanium nitride Standard

Reference Material as one of their highest needs. A prototype SRM has been made by ion beam sputtering onto 75-mm diameter silicon wafers that were then cut into 10-mm squares. The thickness of the TiN was about 100 nm. Four squares plus a blank were analyzed by neutron depth profiling to determine the total nitrogen concentration. The concentration was determined relative to a boron concentration standard. The relative count rates of the nitrogen and boron samples were adjusted by the ratio of the nitrogen to boron cross sections (1.819/3840). Statistical uncertainties are about 1% (1σ) and the overall normalization uncertainty is 2% (1σ) due to the uncertainty of the nitrogen and boron cross sections. An approximate 3% fall-off of the nitrogen concentration from center to edge of the original wafer was observed. A measure of

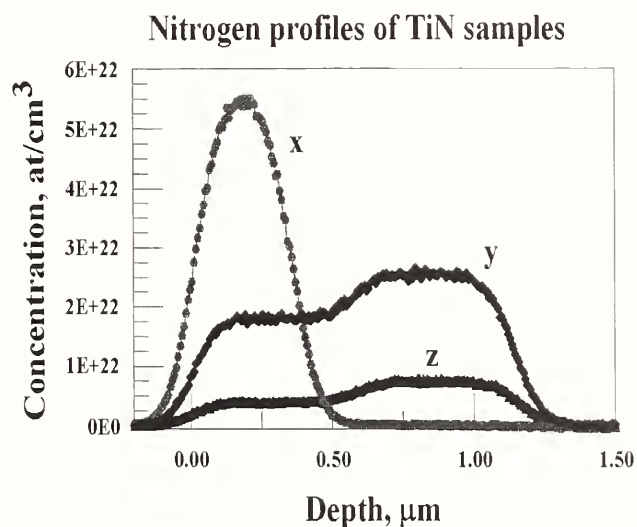


Figure 1. Three titanium samples from a previous study indicating nitrogen non-uniformity and less than a one-to-one stoichiometry.

the titanium concentration on each square was made by the technique of activation analysis. This allows a determination of the stoichiometry of the TiN.

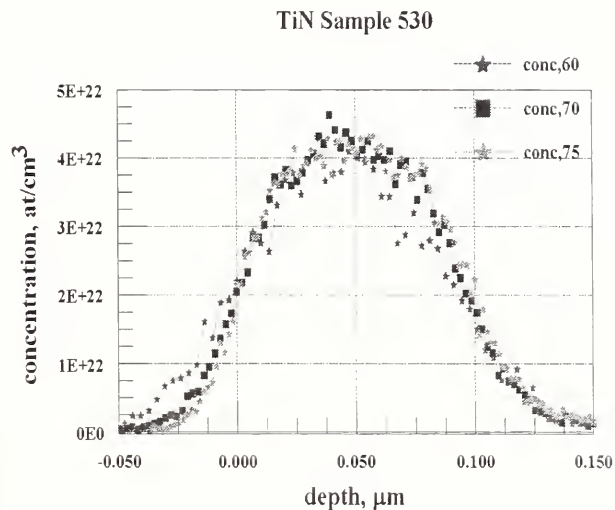


Figure 2. Proposed SRM material with expected stoichiometry. Measurements taken at different angles indicate same nitrogen distribution with differing resolution functions.

Dimensions of Polyelectrolyte Chains with Multivalent Counterions

Yubao Zhang, Brett D. Ermi, and Eric J. Amis, *Polymers Division
NIST, Gaithersburg, MD 20899*

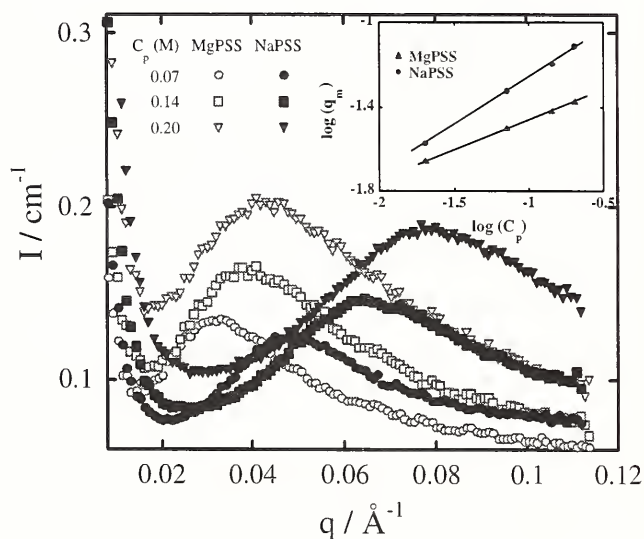
Polyelectrolytes, macromolecules carrying a large number of charges, are the predominant water-soluble synthetic and natural polymers. They have wide industrial application and critical biological function. For industry, polyelectrolytes are used as stabilizers, flocculants, or surface-active agents for water treatment, paper, paints, personal care products, and pharmaceuticals. In biological systems, the binding of proteins and nucleic acids, the functioning of enzymes, and the construction of cellular components are controlled by the tensions imposed by electrostatic interactions. It is also clear that the interaction of polyelectrolytes with multivalent counterions is a critical factor in many industrial applications and biological functions. Although recent years have witnessed an impressive confluence of experiments, simulations, and theory, long-range electrostatic interactions still disrupt most traditional methods and characterization techniques. In the work described here, the method of zero-average-contrast small angle neutron scattering (SANS) is used to overcome this barrier and probe directly the most fundamental polymer property, the chain dimension, as a function of concentration and counterion valence.

For low ionic strength polyelectrolyte solutions SANS shows a maximum at finite wavevector and a steep upturn at low angles; results that are dramatically different from those of neutral polymer solutions[1]. There is no complete theory, only qualitative descriptions for these phenomena that appear for nearly all charged macromolecules. The situation is even more complicated for typical biological systems or for commercial polyelectrolyte applications because of the presence of divalent or trivalent counterions. The specificity of interactions with multivalent ions is critical to applications such as water treatment and to biological processes such as protein folding and DNA packing. Although the multivalent counterions have dramatic effects on the structure and dynamics of polyelectrolyte solutions, experimental work with scattering is both limited and difficult to interpret. A major impediment for simulations and theoretical interpretation is the lack of an adequate description for the single chain structure and dimension. The overwhelming effect of strong intramolecular and in-

termolecular electrostatic interactions of the unscreened charges dominates the scattering, even in dilute solution.

The method of zero-average-contrast (ZAC) in small angle neutron scattering provides a means to overcome this obstacle and measure single chain dimensions in dilute and semidilute solutions[2]. The ZAC method requires matched pairs of deuterated and hydrogenated polymers and a specific H-D solvent composition, but the charge concentration and counterions can be changed over a broad range.

Figure 1. Full contrast SANS for NaPSS (filled) and



MgPSS (unfilled) in D₂O. Monomer concentrations: (●) 0.20 mol/L, (◆) 0.14 mol/L, and (■) 0.07 mol/L. Inset is log-log plot of peak position versus monomer concentration.

Poly(styrene sulfonate) (PSS) with matched degree of polymerization and degree of sulfonation were obtained as deuterated PSS and hydrogenated PSS. The sodium salt of PSS was purified by ion-exchange, dialysis, neutralization titration with NaOH or Mg(OH)₂, and lyophilization. Figure 1 shows typical polyelectrolyte scattering (performed on the NG1 8 m SANS instrument) without added salt. Although qualitatively the two sets are similar, including strong upturns at low q ,

the concentration dependence of the broad maxima is shown in the inset with $q_{\text{max}} \propto c^{0.46}$ for NaPSS and $c^{0.29}$ for MgPSS, where c is the salt concentration. Peaks for the divalent counterion polymer are also shifted to lower q .

All of these features disappear under the zero-average-contrast conditions. ZAC is achieved with an equimolar mixture of deuterated and hydrogenated polymer in a mixture of H_2O and D_2O . The fraction of D_2O in the solution is set at the value necessary to satisfy the "optical theta condition," where the scattering length densities of the hydrogenated and deuterated monomers are equal and opposite. Figure 2 displays the scattering profiles from the ZAC solutions for NaPSS and MgPSS. Each decreases monotonically with angle, as expected for the intraparticle scattering function, and each is fit adequately with a Debye function.

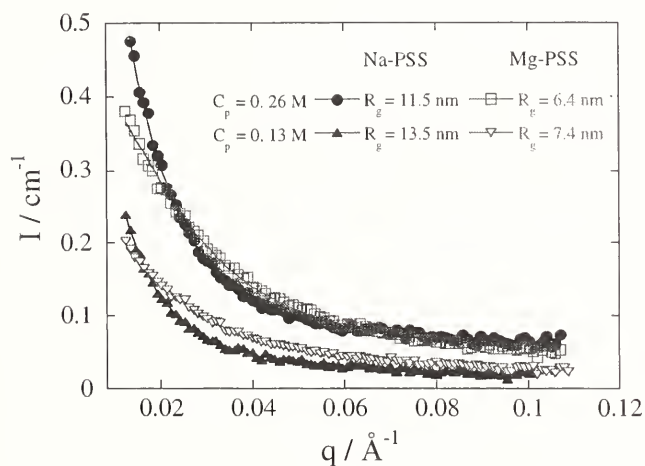


Figure 2. ZAC scattering from Na and Mg polyelectrolyte solutions under conditions of zero average contrast showing single chain scattering. Fits to Debye function.

Figure 3 shows the values of polymer chain radius of gyration as a function of concentration for NaPSS and MgPSS along with calculated estimates for the size of a single chain with degree of polymerization of 300 under random coil and rod-like configurations. For both systems, the chain dimension decreases with increasing concentration with the MgPSS chains nearly a factor of two smaller for each concentration. While the monovalent counterion chains are highly extended, they are not at the rod-like limit. At the same time, both systems are more expanded than the calcu-

lated ideal Gaussian chain value. This result implies that while the divalent counterions induce a coil contraction they do not produce a coil collapse or a coil-globule transition.

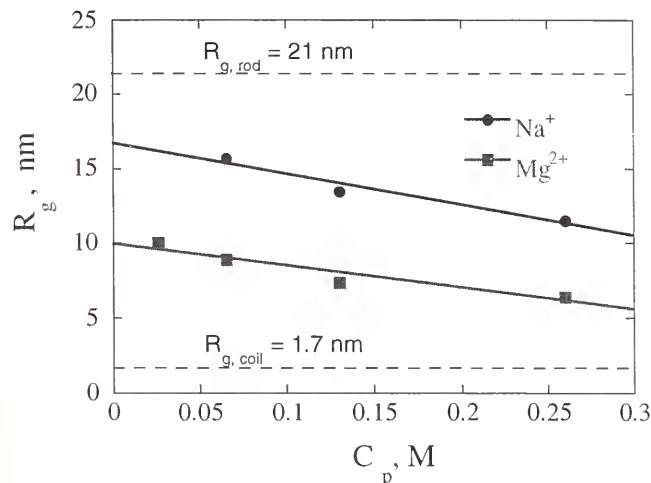


Figure 3. Polyelectrolyte chain dimensions as a function of concentration with comparison to model chain calculations.

This study demonstrates the power of the zero-average-contrast method to extract single chain information even in the presence of strong intermolecular interactions. The method, here used for dilute low ionic strength solutions, has also been applied to measure single chain dimensions in solutions at high concentration and with arbitrary amounts of added salts as needed to explore the range of real conditions important for polyelectrolytes.

References

- [1] Ermi, B. D.; Amis, E. J. *Macromolecules* **30**, 6937 (1997)
- [2] Williams, C. E.; Nierlich, M.; Cotton, J.P.; Jannick, G.; Boué, F.; Daoud, M.; Farnoux, B.; Picot, C.; de Gennes, P. G.; Rinaudo, M.; Moan, M.; Wolff, C.; Rinaudo, M. *J. Polym. Sci., Lett. Ed.* **17**, 379 (1979)

Characterization of New Biomimetic Materials Using Neutron Reflectivity

¹S. Krueger, ¹C.F. Majkrzak, ¹N.F. Berk, ¹J.A. Dura, ²C.W. Meuse and ²A.L. Plant

¹NIST Center for Neutron Research

²Biotechnology Division

NIST, Gaithersburg, MD 20899

All cells are enclosed by a biological membrane, consisting of assemblies of lipid and protein molecules, that defines its boundaries and regulates its interactions with the environment. The lipid molecules form a continuous double layer, or bilayer, which acts as a barrier to water-soluble molecules and provides the framework for the incorporation of the protein molecules. Specialized proteins embedded in lipid bilayers participate in fusion events between cells (*i.e.*, triggered by viruses), regulate ion transport through pores and channels (*i.e.*, neural activities), engage in enzymatic activity at membrane surfaces, and play a role in biological signaling (*i.e.*, receptor proteins activated by hormones). Cell membranes are sufficiently complicated that they cannot be duplicated in the laboratory for study. Thus, model biological membranes, which are simpler than cell membranes but mimic their structure and function, are used to study these complicated systems. Such model membranes are known as biomimetic materials, which emulate biological function such as molecular recognition, dynamic conformational change and spontaneous self-assembly of complex arrays of molecules.

A biomimetic material which is analogous to the lipid membranes of cells and can support active membrane proteins has been made in NIST's Biotechnology Division [1]. This hybrid bilayer membrane (HBM), which is illustrated in Fig. 1, consists of two self-assembling monolayers, one which is non-biological (alkanethiol) and a second which can be found in biological cell membranes (phospholipid). This system is formed spontaneously on a planar gold surface. Since the alkanethiol monolayer is strongly bonded to the gold surface, this HBM is more rugged than a conventional supported phospholipid bilayer, which binds only weakly to a silicon or glass surface. In addition to their obvious importance as a tool for understanding and characterizing membrane protein structure and function, the biomimetic characteristics of the HBMs make them commercially significant for a number of applications including biosensors, tissue engineering, and bioelectronics and biocatalysis. The lipid and protein composition of the HBM can be readily engineered to produce structures with novel physical and chemical properties that do not occur in nature.

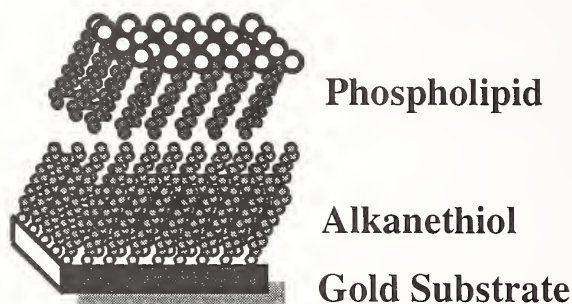


Figure 1. The alkanethiol/phospholipid hybrid bilayer membrane (HBM).

The development of measurement tools for probing the structure and function of these engineered membranes and the cell membrane components incorporated into them is essential for the optimization of their biomimetic character. To this end, the neutron reflectivity technique is being used to assist in the structural characterization of HBMs which are in contact with water. Such *in situ* measurements are only possible because neutrons interact weakly with materials, in contrast to electromagnetic probes such as light, x-rays and electrons. Thus, the planar substrate can be used as the incident medium, allowing the phospholipid side of the HBM to be in full contact with water, as it is in its native state. The neutron reflectivity measurements are being made on the NG1 reflectometer at the NCNR, shown in Fig. 2. Advancements in instrumentation, sample environment and measurement protocols now make it possible to obtain Angstrom-level information about the composition of HBMs along the axis perpendicular to the plane of the membrane.

The results from recent neutron reflectivity measurements of HBMs in water are shown in Fig. 3. The HBMs were formed on single crystal silicon substrates, which had been coated with $\sim 50\text{\AA}$ of gold on a $\sim 15\text{\AA}$ chromium adhesion layer, and were measured in contact with water. The neutron scattering length density (SLD) profile shown in Fig. 3 was obtained by fitting the reflectivity data using the model-independent fitting program, PBS (2). Since the neutron scattering length density of each element in the bilayer depends upon its chemical composition, the SLD profile is essentially a



Figure 2. Members of the experimental group at the NG1 reflectometer at the NCNR. Clockwise from bottom: S. Krueger, A. L. Plant, C. W. Meuse, N. F. Berk and C. F. Majkrzak.

map of the bilayer structure in the plane perpendicular to that of the membrane, generally defined as the Z direction. The silicon substrate is at $Z=0$ by definition. The locations of the gold layer, the alkanethiol monolayer and the phospholipid monolayer relative to the substrate can be easily distinguished in the SLD profile.

Neutron reflectivity measurements have also been made, for the first time, on HBMs in the presence of the membrane protein, melittin, a relatively small peptide toxin that is found in bee venom. Although melittin is an important model compound for pore-forming peptides such as antibiotics, its exact location in the membrane is not known. The structure of HBMs in the absence and presence of melittin now can be directly compared and questions about how deeply melittin penetrates into the bilayer, and whether melittin forms pores that allow water into the bilayer, can be addressed.

Most recently, neutron reflectivity has been used to study the structure of a novel HBM matrix consisting of an ethyleneoxide-containing alkanethiol monolayer and a phospholipid monolayer. The ethyleneoxide moiety tethered to the gold surface was intended to act as a loosely-packed "spacer", allowing water to penetrate into the region near the gold surface, thus providing a suitable environment for the in-

corporation of transmembrane proteins. However, the neutron reflectivity measurements provided direct evidence that the ethyleneoxide region contains no water. Furthermore, the reflectivity measurements confirmed that melittin does not alter the membrane structure in a way that would allow water into this region. These important results have led to the development of new HBMs which more closely mimic biological membranes and are capable of supporting transmembrane proteins.

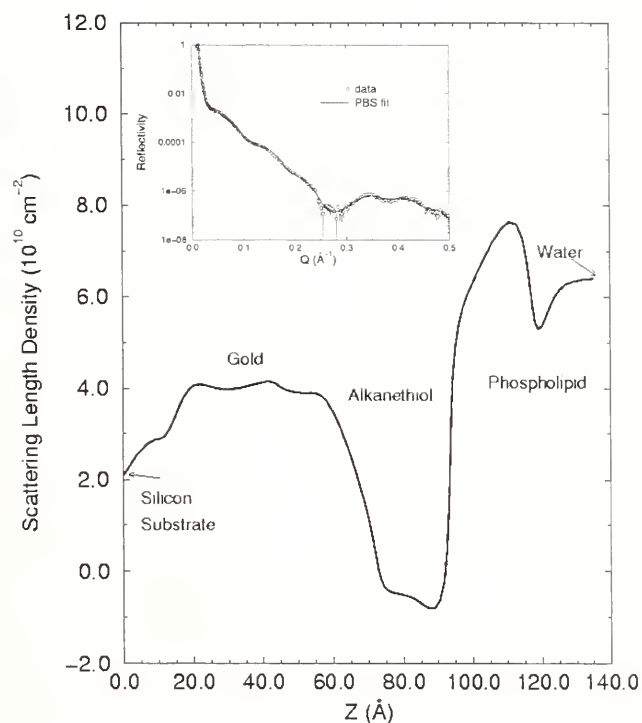


Figure 3. A representative neutron scattering length density profile for a hybrid bilayer membrane. The location of the silicon substrate is defined as $Z=0$. The corresponding neutron reflectivity data are shown in the inset.

References

- [1] Plant, A. L. *Langmuir* 9, 2764 (1993).
- [2] Berk, N. F. and Majkrzak, C.F. *Phys. Rev. B* 51, 11296 (1995).

The Dynamics of Hydrogen in Solid C₆₀

S. A. FitzGerald, T. Yildirim, L. J. Santodonato, D. A. Neumann, J. R. D. Copley, and J.J. Rush
NIST Center for Neutron Research
NIST, Gaithersburg, MD 20899

Carbon is the most studied element in the entire periodic table. For decades it was believed that pure carbon existed in two forms, diamond and graphite. Thus it was quite surprising when a third form of

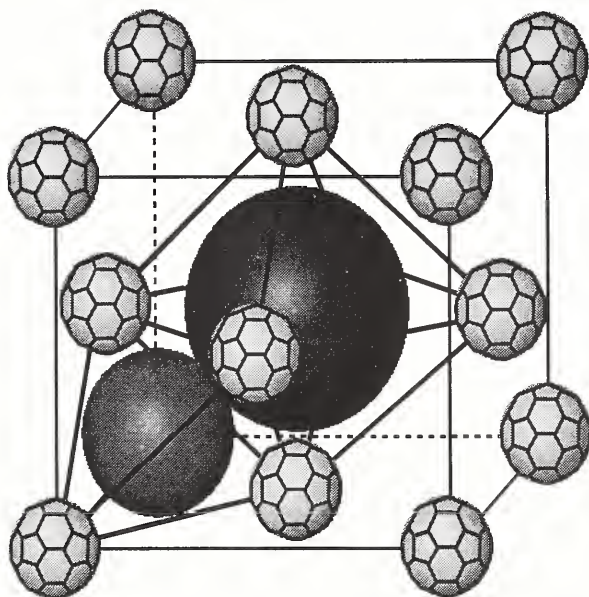


Figure 1. Schematic diagram of the interstitial spaces in a C₆₀ lattice. The gray balls indicate the positions of the C₆₀ molecules while the red ball resides in the larger octahedral site and the blue ball sits on one of the tetrahedral sites. The hydrogen molecules must go into one of these spaces between the “buckyballs”.

pure carbon, called fullerenes, was discovered in the mid 1980's. The most well-known of this new-class molecular materials is the one consisting of 60 carbon atoms which takes the shape of an atomic-scale soccer ball. These beautifully symmetric molecules are commonly called “buckyballs”.

In the solid state C₆₀ molecules form a structure with large interstitial spaces between the molecules. (Figure 1) These spaces are easily large enough to accommodate a wide variety of atomic and molecular

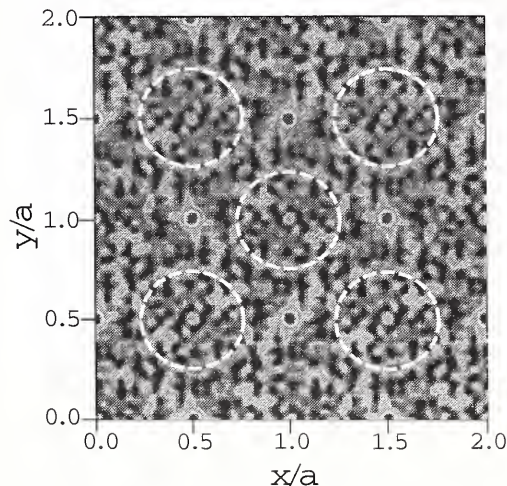


Figure 2. A Fourier difference map of the 100 crystallographic plane which shows the locations of the C₆₀ molecules using dashed white lines and the location of the deuterium molecules by the red and yellow contours at the octahedral position.

species, which can significantly influence the properties of the resulting compound. Most notable are the alkali doped C₆₀ compounds, which display superconductivity at reasonably high temperatures. However it has also been shown that various gases including hydrogen, nitrogen, carbon monoxide, and oxygen can be absorbed into the spaces between C₆₀ molecules. This suggests that solid C₆₀ might be useful as a medium for the safe storage of hydrogen or as a molecular sieve to separate these gases. In spite of this, relatively little effort has been made to understand the interactions which govern these potentially useful properties namely, the interaction of the trapped species with the C₆₀ host. Hydrogen in C₆₀ is also of fundamental interest because it is a nearly perfect example of a simple quantum object (hydrogen) trapped in a classical matrix (C₆₀). Neutron spectroscopy is a direct way of probing the bonding in materials and it is a particularly powerful tool with which to study the dynamics of hydrogen because of the large incoherent

scattering cross-section of hydrogen. Inelastic scattering spectra obtained using the Fermi Chopper Spectrometer (Figure 3) show well-defined peaks, which

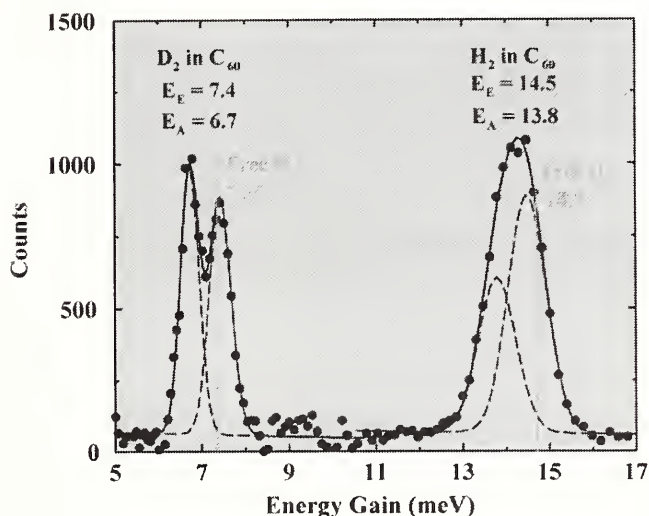


Figure 3. Neutron spectra showing the rotational transitions for hydrogen and deuterium absorbed in solid C_{60} . Note that the transition is a doublet in both cases with a splitting of 0.7 meV. The center of the doublet is slightly shifted from the value expected for the free molecules, which is indicated by the green arrow.

can be attributed to the quantized rotational levels of the hydrogen and deuterium molecules.

These peaks are only slightly shifted from the positions expected for the free rotations of these molecules. The simplicity of this behavior allows us to probe the effects of relatively weak interactions with the host lattice, which lead to the small departure from the free rotor case.

To explore this more quantitatively we have performed model calculations using a simple Born-Meyer type of potential. The rotational potentials felt by hydrogen and deuterium molecules within this model are shown in Fig. 4. The panel on the left shows the calculated potential for the case of complete orientational disorder of the C_{60} molecules while that on the right shows the potential for ordered C_{60} . The difference in energy between the red and blue regions is only ~ 1 meV, in agreement with the experimental observation that the rotations are nearly free. The diagrams below the calculated potentials show the change in the quantum energy levels as the strength of the orientational potential is varied. For the disordered case, no change is seen over this limited range of po-

tential, whereas for the ordered C_{60} case, the level at ~ 14.7 meV splits into 2 states, as is observed experimentally. Thus the degree of splitting is extremely sensitive to the symmetry and the strength of the interactions.

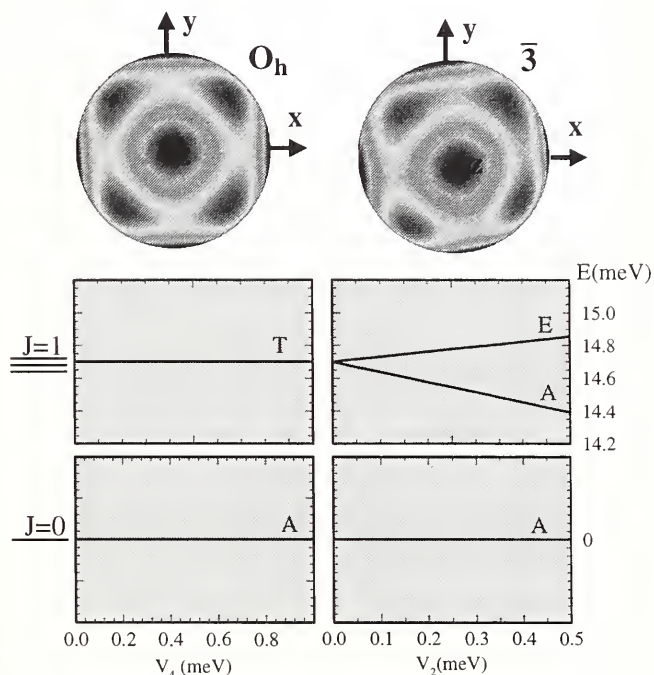


Figure 4. The top diagrams show contour plots of the orientational potential felt by a hydrogen molecule when C_{60} molecules are orientationally disordered (left) and orientationally ordered (right). The total variation in the potential (from red to blue) is about 1 meV indicating that the rotation is only weakly hindered. The bottom diagrams show the quantum rotational levels as a function of the orientational potential when C_{60} molecules are orientationally disordered (left) and orientationally ordered (right).

Neutron scattering combined with self-consistent phonon calculations demonstrates that the symmetry of the interstitial site is $\bar{3}$. Furthermore, the magnitude of the splitting (0.7 meV) is comparable to the size of the rotational barrier arising from the intermolecular interactions between the hydrogen and the C_{60} molecules. Additional studies are underway which will probe how these interactions are changed by the application of pressure and the co-intercalation of charged species into the C_{60} host.

Polarons in Colossal Magneto-resistive Materials

L. Vasiliu-Doloc¹, J. W. Lynn¹, R. Osborn², S. Rosenkranz²,
S. K. Sinha³, O. Seeck³, J. Mesot², J. F. Mitchell²

¹NIST Center for Neutron Research, NIST, Gaithersburg, Maryland 20899

²Materials Science Division, Argonne National Laboratory, Argonne, Illinois 60439

³Advanced Photon Source, Argonne National Laboratory, Argonne, Illinois 60439

The magnetic properties of the lanthanum manganese oxide class of materials have attracted tremendous interest recently because of the dramatic increase in conductivity these systems exhibit when the magnetic moments order ferromagnetically, either by lowering the temperature or by applying a magnetic field. This huge increase in the carrier mobility, which has been given the name ‘‘colossal magnetoresistance’’ (CMR), is both of scientific and technological interest. In particular, it is anticipated that these materials may provide the next generation of read/write heads for the magnetic data storage industry, while the ‘‘half-metallic’’ behavior provides fully spin polarized electrons for use in magneto-electronics applications, and for sensors in a variety of applications such as in the automotive industry.

CMR can be strongly enhanced in systems with reduced dimensionality and so there has been considerable interest in the two-layer Ruddlesden-Popper compounds, $\text{La}_{2-2x}\text{Sr}_{1+2x}\text{Mn}_2\text{O}_7$. The reduced dimensionality leads to significant extension of the temperature range over which magnetic correlations are important, and thereby allows a detailed examination of the link between local spin correlations and the resulting magnetotransport. We have therefore investigated the magnetic correlations in $\text{La}_{1.2}\text{Sr}_{1.8}\text{Mn}_2\text{O}_7$ using neutron scattering. Over a large temperature range above $T = 112$ K, we found evidence for two-dimensional magnetic correlations which peak in intensity at the transition. Although the in-plane correlations are predominantly ferromagnetic, a canting of spins in neighboring planes within the bilayers, at an angle that is dependent both on temperature and magnetic field, was observed [1,2].

One of the central questions in the field of manganites concerns the lattice involvement in the mechanism of CMR. While the relation between ferromagnetism and conductivity was explained in terms of double exchange, it is now clear that a full understanding of these materials must include the lattice degrees

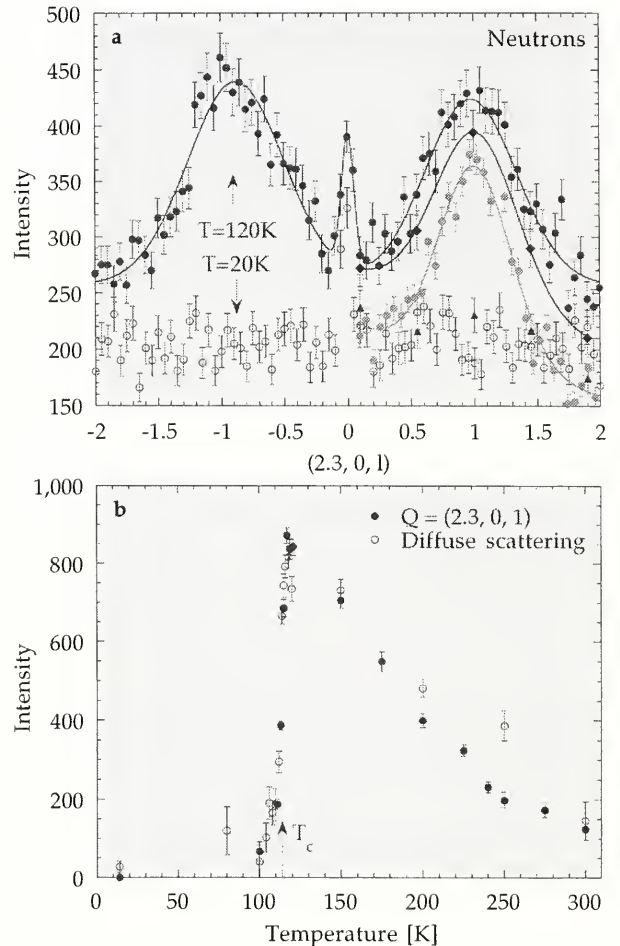


FIG. 1 (a) l -scans through the charge ordering peaks at $(2.3, 0, 1)$ at $T=120$ K: energy-integrated (red), elastic (orange), non-spin-flip scattering measured with polarized neutrons (green diamonds), spin-flip scattering (green triangles). The orange and green data points have been scaled by appropriate factors. The l -scan at $T=20$ K (open purple circles) shows that the charge peaks have vanished. (b) Temperature-dependence of the intensity of the superlattice peak $(2.3, 0, 1)$ (red), and of the diffuse scattering after correction for the phonon scattering (blue), showing that the charge order and lattice polarons collapse at the Curie temperature.

of freedom. In particular, the formation of lattice polarons above the Curie temperature has been inferred from a variety of measurements, but direct evidence has been lacking.

Neutron measurements carried out at NIST, and X-ray measurements at the Advanced Photon Source, have revealed charge localization in the paramagnetic-insulating phase of the layered $\text{La}_{1.2}\text{Sr}_{1.8}\text{Mn}_2\text{O}_7$ CMR material, with the associated diffuse polaron scattering that originates from the lattice distortions around the localized charges. Figure 1(a) shows two of the observed incommensurate superlattice peaks associated with the charge ordering, characterized by the wave vector $(0.3, 0, 1)$. Polarized neutron scattering has shown that the incommensurate superlattice peaks are pure structural reflections, originating most likely from Mn^{3+} - Mn^{4+} charge correlations. These correlations are quasi-static on a time scale ps set by the energy resolution of the instrument. The superlattice peaks are broader than the q resolution in both h and l directions, showing that both the in-plane and out-of-plane charge correlations remain short range at all temperatures. The charge order melts as the insulator-to-metal transition is traversed and long-range ferromagnetic order is established [3], as shown in Fig. 1 (b). By similarity with the 3D perovskite manganites and with the cuprates, this scattering may originate from a charge-ordered stripe phase above T_C , which is destroyed when the double exchange mechanism drives the system metallic. The lattice strain induced by the localized charges gives rise to a four-lobed pattern of diffuse scattering around the Bragg peaks. The upper panel in Fig. 2 shows a contour plot of the diffuse X-ray scattering in the $[h, 0, l]$ plane around the $(2, 0, 0)$ reflection. Only the $l > 0$ half is shown, but the pattern is symmetric with respect to $l = 0$, as proved by the neutron l -scans in the lower panel of Fig. 2. The sharp rod of scattering along the $[0, 0, l]$ direction is resolution limited in the $[h, k, 0]$ plane and is associated with stacking faults. Part of the lobe-shaped diffuse scattering is due to conventional acoustic phonons, while the temperature dependence of the additional, polaron scattering (blue open circles in Fig. 1(b)), arises from static or quasi-static atomic displacements as revealed by elastic neutron scattering (see Fig. 2 (bottom)). The lattice strain caused by the polarons relaxes when the short-range charge order melts at the Curie temperature, providing compelling evidence of the role of polarons in the origin of CMR. Further work is now in progress to determine if the charge melting can be controlled by the application of magnetic or electric fields, which would open up completely new

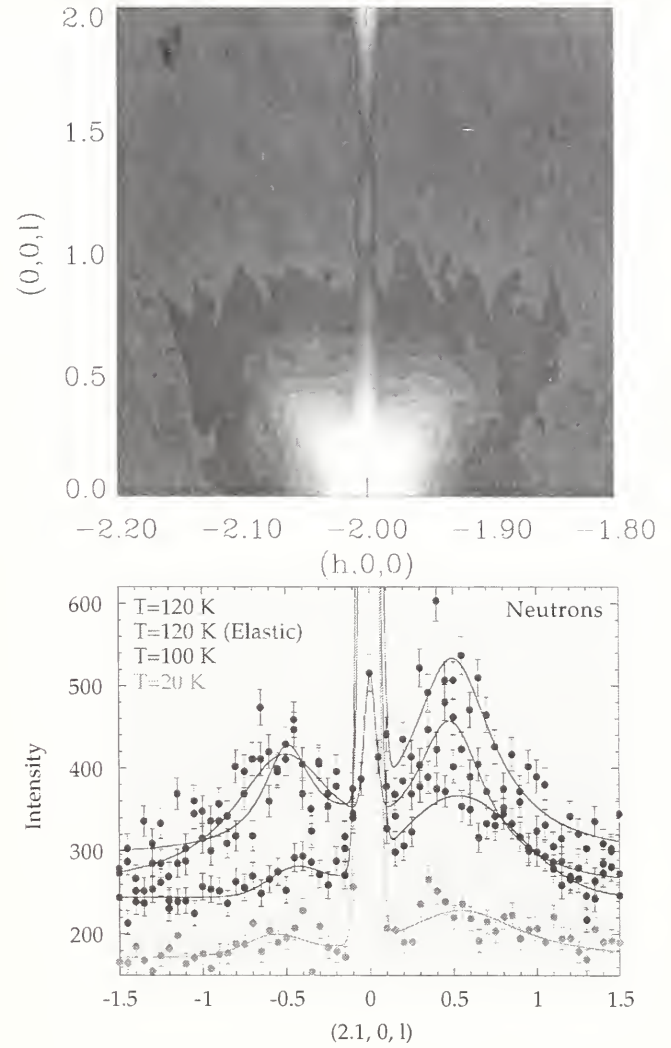


FIG. 2 (Top) Contour plot showing the lobe-shaped pattern of diffuse scattering around $(2, 0, 0)$. (Bottom) Neutron energy-integrated l -scans across the diffuse scattering in the upper panel, for $T=120, 100,$ and 20 K. The scan at $T=120$ K (red circles) is an elastic scan, and has been scaled by an appropriate factor.

avenues for applications.

References

- [1] R. Osborn, S. Rosenkranz, D. N. Argyriou, L. Vasiliu-Doloc, J. W. Lynn, S. K. Sinha, J. F. Mitchell, K. E. Gray, S. D. Bader, Phys. Rev. Lett. **81**, 3964 (1998).
- [2] S. Rosenkranz, R. Osborn, J. F. Mitchell, L. Vasiliu-Doloc, J. W. Lynn, S. K. Sinha, D. N. Argyriou, J. Appl. Phys. **83**, 7348 (1998).
- [3] L. Vasiliu-Doloc, S. Rosenkranz, R. Osborn, S. K. Sinha, J. W. Lynn, J. Mesot, O. Seeck, J. F. Mitchell, submitted to Nature.

Neutron Interferometry and Optics Facility (NIOF)

M. Arif, D. Jacobson, A. Ioffe, P. Huffman, T. Gentile, and A. Thompson

*Ionizing Radiation Division
NIST, Gaithersburg, MD 20899*

A neutron interferometer (NI) is analogous to a classical Mach-Zehnder type optical interferometer and it is the only device that allows direct measurement of the phase of a neutron wave. The first neutron interferometer was operated over two decades ago in Vienna, Austria. In the USA, a very successful group has been operating at the University of Missouri-Columbia for the last two decades. Gravitationally induced quantum interference of neutron waves, 4π spinor rotation of neutrons in a magnetic field, and observation of the Aharonov-Casher effect (neutron analog of the Aharonov-Bohm effect for electrons) are among the seminal experiments that were carried out during this period. By measuring the phase shift of the neutrons that pass through a sample it is possible to accurately determine the neutron refractive index, n , of the material. The NI method of determination of n is, for the most part, independent of the microscopic details of the sample and perhaps the most accurate method that is available today. The refractive index, n , of many solids (e.g. uranium, chromium, vanadium) and gases (hydrogen, helium etc.) that are important to condensed

matter and solid state physics have been measured and are being measured today.

The NIST Neutron Interferometry and Optics Facility (NIOF) is one of the premier facilities for neutron optics research. Located in the NCNR guide hall, it uses single crystal neutron interferometers (perhaps the best in the world today) with exceptional phase stability and fringe visibility that are crucial for the success of experiments in both fundamental and applied research. This exceptional performance is in part attributed to the state-of-the-art thermal, acoustical and vibration isolation system that has been successfully designed and built during the past few years.

During the past year the NIST NIOF has provided unique research opportunities for both applied and fundamental research and a diverse selection of experiments have been successfully carried out. Two Ph.D. dissertation research were carried during this period and six articles have been written for publications. Research collaborations have been established with the University of Missouri-Columbia, the Hahn-Meitner-Institute and the University of Innsbruck and EXXON.

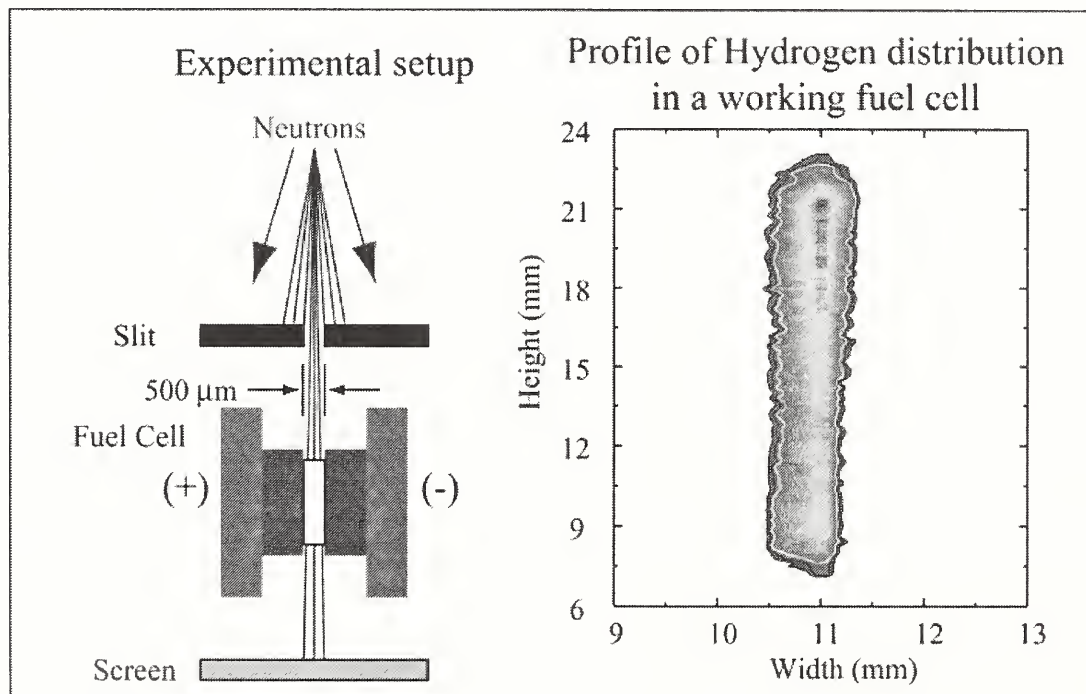


Figure 1. Neutron image of the water gradient inside a fuel cell.

Special effort has been made to apply neutron-imaging techniques for industrial research. The NIOF is equipped with a high resolution CCD type 2-D position sensitive neutron detector to perform high-resolution neutron radiography of samples using a mono- or a poly-energetic energetic neutron beam. Early performance tests of a neutron tomography station have been successfully carried out. In addition to radiography, many other types of diffraction imaging experiments may be performed at the NIOF. Researchers from EXXON have exploited the convenience of this facility for both hydrogen fuel cell research and for studying hydrocarbons. For the first time the water gradient inside a working fuel cell has been successfully imaged (fig.1). Results from these experiments have allowed verification of theoretical predictions of water transport mechanism in a working fuel cell [1]. Researchers from the University of Innsbruck, Austria, have also used this facility to study the diffraction of neutrons ($\lambda=0.235$ nm) from macroscopic objects ~ 0.1 mm in size. Finally, a semi-finalist in the 57th Westinghouse Science Talent Search has demonstrated the Neutron Phase Contrast Imaging technique.

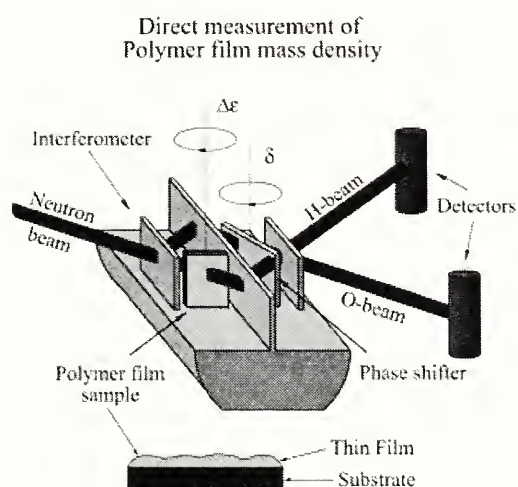


Figure 2. Schematic of the polymer thin film measurement setup.

The first successful neutron interferometric measurements of scattering length density in polymer thin films ($1 < \mu\text{m}$) have been carried out in collaboration with the NIST Polymers Division (fig. 2). This technique is independent of calibration standards and complex mathematical modeling of the physical process of interaction. This measurement has opened the possibility of using NI as an important tool for establishing well defined densities of thin films that is critical in many analysis techniques in surface physics research

[2].

An important experiment has been carried out to verify the recent predictions of quantum entanglement of the nuclear states in a mixture of fluids. The existence of such entanglement would suggest that the refractive index, ' n ', of a mixture cannot be calculated only from the knowledge of fractional abundance and n of the constituent elements. If this were true, the implications would be profound for many neutron scattering techniques. A NIOF experiment measured scattering length density, Nb , for various mixtures of H_2O and D_2O . It had been proposed that for these mixtures a 5-10% deviation from the traditional theory might occur because of quantum entanglement of H and D at room temperature. However, the experimental data agreed with the traditional theory within the statistical fluctuation of the data, which was of order 0.4% and within this limit no deviation from standard theory has been observed [3].

The capability of the facility has been augmented by the addition of a transmission neutron polarizer and RF gradient flipper. Neutron polarization in excess of 98% has been obtained with thermal neutrons. This new capability was exploited in an experiment which observed the 4π spin rotation symmetry of the neutron wave function. This experiment was unique in that the neutron guide field was gently rotated by 180° allowing the neutron spin direction to adiabatically follow the field. This experiment provides the first *direct* observation of 4π spin rotation symmetry of neutrons under space rotation.

New experiments such as the measurement of the internal charge structure of a neutron, measurement of mass densities of thin films as a function of thickness and scattering length of samples (such as D_2 gas) that important for many body calculations are being planned. Future plans also include constructing large separated-section interferometers. Such interferometers are crucial for phase transition studies in samples and fundamental physics experiments with at least an order of magnitude more sensitivity than what is possible today.

References

1. R. J. bellows, M. Y. Lin, M. Arif, A. K. Thompson and D. Jacobson (Submitted to Journal of the Electrochemical Society).
2. W. E. Wallace, D. L. Jacobson, M. Arif and A. Ioffe. (Submitted to Applied Physics Letters).
3. A. Ioffe, M. Arif, D. L. Jacobson and F. Mezei (Submitted to Physical Review Letters August 1998)

Protein Conformations and Interactions in Biochemical Regulation

Jill Trehwella¹, Joanna K. Krueger¹, Glenn A. Olah¹, Jinkui Zhao¹, James T. Stull², and Donal A. Walsh³

¹*Los Alamos National Laboratory, Los Alamos, NM 87545*

²*UT Southwestern Medical Center*

³*University of California at Davis, Davis, CA*

Small-angle neutron scattering, with contrast variation, has provided key insights into the regulation of protein activities. Life functions at the molecular level via a large number of highly regulated molecular networks through which messages are communicated so that cells can maintain vital ongoing functions and also can respond as needed to external stimuli. Proteins are the work-horses of life carrying out all the functions required for survival, growth and reproduction. They are responsible for motility, transport, signal transduction, catalysis, protein synthesis and degradation, energy capture, transport and conversion, damage recognition and repair, replication and transcription, etc. These activities all must be strictly coordinated, and there are a variety of mechanisms for regulating protein function that are key to healthy function. One of the most common regulatory mechanisms of protein activity is the addition, or removal, of phosphate groups from hydroxyl groups on proteins. Protein phosphorylation reactions are catalyzed by a family of enzymes called the protein kinases of which several hundred have been identified to date. Protein kinase activities themselves are frequently regulated by “second messengers” that are released into the cellular cytoplasm in response to a “first messenger” signal, such as a hormone binding to a cell surface receptor. Two commonly used second messengers are divalent calcium ions and cyclic nucleotides. These messengers modulate kinase activities generally by binding to intermediary regulatory proteins that then either bind to or modulate their interaction with the kinase such that the kinase activity is switched on or off.

Small-angle scattering from proteins in solution gives information on their overall shapes and is particularly sensitive to domain movements as well as protein-protein associations. In the case of neutron scattering, the differences in the scattering properties of hydrogen and deuterium allow one to use specific deuterium labeling with contrast variation to extract structural data on individual components within complexes. We have used neutron scattering with contrast variation to characterize the conformational transitions and associations in the activation mechanism of two

model kinases; the Ca²⁺/calmodulin-dependent kinase myosin light chain kinase (MLCK), and the cyclic nucleotide (cAMP)-dependent protein kinase.

In our neutron scattering studies of the Ca²⁺/calmodulin/MLCK activation mechanism we have determined the conformational transitions undergone by both the kinase and calmodulin upon complex formation [2], and the effects of substrate binding on the complex [3]. These experiments were performed using samples prepared with the MLCK enzyme complexed with deuterated calmodulin. Data were measured for the complex in solvents having a range of D₂O levels. The basic scattering functions for calmodulin and MLCK within the complex, as well as the cross term, were extracted from these neutron data. Uniform two-ellipsoid models were used to aid in the interpretation of the scattering data. Figure 1 shows the conformations of calmodulin and MLCK in the complex with and without substrate as determined by the neutron scattering experiment. By fitting the high resolution crystal or NMR structures available on the components of these complexes into our ellipsoid models we have been able to gain new insights into the molecular basis for the kinase regulation. Figure 2 summarizes the information derived from the solution scattering studies concerning the activation mechanism.

Our more recent solution scattering studies of the cAMP-dependent protein kinase [4] have revealed the quaternary structure of this kinase which has two identical catalytic and two identical regulatory subunits that bind the cAMP second messenger. This binding results in the dissociation and activation of the catalytic subunits. Again by fitting the high resolution structures into the molecular envelopes defined by the neutron data, we have been able to compare and contrast the different regulatory mechanisms for the highly conserved catalytic core of the two kinases we have studied thus far.

Our neutron contrast variation studies provide critical information about the dynamic conformational transitions underlying the regulatory mechanisms we are studying. The ability to study the global shapes of the component structures within complexes in which

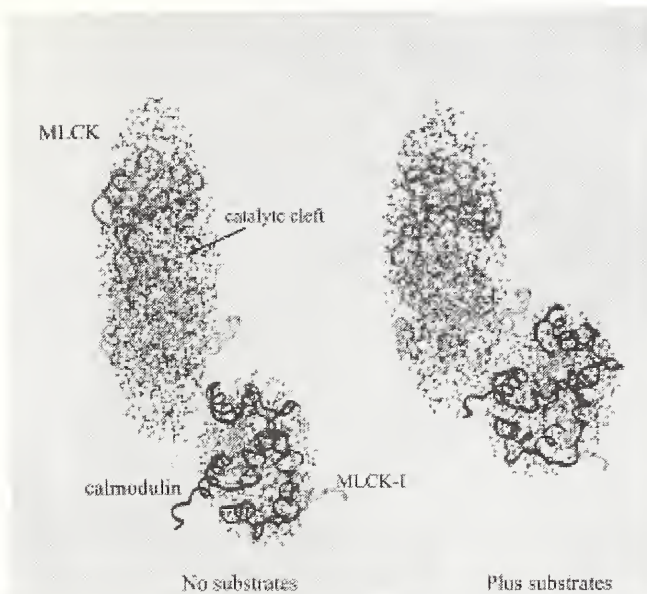


Figure 1. Ellipsoid models derived from the neutron scattering data for 4Ca^{2+} •calmodulin•MLCK complexes with (right) and without (left) substrates. Superimposed within the ellipsoids are the known structures for the upper (orange ribbon) and lower (yellow ribbon) lobes of the MLCK catalytic core. Within the smaller ellipsoid Calmodulin is represented as a red ribbon, with the MLCK calmodulin-binding domain (MLCK-I) in yellow. Upon substrate binding there is movement of the calmodulin closer to the catalytic cleft. At the same time the catalytic cleft of MLCK closes, presumably about its substrate.

there is inherent flexibility provides a critical framework into which higher resolution structural data on the individual components can be fit. These types of problems cannot be studied by high resolution crystallography when flexibility inhibits crystallization. Neither can they be studied by NMR when the structures are larger than ~ 40 kDa. Thus neutron small-angle scattering and contrast variation fills an important niche that helps to assemble the molecular jigsaw puzzles that we need to solve in order to understand the way in which molecular networks operate. This understanding is key to medical and biotechnology applications that utilize biomolecules and their unique properties.

References

- [1] Krueger, J. K., Olah, G. A., Rokop, S. E., Zhi, G., Stull, J. T., & Trewella, J. "The Structure of 4Ca^{2+} •Calmodulin and a Functional Myosin Light Chain Kinase in the Activated Complex," *Biochemistry* **36**, 6017-6023, 1997.
- [2] Krueger, J., Zhi, G., Stull, J. T., & Trewella, J. "Neutron Scattering Studies Reveal Further Details of the Ca^{2+} /Calmodulin-Dependent Activation Mechanism of Myosin Light Chain Kinase," in

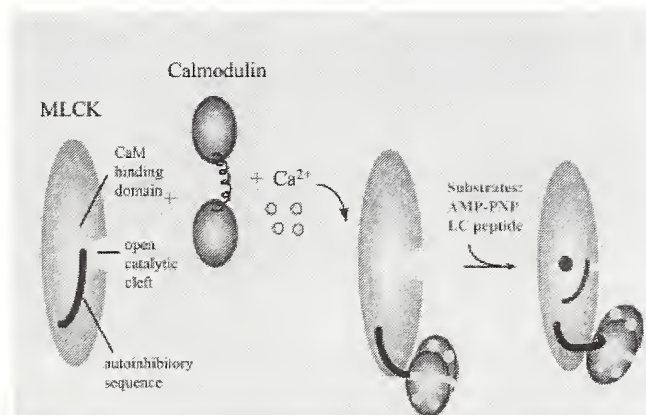


Figure 2. Schematic summarizing the sequential conformational transitions for calmodulin activation of MLCK. In its inactive conformation, MLCK maintains an open catalytic. Upon binding 4Ca^{2+} , calmodulin undergoes a conformational collapse as it interacts with hydrophobic residues at each end of the calmodulin-binding sequence that forms a helix. Substrate binding induces closure of the kinase catalytic cleft. Thus the fully activated complex is formed.

press, 1998

- [3] Zhao, J., Hoyer, E., Boylen, S., Walsh, D. A., & Trewella, J. "Quaternary Structure of the cAMP-Dependent Protein Kinase by Neutron Contrast Variation," in press, 1998.

Microstructure Transformation During Microemulsion and Micellar Polymerizations

Carlos C. Co¹, Eric W. Kaler¹ and Steven R. Kline²

¹*Center for Molecular and Engineering Thermodynamics
Dept. of Chemical Engineering, University of Delaware*

²*NIST Center for Neutron Research
NIST, Gaithersburg, MD 20899*

Emulsion polymerization is the most widely used process to prepare polymer colloids (latexes) of sizes 100 to 10,000 nm, finding use in applications such as paints and adhesives. Microemulsion systems contain larger amounts of surfactant relative to the monomer and produce much smaller polymer particles of 20 to 50 nm diameter. The surfactant molecules themselves can be functionalized and polymerized producing even smaller structures of 3 to 5 nm, still retaining a well-defined shape. The reduced size and increased surface area of these structures allows for a variety of new applications beyond conventional emulsion latexes, such as adsorbents and receptor binders for biomedical compounds [1].

In all of these reaction systems there is a definite need to understand the details of the underlying mechanisms in order to control the final product. A number of models for free-radical polymerization kinetics have been proposed, and all depend on the location of monomer relative to the growing polymer chain. This partitioning of monomer determines the overall rate of reaction as well as the dominant free-radical

termination events. The widely different initial microstructure of emulsion, microemulsion, and micellar systems leads to important differences in the localization of monomer and polymer. Typical experiments attempt to correlate the overall rate of reaction with the initial and final properties of the microemulsion and latex respectively, with little information about the specifics of the compartmentalized monomer and polymer. In order to elucidate the mechanistic details, polymerization reactions can be performed on-line, using Small-Angle Neutron Scattering (SANS) to provide microstructural information as a function of conversion (or time). SANS is well suited to investigate polymerization reactions, non-invasively probing appropriate length scales in as short as one-minute intervals.

A microemulsion polymerization of hexyl methacrylate was performed on-line using SANS while simultaneously measuring the conversion [2]. Representative SANS spectra at increasing conversion are shown in Figure 2. As the reaction proceeds, the diminishing peak in the spectra shows the smooth decrease in the size of the monomer-swollen microemulsion droplets. Simultaneously, the increase in the low- q scattering indicates a steady growth of latex particles.

Quantitative modeling shows that the average diameter of the latex particles remains nearly constant, simply increasing in number with time. These results support a model of polymerization in which the propagation reaction occurs in a monomer-rich shell surrounding a growing polymer particle that is not swollen with monomer. It also provides insight into the behavior of monomers with different partition coefficients.

Micelle polymerization should behave even less like an emulsion polymerization than a microemulsion. There is now no monomer to partition, since the surfactant is the monomer and is constrained to a specific location in the aggregate. If there is no transfer of monomer between aggregates during the polymerization, the process can be thought of as a "zippering" of the individual micelles.

Unlike most microemulsions, micellar aggre-

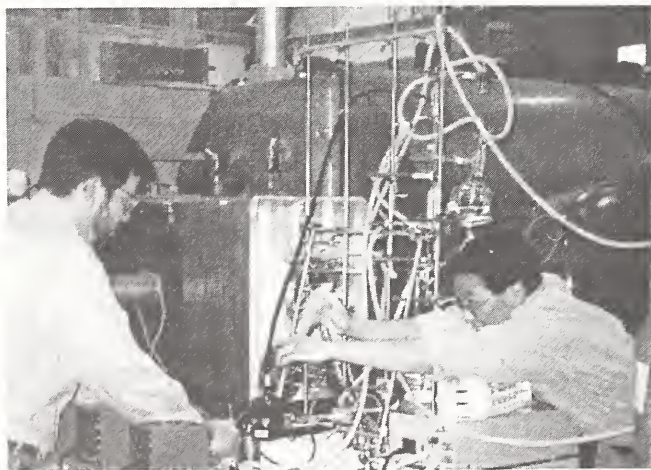


Figure 1. Prof. Kaler (L) and graduate student Carlos Co (R) withdraw a polymerization sample for SANS measurement.

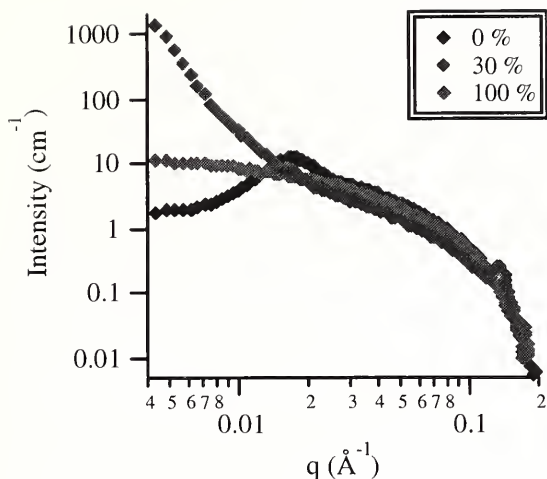


Figure 2. SANS spectra of the polymerizing hexyl methacrylate microemulsion as a function of monomer conversion.

gates are not limited to globular structures. In particular, cylindrical surfactant structures can be polymerized. The surfactant cetyltrimethylammonium 4-vinylbenzoate forms viscoelastic solutions in water containing cylindrical micelles of 4 nm diameter and thousands of nanometers long. The SANS curves in Figure 3 show the evolution of structures from the initial charged micelles to the final polymerized cylinders. At intermediate (20 - 70%) conversion the reacting system passes through a highly turbid and ordered phase, with a sharp peak indicating a well-defined spacing of 5 nm. The ordered phase abruptly disappears, resulting in a stable dispersion of discrete, polymerized cyl-

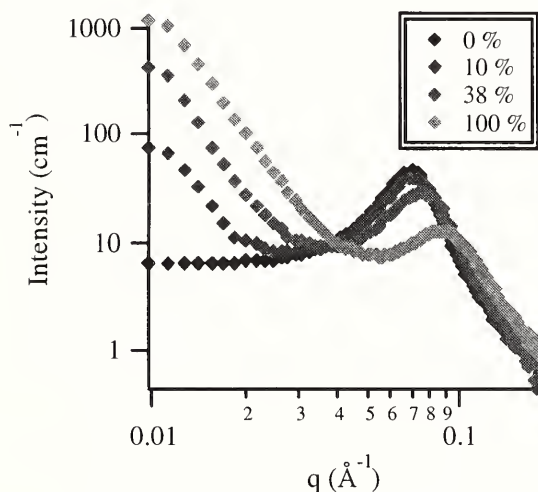


Figure 3: SANS spectra of polymerizing cetyltrimethylammonium 4-vinylbenzoate micelles as a function of time (increasing conversion).

inders 4 nm x 80 nm [3]. This novel ordering behavior is not fully understood, but is in sharp contrast to the smooth structural changes seen in microemulsion polymerization. On-line polymerization SANS measurements provide a visualization of the evolving microstructure that cannot be provided by other methods, permitting validation of polymerization mechanisms.

References

- [1] *Polymerization in Organized Media*; C. M. Paleos, Ed.; Gordon and Breach: Philadelphia, PA, 1992.
- [2] Co, C. C.; Kaler, E. W. *Macromolecules*, **1998**, *31*, 3203.
- [3] Kline, S. R. private communication.

Arborescent Graft Polymers

S. Choi¹, R. M. Briber¹, B. J. Bauer², A. Topp², M. Gauthier³ and L. Tichagwa³

¹University of Maryland, College Park, MD

²Polymers Division, NIST, Gaithersburg, MD 20899

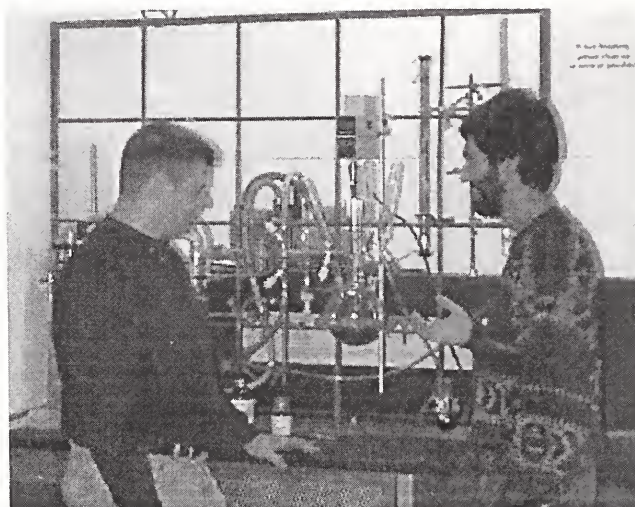
³University of Waterloo, Waterloo, Ontario, Canada

Arborescent graft polymers (AGP) are a new class of polymer molecules with potential for use as drug delivery systems, monomolecular micelles for catalyst dispersions, waste water treatment and flow modifiers. AGP's are highly branched (i.e. treelike or arborescent) macromolecules synthesized by successive generations of functionalization and grafting reactions [1]. These molecules fall into a class of controlled architecture polymers that have generated considerable research interest in recent years and include dendrimers, arborescent, and hyperbranched polymers [2]. The applications envisaged for these types of polymers are based on exploiting the highly branched architecture of the polymers and require an understanding of the size and shape of the molecules in solutions and mixtures with other polymers. Small-angle neutron scattering (SANS) has been used to provide the foundation for understanding the shape-property relationships in these systems.

The chain architecture of AGP's is shown schematically in figure 1. The synthesis goal is to provide methods for producing polymers with controllable size, shape and functionality for use in such applications as coatings, membranes, drug release systems and flow modifiers. By synthesizing molecules with an outside shell of a hydrophilic polymer and an inner core of a hydrophobic polymer these molecules can act as water dispersible monomolecular micelles which can absorb organic molecules from waste water or help to disperse water insoluble catalyst systems. In order to design APG's for specific applications it is necessary to have detailed information on the intermolecular density profile, molecular size and shape in solutions and in mixtures with other polymers. We have been using small angle neutron scattering (SANS) to measure the size and shape of APG's under a range of different conditions.

SANS curves for a series of polystyrene AGP's as a function of generation in deuterated cyclohexane at 30°C is shown in figure 2. The radii of gyration (R_g) of the polymers were measured and are plotted as a function of generation in figure 3.

For generations 0 and 1 the size of the molecules is essentially equivalent under all measured con-



Andy Kee (left) and Mario Gauthier (right) discussing the synthesis of arborescent polymers.

ditions while for generations 2 and 3 the molecules vary in size significantly (particularly for generation 3) depending on the solvent or matrix polymer. The generation 3 molecules show the largest expansion in (deuterated) toluene which has the highest solvent power of the various systems studied. The most compact structure for the generation 3 molecule occurs in linear (deuterated) polystyrene. For comparison the R_g of a

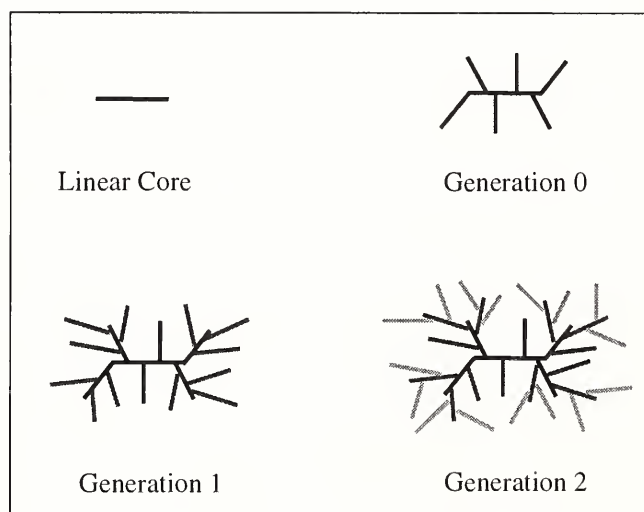


Figure 1. Schematic representation of arborescent graft polymer chain architecture.

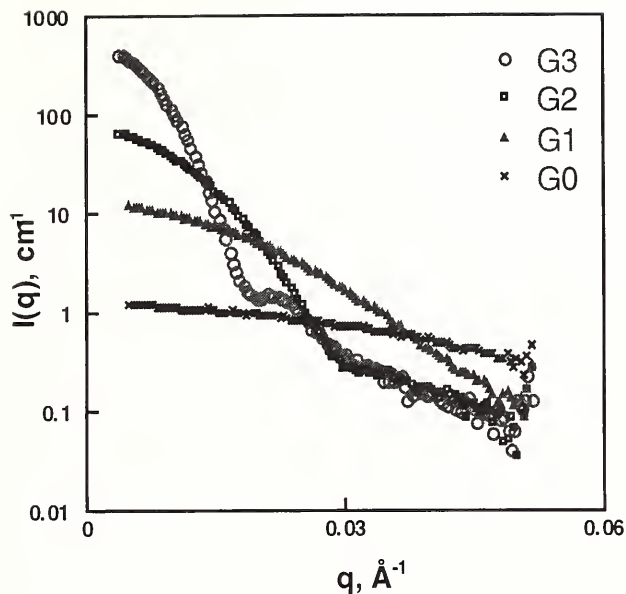


Figure 2. SANS data for all generations of polystyrene

sphere was calculated assuming the generation 3 molecule was collapsed to bulk density. The R_g obtained was 170 Å which is close to the R_g of the generation 3 polymer in linear (deuterated) polystyrene. This indicates that the generation 3 molecules should be essentially non-interpenetrating and the linear polystyrene matrix chains are largely excluded from the arborescent graft molecules. This data is important for esti-

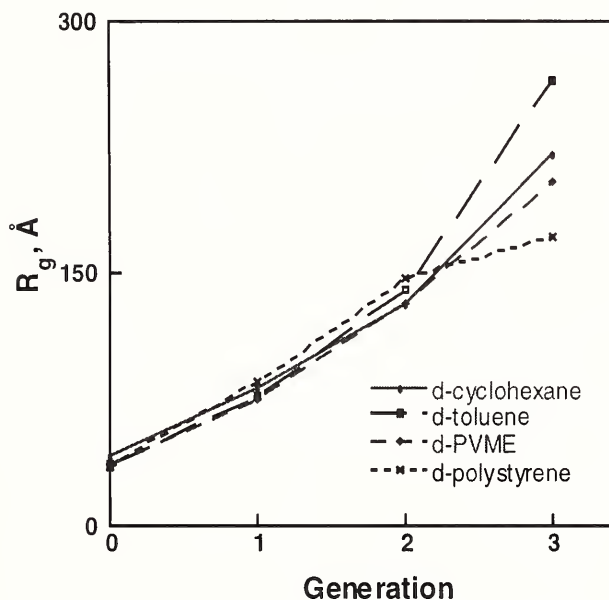


Figure 3. Radius of gyration of polystyrene AGP's in solutions and blends for all generations.

imating the solvating power of these systems for use as monomolecular micelles and for understanding the role of entanglements in determining their flow properties.

The SANS data for generation 3 arborescent graft polymers in deuterated cyclohexane showed a clear Guinier region and a second interference peak at

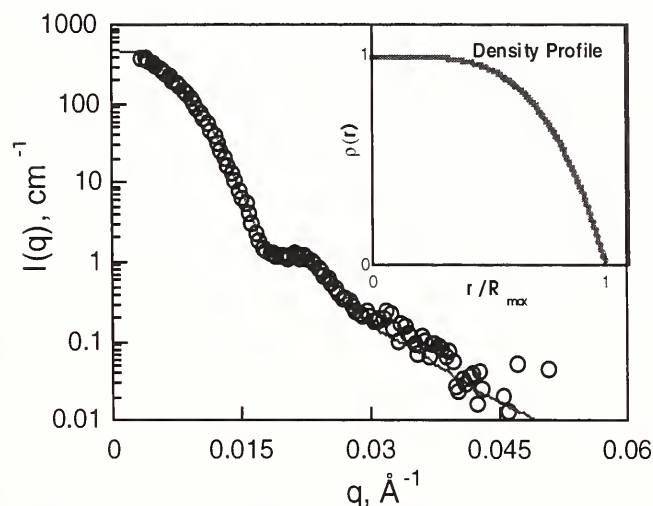


Figure 4. Scattering function calculated (solid line) compared with SANS data.

higher q which can be attributed to the single particle form factor (figure 4). A power law function was used to estimate the intermolecular density profile and calculate the scattering for comparison with experiment (see $\rho(r)$ inset in figure 4).

Our neutron scattering work indicates that for the largest molecules studied (generation 3) the shape of the molecules is quite compact, and in mixtures with linear polymer chains there is relatively little interpenetration of the arborescent molecules by the linear chains. These results will help guide chemists in synthesizing new types and variations of arborescent graft polymers to exploit the unique possibilities of shape-tailored molecules for a range of applications.

References

- [1] M. Gauthier, L. Tichagwa, J. S. Downey, and S. Gao, *Macromolecules*, **29**, 519 (1996).
- [2] D. A. Tomalia, A. M. Naylor, W. A. Goddard, *Angew. Chem. Int. Ed. Engl.*, **29**, 138 (1990).

The Vibrational Isocoordinate Rule in Se-As-Ge Glasses

¹R. L. Cappelletti, ¹Birgit Effey and ²W. A. Kamitakahara

¹Condensed Matter and Surface Sciences Program

Department of Physics and Astronomy, Ohio University, Athens, OH 45701

²NIST Center for Neutron Research

NIST, Gaithersburg, MD 20899

Inorganic glasses are among the most widely used classes of materials, yet they remain poorly understood at the atomic level, because the lack of long-range atomic order makes it difficult to obtain detailed information. Drawing unifying concepts from data on many materials, and identifying exceptional cases that can have potential value to technology, are the goals of a neutron scattering program at the NCNR.

Chalcogens (S, Se or Te) combined with Column IVB or VB elements form a large variety of covalent systems which readily form glasses when quenched from the melt [1]. They offer a wide range of optical and electronic applications. For example, transmission bands in the infrared region of the spectrum permit applications such as fibers for IR laser surgery, cutting and welding, night-vision devices, etc. which are based on selecting materials to optimize transmission in a particularly useful IR band. Chalcogenide glasses are also used in extremely fast switching devices, in X-ray imaging, and in imagers for video cameras. In terms of basic physics, these materials present a fertile testing ground for studying the effect of network topology on glass properties.

In the Se-As-Ge system, Se atoms are almost always covalently bonded to two other atoms, while As and Ge are respectively almost always 3- and 4-coordinated. An isocoordinate rule is one that identifies a property of a multicomponent covalent network glass system that stays constant for all compositions which have the same average coordination number, $\langle r \rangle$. There are several of these evident in ternary Se-based glass alloys. Examples are the glass transition temperature, softening temperature, elastic constants, measures of hardness, and Se-H spectral hole-burning relaxation. Most of these rules cover behavior that is nearly static and on a macroscopic length scale. Our neutron scattering experiments extend the range of times involved in these rules by many orders of magnitude. We have identified a simple feature in the *dynamics* of chalcogenide glasses, the vibrational isocoordinate rule (VIR), which states that *up to some frequency the vibrational density of states (VDOS) is the same for alloys*

having the same $\langle r \rangle$ [2]. This observation extends the time scale for the operation of such rules to the picosecond regime and the length scale to a few bondlengths.

Fig. 1 shows the Generalized Vibrational Density of States (GVDOS) measured by neutron TOF inelastic scattering for several Se-As-Ge glasses. Some data sets were measured at NIST-CNR using the Fermi Chopper Spectrometer (FCS) and some at the IN4 TOF spectrometer at ILL. There are two or three curves for each value of $\langle r \rangle$ which correspond to the compo-

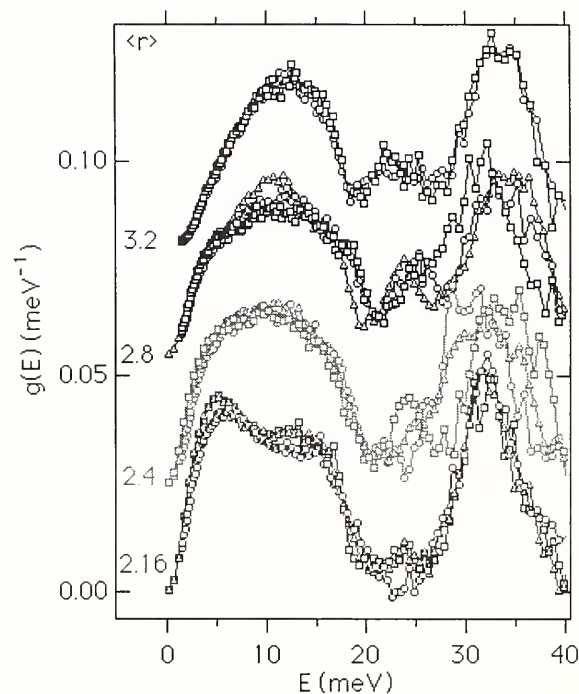


Figure 1. The VIR is best shown by plotting GVDOS of isocoordinated alloys on top of each other. $\langle r \rangle = 2.16$: ? $\text{Se}_{92}\text{Ge}_{08}$ (IN4), $^a\text{Se}_{89}\text{As}_{06}\text{Ge}_{05}$ (IN4), $^o\text{Se}_{84}\text{As}_{16}$ (FCS); $\langle r \rangle = 2.4$ including the binary alloys terminating the isocoordinate line are shown: $^a\text{Se}_8\text{Ge}_2$ (IN4), ? $\text{Se}_{675}\text{As}_{250}\text{Ge}_{075}$ (IN4), $^o\text{Se}_3\text{As}_2$ (FCS). $\langle r \rangle = 2.8$: $^a\text{Se}_{51}\text{As}_{18}\text{Ge}_{31}$ (IN4), $^o\text{Se}_4\text{As}_4\text{Ge}_2$ (FCS), ? $\text{Se}_3\text{As}_6\text{Ge}_1$ (FCS); $\langle r \rangle = 3.2$: $^o\text{Se}_{25}\text{As}_{30}\text{Ge}_{45}$ (FCS), ? $\text{Se}_{175}\text{As}_{450}\text{Ge}_{375}$ (FCS). Starting from the bottom, successive data curves are shifted up by 0.025 units on the vertical scale.

sitions indicated in the figure caption. The data at $\langle r \rangle = 2.4$ are particularly remarkable in that they include As_2Se_3 having a nearly 2-D network and Ge_2Se_8 which has a network closer to 3-D in character. The energy bands below 20 meV are nearly identical. Near 25 meV the VIR breaks down since the tetrahedral breathing mode appears in the Ge glass but not in the As one, i.e. the short range order of the network matters for this mode. Apparently the VIR holds when *network connectivity and not short-range order* is important.

A clear departure from the VIR for $\langle r \rangle = 2.6$ is shown in Fig. 2. The GVDOS of the lower curve, which clearly follows the trend of Fig. 1, is for $\text{Se}_{55}\text{As}_{30}\text{Ge}_{15}$. The upper curve displaying several sharp features is for glassy As_3Se_2 . Surprisingly, these features are not evident in Raman scans in this glass. The origin of these features is not yet certain, but it is probable that they arise from a nanoscopic phase separation of isolated molecules within the glass that retain their well-defined molecular vibrational modes. Evidence supporting this view is that one can make several $\text{As}_x\text{Se}_{1-x}$ glasses for $x > 0.5$ which display sharp features at the *same* frequencies, thus pointing to the

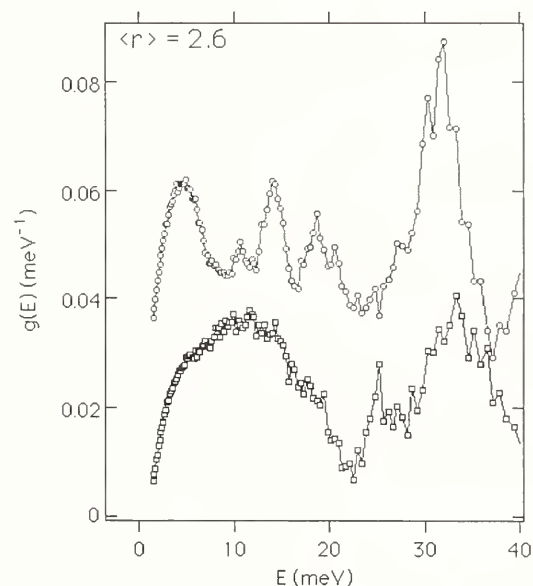


Figure 2. The bottom curve: $\text{Se}_{55}\text{As}_{30}\text{Ge}_{15}$ (FCS) follows the VIR. The top curve: As_3Se_2 (FCS) is an exception to the VIR. Both datasets are for $\langle r \rangle = 2.6$. Starting from the bottom, successive data curves are shifted up by 0.030 units on the vertical scale.

same molecular species.

The conclusions of this research are twofold:

(1) The VIR is followed closely across the entire glass-forming region of the Se-As-Ge phase diagram, with

the exception of a small region near the composition As_6Se_4 . (2) Highly unusual behavior is observed for As_6Se_4 , indicating the formation of molecular clusters or small structural units. The combination of (1) and (2) is intriguing, and may be relevant to unusual photocontractive effects that recently have been observed in As-Se thin films. Better understanding of the structural properties of the Se-As-Ge forms an improved basis for potential applications.

References

- [1] Valentina F. Kokorina, Glasses for Infrared Optics, CRC Press, Boca Raton (1996).
- [2] B. Effey and R. L. Cappelletti, Phys. Rev. B (in press).

Membrane Mediated Polymer Interdiffusion

Alan R. Esker¹, Holger Gröll¹, Gerhard Wegner¹, Charles C. Han¹, and Sushil K. Satija²

¹Polymers Division

²NIST Center for Neutron Research

NIST, Gaithersburg, MD 20899

Understanding the interdiffusion of polymer chains at interfaces is critical to many applications such as coatings, adhesion, composite lamination and fracture strength development. Neutron reflectivity has proven to be a very powerful technique for studying polymer interdiffusion at polymer-polymer interfaces [1]. These studies have examined the role of temperature and molecular weight on interdiffusion between hydrogenated and deuterated polymer bilayers. More recently, the sensitivity of the neutron reflectivity technique has allowed the analysis of thickness dependent diffusion when the film thickness approaches the radius of gyration of the polymer.

The present study probes how the introduction of ultra-thin barrier layers between the interdiffusing polymers affects their dynamics. The study of interdiffusion through barrier membranes is of significant importance in many areas of material science, including metallurgy, biology and polymer science. As an example, consider a system where the barrier is in fact an oxidized layer brought about by degradation of one of the materials. This is an important aspect in materials science where the effects of oxide layers on the interdiffusion in metallic systems have received considerable attention [2]. For polymeric systems one can create an ultra-thin barrier membrane composed of a crosslinked polymer. The crosslinking makes the barrier insoluble in the surrounding polymers while still allowing the interdiffusion of polymers through the membrane.

The geometry of a model system designed for this study is shown in Fig. 1. It is a trilayer system, containing two polystyrene (PS) layers separated by a membrane. One of the polymer layers (either the top or bottom layer) is hydrogenated while the other is deuterated. Molecular weights of both the hydrogenated and deuterated polymer layers were closely matched (hPS: $M = 40 \text{ kg}\cdot\text{mol}^{-1}$; dPS: $M = 39 \text{ kg}\cdot\text{mol}^{-1}$).

The sample was prepared in three stages. First, a polymer layer was spin coated on a silicon substrate covered with a uniform oxide layer ($\sim 10 \text{ \AA}$). The barrier membrane itself consisted of a blend of isopentylcellulose cinnamate (IPCC) and PS (34 wt%). It was transferred on top of the bottom polymer layer

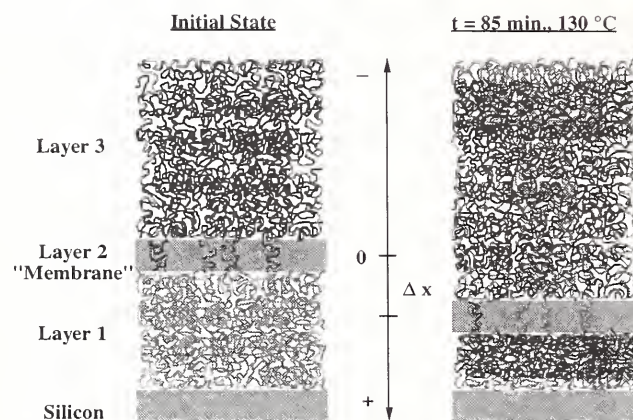


Figure 1: Schematic drawing of the sample geometry for Air/hPS/IPCC(34 wt% PS)/dPS//SiO₂/Si. Red (dPS) and blue (hPS) are used to distinguish between isotopically different polymer chains. The membrane (green) is displaced by Δx from its original position as hPS and dPS mix during annealing.

by the Langmuir-Blodgett technique. The IPCC/PS layers can be transferred in increments of 10 \AA . Using a blend of IPCC and PS as a membrane material allows for the control of the membrane's porosity as the PS component is free to leave the barrier layer during the experiment thereby creating holes and channels in the membrane's network which facilitate PS transport across the membrane. In the present case the IPCC (34 wt%PS) membrane is 60 \AA (6 layers) thick. After transfer the IPCC in the film was cross-linked for 15 min. by UV irradiation under a nitrogen atmosphere. The third and final PS layer was floated on top of the sample. The trilayer system was dried under vacuum at $70 \text{ }^\circ\text{C}$ to remove residual solvents from the polymer. The thickness and roughness of the trilayer system was characterized at each stage by x-ray reflectivity.

A neutron reflectivity curve from the as prepared sample

Air // hPS/IPCC(34 wt% PS)/dPS // SiO₂/Si

is shown in Fig. 2. The orange curve is a fitted reflectivity profile based on the corresponding scattering length density profile (sld) shown in the inset (also orange). The position of the three films, dPS ($\sim 500 \text{ \AA}$), IPCC(34 wt% PS) membrane ($\sim 60 \text{ \AA}$), and hPS ($\sim 800 \text{ \AA}$) can be accurately determined by neutron

reflectivity. After annealing the sample at 130 °C for 80 minutes, changes in the thicknesses and compositions of the PS layers as well as the location of the membrane can be obtained by fitting the reflectivity data (brown). The inset shows the corresponding sld profile (also brown) for the annealed sample revealing an excess of dPS at both the air and SiO₂ interfaces as has been observed in blank experiments² with bilayers of dPS and hPS without the membrane. It takes about 10 times longer to achieve this final state with the membrane present (80 min) than the corresponding time without a membrane (8 min).

More important, we see a movement of the membrane, Δx , relative to its initial position as measured from the Si interface. Neutron reflectivity measurements are very sensitive to the location of the membrane in this trilayer system and its position can be very accurately tracked as a function of annealing time which is shown for this sample in the upper half of Fig. 3. At later annealing times (80 min), the membrane has moved by ~ 120 Å from its original position in the

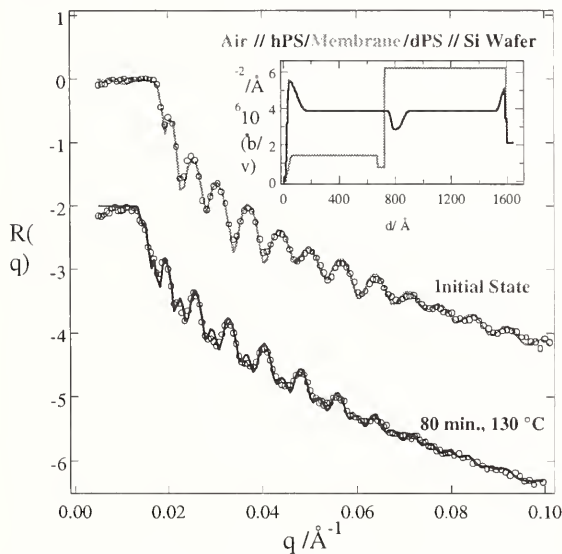


Figure 2: Neutron reflectivity data for initial and final state of the sample Air//hPS/IPCC(34wt% PS)/dPS//SiO₂/Si. The lines are the best fit to the data.

film relative to Si.

An interesting result is observed in a sample where the position of the dPS and hPS layers have been switched. The bottom panel of Fig. 3 shows the relative movement of the membrane in a sample

Air // dPS/IPCC(34 wt% PS)/hPS // SiO₂/Si

as a function of annealing time. It is obvious that the two different geometries result in a reversal of the travel direction of the membrane. In both cases, the membrane moves towards the dPS rich side of the mem-

brane indicating a higher mobility of dPS through the membrane as compared to hPS.

In bilayer interdiffusion studies the influence of unmatched molecular weights has been investigated where the movement of the diffusion boundary has been tracked by observing the movement of gold marker particles (3). Those results show a movement of the interdiffusion boundary towards the direction of the lower molecular weight component. In the present study, the molecular weights of the hPS and the dPS were closely matched, therefore the observed movement of the membrane can be connected to slightly different interactions between the membrane's material (IPCC) and the two isotopically different polymers hPS and dPS leading to a higher permeability of dPS through the barrier.

This result opens up the possibility of a number of new experiments in this area. These include the

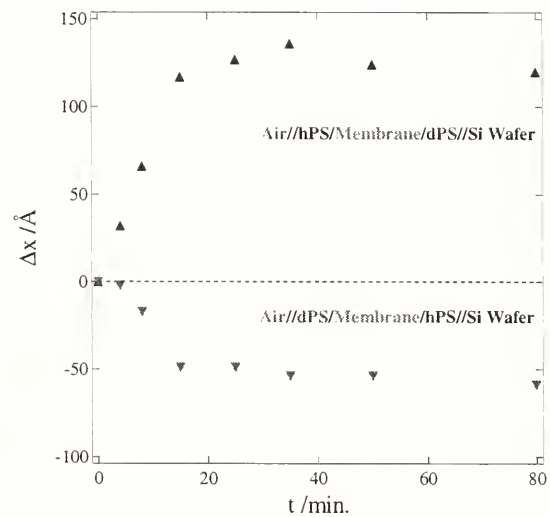


Figure 3: Displacement of the membrane relative to Si effects on the mobility of polymers through membranes as a function of: 1) the molecular weight of the polymer, 2) the degree of crosslinking of the barrier layer, 3) the wt% of PS in the membrane (porosity), and 4) the thickness of the barrier. Besides providing valuable insight into the transport properties of ultra-thin membranes, this project serves as a stepping stone for designing future reflectivity experiments to probe transport properties in biological membranes.

References:

- [1] T.P. Russell, Materials Science Reports **5**, 171 (1990).
- [2] K.M. Lui, K.P. Chik, R.W.M. Kwok, W.H. Choy, and I.H. Wilson, Appl. Phys. Lett. **72**, 2701 (1998).
- [3] P.F. Green, C. J. Palmstrom, J. W. Mayer, and E.J. Kramer, Macromolecules **18**, 501 (1985).

Interactions

A User Facility: Neutrons for the U.S. Research Community

The NCNR is a national resource, providing state-of-the-art neutron beam instrumentation for industry, government, and university research programs. User activity has increased rapidly as the number and capability of the instruments has risen. As shown in Fig. 1, user participation has tripled since the start of operations in the NCNR guide hall in 1990.

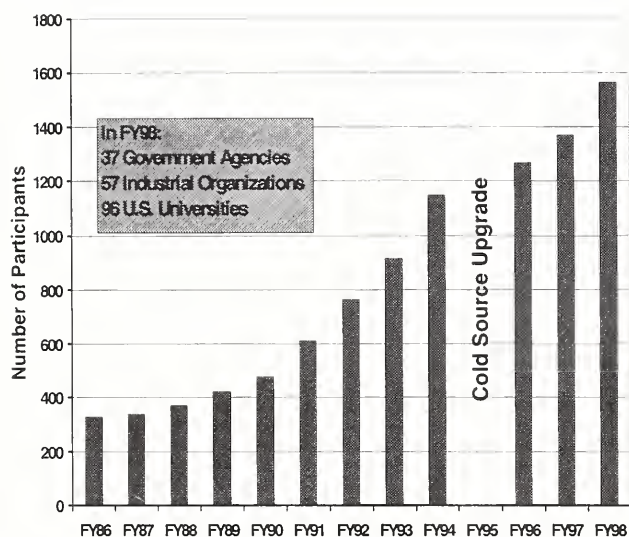


Fig. 1. Research participants at the NCNR.

The bar at far right in Fig. 1 represents participants from 96 universities, 37 government institutions, 57 U.S. industrial laboratories, and 168 foreign institutions. Participants include those who were at the NCNR at least once for an experiment or collaborated in other ways, such as sample preparation or co-authoring a publication. NIST researchers comprise a small fraction of the total user population, but are naturally a critical factor, often enabling other users to perform the best measurements possible.

The NCNR has always striven to enable researchers to obtain access through procedures that are appropriate for their needs, without excessive delay or bureaucracy. In practice, that has meant allowing several different modes of access through formal proposals, informal collaborations, and Participating Research Teams. In some cases, industrial R&D of a proprietary nature is carried out at the NCNR, provided that appropriate beam-time charges are paid on a

full-cost-recovery basis to the U.S. government.

Formal User Program

The Program Advisory Committee (PAC) is the body primarily responsible for proposal review and user policies. The PAC advises the NCNR Director on these and other aspects of the NCNR operation. Its current (1997-1998) membership includes Jill Trehwella (chair, Los Alamos National Laboratory), William Graessley (Princeton University), Sanat Kumar (Penn State University), Gabrielle Long (NIST), Laurence Passell (Brookhaven National Laboratory), Sunil Sinha (Argonne National Laboratory), Thomas Russell (University of Massachusetts), and Emile Schweikert (Texas A&M University). The PAC membership represents a wide range of expertise in neutron beam research, and advises NIST on many aspects of the research activities and instrumentation at the NCNR, especially those concerning user interaction.

The most direct area of involvement for the PAC lies in the formal research proposal system, which is based on a submission deadline and subsequent review at six- to eight-month intervals. After each deadline, proposals are peer-reviewed by mail or electronic mail by experts in the research area specific to each proposal. The PAC then meets to consider the proposals with their reviews, together with technical and safety reviews provided by NCNR staff, and makes recommendations for approval or rejection and allocation of specific amounts of beam time for each proposal.

The PAC met twice at NIST during FY 1998, first on November 21, 1997, and again on July 13-14, 1998. 130 proposals were reviewed on the first occasion, and 162 proposals requesting 1563 instrument-days on the second. The review was confined to proposals for small-angle neutron scattering (SANS), reflectometry, cold-neutron triple-axis spectrometry, and time-of-flight spectroscopy. Other categories of proposals, such as powder diffractometry and chemical analysis, are reviewed on a continuing basis rather than at the regular PAC meetings. Both the number of proposals and the number of requested instrument-days show a continuing growth. For comparison, the call for proposals in August 1995 stimulated 100 proposals requesting 549 instrument-days.

The two 30-m SANS diffractometers still account for the largest category of proposals (67 during the last proposal round), but proposals for the two reflectometers have risen to a comparable number (58 during the last round). The demand for SANS is now rising relatively slowly, while that for reflectometry still shows strong growth. The oversubscription in number of instrument-days (i.e., days requested divided by days available) was approximately 3 for reflectometry, and approximately 2 for SANS and inelastic scattering. The oversubscription for the reflectometers was high at both PAC meetings in FY 1998, despite the provision of more instrument-days for users at the second meeting. There are plans to construct another reflectometer in the near future to accommodate the increasing demand, especially in the area of biology, where experiments can require large blocks of beam time.

The demand for high-resolution inelastic neutron scattering is also increasing. The number of proposals for the SPINS spectrometer (cold-neutron triple-axis with polarized beam option) was 15 in Nov. 1997, and 24 in July 1998. In the last instance, the oversubscription in instrument-days was 2.9. Requests for the Fermi-chopper time-of-flight spectrometer also showed growth, with 9 proposals in 1996, 13 proposals in Nov. 1997, and 15 proposals in July 1998, with an oversubscription of 1.4 at the last PAC meeting. The three new inelastic scattering instruments about to come into operation will stimulate further demand, so that this proposal category should show a substantial increase in the near future. The next call for proposals will offer the backscattering spectrometer, which is now operational, to users on a limited basis. The disk-chopper time-of-flight spectrometer and the spin-echo spectrometer are nearing completion and will be offered to users in the near future.

In addition, time on the 32-detector powder diffraction instrument at BT-1 is also available for users through proposals. For the present, sufficient time is available for all proposals received, and time is directly scheduled by the NCNR staff when proposals are received. During the past year, approximately 80 proposals were granted time on this instrument, approximately half of which were from outside users.

Some users devote a substantial part of their research effort to neutron scattering measurements at the NCNR. At the most recent PAC meeting, it was felt that these users would make best use of their instrument time if they could be assured of access to beam time distributed over an extended period of about two years. The PAC therefore recommended that a

new proposal category be instituted, called program proposals. The latter would be longer and more detailed than a regular proposal, describing a course of measurement rather than a single experiment. NCNR management agreed to implement program proposals on a trial basis.

Collaborations

Direct collaborations remain a common way to access the instruments at the NCNR, accounting for approximately 60% of the number of instrument-days. The thermal-neutron triple-axis spectrometers are mainly scheduled in this way. Most of the time reserved for NIST researchers on other instruments is also devoted to experiments that are collaborations with non-NIST personnel.

Participating Research Teams

Another mode of access to NCNR instrumentation takes place through Participating Research Teams (PRT). In this case, groups of researchers join together to build and operate an instrument, using additional funding derived outside of NIST (although NIST does participate in some PRTs). Three-quarters of the time on such instruments is reserved for the PRT, and the balance is allocated to general user proposals. Several instruments have been developed in this way, and others are under consideration. One particular version of this is the Center for High Resolution Neutron Scattering (CHRNS), which is funded by the National Science Foundation (NSF) and NIST. The instruments include a 30 m SANS machine, a Spin Polarized Inelastic Neutron Spectrometer (SPINS), and a perfect crystal very low angle SANS now under development at BT-5. In CHRNS, all of the NSF time is returned to the general user community for allocation by the PAC. A detailed description of the activities of CHRNS is prepared as an annual report to the NSF, and is available on request.

Feedback from Users

Users are encouraged to offer their comments concerning the instrumentation, operations, and policies at the NCNR. Their input is being obtained in several ways. First, the NCNR local contact personnel interact directly with each research group using the facility. This informal method typically identifies concerns about a specific instrument. Responsibility for

action then resides with the cognizant NCNR instrument scientist. Users may also offer comments on a form provided on the facility Web pages. The NCNR Researcher's Group, an independent body currently chaired by Professor Anne Mayes of MIT, is in the process of obtaining further information through a survey of its membership.

Other communication with users

For the past several years, the primary means of communication with the NCNR user community has been through electronic mail and the facility Web pages at <http://rrdjazz.nist.gov>. For almost all the major neutron scattering instruments, beam time requests that are not formal proposals must be submitted through a Web page form. Most formal proposals for beam time are submitted using the same form, accounting for approximately 80% of proposals received in response to the last call. The current hit rate for the NCNR web page is 1 M/year. Electronic submission has many advantages, facilitating the compilation of a comprehensive database on investigators, proposals, referees, and experiments. This is extremely useful in the increasingly complicated task of assigning and scheduling beam time and equipment, and in making administrative decisions concerning NCNR operations.

Independent Programs

The **Polymers Division** of the Materials Science and Engineering Laboratory has two major program elements at the NCNR. For the first, the objectives are to help the U.S. microelectronics and supporting infrastructure industries by addressing their most pressing materials measurement and standards issues. In today's ICs and packages the feature size is ever shrinking, e.g., on the chip level the feature size is approaching 250 nm while the size of a polymer molecule is typically 5-10 nm. As feature size shrinks the structure and properties of interfaces play an increasingly important role controlling the properties of the polymer layers used in interconnects and packages. In this program both neutron reflectivity and neutron scattering have played an essential role for characterizing polymer/metal interfaces including local chain mobility, moisture absorption, glass transition temperature and crystalline structure. For the second, the objective is to understand the underlying principles of phase behavior and phase separation kinetics in the bulk and

on surfaces of polymer blends in order to facilitate morphology/structure control during processing. SANS and reflectivity measurements in equilibrium, in transient, and under external field provide essential information for general understanding as well as for specific application of polymer blend/alloy systems. Customers include material producers and users, ranging from chemical, rubber, tire, and automotive companies, to small molding and compounding companies. The focus of research on polymeric materials includes commodity, engineering and specialty plastic resins, elastomers, coatings, adhesives, films, foams, fibers, and non-woven's.

The **Exxon Research and Engineering Company** is a member of the Participating Research Team (PRT) that operates, maintains, and conducts neutron-related research activities at the NCNR's NG7-30M SANS and NG5-Neutron Spin Echo Spectrometer (to be dedicated soon) instruments. The mission is to use those instruments, as well as other neutron scattering techniques, to conduct scientific research that complements the research activities at Exxon's main laboratories as well as at its affiliates' laboratories throughout the world. The aim of these research activities is to deepen knowledge of the nature of the products and processes of the business so as to better serve customers and to improve the return on shareholders' investment. In line with that, and taking full advantage of the unique properties of neutrons, most of the experiments use SANS or other neutron techniques to study the structure and dynamics of hydrocarbon materials, especially in the fields of polymers, complex fluids, and petroleum mixtures. Exxon views its participation in the NCNR and collaborations with NIST and other PRT members as an excellent investment for the company and a good way to contribute to the scientific health of the nation.

The **Nuclear Methods Group** (Analytical Chemistry Division, Chemical Science and Technology Laboratory) has as its principal goals the development and application of nuclear analytical techniques for the determination of elemental compositions with greater accuracy, higher sensitivity and better selectivity. A high level of competence has been developed in both instrumental and radiochemical neutron activation analysis (INAA and RNAA). In addition, the group has pioneered the use of cold neutron beams as analytical probes with both prompt gamma activation analysis (PGAA) and neutron depth profiling (NDP). PGAA

measures the total amount of a particular analyte present throughout a sample by the analysis of the prompt gamma-rays emitted during neutron capture. NDP, on the other hand, determines concentrations of several important elements (isotopes) as a function of depth within the first few micrometers of a surface by energy analysis of the prompt charged-particles emitted during neutron bombardment. These techniques (INAA, RNAA, PGAA, and NDP) provide a powerful combination of complementary tools to address a wide variety of analytical problems of great importance in science and technology, and are used to help certify a large number of NIST Standard Reference Materials. During the past several years, a large part of the Group's efforts has been directed towards the exploitation of the analytical applications of the guided cold-neutron beams available at the NIST Center for Neutron Research. The Group's involvement has been to design and construct state-of-the-art cold neutron instruments for both PGAA and NDP and provide facilities and measurements for outside users, while retaining and utilizing our existing expertise in INAA and RNAA.

The **Center for Food Safety and Applied Nutrition**, U. S. Food and Drug Administration (FDA), directs and maintains a neutron activation analysis (NAA) facility at the NCNR. This facility provides agency-wide analytical support for special investigations and applications research, complementing other analytical techniques used at FDA with instrumental (INAA), neutron-capture prompt-gamma (PGAA), and radiochemical Neutron Activation Analysis (NAA) procedures, radioisotope X-ray fluorescence spectrometry (RXRFS), and low-level gamma-ray detection. This combination of analytical techniques enables diverse multi-element and radiological information to be obtained for foods and related materials. The NAA facility supports agency quality assurance programs by developing in-house reference materials, by characterizing food-related reference materials with NIST and other agencies, and by verifying analyses for FDA's Total Diet Study Program annually. Other studies include the development of RXRFS methods for screening foodware for the presence of Pb, Cd and other potentially toxic elements, use of INAA to investigate bromate residues in bread products, and use of PGAA to investigate boron nutrition and its relation to bone strength. FDA's NAA laboratory personnel frequently provide intra-agency technical assistance, the most recent example being participation in the production of the document "Accidental Radioactive Contamination

of Human Food and Animal Feeds: Recommendations for State and Local Agencies" by the Center for Devices and Radiological Health.

The **Neutron Interactions and Dosimetry Group (Physics Laboratory)** provides measurement services, standards, and fundamental research in support of NIST's mission as it relates to neutron technology and neutron physics. The national and industrial interests served include scientific instrument calibration, electric power production, radiation protection, defense nuclear energy systems, radiation therapy, neutron radiography, and magnetic resonance imaging. The Group's activities may be represented as three major activities. The first is Fundamental Neutron Physics - including operation of a neutron interferometry and optics facility, development of neutron spin filters based on laser polarization of ^3He , measurement of the beta decay lifetime of the neutron, and investigations of other coupling constants and symmetries of the weak interaction. This project involves a large number of collaborators from universities and national laboratories. The second is Standard Neutron Fields and Applications - utilizing both thermal and fast neutron fields for materials dosimetry in nuclear reactor applications and for personnel dosimetry in radiation protection. These neutron fields include thermal neutron beams, "white" and monochromatic cold neutron beams, a thermal-neutron-induced ^{235}U fission neutron field, and ^{252}Cf fission neutron fields, both moderated and unmoderated. The third is Neutron Cross Section Standards - including experimental advancement of the accuracy of neutron cross section standards, as well as evaluation, compilation and dissemination of these standards.

Several universities have also established long term programs at the NCNR. The **University of Maryland** is heavily involved in the use of the NCNR, and maintains several researchers at the facility. **Johns Hopkins University** participates in research programs in solid state physics and in instrument development at the NCNR. The **University of Pennsylvania** is working to help develop biological applications of neutron scattering. It is also, along with the University of California, Santa Barbara, duPont, Hughes, and Allied Signal participating in development of a new filter analyzer neutron spectrometer. The **University of Minnesota** participates in two PRTs; the **University of Massachusetts** participates in one.

Reactor Operations and Engineering



Reactor Operations and Engineering Group after award of Department of Commerce award for outstanding service.

Reactor on-line time for the year was 67% of real time, which is excellent, compared to the maximum achievable of 73%. The reason for the slightly lower on-line time than last year's 70% is two fold. There was a one-week shutdown for shipment of spent fuel and a three-week shutdown for licensing of new personnel and requalifying of current operators. This time was also used to perform maintenance on the guide tubes and refurbish the cooling tower. In addition, towards the end of the year, a very small leak, on the order of 0.01 liter per hour was discovered in the vicinity of the thermal column. As a result, it was decided to shut down the reactor and search for the leak. After an exhaustive search and testing, the source of the leak was not found and the leak had not returned. The situation will continue to be monitored.

Three new operators received their senior operator license following comprehensive written, oral, and operating examinations by the Nuclear Regulatory Commission. They passed their examinations and qualified with distinction achieving near perfect scores in all categories. All 17 currently licensed personnel passed their requalification examinations.

For the first time in ten years, three shipments of spent fuel were made to the DOE facilities at Savannah River, South Carolina. The shipments consisted of 126 elements equivalent to about 5 years of 20 MW operation. This has greatly relieved storage space in the spent fuel pool. Two more shipments are scheduled for the latter part of 1999.

Plans are underway for comprehensive review of all major reactor systems for upgrade or improvement. An outage of 3 – 5 months is scheduled for early 2000 to replace the control rods and the heavy water and to perform other maintenance items. Plans are also being made, if time permits, to replace the existing cooling tower with a larger wet-dry tower of new design and to replace the existing cold source with an advanced version that will double the flux.

An updated safety analysis report is in the final stages of review. It will be submitted to the Nuclear Regulatory Commission next year as the first step in the relicensing of the reactor.

Instrumentation Developments

High-flux Backscattering Spectrometer Commissioned

The first vanadium spectrum from the NCNR high flux backscattering spectrometer (HFBS) was obtained in June of 1998 after a design and construction effort lasting more than six years. The measured energy resolution of $0.9 \mu\text{eV}$ is a factor of 50 better than that routinely obtained using any other spectrometer currently in operation at the NCNR (Figure 1). This exceptional energy resolution will enable the investigation of many types of dynamical processes in materials, including molecular reorientations, diffusion, dynamics of liquids, glasses and polymers, and critical scattering near phase transitions.

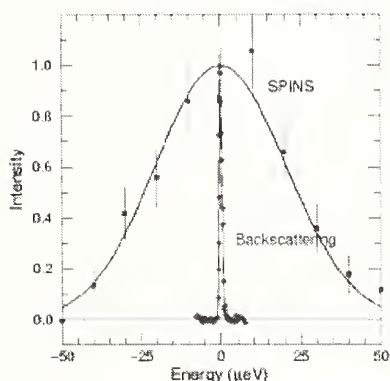


Figure 1. Comparison of resolution of HFBS to SPINS (Cold Neutron Triple Axis spectrometer).

A backscattering spectrometer can be viewed most simply as a limiting case of a triple-axis spectrometer where the scattering angles of the neutrons from both the monochromator and analyzer crystals are 180 degrees[1]. This geometry decouples the beam divergence from the energy resolution allowing the instrument to achieve an ultimate energy resolution defined by the properties of the crystals. The HFBS uses the (111) reflection from bent silicon crystals to both monochromate and analyze the neutron energies. The final energy, defined by the Bragg condition from the silicon analyzers, is 2.08 meV corresponding to a neutron wavelength of 6.27 \AA . The incident energy is varied by shaking the monochromator using a cam-operated drive system thereby Doppler shifting the incident neutron energy. To date, this device has been

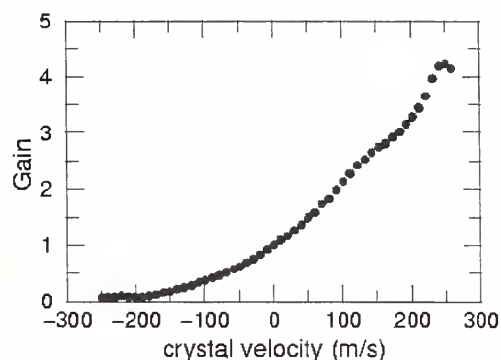


Figure 2. Measured gain from use of phase space transform chopper.

used to obtain energy transfers of $\pm 45 \mu\text{eV}$. The ultimate overall energy transfer range measured by this instrument will exceed $50 \mu\text{eV}$.

The primary design goal of this instrument was to maximize the count rate for a given experiment while maintaining an energy resolution of better than $1 \mu\text{eV}$ full width at half maximum (FWHM). This has been achieved by matching the divergence of the front-end of the instrument with the divergence of the secondary spectrometer, utilizing a phase-space transform (PST) chopper and by maximizing the area of coverage for the analyzer and monochromator crystals. The HFBS design incorporates a 4m long converging guide which increases the incoming beam divergence and results in

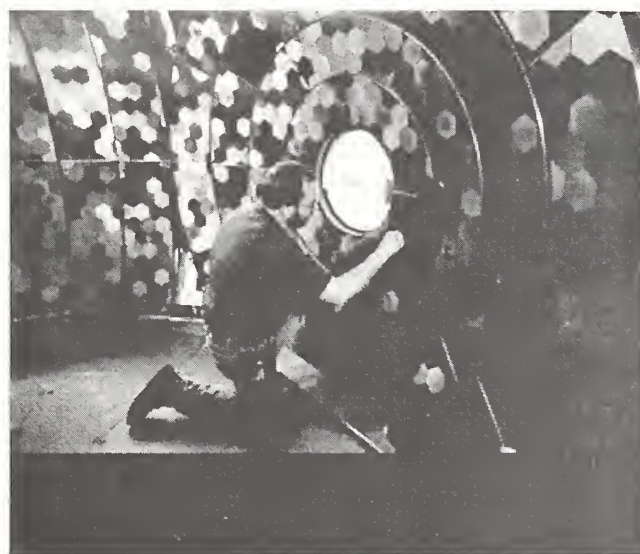


Figure 3. Scott Slifer adjusting the analyzer assembly on the HFBS.

3.9 times more flux at the end of the guide. The PST is a novel device, conceived originally by Schelten and Alefeld[2], which acts as a premonochromator for the instrument: reflecting the beam of neutrons towards the monochromator while focussing their energy distribution towards the narrow value required by the back-scattering monochromator crystal. Measurements carried out at the HFBS have demonstrated for the first time that this device increases the neutron flux from the monochromator by more than a factor of four from that obtained with a stationary crystal (Figure 2). The spherically focussed monochromator and analyzer crystals cover very large areas (the analyzer subtends 20% of the total solid angle) and make the instrument very efficient in its use of the available neutrons (Figure 3).

Monte Carlo simulation of neutron beam lines

Monte Carlo simulation of cold neutron beam tube performance is a powerful tool for predicting neutron fluxes and developing optimized neutron scattering instrumentation. A Monte Carlo program has been developed at the NCNR which makes use of modeled reflectivity curves and parameterized neutron cross-sections to simulate the neutron beam delivery system. The neutron beam system may consist of any combination of straight, bent, focusing and channeled guide sections, circular and rectangular diaphragms, neutron collimators, neutron velocity selectors and variety of commonly-used cooled and room temperature crystal filters. The program can also allow for non-ideal configurations such as random Gaussian

These flux enhancing devices together with the flux available from the NG-2 guide have resulted in a measured flux at the sample position of $1.4 \times 10^5 \text{ cm}^{-2}\text{-sec}^{-1}$ in good agreement with calculations. This flux makes the HFBS competitive with any instrument of its kind in the world.

References

- [1] P. M. Gehring and D. A. Neumann, *Physica B* **64**, 241-243 (1998).
- [2] J. Schelten and B. Alefeld, in *Proc. Of a Workshop on Neutron Scattering Instrumentation for SNQ*, ed. R. Scherm and H. H. Stiller, Report Jul-1954, (1984)

guide section misalignments. Modeled guide coatings include natural Ni, ^{58}Ni , multilayer and supermirror. Using reference neutron spectrum data, gold foil activation data and measured reflectivity data obtained from two of the NCNR cold neutron beam tubes, the Monte Carlo program has been used to characterize the liquid hydrogen cold neutron source brightness. In turn, this brightness model has been incorporated into simulations of all the neutron beam tubes (NG-0-NG-7) installed on the NCNR cold source. Table 1 shows that the agreement of the simulated and measured capture fluxes is remarkably good. The program has been used extensively to predict and optimize the performance of projected future reconfigurations of the NCNR beam tubes as well as to characterize neutron fluxes per unit wavelength at locations where flux measurements are not yet available.

Guide system	$\phi_c^{\text{meas}} (\text{cm}^{-2}\text{s}^{-1})$	$\phi_c^{\text{sim}} (\text{cm}^{-2}\text{s}^{-1})$	$\phi_{\text{int}}^{\text{sim}} (\text{cm}^{-2}\text{s}^{-1})$	$\langle\lambda\rangle (\text{\AA})$
NG-0 before NDP chamber	2.56×10^9	2.336×10^9	6.020×10^8	6.976
NG-1 at reflectometer monochromator	3.1×10^9	3.376×10^9	1.023×10^9	5.93
NG-2 before filter	3.5×10^9	3.498×10^9	1.055×10^9	5.96
NG-2 at HFBS shutter	2.15×10^8	2.094×10^8	6.08×10^7	6.20
NG-2 at HFBS (after converging guide)	8.29×10^8	7.75×10^8	2.25×10^8	6.20
NG-3 before SANS filter	1.7×10^9	1.725×10^9	5.30×10^8	5.85
NG-4 at DCS shutter	2.7×10^9	2.62×10^9	7.94×10^8	5.93
NG-4 at DCS sample (Choppers removed)	9.92×10^8	9.96×10^8	3.39×10^8	5.28
NG-5 at Guide Hall entrance	2.3×10^9	2.148×10^9	6.42×10^8	6.02
NG-6 at Guide Hall entrance	2.3×10^9	2.197×10^9	6.66×10^8	5.93
NG-6 at end of guide	1.37×10^9	1.387×10^9	4.37×10^8	5.71
NG-7 at reflectometer monochromator	1.9×10^9	1.948×10^9	5.90×10^8	5.93
NG-7 before SANS filter	1.56×10^9	1.639×10^9	5.12×10^8	5.75

Table 1. A comparison of measured and simulated capture fluxes for various locations on the NCNR cold neutron beam tubes. The table also gives simulated integrated fluxes ($\phi_{\text{int}}^{\text{sim}} = \int (\frac{d\phi}{d\lambda}) d\lambda$) and average wavelengths ($\langle\lambda\rangle = 1.8 \phi_c^{\text{sim}} / \phi_{\text{int}}^{\text{sim}}$) in the guide at the reference positions.

New capabilities for sample environment and preparation

This year the NCNR added several new sample environment capabilities. The obtainable temperature equivalent magnetic field energy per Bohr magneton was increased from 0.4 Kelvin to 0.52 Kelvin by the procurement of a 9 Tesla vertical field superconducting magnet. In order to reach sample temperatures comparable with this field energy range, a pumped helium-3 refrigerator with a base temperature of 0.29 Kelvin is incorporated into the 9 Tesla magnet system. These low temperatures and high fields are critical for the NCNR's ongoing program of research on low dimensional magnetism. The new superconducting magnet system is top-loading which facilitates quick turn around for studies involving multiple samples. The horizontal field magnet, shown in Fig. 1, was recently returned to service.

A new 2000 K variable temperature vacuum furnace was acquired this year providing new capability for neutron scattering experiments at high tempera-

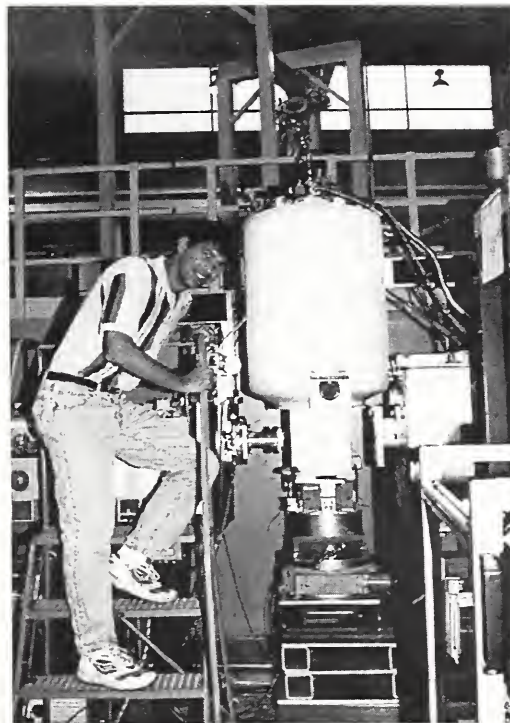


Figure1. John Barker sets up the recently repaired superconducting horizontal field magnet on the NG-7 SANS.

Detector Electronics for the HFBS

The recently commissioned High Flux Backscattering Spectrometer provided a unique design challenge for the ^3He neutron detector electronics. The combination of a large evacuated flight path together with close packing of the half inch diameter detectors meant that the traditional preamplifier/amplifier/discriminator (PAD) modules could only be utilized outside of the vacuum chamber. This option would have resulted in an unacceptable noise susceptibility for the weak detector signals being transmitted over long cables and through vacuum feedthrough devices. The HFBS project opted, instead, to design a small form-factor, fully vacuum rated PAD module that could be located within the vacuum flight chamber and then route the robust digital discriminator outputs to the outside data acquisition electronics.

The NCNR design is based on two commercially available hybrid circuits: a preamplifier/shaping amplifier, and an amplifier/discriminator. Both parts dissipate power at the milliwatt level and are fully vacuum (space) rated. The output stage uses a CMOS

dual inverting/non-inverting driver which also exhibits very low power dissipation, even when driving large loads. The balanced output is used to provide ECL level logic output with excellent common mode rejection for the signal transmitted out of the flight chamber to the data acquisition electronics. Careful component selection and package design resulted in a small form-factor, flat-package design with a thickness of less than 0.45 inches consistent with the detector spacing requirements. Additional features in the NCNR design include: a robust input protection network to protect the preamplifier, on-board regulation of the discriminator level reference voltage, separate high and low level discriminator settings, and convenient on-board connections for daisy chaining high voltage and test pulse inputs to adjacent PAD modules.

Data Acquisition Electronics for the DCS Time-of-flight Spectrometer

The Disk Chopper Time-of-flight Spectrometer (DCS) presents unique requirements for its data acquisition system. The choppers of the DCS instrument (see Figure 1) periodically illuminate the sample with pulses of neutrons which are then scattered towards the detectors. Each period the chopper system produces a signal synchronous with the incoming neutron pulse that starts a free-running clock which is used to time the neutron flight. When a neutron event occurs, the front-end data acquisition electronics create a 30-bit binary event word which encodes which detector, and at what time, registered a scattered neutron. The rest of the data acquisition system is responsible for reading out the event words, decoding the data event words, and histogramming the data. The user workstation processes the stored histograms from the measurement.

Both the large number of detectors (nearly 1000) and the high-energy resolution characterize the NIST DCS instrument. This requires that the time-of-flight measurement to be resolved to better than 100 nanoseconds over a timing interval which can exceed 50 milliseconds (a timing dynamic range of over 10^6). To meet these requirements the detectors must be interrogated at a raw rate exceeding 10^{10} s^{-1} . The actual worst-case neutron event rate (all neutrons in a pulse scattered into one time channel) is under 10^7 s^{-1} , while the time-averaged data rate at which the histogram must be updated is only on the order of 10^5 s^{-1} . Bridging these drastically different data rates is the primary function of the data acquisition electronics. The general approach adopted in the NIST design is to process data hierarchically, in a tree-like structure, which mirrors the data bandwidth requirements. In this concept, multiple front-end elements operate in parallel at high speed, passing valid events to the next level where they are multiplexed and then passed on to be histogrammed into memory.

The DCS data acquisition electronics were successfully tested under test-bench conditions and under "live" conditions during a recent reactor cycle. The NCNR design uses two types of single width, 6U-sized VME modules to process incoming events and multiplex the events for VME readout to the crate controller computer where the events are histogrammed. The input modules are capable of processing events from 30 detectors creating the appropri-

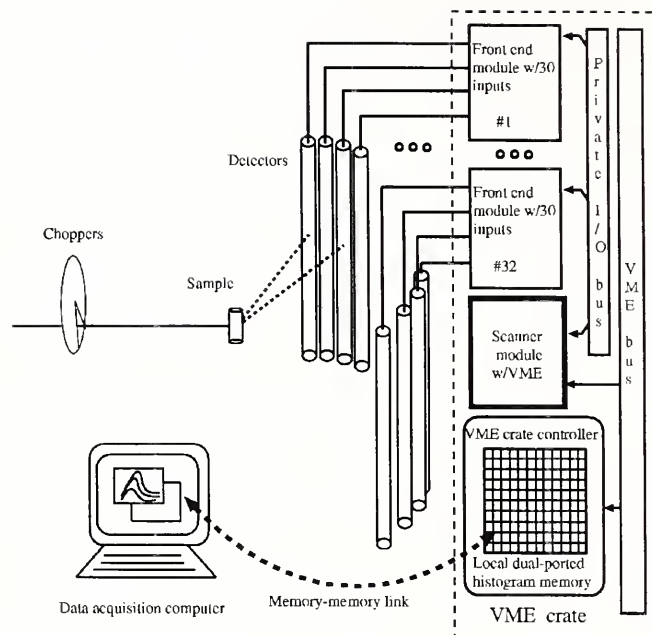


Figure 1. Schematic diagram of DCS Data Acquisition system.

ate time-stamped data words and storing the events in a 64 deep FIFO memory for readout. The DCS instrument requires 31 input modules to handle all of the 913 detectors in the current configuration. A scanner module polls all of the 31 input modules over a private bus to see if they have valid events ready for readout. If data is available, the scanner module reads the valid events from the input modules and stores the data for readout over the VME bus to the VME crate controller. The crate controller computer reads the events from the scanner module, filters valid events, processes the timing information, and histograms events by detector and time channel into a block of memory accessible to the user workstation computer.

Research Topics

The topics listed here represent research undertaken during the year. For further details on any area, please contact the authors directly, or write to Linda Clutter, 100 Bureau Drive Stop 8562, Gaithersburg, MD 20899-8562

Materials Science

A New Phase of Silver Fluoride?

R. Harlow³⁹

A Ring/Plug Reference Specimen for Residual Stress Measurements

T. Gnäupel-Herold¹⁸⁸, P. C. Brand⁹⁸, D. Balzor¹⁰⁵, A. V. Clark¹⁰⁵ and H. J. Prask⁹⁸

Acid Sites in Zeolite ZSM-5

A. Peters³⁶, R.-H. Hu²¹², S. Purnell²¹², B. H. Toby⁹⁸, R. Senesi¹⁴², D. A. Neumann⁹⁸ and D. H. Olson¹⁹⁹

Aerogels Investigated by SANS with Contrast Masking Solutions

C. Merzbacher⁹⁵, M. Anderson⁹⁵ and J. Barker⁹⁸

Amorphous Content Determination Methodology

J. K. Stalick⁹⁸, R. Senesi¹⁴² and B. Toby⁹⁸

A Structural Study of the Ruddlesden-Popper Calcium Manganate

$\text{Ca}_4\text{Mn}_3\text{O}_{10}$

M. Greenblatt¹³⁵ and I. Fawcett¹³⁵

Ceramic Mixed Conducting Membrane Materials

H. Prask⁹⁸ and E. Drescher-Krasicka¹⁰⁶

Characterization of Microcracking in Iron Titanate by SANS

A. Allen¹⁰² and E. Fuller¹⁰²

Characterization of Standard Reference Specimens for Residual Stress Measurements as Part of VAMAS

T. Gnäupel-Herold¹⁸⁸, P. C. Brand⁹⁸, H. J. Prask⁹⁸ and G. A. Webster⁵⁷

Charge, Orbital and Magnetic Ordering in the Manganate Perovskites

P. Woodward²⁰ and T. Vogt²⁰

Chemical Ordering in Ni-Mn-Ga Heusler Alloys

R. Overholser¹⁸⁸, M. Wuttig¹⁸⁸ and D. A. Neumann⁹⁸

SANS from Oil Bearing Sedimentary Rocks

A. Radlinski¹³ and G. Wignall¹¹⁵

Comparison of Residual Stress Measurement Techniques

T. Gnäupel-Herold¹⁸⁸, P. C. Brand⁹⁸, H. J. Prask⁹⁸, S. Spooner¹¹⁵, B. Pardue¹⁵³, D. Nelson¹⁴¹ and S. Foss⁷¹

Complex Oxide Structures

A. Sleight¹¹⁹, I. Radosavljevic¹¹⁹ and T. Amos¹¹⁹

'CONV' and 'STRESS': New Codes for Data Reduction in Neutron Diffraction Residual Stress Measurements

P. C. Brand⁹⁸ and T. Gnäupel-Herold¹⁸⁸

CPD Round Robin on Quantitative Phase Analysis

J. K. Stalick⁹⁸

Crystal Chemistry of Protonic Centers in Zeolites

D. H. Olson¹⁹⁹ and Brian Toby⁹⁸

Determination of Residual Stresses in an Al plate for Helicopter Applications

P. C. Brand⁹⁸, H. J. Prask⁹⁸, T. Gnäupel-Herold¹⁸⁸ and D. Ludin¹⁹

Effect of Annealing on ZrO_2 Phase Composition

J. K. Stalick⁹⁸ and J. Ilavsky³⁴

Fast Ion Conductors

J. K. Stalick⁹⁸, B. Wuensch⁸¹ and E. Ku⁸¹

Grazing Incidence SANS from Plasma Sprayed Coatings

A. Allen¹⁰² and H. Boukar¹⁰²

Hydrogen-Induced Lattice Migration in Palladium/Nickel Alloys

T. Flanagan²¹⁰ and J. Barker⁹⁸

Hydrogen Location in Graphite Nano-Fibers

S. F. Trevino^{98,11} and P. Anderson¹¹²

Identification Of A Hydrogen-Induced Tetragonal Phase In $\text{Ti}_{48}\text{Al}_2\text{Nb}_2\text{Cr}$ Alloys.

M. DeGraef²³ and B. Mollosseau²³

Influence of Thermal Treatment on Void Morphology in Polyethylene-Carbon Black Composites

D. Marr³⁰, J. Oakley³⁰, K. Schwartz¹²⁹ and M. Wartenberg¹²⁹

Investigation of the $\text{Zr}_9\text{Pt}_{11}$ Structure Type

J. K. Stalick⁹⁸ and R. Waterstrat⁹⁸

Kinetics of Gellation of Silica under Shear

C. Muzny¹¹¹, H. Hanley¹¹¹ and G. Straty¹¹¹

Low Temperature Crystal Structure Study of $\text{DZSM-5-4D}_2\text{O}$ (Si:Al=26)

D. H. Olson¹⁹⁹

Magnetic Structure of Layered Perovskites as a Function of Temperature

A. K. Cheetham¹⁷⁷ and B. J. Campbell¹⁷⁷

Measurement and Modeling of Residual Stresses in Multi-pass Weldments

T. Gnäupel-Herold¹⁸⁸, H. J. Prask⁹⁸, P. C. Brand⁹⁸, R. Lloyd⁵⁵ and W. Reuter⁵⁵

Measurement of Diffraction Elastic Constants of γ -Alumina and Zirconia Plasma Sprayed Coatings

T. Gnäupel-Herold¹⁸⁸, J. Matejicek¹⁴² and H. J. Prask⁹⁸

Micro-Porosity in Amorphous Carbons and Li-Carbons

J. E. Fischer¹⁹⁹, P. Zhou¹⁹⁹, Y. Sorek¹⁹⁹, A. Claye¹⁹⁹ and W. Kamitakahara⁹⁸

Microstructure of Permeable Hydrogel Lens Materials

J. S. Huang⁴⁴, J. Li⁴⁴ and P. Vilant¹⁶

Microstructure of Silica-Aerogel Sensor Materials

R. Reidy¹³¹ and A. Allen¹⁰²

Morphological and Kinetic Study of Early Calcium-Silicate-Hydrate Gel Development during the Hydration of Cement and Tricalcium Silicate

H. M. Jennings¹¹², J. J. Thomas¹¹² and A. J. Allen¹⁰²

Neutron Diffraction Data of Beta- PtO_2

B. Chamberland⁹ and M. O'Keefe⁹

Neutron Diffraction Measurements of Nanostructured, Non-Equilibrium Spinell Ferrites

V. G. Harris⁹⁵

Neutron Diffraction Studies of AlFeMn Solid Solutions

V. G. Harris⁹⁵ and Q. Huang^{98,188}

Neutron Diffraction Studies of the Zeolites Cancrinite and (Ba,K)G-L

A. Burton¹⁸¹, M. Feuerstein¹⁸¹ and R. Lobo¹⁸¹

Neutron Diffraction Validation of Scanning Acoustic Imaging Residual Stress Measurements

T. Gnäupel-Herold¹⁸⁸, H. J. Prask⁹⁸ and E. Drescher-Krasicka¹⁰⁶

Order-Disorder in CoFe/Carbon Composites

J. H. Scott¹¹⁰, M. E. McHenry²³, Z. Turgut²³ and M. Storch²³

Polymerized Fullerenes

S. F. Trevino^{98,11}, N. Beck-Tan¹¹ and L. Balogh⁸⁶

Pore Size Distribution Analysis of Activated Carbons

P. Pendleton²⁰¹ and C. Howard¹⁴

Radiation-Induced Microstructure in Reactor Pressure Vessel Steels

G. R. Odette¹⁷⁷, B. Wirth¹⁷⁷ and D. Klingensmith¹⁷⁷

Residual Stresses around Weldments in Various Steel-Plate Configurations

T. Gnäupel-Herold¹⁸⁸, P. C. Brand⁹⁸, I. Varhol¹²⁴ and H. J. Prask⁹⁸

Residual Stresses in a Failed Steel Structural Member

P. C. Brand⁹⁸, H. J. Prask⁹⁸, T. Gnäupel-Herold¹⁸⁸, E. Drescher-Krasicka¹⁰⁶ and C. Ostertag¹⁷²

Residual Stresses in a Powder Metallurgy Gear

T. Gnäupel-Herold¹⁸⁸, H. J. Prask⁹⁸, B. Chelluri⁵³

Residual Stresses in Powder Metallurgy Test Specimens

T. Gnäupel-Herold¹⁸⁸, H. J. Prask⁹⁸, M.-J. Yang¹²³ and R. German¹²³

Residual Stresses in a Shrink-Fit Ti/SiC Ring

T. Gnäupel-Herold¹⁸⁸ and S. F. Trevino^{98,11}

Residual Stresses in Thermally-Sprayed Coatings

J. Matejicek¹⁴², T. Gnäupel-Herold¹⁸⁸, P. C. Brand⁹⁸, H. J. Prask⁹⁸, S. Sampath¹⁴² and H. Herman¹³

Residual Stresses in Ti Rib Implants for Children

T. Gnäupel-Herold¹⁸⁸, H. J. Prask⁹⁸ and R. Roberts⁵

Residual Stress Measurements on Railroad Rails

T. Gnäupel-Herold¹⁸⁸, P. C. Brand⁹⁸, J. Gordon¹⁶⁰, J. Magiera³³, J.

- Orkisz³³ and H. J. Prask⁹⁸
Residual Stresses, Texture and Grain Size in Aluminum/Alumina Composite Materials
 P. C. Brand⁹⁸, T. Gnäupel-Herold¹⁸⁸ and S. Skirl¹⁴⁷
- SANS Investigation of Hydrogen Trapping at Lattice Defects in Palladium**
 B. Heuser¹⁸⁴ and J. King¹⁹⁰
- SANS Investigation of the Role of Templating Molecules in Zeolite Synthesis**
 C. Glinka⁹⁸ and L. Beck²¹
- Search for Hydride Formation in Hydrogen Charged Aluminum Single Crystals**
 C. Buckley¹⁸⁵, H. Birbaum¹⁸⁵ and J. Barker⁹⁸
- Single-Crystal Elastic Constants from Measurements on Polycrystals**
 T. Gnäupel-Herold¹⁸⁸, H. J. Prask⁹⁸ and P. C. Brand⁹⁸
- Single-Crystal Rene N5-Sc under Load**
 T. Gnäupel-Herold¹⁸⁸, H. J. Prask⁹⁸, P. C. Brand⁹⁸ and R. Fields¹⁰⁶
- Size Distribution and Volume Fraction of Copper-Rich Precipitates in Model Reactor Pressure Vessel Steels**
 D. Balzar¹⁰⁵ and C. Glinka⁹⁸
- Size Distribution of Zeolite Precursor Particles**
 C. J. Glinka⁹⁸, R. Thompson²¹⁹ and B. Shoeman³⁷
- Strains in New Dental Materials**
 H. Prask⁹⁸, A. Saigal¹⁵⁹ and T. Gnäupel-Herold¹⁸⁸
- Structural Characterization of Fluorocarbon-Zeolite Interactions**
 C. Grey¹⁴² and M. Ciruolo¹⁴²
- Structural Characterization of Gas Adsorbent Zeolites**
 J. B. Higgins⁴
- Structural Investigations in the SrRu_{1-x}Ir_xO₃ System**
 T. Vogt²⁰
- Structural Studies in Alkaline Ga Borates**
 A. Mehta¹⁴⁰, R. Smith¹⁹⁵ and B. H. Toby⁹⁸
- Structural Studies Ba/La-Titanates**
 C. J. Rawn¹¹⁷ and B. H. Toby⁹⁸
- Structural Studies of Ca-Ir and Ca-Rh Deuterides**
 R. O. Moyer¹⁵⁸ and B. H. Toby⁹⁸
- Structural Studies of Germanium Zeolites**
 J. B. Parise¹⁴², G. M. Johnson¹⁴² and A. Tripathi¹⁴²
- Structural Studies of Iodine-Loaded ZSM-5**
 D. H. Olson¹⁹⁹
- Structural Studies of Sr₂Rh_{1-x}Ru_xO₄ Layered Perovskites**
 P. Woodward²⁰, B. Kennedy²⁰³ and T. Vogt²⁰
- Structural Studies of Strontium Niobium Oxides**
 W. Wong-Ng¹⁰², W. Greenwood¹⁸⁸ and B. H. Toby⁹⁸
- Structure of Porous Silica Thin Films**
 W. Wu¹⁰⁷ and D. Pochan¹⁰⁷
- Surfactant Stabilized Nanocrystalline Palladium Clusters**
 R. Kirchheim¹⁸³ and J. Barker⁹⁸
- Temperature Dependence in the Structure of Yttrium Tungstate**
 A. Sleight¹¹⁹, P. Forster¹¹⁹ and A. Yokochi¹¹⁹
- Variable Temperature Structure of Rh Doped Sr₂RuO₄**
 B. Kennedy¹⁴⁵ and Tom Vogt²⁰
- Zeolite SRM Characterization**
 B. H. Toby⁹⁸ and R. Senesi^{142,98}
- X-Ray Reflectometry Analysis of Alkanethiol Deposited on AuO**
 K. T. Forstner⁹⁸, J. A. Dura⁹⁸, C. F. Majkrzak⁹⁸, J. Woodward¹⁰⁰, A. Plant¹⁰⁰
- M. Lin⁴⁴ and D. Peiffer⁴⁴
Critical Neutron Reflection Tests of Polymer Interdiffusion Dynamics
 R. P. Wool¹⁸¹, K. A. Welp¹⁸¹ and W. Dozier¹⁸¹
- Demixing Kinetics of Polyolefin Blends**
 N. Balsara¹²⁵, H. Wang¹²⁵ and B. Hammouda⁹⁸
- Diblock Copolymer Mixtures in Aqueous Solutions**
 Z. Li⁴⁴, J. Sung⁴⁴ and J. S. Huang⁴⁴
- Dynamics of Polymer Interdiffusion**
 S. K. Satija⁹⁸
- Effects of Polymer Additives on the Formation of Hydrate Crystals in Petroleum Pumping**
 J. Hutter⁴⁴ and H. King⁴⁴
- Effects of Pressure on the Lower Critical Ordering Temperature of Diblock Copolymers**
 A.-V. Ruzette⁸¹ and A. Mayes⁸¹
- Effects of Shear on the Phase Behavior of Polyolefin Blends**
 N. Balsara¹²⁵ and A. Lefebvre¹²⁵
- Effects of Substrate Interactions on the Ordering of Block Copolymer Films**
 E. Huang¹⁸⁹, J. DeRouchey¹⁸⁹ and T. Russell¹⁸⁹
- Effects of Supercritical CO₂ on the Phase Behavior of Block Copolymer Melts**
 J. Watkins¹⁸⁹, M. Pollard¹⁸⁹, G. Brown¹⁸⁹, S. Kumar¹²³ and T. Russell¹⁸⁹
- Effects of Surfactants on the Conformation of Grafted Polymer Brushes**
 T. Cosgrove¹⁶⁹, J. Hone¹⁶⁹ and R. Wesley¹⁶⁹
- Electric Field-Induced Orientation of Diblock Copolymers in Thin Films**
 J. DeRouchey¹⁸⁹ and T. Russell¹⁸⁹
- Glass-Transition Effects on Microphase Separation in PS/PVME Polymer Blends**
 S. Kumar¹²³, R. Jones¹²³, S. Kanath¹²³, R. Briber¹⁸⁸ and L. Ho¹⁸⁴
- In-Situ SANS Study of Living Anionic Polymerization of Homopolymers**
 D. Allgaier⁶¹, J. Stellbrink⁶¹, L. Willner⁶¹ and L. Fetters⁴⁴
- Interfacial Scattering from Phase-Separated Polymer Blends**
 H. Jinnai⁷⁶, M. Hayashi⁷⁶ and C. Han¹⁰⁷
- Kinetics of Shear Alignment of Block Copolymer Blends**
 R. Krishnamoorti¹⁸⁴, S. Rai¹⁸⁴ and B. Hammouda⁹⁸
- Microstructure of Dendrimer Blends**
 A. Ramzi¹⁰⁷ and B. Bauer¹⁰⁷
- Microstructure and Properties of Hyperbranched Polymers**
 N. Wagner¹⁸¹ and Y. Kim⁴⁰
- Morphology of Single Graft Block Copolymers**
 S. Trevino^{98,11}, N. Beck-Tan¹¹, S. Guido¹⁸⁹ and C. Lee¹⁸⁹
- Neutron Reflectivity Study of the Phase Separation in dPB/PI Blends Using a Unique Back Transformation Technique**
 A. Schreyer^{188,98}, C. F. Majkrzak⁹⁸, N. Berk⁹⁸, H. Gruell¹⁰⁷, C. Han¹⁰⁷
- Neutron Studies of Polymer Dynamics in Intercalated Polymer-Clay Nanocomposites**
 R. Ivkov¹⁰⁷, P. M. Gehring⁹⁸, N. Maliszewskyj⁹⁸, P. Papanek^{98,199} and R. Krishnamoorti¹⁸⁴
- Nucleation and Growth in Binary Polymer Mixtures Initiated by Pressure Jumps**
 N. Balsara¹²⁵, A. Lefebvre¹²⁵, H. Lee¹²⁵ and B. Hammouda⁹⁸
- Phase Separation in Polymer Thin Films**
 H. Gruell¹⁰⁷, C. Han¹⁰⁷ and S. Kumar¹²³
- Polybutadiene/XP-50 Polymer Blends**
 M. Rabeony⁴⁴, C. Elspass⁴⁴ and R. Garner⁴⁴
- Polyolefin Star Polymer, Linear Polymer Blends**
 R. Garner⁴⁴ and M. Lin⁴⁴
- Polymer Chain Conformation in Thin Films: Deviations from Bulk Behavior in d-PS/PS Films**
 S. Kumar¹²³, R. Jones¹²³, R. Briber¹⁸⁸, L. Ho¹⁸⁴ and T. Russell¹⁸⁹
- Polymer Interdiffusion Near the Polymer/Solid Interface**
 E. K. Lin¹⁰⁷, D. J. Pochan¹⁰⁷, W. Wu¹⁰⁷, S. K. Satija⁹⁸ and R. Kolb⁴⁴
- Pressure Dependence of the Order-Disorder Transition in Diblock Copolymers**
 M. Pollard¹⁸⁹ and T. Russell¹⁸⁹
- Pressure Effects on Crystallization and Phase Behavior of Binary Polyolefin Blends**
 R. Krishnamoorti¹⁸⁴, M. Modi¹⁸⁴ and B. Hammouda⁹⁸
- PS-PANa Diblock Copolymers in Solution**

Polymers

Block Copolymer Domain Morphology

S. Trevino^{98,11}

Chain Conformation and Interaction Parameters of Polyolefin Polymer Blends

D. Lohse⁴⁴, M. Rabeony⁴⁴ and R. Garner⁴⁴

Conformation of Polymer Chains Confined in Controlled Pore Glass

R. Briber¹⁸⁸, D. Ho¹⁸⁴ and I. Teraoka¹²⁵

Conformation of Random Copolymers in Solution

J. Li⁴⁴ and M. Lin⁴⁴

SANS Study of Block Copolymer (“Crew Cut”) Micelles as Solubilizing Agents

D. Nguyen¹²⁶ and M. Moffitt⁸³,

SANS Study of Phase Separation in Model Polymer Networks

B. Viers¹⁸⁰

SANS Study of the Thermodynamics of Blends of Star and Linear Polymers

M. Foster¹⁶⁹, T. Zook¹⁶⁹ and C. Greenberg¹⁶⁹

Self-Assembly of Polyethylene-Propylene-Ethylene Triblock Copolymers in Selective Solvents

L. Fetters⁴⁴, D. Richter⁶¹, M. Monkenbush⁶¹ and W. Leube⁶¹

Shear-Induced Order-Disorder Transition in Diblock Copolymer Solutions

C.-I. Huang¹⁹¹, T. Lodge¹⁹¹ and C. Han¹⁰⁷

Shear Induced Polymer Desorption

E. Lin¹⁰⁷, R. Kolb¹⁰⁷ and W. L. Wu¹⁰⁷

Shear-Induced Polymer Melt Desorption from an Attractive Solid Surface

E. K. Lin¹⁰⁷, D. J. Pochan¹⁰⁷, W. Wu¹⁰⁷, S. K. Satija⁹⁸ and R. Kolb⁴⁴

Shear-Induced Structure of Ethylene-Propylene Copolymer Aggregates in Selective Solvents

H. Ou-Yang⁷⁷ and M. Islam¹⁰⁷

Solution Structure of Arborescent Graft Polymers

R. Briber¹⁸⁸, S. Choi¹⁸⁸, M. Gauthier²¹³, B. Bauer¹⁰⁷ and A. Topp¹⁰⁷

Spinodal Decomposition in PS/PI Blends

H. Jinnai⁷⁶, Hayashi⁷⁶ and C. Han¹⁰⁷

Surface Segregation in Binary Blends of Topologically Distinct Polymers

M. D. Foster¹⁶⁹, C. C. Greenberg¹⁶⁹ and D. M. Teale¹⁶⁹

Structure and Morphology of Semicrystalline Polymer Thin Films

D. J. Pochan¹⁰⁷, E. K. Lin¹⁰⁷, W. Wu¹⁰⁷, C. F. Majkrzak⁹⁸, S. K. Satija⁹⁸ and R. Kolb⁴⁴

Structure of Genetically Engineered Triblock Copolymer Gels

S. Kennedy¹⁸⁹ and T. Russell¹⁸⁹

Thermal Expansion and Glass Transition Behavior of Polymer Films: Effect of the Free Surface and Confinement between Non-interacting Surfaces

D. J. Pochan¹⁰⁷, E. K. Lin¹⁰⁷, W. Wu¹⁰⁷, S. K. Satija⁹⁸ and S. Z. D. Cheng¹⁶⁹

Two-Stage Spinodal Decomposition in a Rubber Blend

M. Hayashi⁷⁶ and C. Han¹⁰⁷

Complex Fluids

Clay Platelet Correlations Under Shear

C. J. Glinka⁹⁸ and J. Ramsay¹⁶⁵

Compatibility of Oil Mixtures at High Temperatures

H. Aldrich⁴⁴ and M. Lin⁴⁴

Conformation and Interactions in Polystyrene Sulfonate Aqueous Polyelectrolyte Solutions

B. Ermi¹⁰⁷, Y. Zhang¹⁰⁷ and E. Amis¹⁰⁷

Dendrimer Interactions in Solution

R. Ivkov¹⁰⁷, G. Nisato¹⁰⁷ and E. Amis¹⁰⁷

Effects of Polymers on Colloidal Interactions

R. Ivkov¹⁰⁷ and E. Amis¹⁰⁷

Effects of Polyacrylic Acid on the Suspension of Natural and Synthetic Clays in Aqueous Solutions

R. Ivkov¹⁰⁷ and E. Amis¹⁰⁷

Electrostatic and Counterion-Specific Effects on Micelle Morphology Probed with SANS

L. Magid²⁰⁴, P. Butler⁹⁸ and Z. Han¹⁰⁷

Flocculation and Sedimentation of Ratawi Asphaltenes

E. Sheu¹⁵⁴

Flow-Induced Microstructural Transitions in Polyampholyte-Polymer Colloid Mixtures

N. Wagner¹⁸¹, K. A. Vaynberg¹⁸¹ and R. Sharma¹⁸¹

Kinetics of Poiseuille Flow-Induced Structures in Solutions of Thread-like Micelles

W. Hamilton¹¹⁴, P. Butler⁹⁸, Z. Han¹⁵⁴ and L. Magid²⁰⁴

Kinetics of Polymerization of Rod-Like Micelles

S. Kline⁹⁸

Microstructure of Alkylpolyglucoside Micelles and Microemulsions

L. Ryan¹⁸¹, D. Ianspetro¹⁸¹, C. McKelvey¹⁸¹, J. Silas¹⁸¹ and E. Kaler¹⁸¹

Microstructure of Shear Thickening and Shear Thinning Suspensions

N. Wagner¹⁸¹, J. Amante¹⁸¹, B. Moranzano¹⁸¹ and R. Butera⁴¹

Mixed Cationic/Anionic Vesicle Formation Kinetics Using Time-Resolved SANS

P. Huibers⁸¹, L. Shen⁸¹ and I. Goldmints⁸¹

Ordered Structures of Pluronic Micelles in Formamide Solutions

P. Alexandridis¹⁴², L. Yang¹⁴², S. Ahn¹⁴² and Y. Lin¹⁴²

Poiseuille-Flow-Induced Changes in the Structure of Surfactant Micelles

L. Walker²³, B. Thebaud²³, B. Poore²³, M. Truong²³, Y. Christanti²³ and B. Hammouda⁹⁸

Pressure-Induced Swelling of Polymer Micelles in Supercritical Fluids

M. McHugh⁷², T. diNoia⁷², J. van Zanten⁷², C. Kirby⁷², T. Kermis⁷² and S. Conroy⁷²

Reverse Micelles

S. Trevino^{98,11}, N. Beck-Tan¹¹, K. Freeman³⁸, S. Lee³⁸ and J. Deitzel^{98,11}

SANS Characterization of Amine-Based Heavy Oil Emulsifiers

E. Sheu¹⁵⁴

SANS Determination of the Persistence Length in Rod-Like Micelles

L. Magid²⁰⁴ and P. Butler⁹⁸

SANS Investigation of Stimuli Responsive Hybrid Linear-Dendrimer Copolymers in Various Solvents

M. Diallo²¹, B. Bauer¹⁰⁷ and B. Hammouda⁹⁸

SANS Measurements of Liposome Size Distributions

S. Trevino^{98,11}, F. Lebeda²¹⁶ and G. R. Matyas¹²

SANS Study of the Factors Affecting the Crystallization of Wax in Fractionated Petroleum

J. Hsu¹⁵⁴ and E. Sheu¹⁵⁴

SANS Study of Interfacial Curvature in Microemulsions

S.-H. Chen⁸¹ and S.-M. Choi⁸¹

SANS Study of Organic-Template-Driven Synthesis of Transition Metal Mesoporous Oxides

S. Elder¹¹⁵ and P. Butler⁹⁸

Search for Surface Enrichment in Ultrafine Aerosol Droplets Using SANS

B. Wyslouzil²¹⁹, J. Cheung²¹⁹, G. Wilemski¹⁹³ and R. Strey⁶⁰

Shear-Induced Structure in Dilute Aqueous Solutions of Thread-like Surfactant Micelles

T. Slawecki⁹⁸ and C. Glinka⁹⁸

Shear-Induced Structural Transitions in Triblock Copolymer Micellar Solutions

T. Slawecki⁹⁸, C. Glinka⁹⁸ and B. Hammouda⁹⁸

Shear-Induced Structure in Rodlike Micelles

P. Butler⁹⁸ and C. Sommer³³

Static and Shear Flow Structure of Laponite Clay Aqueous Dispersions

D. Ho¹⁸⁸, R. Briber¹⁸⁸, C. Glinka⁹⁸ and R. Krishnamoorti¹⁸⁴

Structure and Aggregation of Soot in Flowing Motor Oil

M. Lin⁴⁴ and M. Francisco⁴⁴

Structure and Interactions in Dense Colloidal Mixtures

S. Kline⁹⁸ and E. Kaler¹⁸¹

Structure and Polymerization of CTAT-/Styrene/D₂O Microemulsions

S. Kline⁹⁸

Structure of Ni(OH)₂ Sheared Dispersions of Colloidal Hard Plates

A. Rennie²² and A. Brown²²

Solvent Effects on the Size and Shape of Dendrimers

S. Trevino^{98,11} and N. Beck-Tan¹¹

Static and Flowing Microstructure of Drilling Muds

M. Paquette³⁷, N. Moll³⁷ and C. Glinka⁹⁸

Structure of PEO-PPO-PEO Tri-Block Copolymer Micelles

I. Goldmints⁸¹ and P. Huibers⁸¹

Temperature and Concentration Dependence of Polymer (PEO)–Surfactant (SDS) Complexes in Aqueous Solutions

K. Chari⁴² and M. Lin⁴⁴

Condensed Matter Physics

A Bond-Valence Analysis of the Structure of $\text{Ba}_{0.875}\text{Sr}_{0.125}\text{RuO}_3$

A. Santoro⁹⁸, I. Natali Sora^{98,167} and Q. Huang^{98,188}

A Bond-Valence Analysis of the Structure of $\text{YBa}_2\text{Fe}_3\text{O}_8$

I. Natali Sora^{98,167} and A. Santoro⁹⁸

Anisotropic Spin Hamiltonians Due to Spin-Orbit and Coulomb Exchange-Interactions

T. Yildirim⁹⁸, A. B. Harris¹⁹⁹, A. Aharony¹⁷³ and O. Entin-Wohlman¹⁷³

Antiferromagnetic Ordering of $\text{La}_{0.33}\text{Ca}_{0.67}\text{MnO}_3$ Thin Films

Y. Ijiri⁹⁸, J. A. Borchers⁹⁸, J. W. Lynn⁹⁸, R. W. Erwin⁹⁸, M. Rajeswari¹⁸⁸, M. C. Robson¹⁸⁸, R. Ramesh¹⁸⁸ and V. Venkatesan¹⁸⁸

Antiferromagnetic Spin Ordering in $\text{FeMn/Ni}_{80}\text{Fe}_{20}$ Superlattices

Y. Ijiri⁹⁸, J. A. Borchers⁹⁸, D. Dender^{98,188} and R. W. Erwin⁹⁸, J.-C. A. Huang⁸⁹ and C-H Lee⁹⁴

Characterization of the Antiferromagnetic Order in Exchange-biased $\text{Ni}_{80}\text{Fe}_{20}/\text{CoO}$ Bilayers

N. Gokemeijer⁷⁰, C. L. Chien⁷⁰, Y. Ijiri⁹⁸, J. A. Borchers⁹⁸ and R. W. Erwin⁹⁸

Characterization of the Crystal and Magnetic Structures of Dicyanamide Complexes by Neutron Powder Diffraction

C. R. Kmety-Stevenson¹¹⁶, J. L. Manson²⁰⁹, Q. Huang^{98,188}

Charge and Magnetic Ordering in $\text{La}_{1/2}\text{Ca}_{1/2}\text{MnO}_3$

Q. Huang^{98,188}, J. W. Lynn⁹⁸, V. Smolyaninova¹⁸⁸, K. Ghosh¹⁸⁸ and R. L. Greene¹⁸⁸, D. Dender⁹⁸ and R. W. Erwin⁹⁸

Critical Magnetic Scattering in LaCaMnO_3

L. Vasiliiu-Doloc^{98,188} and J. Lynn⁹⁸

Crystal and Magnetic Structures in $\text{Co}_{2.25}\text{Ru}_{0.75}\text{O}_4$ and $\text{Co}_{2.25}\text{Sn}_{0.25}\text{Ru}_{0.50}\text{O}_4$

Q. Huang^{98,188}, J. W. Lynn⁹⁸, R. W. Erwin⁹⁸, M. Crawford³⁹, R. L. Harlow³⁹ and E. M. McCarron³⁹

Crystal and Magnetic Structures of NiF_3

L. Chacon¹⁷², N. Rosov⁹⁸ and J. W. Lynn⁹⁸

Structural Change and Charge Ordering in Bilayered $\text{La}_{2-2x}\text{Sr}_{1+2x}\text{Mn}_2\text{O}_7$

W.-H. Li⁸⁸, S. Y. Wu⁸⁸ and H. D. Yang⁹²

Crystal Structure and Magnetic Ordering in CoMoO_3

Q. Huang^{98,188}, J. W. Lynn⁹⁸, R. W. Erwin⁹⁸ and M. Crawford³⁹

Crystal Structure and Magnetic Order in the Nd-based CMR Compounds

W.-H. Li⁸⁸, K. C. Lee⁸⁸, R. S. Liu⁹³, C. Y. Huang^{98,188} and J. W. Lynn⁹⁸

Crystal Structure of the Ca-Doped $(\text{La}/\text{Sr})_3\text{Mn}_2\text{O}_7$

W.-H. Li⁸⁸, S. Y. Wu⁸⁸ and H. D. Yang⁹²

Determination of the Crystal Structure of Conducting Polymer $\text{Fe}(\text{OCl})$ and Aniline $\text{Fe}(\text{OCl})$

W.-H. Li⁸⁸, S. Y. Wu⁸⁸ and C.-G. Wu⁸⁸

Determination of the Spin Hamiltonian for a Spin-1/2 Antiferromagnetic with a Spin Gap

M. Stone⁷², J. Rittner⁷², D. H. Reich⁷² and C. Broholm^{72,98}

Effect of Si-Doping on the Spin-Peierls Phase of CuGeO_3

S.-H. Lee^{98,188}, P. M. Gehring⁹⁸, K. Hirota¹⁵⁶, G. Shirane²⁰, T. Masuda²⁰⁵, K. Uchinokura²⁰⁵ and M. Hase⁶²

Effect of Superconductivity on the Lattice Dynamics of $\text{Ba}_{0.6}\text{K}_{0.4}\text{BiO}_3$

C. P. Adams^{98,188}, J. W. Lynn⁹⁸ and S. N. Barilo¹⁷

Effect of Zn Substitution on the Magnetic Resonance Peak in $\text{YBa}_2\text{Cu}_3\text{O}_7$

H. F. Fong¹²⁷, B. Keimer¹²⁷ and R. W. Erwin⁹⁸

Effects of Field Cycling on Co/Cu and Co/Ag Multilayers

J. A. Borchers⁹⁸, J. A. Dura⁹⁸ and C. F. Majkrzak⁹⁸, S. Y. Hsu⁸⁷, R. Loloee⁸⁷, W. P. Pratt, Jr.⁸⁷ and J. Bass⁸⁷

Effects of H on Magnetic Coupling in FeV Superlattices

B. Horvarsson¹³², G. Andersson¹³², J. A. Dura⁹⁸, T. Udovic⁹⁸, C. F.

Majkrzak⁹⁸

Effects of Si-Doping on Magnetic Excitations in the Spin-Peierls System, CuGeO_3

S.-H. Lee^{98,188}, G. Shirane²⁰, P. M. Gehring⁹⁸ and K. Hirota¹⁵⁶

Flux Lattice Structure in Nb and BaKBiO_3

D. Dender^{98,188}, C. Adams^{98,188} and J. Lynn⁹⁸

Ground-State Selection in FCC and FCT Antiferromagnets Due to Quantum Disorder

T. Yildirim⁹⁸, A. B. Harris¹⁹⁹ and E. F. Shender¹⁷²

Incommensurate and Commensurate Magnetic Structures in the Magnetoinsensitive $\text{R}_2\text{Ni}_3\text{Si}_5$ Materials

F. Bourdarot³¹, S. Skanthakumar⁸, J. W. Lynn⁹⁸ and L. C. Gupta¹⁴⁶

Incommensurate Spin Fluctuations and Structural Transitions in Excess Oxygen-doped $\text{La}_2\text{CuO}_{4+x}$

R. J. Birgeneau⁸¹, Y. S. Lee⁸¹, R. J. Christianson⁸¹, M. A. Kastner⁸¹ and R. W. Erwin⁹⁸

Influence of Interface Structure on the Magnetic Polarizability of a Pd-Co Alloy Overlayer in Close Proximity to CoPt_3

M. Fitzsimmons⁷⁸, F. Hellman¹⁷⁵, B. Maran¹⁷⁵, A. Shapiro¹⁷⁵

Interfacial Spin States in Magnetic Tunnel Junction Multilayers

C. Platt¹⁷⁵, A. E. Berkowitz¹⁷⁵, J. A. Borchers⁹⁸, J. A. Dura⁹⁸ and C. F. Majkrzak⁹⁸

Interlayer Spin Coupling in FeMn-based Spin Valves

J. A. Borchers⁹⁸, C. F. Majkrzak⁹⁸, A. Reilly⁸⁷, W. P. Pratt, Jr.⁸⁷ and J. Bass⁸⁷

Lattice Dynamics of a Material with Negative Thermal Expansion, ZrW_2O_8

G. Ernst⁸⁰, C. Broholm^{72,98}, A. P. Ramirez⁸⁰, G. Kovacs⁸⁰ and G. Gasparovic⁷²

Low-Temperature Neutron Diffraction Studies of $\text{Pr}_3(\text{Fe},\text{Co})_{27.5}\text{Ti}_{1.5}$ Permanent Magnets

V. G. Harris⁹⁵ and Q. Huang^{98,188}

Magnetic and Crystal Structure Phase Transitions in $\text{R}_{1-x}\text{Ba}_x\text{CoO}_{3-y}$ ($\text{R}=\text{Nd},\text{Gd}$)

I. O. Troyanchuk¹⁷, D. D. Khalyavin¹⁷, T. K. Solovykh¹⁷, H. Szymczak¹⁷, Q. Huang^{98,188} and J. W. Lynn⁹⁸

Magnetic Correlations and Lattice Distortions in the Bilayer Manganite $\text{La}_{1.2}\text{Sr}_{1.8}\text{Mn}_2\text{O}_7$

L. Vasiliiu-Doloc^{98,188}, S. Rosenbranz⁸, R. Osborn⁸, S. K. Sinha⁸, J. W. Lynn⁹⁸ and J. F. Mitchell⁸

Magnetic Correlations in Discontinuous Co-SiO_2 Thin Films and Multilayers

S. Sankar¹⁸⁸, A. E. Berkowitz¹⁷⁵, D. Dender^{98,188}, J. A. Borchers⁹⁸, R. W. Erwin⁹⁸, S. R. Kline⁹⁸, J. A. Dura⁹⁸ and C. F. Majkrzak⁹⁸

Magnetic Depth Profile of CMR Perovskite Films and Spin Valves

Y. Ijiri⁹⁸, J. A. Borchers⁹⁸, J. W. Lynn⁹⁸, R. W. Erwin⁹⁸, C. F. Majkrzak⁹⁸, M. Robeson¹⁸⁸, R. Ramesh¹⁸⁸, V. Venkatesan¹⁸⁸ and R. Greene¹⁸⁸

Magnetic Domains in Co/Cu Multilayers

J. A. Borchers⁹⁸, J. A. Dura⁹⁸, C. F. Majkrzak⁹⁸, J. Unguris¹⁰³, D. Tulchinsky¹⁰³, M. H. Kelley¹⁰³, R. Celotta¹⁰³, S. Y. Hsu⁸⁷, R. Loloee⁸⁷, W. P. Pratt, Jr.⁸⁷ and J. Bass⁸⁷

Magnetic Domain Structure in CoPt Thin Films

C. Glinka⁹⁸ and M. Toney⁵⁴

Magnetic Domain Structure of Thermally Treated Nanocrystalline Ni_3Fe

H. Frase²¹ and L. Robertson¹¹⁵

Magnetic Ordering in the Spin-Ladder Compound CaCu_2O_3

V. Kiryukhin⁸¹, Y.-J. Kim⁸¹, R. Erwin⁹⁸, R. J. Birgeneau⁸¹

Magnetic Ordering in the System $\text{La}_{1-x}\text{Pr}_x\text{BaCuFeO}_5$

W. Momburu¹⁶², F. Araujo-Moreira¹⁸⁸, L. Suescun²⁰⁸

Magnetic Structure and Site Occupancies in $\text{YFe}_{11-x}\text{Co}_x\text{Ti}$ for $x=1,3,7$, and 9

J. K. Liang⁵⁹, Q. Huang^{98,188} and A. Santoro⁹⁸

Magnetic Field Effects on Antiferromagnetic Ordering in a Fe/FeF_2 Bilayer

Y. Ijiri⁹⁸, J. A. Borchers⁹⁸, R. W. Erwin⁹⁸, M.-C. Cyrille¹⁷⁵, I. K. Schuller¹⁷⁵, J. Nogues¹⁶³ and D. Lederman²¹⁸

Magnetic Order and Crystal Field Effects in RNiBC

F. Bourdarot^{26,98}, J. W. Lynn⁹⁸, Q. Huang^{98,188}, D. R. Sanchez²⁸, M. B. Fontes²⁸, J. C. Trochez²⁸ and E. Baggio-Saitovitch²⁸

Magnetic Order and Fluctuations in a Zig-Zag Spin-1/2 Chain

I. A. Zaliznyak^{72,98}, C. Broholm^{72,98}, M. Kibune²⁰⁵ and H. Takagi²⁰⁵

Magnetic Order in Pr-Containing Cuprate Superconductors

W.-H. Li⁸⁸, K. C. Lee⁸⁸, H. C. Ku⁹⁴ and J. W. Lynn⁹⁸

- Magnetic Order in Tb-Containing Cuprate Superconductors**
W.-H. Li⁹⁸, K. C. Lee⁸⁸ and H. D. Yang⁹² and J. W. Lynn⁹⁸
- Magnetic Order in the Superconductor RNi₂B₂C**
J. W. Lynn⁹⁸, S. Skanthakumar⁸, Z. Hossain¹⁴⁶, L. C. Gupta¹⁴⁶, R. Nagarajan¹⁴⁶ and C. Godart²⁷
- Magnetic Order, Structure, and Spin Dynamics of (La_{1-x}Ca_x)MnO₃**
J. W. Lynn⁹⁸, R. W. Erwin⁹⁸, J. A. Borchers⁹⁸, Q. Huang^{98, 188}, A. Santoro⁹⁸, K. Ghosh¹⁸⁸ and R. L. Greene¹⁸⁸
- Magnetic Properties of HoVO₄**
C. K. Loong⁸, S. Skanthakumar⁸, J. W. Lynn⁹⁸ and G. K. Liu¹⁸⁸
- Magnetic Ordering and Structure of PrBa₂Fe₃O₈**
N. Rosov⁹⁸, J. W. Lynn⁹⁸, M. Seyedahmadian⁸⁰ and T. Yeun⁸⁰
- Magnetic Ordering in Dy₅O₅Ge₁₀**
S. Skanthakumar⁸, J. W. Lynn⁹⁸, L. C. Gupta¹⁴⁶, M. Lin⁴⁴ and S. K. Sinha⁸
- Magnetic Ordering of Exchange-Biased Fe₃O₄/NiO Superlattices**
J. A. Borchers⁹⁸, R. W. Erwin⁹⁸, Y. Ijiri⁹⁸, D. M. Lind⁴⁶ and P. G. Ivanov⁴⁶
- Magnetic Ordering of Mn in Nd_{1-x}Ca_xMnO₃**
S. Y. Wu⁸⁸, W.-H. Li⁸⁸, K. C. Lee⁸⁸, J. W. Lynn⁹⁸, R. S. Liu⁹³, J. B. Wu⁹³ and C. Y. Huang^{98, 188}
- Magnetism of Ferrihydrite Nanoparticles**
M. S. Seehra²¹⁸, V. Suresh Babu²¹⁸ and J. W. Lynn⁹⁸
- Nature of Spin And Charge Ordering In Different Phases Of La_{2-8x}Pr_xCa_yMnO₃**
S.-H. Lee⁹⁸, T. Kim¹³⁵ and S.-W. Cheong¹³⁵
- Neutron and X-ray Diffraction Study of the Crystal Structure of Bi₁₀Sr₈O_x**
Q. Huang^{98, 188} and W. Wong-Ng¹⁰²
- Neutron and X-ray Diffraction Study of the Crystal Structure of Sr_{0.495}Ca_{0.165}Bi_{0.39}O_x**
Q. Huang^{98, 188} and W. Wong-Ng¹⁰²
- Neutron and X-ray Powder Diffraction Study of RBa₂Fe₃O_{8+y} Phases**
P. Karen¹⁹⁸, A. Kjekshus¹⁴, Q. Huang^{98, 188}, J. W. Lynn⁹⁸, N. Rosov⁹⁸, I. Natali-Sora⁹⁸, V. L. Karen⁹⁸, A. D. Mighell⁹⁸ and A. Santoro⁹⁸
- Neutron Powder Diffraction Determination of the Structure of Sr₃Ru₂O₇**
Q. Huang^{98, 188}, J. W. Lynn⁹⁸, R. W. Erwin⁹⁸, A. Santoro⁹⁸ and R. J. Cava¹²⁷
- Neutron Powder Diffraction Study of the Crystal Structure and Magnetic Ordering of Ca₂Y₂Cu₅O₁₀**
T. Fong¹²⁷, Q. Huang^{98, 188}, J. W. Lynn⁹⁸, A. Hayashi²⁰, R. J. Cava¹²⁷ and B. Keimer¹²⁷
- Neutron Reflectivity Studies of Fe₃O₄/NiO Exchange-Biased Bilayers**
D. M. Lind⁴⁶, J. A. Dura⁹⁸ and C. F. Majkrzak⁹⁸
- Neutron Scattering Study of the Nuclear and Magnetic Structure of RD₃**
T. J. Udovic⁹⁸, Q. Huang^{98, 188}, J. W. Lynn⁹⁸, R. W. Erwin⁹⁸ and J. J. Rush⁹⁸
- Neutron Studies of New Incommensurate Magnetic Correlations Near the Lower Critical Concentration for Stripe Order in La_{1.6-x}Nd_{0.4}Sr_xCuO₄**
J. M. Tranquada²⁰, N. Ichikawa²⁰⁵, P. M. Gehring⁹⁸ and S.-H. Lee^{98, 188}
- Observation of Pr Magnetic Order in PrBa₂Cu₃O₇**
S. Skanthakumar⁸, J. W. Lynn⁹⁸, N. Rosov⁹⁸, G. Cao⁴⁶, J. E. Crow⁴⁶, S. Uma⁸³ and A. Erb¹⁸²
- Off-Specular Scattering from Magnetic Domains in Co/Cu/Co Spin Valves**
J. A. Borchers⁹⁸, N. Persat¹³⁸ and H. A. M. van den Berg¹³⁸
- Polarized Neutron Diffraction Studies of Magnetic Ordering in Exchange-Biased Fe₃O₄/CoO Superlattices**
Y. Ijiri⁹⁸, J. A. Borchers⁹⁸, R. W. Erwin⁹⁸, S.-H. Lee^{98, 188}, C. F. Majkrzak⁹⁸, P. J. van der Zaag¹²⁴ and R. M. Wolf¹²⁴
- Polarized-Neutron Scattering Measurements of the Oxygen Moment in (La,Sr)MnO₃**
P. M. Gehring⁹⁸, G. Shirane²⁰ and H. Hirota¹⁵⁶
- Polarized Neutron Studies of Magnetic Interfacial Roughness in EuTe/PbTe Superlattices**
H. Kapa^{119, 98}, T. Giebultowicz¹¹⁹, G. Bauer¹¹⁹, C. F. Majkrzak⁹⁸
- Pressure Dependence Nuclear and Magnetic Structures in La_{0.67}Ca_{0.33}MnO₃**
Q. Huang^{98, 188}, J. W. Lynn⁹⁸, A. Santoro⁹⁸, S. F. Trevino^{98, 11}
- Q-Dependence of the Spin Flip Scattering from Exchange Coupling across Fe-Fe₂ Interfaces Measured with Spin Polarized Neutron Diffraction with Polarization Analysis**
M. Fitzsimmons⁷⁹ and I. Schuller¹⁷⁵
- Reflectivity Measurements on Spin Valve Structures**
D. Sarkisov²⁰⁰ and M. Dabaghian²⁰⁰
- Single-Ion Anisotropy and Crystal Field Effects in R₂CuO₄ (R=Nd, Sm, Pr, ...)**
T. Yildirim⁹⁸, R. Sachidanandam¹⁵², A. Aharony¹⁵² and A. B. Harris¹⁵⁹
- Site Distributions and Magnetic Structures in Al_{0.5}Fe_{0.5-x}Mn_x, x=0.05,0.1,0.15**
V. Harris⁹⁵, D. J. Farnell⁹⁵, K. B. Hathaway⁹⁵, Q. Huang^{98, 188}, A. Mohan¹⁹³ and G. J. Long¹⁹³
- Site Distributions and Magnetic Structures in La₂(Co_{1-x}Fe_x)₁₆Ti for x=0,0.2,0.4**
J. K. Liang⁵⁹, Q. Huang^{98, 188} and A. Santoro⁹⁸
- Small-Angle Magnetic Scattering from Nanocrystal-line Cobalt**
J. Weismüller¹⁶⁶, R. D. Shull¹⁰², R. McMichael¹⁰², U. Erb¹²⁸ and J. Barker⁹⁸
- Spin Chain Direction in Copper Pyrazine Nitrate**
M. Stone⁷², D. H. Reich⁷² and C. Broholm^{72, 98}
- Spin Dynamics of Er³⁺ in ErBa₂Cu₃O₇**
S. Skanthakumar⁸, J. W. Lynn⁹⁸ and F. Dogan²¹²
- Spin Dynamics of the Mn Ions in La_{1-x}Ba_xMnO₃ and Pr_{1-x}Ba_xMnO₃**
J. W. Lynn⁹⁸, L. Vasiliiu-Doloc^{98, 188}, K. Ghosh¹⁸⁸, R. L. Greene¹⁸⁸ and S. Barilo¹⁷
- Spin-Flop Tendencies in Exchange-biased Co/CoO Thin Films**
J. A. Borchers⁹⁸, Y. Ijiri⁹⁸, S.-H. Lee^{98, 188}, C. F. Majkrzak⁹⁸, G. Felcher⁸, R. Kodama⁹⁵, K. Takano¹⁷⁵ and A. E. Berkowitz¹⁷⁵
- Spin Freezing in a Geometrically Frustrated Antiferromagnet, Y₂Mo₂O₇**
J. Gardner⁸⁴, B. Gaulin⁸⁴, C. Broholm^{72, 98} and S.-H. Lee^{98, 188}
- Spin Gap in a Three Dimensional Frustrated Magnet, ZrCr₂O₄**
S.-H. Lee^{98, 188}, C. Broholm^{72, 98} and S.-W. Cheong⁸⁰
- Spin Wave Dispersion Relations in the Magnetoresistive Pyrochlore Tl₂Mn₂O₇**
J. W. Lynn⁹⁸, L. Vasiliiu-Doloc^{98, 188} and M. A. Subramanian⁷⁹
- Static and Dynamic Properties of Spin and Charge Ordering in La_{2-x}Sr_xNiO₄**
S.-H. Lee^{98, 188}, S.-W. Cheong⁸⁰ and G. Aeppli⁹⁶
- Structure and Magnetic Order in Ba₂MRu₂O₆, M=Cu, Fe, Co, Ni, In**
J. T. Rijssenbeek¹²³, Q. Huang^{98, 188}, R. W. Erwin⁹⁸ and R. J. Cava¹²⁷
- Structure and Magnetic Order in Sr₃CaRu₂O₉**
Q. Huang^{98, 188} and R. J. Cava¹²⁷
- Structure and Magnetic Order in Sr₂Y_{0.8}Ca_{0.2}Co₂O₆**
Q. Huang^{98, 188}, J. W. Lynn⁹⁸, R. W. Erwin⁹⁸ and R. J. Cava¹²⁷
- Structure Determination of Tl₂(Ba_{0.6}Sr_{0.4})₂Ca₂Cu₃O_y (1-2) Superconductors**
F. Izumi⁹⁰ and Q. Huang^{98, 188}
- Structure Determination of KCa₂Nb₃O₁₀-Li (T_c=5.5) Superconductors**
F. Izumi⁹⁰ and Q. Huang^{98, 188}
- Structure Determination of Zeolites AFI Series AlPO₄-5, Al₁₂P₁₂O₄₈**
F. Izumi⁹⁰ and Q. Huang^{98, 188}
- Structure of LaRuO₃**
Q. Huang^{98, 188}, A. Santoro⁹⁸ and R. J. Cava¹²⁷
- Structure of YCo_{0.5}Mn_{0.5}O_{3-x}, Tb_{0.5}Ba_{0.5}CoO₄ and Nd_{0.5}Ba_{0.5}CoO₄**
Q. Huang^{98, 188}, J. W. Lynn⁹⁸, R. W. Erwin⁹⁸ and I. Troyanchuk⁵
- Structures of HgMo_{0.25}Ba₂CuO_{4+y} High T_c Superconductors**
Q. Huang^{98, 188}, M. Marezio⁶⁵, F. Licci⁶⁵ and A. Santoro⁹⁸
- Structures and Magnetic Properties of Pr₃(Fe_{1-x}Co_x)_{27.5}Ti_{1.5}**
V. Harris⁹⁵ and Q. Huang^{98, 188}
- Structure of Ba_{0.8}Sr_{0.2}CoO_y**
Q. Huang^{98, 188} and R. J. Cava¹²⁷
- Structures of YM₂Cu_{2.885}Re_{0.15}O_{7+x} (M=Ba and Sr) High T_c Superconductor**
Q. Huang^{98, 188}, M. Marezio⁶⁵, F. Licci⁶⁵ and A. Santoro⁹⁸
- Structure Change of BaRuO₃ Under High Pressure**
Q. Huang^{98, 188}, S. Trevino^{98, 11}, A. Santoro⁹⁸, R. J. Cava¹²⁷
- Structural Phase Transition and Magnetic Order in Heavy Fermion Compounds Ce₃M with M=Al, In, and Sn**
W.-H. Li⁸⁸, K. C. Lee⁸⁸ and Y. Y. Chen⁸⁰
- Structural Scattering from BKBO Cubic Superconductor**
S. Barilo¹⁷ and J. Lynn⁹⁸
- Structure and Magnetic Ordering of M^{II}[N(CN)₂]₂ (M=Co, Ni, Mn)**
J. L. Manson²⁰⁹, C. R. Kmetz-Stevenson¹¹⁶, Q. Huang^{98, 188}, J. W. Lynn⁹⁸, G. Bendele¹⁴², S. Pagola¹⁴², P. W. Stephens¹⁴², L. M. Kiable-Sands²⁰, A.

- L. Rheingold²⁰, A. J. Epstein¹¹⁶ and J. S. Miller²⁰⁹
Studies of Magnetic Critical Scattering in Strained and Lattice-Matched (Y/Lu)Ho(Y/Lu) Films
 P. M. Gehring⁹⁸, C. F. Majkrzak⁹⁸, L. D. Gibbs²⁰, A. Vigliante²⁰, A. C. Lake¹²¹, J. Goff¹²¹ and R. A. Cowley¹²¹
- Studies of Spin Waves in the Ladder Compound $\text{La}_5\text{Ca}_9\text{Cu}_{24}\text{O}_{41}$**
 M. Matsuda⁶⁸, G. Shirane²⁰, S.-H. Lee^{98, 188} and P. M. Gehring⁹⁸
- Study of the Origin of Incommensurate Spin Fluctuations in $\text{La}_{2-x}\text{Sr}_x\text{Cu}_1\text{Zn}_y\text{O}_4$**
 H. Kimura¹⁵⁶, S. Wakimoto¹⁵⁶, K. Yamada¹⁵⁶, S.-H. Lee^{98, 188}, C. F. Majkrzak⁹⁸, R. Erwin⁹⁸, G. Shirane²⁰, Y. S. Lee⁸¹ and R. Birgeneau⁸¹
- Superconductivity in $\text{La}_{2-x}\text{Sr}_x\text{CuO}_4$**
 S. Wakimoto¹⁵⁶, S. Ueki¹⁵⁶, K. Hirota¹⁵⁶, K. Yamada¹⁵⁶, Y. Endoh¹⁵⁶, R. J. Birgeneau⁸¹, Y. S. Lee⁸¹, M. A. Kastner⁸¹, G. Shirane²⁰, S.-H. Lee^{98, 188} and P. M. Gehring⁹⁸
- Superconductivity, Magnetic Fluctuations, and Magnetic Order in $\text{TbSr}_2\text{Cu}_{2.69}\text{Mo}_{0.31}\text{O}_7$**
 W.-H. Li⁸⁸, W. Y. Chuang, S. Y. Wu⁸⁸, K. C. Lee⁸⁸, J. W. Lynn⁹⁸, H. L. Tsay⁹² and H. D. Yang⁹²
- TbNiBC Diffraction and Critical Scattering**
 F. Bourdaut⁹⁸, Q. Huang^{98, 188} and J. Lynn⁹⁸
- Temperature Dependence of the Exchange Coupling in Fe/Cr Superlattices**
 A. Schreyer⁹⁸, C. F. Majkrzak⁹⁸, T. Schmitte¹⁵⁴
- The Invar Effect in $\text{Fe}_{65}\text{Ni}_{35}$**
 N. Rosov⁹⁸, J. W. Lynn⁹⁸ and M. Acet¹⁶⁴
- The Magnetic Structure of [MnTPP][TCNE] 2PhMe by High-Resolution Neutron Powder Diffraction**
 C. R. Kmetz-Stevenson¹¹⁶, A. J. Epstein¹¹⁶ and J. S. Miller²⁰⁹, E. J. Brandon²⁰⁹
- Three-Dimensional Spin Structure of $\text{Sr}_2\text{CuO}_2\text{Cl}_2$: Field Dependent Neutron Scattering Study**
 T. Yildirim⁹⁸, S. Skanthakumar⁸ and J. W. Lynn⁹⁸
- Ultra-high Energy Resolution Studies of the Second Length Scale in Single Crystal Terbium**
 J. E. Lorenzo⁶⁶, B. Farago⁶⁶, B. F. Frick⁶⁶, P. M. Gehring⁹⁸, C. F. Majkrzak⁹⁸ and G. Shirane²⁰
- Vortex Lattice and Melting in Nb**
 J. W. Lynn⁹⁸, D. Dender^{98, 188} and N. Rosov⁹⁸
- Vortex Lattice Structure and Melting in $\text{Ba}_{0.6}\text{K}_{0.4}\text{BiO}_3$**
 D. Dender^{98, 188}, J. W. Lynn⁹⁸, N. Rosov⁹⁸, C. P. Adams^{98, 188} and S. N. Barilo¹⁷
- Vortex Lattice Structure in High-Tc Bi-2212**
 B. Keimer¹²⁷ and T. Fong¹²⁷
- X-ray Diffraction Characterization of Annealed Metallic Spin-Valve Structures**
 J. A. Borchers⁹⁸, Y. Ijiri⁹⁸, A. M. Zeltser⁴² and N. Smith⁴²

Biomolecular Science

- Aggregation of the Antibiotic Rifamycin and Implications for Chiral Recognition**
 L. Magid²⁰⁴, D. Armstrong¹⁹² and P. Butler⁹⁸
- Characterization of Solvent Bound to Lysozyme**
 A. Tsai²⁵ and S. Krueger⁹⁸
- Colloidal Structure of Collagen Solutions**
 R. Ivkov¹⁰², C. Goh²⁰⁶, S. Ismailova²⁰⁶, M. Paise²⁰⁶ and J. Rainey²⁰⁶
- Conformational Changes of Chaperonin Complexes Involved in Protein Refolding**
 E. Eisenstein²⁵, J. Zondlo²⁵ and S. Krueger⁹⁸
- Determination of the Location of the Lipid Anchor in Outer Surface Protein A of *Borrelia burgdorferi* by SANS**
 D. Schneider²⁰, C. Lawson²⁰ and V. Graziano²⁰
- Gelation of Methylcellulose**
 C.-I. Huang¹⁹¹ and T. Lodge¹⁹¹
- Internal Organization of Peptide-Nucleic Acid Complexes Derived from SANS**
 F. Schwarz²⁵ and S. Krueger⁹⁸
- In-Situ Measurements of Melittin Insertion into Hybrid Bilayer Membranes**
 S. Krueger⁹⁸, C. F. Majkrzak⁹⁸, J. A. Dura⁹⁸, A. Plant¹⁰⁰ and C. Meuse¹⁰⁰

- Investigation of Cellulase Dimerization in Solution**
 S. Henderson¹⁹⁷
- Location of Peptides in Hybrid Bilayer Membranes**
 A. Plant¹⁰⁰, C. Meuse¹⁰⁰, S. Krueger⁹⁸, C. F. Majkrzak⁹⁸ and J. A. Dura⁹⁸
- Magnetic Field Alignment of Discotic Micelles**
 J. Zhao⁷⁸, J. Trehwella⁷⁸ and A. Bax⁹¹
- Magnetic Field Alignment of Mixed Lipid Discotic Micelles**
 J. Katsaras²⁹, R. Prosser⁷⁴, S. Krueger⁹⁸ and C. Glinka⁹⁸
- Membrane Active Peptides: Phase Transitions and Supramolecular Assemblies of Peptides in Membranes**
 H. W. Huang¹³⁰, W. Heller¹³⁰, T. Harroun¹³⁰ and L. Yang¹³⁰
- Microbial Sphorolipids: Effect of Chain Structure on Bilayer Morphology**
 W. Orts¹⁶¹, R. A. Gross⁸¹, S. Krueger⁹⁸ and C. F. Majkrzak⁹⁸
- Neutron Diffraction Studies of Peptides in Fluid Lipid Bilayers**
 S. White¹⁷⁴ and K. Hristova¹⁷⁴
- Neutron Reflectivity Studies of Protein Adsorption/Desorption on the Surfaces of Self-Assembled Monolayers**
 M. D. Foster¹⁶⁹, S. Petrash¹⁶⁹ and C. F. Majkrzak⁹⁸
- SANS Search for Conformational Changes in Troponin**
 D. Schneider²⁰ and R. Mendelson¹⁷⁶
- SANS Studies of Calmodulin/Target Enzyme Interactions**
 J. Krueger⁷⁸, J. Trehwella⁷⁸, N. Bishop⁷⁸ and A. Wang¹⁰⁰
- SANS Study of Catechol Dioxygenases from *Pseudomonas putida* SH¹**
 S.-L. Huang⁸⁸, W.-H. Li⁸⁸ and J. W. Lynn⁹⁸
- SANS Study of Cyclic-AMP-Dependent Protein Kinase**
 J. Zhao⁷⁸, J. Trehwella⁷⁸, D. Walsh¹⁷³ and R. Bruschia¹⁷³
- SANS Study of the DNA/Flap Endonuclease Complex**
 J. Trehwella⁷⁸, C. Kim⁷⁸ and S. Gallagher⁷⁸
- SANS Study of the Pressure- and Temperature-Dependent Morphology of the Bile Salt/Lecithin System**
 R. Hjelm⁷⁸ and J. Mang⁷⁸
- SANS Study of Protein Folding Mechanisms**
 R. Briber⁸⁸, R. Perez-Salaz¹⁸⁸ and S. Krueger⁹⁸
- SANS Study of the Ferredoxin/TOL Component of Toluence Dioxygenase from *Pseudomonas Putida* F1**
 S.-L. Huang⁸⁸, D. T. Gibson¹⁸⁷, W.-H. Li⁸⁸ and J. W. Lynn⁹⁸
- Self Assembly of Peptide Amphiphiles**
 H. Bianco¹⁹¹, T. Gore¹⁹¹, Y. Dori¹⁹¹ and M. Tirrell¹⁹¹
- Structural Configurations of Microtubules**
 R. Nossal⁹¹, D. Sackett⁹¹ and S. Krueger⁹⁸
- Structure of Microtubule-based Cellular Motors Investigated by SANS**
 R. Mendelson¹⁷⁶, D. Stone¹⁷⁶ and R. Hjelm⁷⁸
- Vectorially-Oriented Protein Monolayers: Neutron Reflectivity Studies**
 J. K. Blasic¹⁹⁹, L. Kneller¹⁹⁹, E. Nordgren¹⁹⁹, J. Strzalka¹⁹⁹ and A. Edwards¹⁹⁹

Chemical Physics of Materials

- Crystal and Magnetic Structures of Aluminum Silicides**
 K. Prassides¹⁴⁴, S. Margadonna¹⁴⁴, B. Sieve⁸⁷, M. Kanatzidis⁸⁷ and D. A. Neumann⁹⁸
- Deposition Interdiffusion at Room Temperature and the Kinetics of Interlayer Diffusion in Barium Stearate Langmuir-Blodgett Films at the Temperature Just Below the Melting Point**
 L. A. Feigin⁶⁷ and I. I. Samoilenko⁶⁷
- Dynamics of Arsenic-Selenium Glasses**
 B. Effey¹¹⁷, R. L. Cappelletti¹¹⁷ and W. A. Kamitakahara⁹⁸
- Dynamics of Hydrogen Trapped by Defects in Pd**
 R. Kichheim²⁰², T. J. Udovic⁹⁸ and J. J. Rush⁹⁸
- Dynamics of Hydrogen Trapped by N-Doped Ta**
 M. Heene³⁵, H. Wipf³⁵, T. J. Udovic⁹⁸ and J. J. Rush⁹⁸
- Dynamics of Layered Silicates: Intercalated Water**
 N. Wada¹⁵⁷ and W. A. Kamitakahara⁹⁸
- Dynamics of Li-Doped Carbon Electrode Materials**
 P. Papanek^{98, 199}, P. Zhou¹⁹⁹, J. E. Fischer^{191, 199} and W. A. Kamitakahara⁹⁸
- Dynamics of Hydrogen in C-15 Laves Phase Hydrides**
 A. V. Skripov⁸⁵, J. C. Cook^{188, 98}, C. Karmonik^{98, 188} and D. A. Neumann⁹⁸

- Evolution of the Structure of the K_2NiF_4 Phases of $La_{2-x}Sr_xNiO_{4-\delta}$ with Oxidation State: Octahedral Distortion and Phase Separation ($0.2 < x < 1.0$)**
J. E. Millburn¹²¹, M. A. Green¹²¹, M. J. Rosseinsky¹²¹ and D. A. Neumann⁹⁸
- First-Principles Calculations of Structural, Vibrational and Electronic Properties of Solid Cubane**
T. Yildirim⁹⁸
- Fulleride Superconductors**
T. Yildirim⁹⁸
- Hydrogen Dynamics in K_3MnH_5**
G. Auffermann¹⁶⁸, T. J. Udovic⁹⁸, J. J. Rush⁹⁸ and C. Karmonik^{98, 188}
- Hydrogen Dynamics in $ZrBeH_{1.5}$**
F. Altorfer^{98, 122}, T. J. Udovic⁹⁸ and B. Hauback⁶³
- Inelastic Neutron Scattering Study of the Dynamics of Crown Ethers in Potassium Electrides**
N. C. Maliszewskyj⁹⁸, D. A. Neumann⁹⁸, M. Wagner⁵⁰ and J. L. Dye⁸⁷
- Inelastic Neutron Scattering Study of the Dynamics of Guanidinium-Based Clathrate Materials**
A. Pivovar¹⁹¹, M. Ward¹⁹¹, D. A. Neumann⁹⁸, T. Yildirim⁹⁸ and J. J. Rush⁹⁸
- Inelastic Neutron Scattering Study of the Hydration of Tricalcium Silicate**
S. A. FitzGerald⁹⁸, D. A. Neumann⁹⁸, J. J. Rush⁹⁸, R. J. Kirkpatrick¹⁸⁵, X. Cong¹⁸⁵ and R. A. Livingston⁴⁵
- Inelastic Neutron Scattering Study of Rare Earth Trihydrides and Trideuterides**
T. J. Udovic⁹⁸, J. J. Rush⁹⁸ and Q. Huang^{98, 188}
- Inelastic Neutron Scattering Study of Al Charged with Hydrogen**
T. J. Udovic⁹⁸, J. J. Rush⁹⁸, C. Buckley¹⁸⁵ and H. K. Bimbaum¹⁸⁵
- Inelastic Neutron Scattering Study of $H_5O_2^+$ Ions and their Partially Deuterated Analogs in $(H_5O)_3PW_{12}O_{40}$**
N. C. Maliszewskyj⁹⁸ and T. J. Udovic⁹⁸
- In Situ Neutron Reflectometry Study of Self-Assembled Poly(Dimethyl Siloxane) Film**
M.-W. Tsao¹⁸¹, J. Rabolt¹⁸¹, A. Kalambur¹⁸¹, L. Sung^{98, 188} and C. F. Majkrzak⁹⁸
- Investigation of the Powder-Averaged Structure of LaF_3**
T. J. Udovic⁹⁸ and Q. Huang^{98, 188}
- Neutron and X-ray Reflectometry Studies of Rough Interfaces in a Langmuir Blodgett Film**
H. Kepa¹¹⁹, L. J. Kleinwalks¹⁵⁵, N. F. Berk⁹⁸, C. F. Majkrzak⁹⁸, T. S. Berzina, V. I. Troitsky¹⁵¹, R. Antolini²⁰⁷ and L. A. Feigin⁶⁷
- Neutron Investigation of Molecular Reorientations in Solid Cubane**
T. Yildirim⁹⁸, P. M. Gehring⁹⁸, D. A. Neumann⁹⁸, P. E. Eaton¹⁷⁹ and T. E. Emrick¹⁷⁹
- Neutron Scattering Studies of Hydration Reaction of Tricalcium Silicate in Various Atmospheres**
S. A. FitzGerald⁹⁸, D. A. Neumann⁹⁸, J. J. Rush⁹⁸ and R. A. Livingston⁴⁵
- Neutron Scattering Studies of the Dynamics of Hydrofluorocarbons Encaged in NaX and NaY Zeolites**
C. Karmonik^{98, 188}, N. C. Maliszewskyj⁹⁸, T. J. Udovic⁹⁸, J. J. Rush⁹⁸, M. K. Crawford³⁹, D. R. Corbin³ and R. R. Cavanagh¹¹⁰
- Neutron Scattering Studies on the Vibrational Excitations and the Structure of Ordered Niobium Hydrides**
B. Hauer⁶¹, E. Jansen⁶¹, W. Kockelmann⁶¹, W. Schafer⁶¹, D. Richter⁶¹, R. Hempelmann¹⁶⁶, T. J. Udovic⁹⁸ and J. J. Rush⁹⁸
- Neutron Scattering Study of the Structure of Na_2C_{60} as a Function of Pressure and Temperature**
T. Yildirim⁹⁸, D. A. Neumann⁹⁸, S. F. Trevino^{98, 11} and J. E. Fischer¹⁹⁹
- Neutron Scattering Study of the Dynamics of Hydrogen and Deuterium Solved in Crystalline Pd_9Si_2**
C. Karmonik^{98, 188}, T. J. Udovic⁹⁸, Q. Huang^{98, 188}, J. J. Rush⁹⁸, Y. Andersson²¹⁰ and T. B. Flanagan²¹⁰
- Neutron Scattering Study of the Vibrational Modes of Cubane**
T. Yildirim⁹⁸, P. M. Gehring⁹⁸, D. A. Neumann⁹⁸, P. E. Eaton¹⁷⁹ and T. E. Emrick¹⁷⁹
- Layer Shearing Modes in Li-Graphite Compounds**
W. A. Kamitakahara⁹⁸, C. Bindra¹⁹⁹ and J. E. Fischer¹⁹⁹
- Low Energy Dynamics of Alkali Silicate Glasses**
J. Toulouse⁷⁷ and D. A. Neumann⁹⁸
- Orientational Order and Disorder in C_{60}**
J. R. D. Copley⁹⁸ and K. H. Michel¹⁷⁰
- Orientational Dynamics of P_4 Molecules in White Phosphorus**
W. A. Kamitakahara⁹⁸, T. Yildirim⁹⁸, D. A. Neumann⁹⁸ and F. Gompf⁷³
- Preferential Isotopic Site Occupation in $Y(D_2H_{1-y}H_{2y})_{3-x}$**
T. J. Udovic⁹⁸, Q. Huang^{98, 188} and J. J. Rush⁹⁸
- Proton Dynamics in Strontium Cerate and Zirconate Ceramics**
C. Karmonik^{98, 188}, T. Yildirim⁹⁸, T. J. Udovic⁹⁸, J. J. Rush⁹⁸, R. L. Paul⁹⁹, K. Lind¹⁶⁶ and R. Hempelmann¹⁶⁶
- Quasielastic Neutron Scattering Study of the Hydration Reaction of Tricalcium Silicate**
S. A. FitzGerald⁹⁸, D. A. Neumann⁹⁸, J. J. Rush⁹⁸, D. P. Bentz¹⁰¹ and R. A. Livingston⁴⁵
- Relaxational Dynamics in GeO_2**
A. Meyer^{98, 188}, J. Neuhaus¹⁴⁹ and H. Schober⁶⁶
- RNaseA Dynamics by Time of Flight Neutron Scattering: A Case Study in Protein Dynamics and its Implications for Drug Design, Formulation and Delivery**
A. Tsai²⁵, T. J. Udovic⁹⁸, J. R. D. Copley⁹⁸, D. A. Neuman⁹⁸, J. J. Rush⁹⁸, M. Tarek^{98, 199}, D. Tobias¹⁷⁴ and G. Gilliland¹⁰⁰
- Rotational dynamics of C_{60} in $(ND_3)_2K_2C_{60}$**
S. Margadonna¹⁴⁴, K. Prassides¹⁴⁴, D. A. Neumann⁹⁸, H. Shimoda² and Y. Iwasa²
- Search for Sublattice Ordering in PrD_{2+x}**
T. J. Udovic⁹⁸ and Q. Huang^{98, 188}
- Slow Motion in Bulk-Glass Forming $Zr_{46.8}Ti_{8.2}Cu_{7.5}Ni_{10}Be_{27.5}$**
A. Meyer^{98, 188}, J. Wuttke¹⁴⁹, W. Petry¹⁴⁹ and H. Schober⁶⁶
- Structural and Magnetic Ordering in DyD_{3-x}**
T. J. Udovic⁹⁸, Q. Huang^{98, 188}, J. Lynn⁹⁸ and R. Erwin⁹⁸
- Structural and Magnetic Ordering in ErD_{3-x}**
T. J. Udovic⁹⁸, Q. Huang^{98, 188}, J. Lynn⁹⁸ and R. Erwin⁹⁸
- Structural Investigation of the High Temperature Protonic Conductors**
C. Karmonik^{98, 188}, Q. Huang^{98, 188}, T. J. Udovic⁹⁸, J. J. Rush⁹⁸ and R. Hempelmann¹⁶⁶
- Structural Ordering in LaD_{3-x}**
T. J. Udovic⁹⁸, Q. Huang^{98, 188} and J. J. Rush⁹⁸
- Structural Study of TmD_{3-x}**
T. J. Udovic⁹⁸, Q. Huang^{98, 188} and J. J. Rush⁹⁸
- Structure and Dynamics of Amorphous Carbon**
P. Papanek^{98, 199}, W. A. Kamitakahara⁹⁸ and J. E. Fischer¹⁹¹
- Structure and Dynamics of Hydrogen in C_{60}**
S. A. FitzGerald⁹⁸, T. Yildirim⁹⁸, L. J. Santodonato⁹⁸, D. A. Neumann⁹⁸, J. R. D. Copley⁹⁸ and J. J. Rush⁹⁸
- Structure and Dynamics of Hydrogen in Na_xC_{60}**
S. A. FitzGerald⁹⁸, T. Yildirim⁹⁸, L. J. Santodonato⁹⁸ and D. A. Neumann⁹⁸
- Structure and Dynamics of K_xC_{60} in the Orthorhombic Phase**
H. M. Guerrero, R. L. Cappelletti¹¹⁷, D. A. Neumann⁹⁸ and T. Yildirim⁹⁸
- Structure of the Ruddlesden-Popper, $(Ln,Ca)_{n+1}Mn_nO_{3n+1}$ Series (Ln=Lanthanide)**
M. Green¹³³ and J. Waldron¹³³
- The Dynamics of Potassium Crytand Complexes**
N. C. Maliszewskyj⁹⁸, D. A. Neumann⁹⁸, D. J. Gilbert⁸⁷ and J. L. Dye⁸⁷
- The Microscopic Glass Transition in Viscous Metallic Liquids**
A. Meyer^{98, 188}, R. Busch²¹, J. Neuhaus¹⁴⁹ and H. Schober⁶⁶
- The Vibrational Isocoordinate Rule in Se-As-Ge Glasses**
B. Effey¹¹⁷, R. L. Cappelletti¹¹⁷ and W. A. Kamitakahara⁹⁸
- Vibrational Densities of States for Cubic and Hexagonal Boron nitride**
W. A. Kamitakahara⁹⁸, D. A. Neumann⁹⁸, G. Doll⁴⁹, B. Sweeting⁴⁹ and A. W. Moore¹

Instrumentation

- Characterization of Fe/Si Reference Layers for Reflectivity Data Inversion**
C. F. Majkrzak⁹⁸
- Construction of the Epoxy Tanzboden for the NIST Neutron Spin Echo (NSE) Spectrometer**
W. Clow⁹⁸
- “DARTS”: A New Neutron Diffractometer for Residual Stress Measure-**

- ment, **Texture Determination and Single Crystal Diffraction**
P. C. Brand⁹⁸, H. J. Prask⁹⁸ and T. Gnäupel-Herold¹⁸⁸
- Development and Installation of a Leak-tight, Top-loading, Horizontal Field Superconducting Magnet**
D. Dender^{98,188} and R. Erwin⁹⁸
- Development and Installation of a Remote Controlled Monochromator Changer for the BT-9 Thermal Triple Axis Spectrometer**
K. T. Forstner⁹⁸, P. Brand⁹⁸, A. Clarkson⁹⁸ and T. Thai⁹⁸
- Development of a Radially-Focussed Polarizing Supermirror Analyzer Array**
M. Murbach¹⁸⁸, P. Brand⁹⁸, and N. Rosov⁹⁸
- Development of a Robust Static Thermal Switch for Fixed Sample Environment Temperatures from 15-650K**
L. Santodonato⁹⁸
- Development of Synthetic Mica Monochromators**
K. T. Forstner⁹⁸ and L. Passell²⁰
- Development and Testing of Fe/Ni Supermirror Plates for the NSE Analyzer**
N. Rosov⁹⁸, S. Rathgeber⁶¹, C. F. Majkrzak⁹⁸ and J. Wood¹²⁰
- Development of a VME-Based Data Acquisition System for the HFBS**
P. D. Gallagher⁹⁸, N. C. Maliszewskyj⁹⁸ and M. Kirsch¹⁴³
- Development and Testing of the Doppler Drive System for the HFBS**
R. Christman⁹⁸, P. Brand⁹⁸ and C. Karmonik^{98,188}
- Development of a Vacuum Rated Pre-amplifier/Amplifier/-Discriminator for He Neutron Detectors**
J. Ziegler⁹⁸
- Design of a Cable and Hose Management System for the NSE Spectrometer**
D. Fulford⁹⁸
- Design and Development of the Filter Analyzer Spectrometer**
D. J. Pierce⁹⁸, R. Christman⁹⁸, J. Kenney⁹⁸ and D. A. Neumann⁹⁸
- The High Flux Backscattering Spectrometer (HFBS)**
P. M. Gehring⁹⁸, D. A. Neumann⁹⁸, C. Karmonik^{98,188} and A. Meyer⁹⁸
- The Disk Chopper Time-of-Flight (DCS)**
J. R. D. Copley⁹⁸, J. C. Cook^{188,98} and F. B. Altofer⁹⁸
- Design and Fabrication of the Voltage and Signal Distribution System for the DCS Detectors**
H. Layer⁹⁸, J. Raebiger⁶¹, M. Garland⁹⁸, D. Kulp⁹⁸, P. Tobin⁹⁸ and T. Thai⁹⁸
- Design and Installation of the Sample Chamber, Flight Chamber and Detector Assembly for the DCS**
C. Bocker⁹⁸, M. Rinehart⁹⁸, G. M. Baltic⁹⁸ and Slifer⁹⁸
- Design and Performance Testing of the DCS Data Acquisition System Electronics**
H. Layer⁹⁸, J. Raebiger⁶¹, P. Klosowski⁹⁸ and N. C. Maliszewskyj⁹⁸
- Evaluation of New Neutron Area-Detectors**
Y. T. Cheng^{99,97}
- Evaluation of a Beryllium Single Crystal as a Monochromator for "DARTS"**
P. C. Brand⁹⁸ and T. Gnäupel-Herold¹⁸⁸
- The Filter Analyzer Spectrometer**
D. A. Neumann⁹⁸, P. Papanek¹⁹⁹, J. E. Fischer¹⁹⁹, J. J. Rush⁹⁸, M. L. Klein¹⁹⁹ and A. C. Cheetham¹⁷⁷
- Hydrogen Cold Source Development**
R. E. Williams⁹⁸, P. A. Kopetka⁹⁸ and J. M. Rowe⁹⁸
- Installation and Alignment of the Spherically Focussed Si(111) Analyzer Assembly for the HFBS**
C. H. Appel¹²⁰, R. Wise¹²⁰, G. M. Baltic⁹⁸, M. Rinehart⁹⁸ and S. Slifer⁹⁸
- Installation and Testing of the New Thermal Beam Tube Shutter Design Using a Remote Actuated Cast System**
J. Moyer⁹⁸, C. Wrenn⁹⁸, P. Brand⁹⁸, A. Clarkson⁹⁸, G. M. Baltic⁹⁸, D. Clem⁹⁸, M. Rinehart⁹⁸ and S. Slifer⁹⁸
- Laue Focussing and Its Applications**
V. K. Kvardakov⁷⁵, V. A. Somenkov⁷⁵, S. Shilstein⁷⁵, J. W. Lynn⁹⁸, D. R. Mildner⁹⁹ and H. Chen⁹⁹
- MBE Chamber for *In-Situ* Neutron Scattering: Instrument Development**
J. A. Dura⁹⁸
- Mica and Ge Reflectivity**
K. T. Forstner⁹⁸ and C. F. Majkrzak⁹⁸
- Monte Carlo Methods for Nuclear Applications**
R. E. Williams⁹⁸
- Monte Carlo Simulation of the NIST Cold Neutron Beamlines**
J. C. Cook^{188,98}
- Neutron Powder Diffraction Study of the Crystal Structure of Ba_{0.78}Sr_{0.22}RuO₃**
I. Natali Sora^{98,171}
- The NIST Neutron Spin Echo Spectrometer (NSE)**
N. Rosov⁹⁸, S. Rathgeber⁶¹ and M. Monokenbusch⁶¹
- Osmic and Mica Supermirror Tests**
K. T. Forstner⁹⁸ and C. F. Majkrzak⁹⁸
- The Perfect Crystal SANS Diffractometer**
J. G. Barker⁹⁸, C. J. Glinka⁹⁸, A. Drews⁹⁸ and M. Agamalian¹¹⁵, and J. Moyer⁹⁸
- Performance Tests of the Optical Filter and Chopper System for the DCS, Including Crystal Filter Options**
J. R. D. Copley⁹⁸, J. C. Cook^{188,98}, N. C. Maliszewskyj⁹⁸ and D. J. Pierce⁹⁸
- Performance Tests of the Phase Space Transform Chopper on NG-2**
P. M. Gehring⁹⁸, D. A. Neumann⁹⁸ and C. Karmonik^{98,188}
- Spin Echo Supermirror Development**
N. Rosov⁹⁸ and C. F. Majkrzak⁹⁸
- Supermirror Reflectivity Measurements**
C. F. Majkrzak⁹⁸
- Testing and Optimization of a Rise-Time Encoding 2-D Neutron Detector for the NSE**
S. Rathgeber⁶¹ and J. Ziegler⁹⁸

Neutron Physics

- Accurate Determination of Neutron Capture Flux**
M. S. Dewey¹⁰⁴, M. Arif¹⁰⁴, D. Gilliam¹⁰⁴, G. L. Greene⁷⁸, W. M. Snow⁵⁸, J. Pauwels⁶⁴, and R. Scott⁸²
- Benchmark Measurements and Calculations of Neutron Transport**
D. Gilliam¹⁰⁴, M. S. Dewey¹⁰⁴, J. Nico¹⁰⁴, C. Eisenhauer¹⁰⁴, J. Grundl¹⁰⁴, and H. Gerstenberg¹⁰
- Certified Neutron Fluence Standards from the Cavity Fission Source**
J. Adams¹⁰⁴ and J. Grundl¹⁰⁴
- Defined-Geometry Alpha Counting**
D. Gilliam¹⁰⁴ and J. Nico¹⁰⁴
- Determination of the Neutron Lifetime**
M. S. Dewey¹⁰⁴, J. Nico¹⁰⁴, D. Gilliam¹⁰⁴, W. M. Snow⁵⁸, G. L. Greene⁷⁸ and X. Fei⁵⁸
- Highly Accurate Neutron Wavelength Measurements**
M. S. Dewey¹⁰⁴, K. Coakley¹⁰⁹, W. M. Snow⁵⁸, and M. Arif¹⁰⁴
- Intercomparison of NIST and PNL Calibration Facilities**
A. Thompson¹⁰⁴, R. Schwartz¹⁰⁴, J. McDonald¹⁵, and M. Murphy¹⁵
- LASER Polarization of ³He for Neutron Spin Filters and Medical MRI**
A. Thompson¹⁰⁴, T. Gentile¹⁰⁴, M. S. Dewey¹⁰⁴, G. L. Jones^{104,58}, F. Wietfeldt^{104,52}, W. M. Snow⁵⁸, and R. Rizzi¹⁹⁹
- Neutron Calorimetry**
W. M. Snow⁵⁸, Z. Chowdhuri⁵⁸, X. Fei⁵⁸, and M. S. Dewey¹⁰⁴
- Neutron Fluence Rate Measurements**
D. Gilliam¹⁰⁴, J. Nico¹⁰⁴, and J. Adams¹⁰⁴
- Neutron Interferometry and Optics**
M. Arif¹⁰⁴, D. Jacobson¹⁰⁴, R. Clothier¹⁸, A. Thompson¹⁰⁴, S. Werner¹⁹², A. Ioffe^{192,104}, A. Zeilinger¹⁸⁶, K. Raum¹⁹⁴, B. Schillinger¹⁹⁴, C. Rausch¹⁹⁴, and W. Richards⁸²
- Neutron Radiography/Tomography**
T. Gentile¹⁰⁴, M. Arif¹⁰⁴, and D. Jacobson¹⁰⁴
- Parity Non-Conserving Neutron Spin Rotation**
B. Hecke¹²¹², D. Markoff²¹², E. Adelberger²¹², S. Penn²¹², and F. Wietfeldt^{104,52}
- Quality Assurance Checks on Masses and Impurities in Neutron Dosimeters for NRC Reactor Pressure Vessel Embrittlement Surveillance**
J. Adams¹⁰⁴, D. Gilliam¹⁰⁴, and J. Grundl¹⁰⁴
- Response of Albedo Dosimeters Versus Distance from a Neutron Source**
R. Schwartz¹⁰⁴ and A. Thompson¹⁰⁴
- Response of Albedo Neutron Dosimeters as a Function of Angle**
R. Schwartz¹⁰⁴
- Study of Time Reversal Invariance in Neutron Beta Decay**

J. Wilkerson²¹⁷, E. Wasserman¹⁷², J. Nico¹⁰⁴, R. G. H. Robertson¹⁷², S. Freedman¹⁷², A. Garcia¹⁹⁶, T. Chupp¹⁴, K. Coulter¹⁴, M. S. Dewey¹⁰⁴, G. L. Greene⁷⁸, A. Thompson¹⁰⁴, B. Fujikawa¹⁷², G. L. Jones^{104,58}, J. Adams¹⁰⁴, F. Wietfeldt^{104,52}, L. Lising¹⁷², S. Hwang¹⁴ and T. Steiger²¹²

Trapping of Ultra Cold Neutrons

J. Doyle⁵², S. Lamoreaux, R. Golub⁵¹, G. L. Greene⁷⁸, M. S. Dewey¹⁰⁴, P. Huffman⁵², C. Brome⁵², C. Mattoni⁵², J. Butterworth⁵², and D. McKinsey⁵²

Utilization of the Materials Dosimetry Reference Facility-Tests of New IRMM ²³⁷Np and ²³⁸U Fast Neutron Dosimeters

J. Adams¹⁰⁴, J. Grundl¹⁰⁴, C. Eisenhauer¹⁰⁴, D. Gilliam¹⁰⁴, and P. Simpson¹⁴

Materials Analysis

A Bender-Focuser for Prompt Gamma Activation Analysis

E. A. Mackey⁹⁹, H. H. Chen-Mayer⁹⁹, R. M. Lindstrom⁹⁹, D. F. R. Mildner⁹⁹, R. L. Paul⁹⁹, Q.-F. Xiao²¹¹ and V. A. Sharov²²⁰

Analytical Applications of Cold Neutrons

H. H. Chen-Mayer⁹⁹, R. Demiralp⁹⁹, R. R. Greenberg⁹⁹, G. P. Lamaze⁹⁹, J. K. Langland⁹⁹, R. M. Lindstrom⁹⁹, E. A. Mackey⁹⁹, D. F. R. Mildner⁹⁹, R. L. Paul⁹⁹ and V. A. Sharov²²⁰

Applications of Neutron Laue Diffraction Focusing Methods

H. H. Chen-Mayer⁹⁹, V. V. Kvardakov¹²³, J. W. Lynn⁹⁸, D. F. R. Mildner⁹⁹ and V. A. Sharov²²⁰

Application of Radioisotope-Induced X-Ray Emission to the Identification of Lead and Other Elements in Ceramic Glazes and Housewares

D. L. Anderson⁴⁷ and W. C. Cunningham⁴⁷

Archeological Applications of NAA

R. Bishop¹³⁹, M. J. Blackman⁹⁹ and J. E. Myers⁹⁹

Bromation in Breadmaking

W. C. Cunningham⁴⁷ and C. R. Warner⁴⁷

Bio-Analytical and Specimen Bank Research

K. A. Fitzpatrick⁹⁹, R. R. Greenberg⁹⁹, G. V. Iyengar¹⁰⁸, J. K. Langland⁹⁹, E. A. Mackey⁹⁹, B. J. Porter⁹⁹ and R. Zeisler⁹⁹

Certification of Standard Reference Materials by Neutron Activation Analysis

D. A. Becker⁹⁹, R. Demiralp⁹⁹, R. R. Greenberg⁹⁹, R. M. Lindstrom⁹⁹, E. A. Mackey⁹⁹ and R. Zeisler⁹⁹

Characterization of Sources and Fluxes of Particulate Pollutants Depositing to Great Waters

P. F. Caffrey¹⁸⁸, A. E. Suarez¹⁸⁸ and J. M. Ondov¹⁸⁸

Characterization of Submicrometer Aerosol Particles

J. M. Ondov¹⁸⁸, S. F. Heller-Zeisler¹⁸⁸ and R. Zeisler⁹⁹

Determination of Hydrogen by PGAA

R. R. Greenberg⁹⁹, R. M. Lindstrom⁹⁹, E. A. Mackey⁹⁹ and R. L. Paul⁹⁹

Determination of Phosphorus via RNAA with Beta Counting

R. L. Paul⁹⁹

Development of a Position-Sensitive Video Radiation Detector

H. H. Chen-Mayer⁹⁹ and C. J. Zeissler¹¹⁰

Development of Radiochemical Separation for NAA

D. A. Becker⁹⁹, R. R. Greenberg⁹⁹ and E. A. Mackey⁹⁹

Elemental Characterization of High Temperature Superconductors

D. A. Becker⁹⁹, R. R. Greenberg⁹⁹, R. M. Lindstrom⁹⁹ and R. L. Paul⁹⁹

Evaluation of Accuracy and Precision in INAA of Botanical Materials

D. A. Becker⁹⁹

Evaluation of Errors and Interferences in NAA

D. A. Becker⁹⁹, M. J. Blackman¹³⁹, R. R. Greenberg⁹⁹, R. M. Lindstrom⁹⁹ and R. Zeisler⁹⁹

Focusing Methods for Radiography and Topography

H. H. Chen-Mayer⁹⁹, D. F. R. Mildner⁹⁹, K. M. Podurets⁷⁵, V. A. Sharov²²⁰ and S. Shilstein⁷⁵

High Sensitivity Gamma-Ray Spectrometry

R. M. Lindstrom⁹⁹

Homogeneity and Composition of Small Solid Samples

R. Zeisler⁹⁹

Hydrogen Detection in Industrial Materials by Incoherent Neutron Scattering

H. H. Chen-Mayer⁹⁹, V. V. Kvardakov⁷⁵, D. F. R. Mildner⁹⁹ and V. A. Somenkov⁷⁵

Improvements to INAA Methodology

D. A. Becker⁹⁹, R. Demiralp⁹⁹, R. R. Greenberg⁹⁹, R. M. Lindstrom⁹⁹, E. A. Mackey⁹⁹ and R. Zeisler⁹⁹

Improvements to PGAA Methodology

D. L. Anderson⁴⁷, R. M. Lindstrom⁹⁹, E. A. Mackey⁹⁹ and R. L. Paul⁹⁹

Lithium Migration in Electrochromic Thin Films

G. P. Lamaze⁹⁹, H. H. Chen-Mayer⁹⁹, M. Badding¹³⁶, A. Gerouk¹⁵⁹ and R. Goldner¹⁵⁹

Multielement Analysis of Foods and Related Materials by NAA

D. L. Anderson⁴⁷ and W. C. Cunningham⁴⁷

Neutron Absorption Measurements Using Converging Beams

H. H. Chen-Mayer⁹⁹, E. A. Mackey⁹⁹, D. F. R. Mildner⁹⁹ and R. L. Paul⁹⁹

Neutron Autoradiography of Paintings

Y.-T. Cheng^{97,99} and J. Olin¹¹⁸

Neutron Beam Spatial Distributions Using Imaging Plate Technology

H. J. Bahre⁴⁸, H. H. Chen-Mayer⁹⁹, Y.-T. Cheng^{97,99}, D. F. R. Mildner⁹⁹ and V. A. Sharov²²⁰

Neutron Depth Profiling of AlN Thin Films

H. H. Chen-Mayer⁹⁹, G. P. Lamaze⁹⁹ and S. McGuire³²

Neutron Depth Profiling of c-BN

H. H. Chen-Mayer⁹⁹, G. P. Lamaze⁹⁹ and L. Pilione¹⁵

Nitrogen Profiling of Thin Titanium Nitride Films

G. P. Lamaze⁹⁹, H. H. Chen-Mayer⁹⁹, N. Cox⁶⁹ and E. B. Steel¹¹⁰

Neutron Focusing for Analytical Chemistry

H. Chen-Mayer⁹⁹, G. P. Lamaze⁹⁹, J. K. Langland⁹⁹, R. M. Lindstrom⁹⁹, E. A. Mackey⁹⁹, D. F. R. Mildner⁹⁹, V. A. Sharov²²⁰ and J. R. Swider¹¹⁰

Neutron Distribution Measurements by Neutron Induced Autoradiography

Z. En²¹¹, J. S. Brenizer²¹¹ and D. A. Becker⁹⁹

Neutron Dosimetry for Instrument Development

R. M. Lindstrom⁹⁹

Neutron Scattering Effects on PGAA

R. R. Greenberg⁹⁹, R. M. Lindstrom⁹⁹, E. A. Mackey⁹⁹ and R. L. Paul⁹⁹

Neutron Transmission through Tapered Capillaries

H. H. Chen-Mayer⁹⁹, D. F. R. Mildner⁹⁹ and V. A. Sharov²²⁰

New Developments in Monitor Activation Analysis

G. P. Lamaze⁹⁹, R. M. Lindstrom⁹⁹, E. A. Mackey⁹⁹ and R. L. Paul⁹⁹

New Developments in NDP

H. H. Chen-Mayer⁹⁹, G. P. Lamaze⁹⁹ and J. K. Langland⁹⁹

Quality Assurance Improvements for NAA

D. A. Becker⁹⁹, R. Demiralp⁹⁹, R. R. Greenberg⁹⁹, R. M. Lindstrom⁹⁹, E. A. Mackey⁹⁹ and R. Zeisler⁹⁹

Quality Assurance Programs

D. L. Anderson⁴⁷ and W. C. Cunningham⁴⁷

Reactor Characterization for NAA

D. A. Becker⁹⁹

Radionuclides in Foods

D. L. Anderson⁴⁷ and W. C. Cunningham⁴⁷

Revalidation of Food SRMs

D. L. Anderson⁴⁷ and W. C. Cunningham⁴⁷

Size Distribution and Deposition of Toxic Elements to Lake Michigan, by Size and by Source.

P. F. Caffrey¹⁸⁸ and J. M. Ondov¹⁸⁸

Studies in Elemental Speciation

D. A. Becker⁹⁹, E. A. Mackey⁹⁹ and R. Zeisler⁹⁹

Test of a Novel High Sensitivity Neutron Detector

B. Feller¹¹³, H. H. Chen-Mayer⁹⁹ and G. P. Lamaze⁹⁹

Trace Elemental Characterization of Silicon Semiconductor Materials

D. A. Becker⁹⁹ and R. M. Lindstrom⁹⁹

Affiliations:

- 1 Advanced Ceramics Corporation
- 2 Advanced Institute of Science and Technology, Japan
- 3 AEA Technology, United Kingdom
- 4 Air Products Incorporated
- 5 American Manufacture Technology
- 6 Ames National Laboratory
- 7 Appalachian University

8 Argonne National Laboratory
 9 Arizona State University
 10 Armed Forces Radiobiology Research Institute
 11 Army Research Laboratory
 12 Army Medical Research Institute
 13 Australian Geological Survey, Australia
 14 Australian Nuclear Science and Technology Organization, Australia
 15 Battelle Pacific Northwest Laboratory
 16 Bausch and Lomb Incorporated
 17 Belarus Academy of Sciences, Belarus
 18 Bethany College
 19 Boeing Helicopter Group, Philadelphia
 20 Brookhaven National Laboratory
 21 California Institute of Technology
 22 Cambridge University, United Kingdom
 23 Carnegie Mellon University
 24 Caterpillar, Incorporated
 25 Center for Advanced Research in Biotechnology
 26 Centre d-etudes Nucleaires de Grenoble, France
 27 Centre National de Recherche Scientifique, France
 28 Centro Brasileiro de Pesquisas Fisicas, Brazil
 29 Chalk River Laboratories, Canada
 30 Colorado School of Mines
 31 Commissariat a l'Energie-Atomique, France
 32 Cornell University
 33 Cracow University of Technology, Poland
 34 Czechoslovakia Academy of Sciences, Czechoslovakia
 35 Darmstadt University, Germany
 36 Davidson Chemical Company
 37 Dow Chemical Company
 38 Duke University
 39 Dupont Company
 40 Dupont Experimental Station, Wilmington
 41 Dupont Marshall Laboratory
 42 Eastman Kodak
 43 Eidgenössische Technische Hochschule, Switzerland
 44 Exxon Research and Engineering Company
 45 Federal Highway Administration
 46 Florida State University
 47 Food and Drug Administration
 48 Fuji Medical Systems USA, Incorporated
 49 General Motors Research and Development Center
 50 George Washington University
 51 Hahn-Meitner Institute, Germany
 52 Harvard University
 53 IAP Research, Incorporated
 54 IBM, Almaden
 55 Idaho National Engineering and Environment Laboratory
 56 Imaging and Sensing Technology
 57 Imperial College, United Kingdom
 58 Indiana University
 59 Institute of Physics, Peoples Republic of China
 60 Institut Für Physikalische Chemie, Germany
 61 Institut für Festkörperforschung, Germany
 62 Institute for Chemical Research, Japan
 63 Institute for Energiteknikk, Norway
 64 Institute for Reference Materials and Measurements, Belgium
 65 Institute for Special Materials, CNR, Parma, Italy
 66 Institute Laue-Langevin, France
 67 Institute of Crystallography, Russia
 68 Institute of Physical and Chemical Research, Japan
 69 Intel Corporation
 70 Iowa State University
 71 John Deere Corporation
 72 Johns Hopkins University
 73 Karlsruhe Nuclear Research Center, Germany
 74 Kent State University
 75 Kurchatov Institute, Russia
 76 Kyoto University, Japan
 77 Lehigh University
 78 Los Alamos National Laboratory
 79 Los Alamos Neutron Science Center
 80 Lucent Technologies, Bell Laboratories
 81 Massachusetts Institute of Technology
 82 McClellan Nuclear Radiation Center
 83 McGill University, Canada
 84 McMaster University, Canada
 85 Metal Physics Institute, Russia
 86 Michigan Molecular Institute
 87 Michigan State University
 88 National Central University, Taiwan
 89 National Cheng Kung University, Taiwan
 90 National Institute for Research in Inorganic Materials, Japan
 91 National Institute of Health
 92 National Sun Yat-Sen University, Taiwan
 93 National Taiwan University, Taiwan
 94 National Tsing Hua University, Taiwan
 95 Naval Research Laboratory
 96 NEC Research Institute Incorporated
 97 Neutek Incorporated
 98 NIST Center for Neutron Research
 99 NIST, Analytical Chemistry Division
 100 NIST, Biotechnology Division
 101 NIST, Building Materials Division
 102 NIST, Ceramics Division
 103 NIST, Electron and Optical Physics Division
 104 NIST, Ionizing Radiation Division
 105 NIST, Materials Reliability Division
 106 NIST, Metallurgy Division
 107 NIST, Polymers Division
 108 NIST, Standard Reference Materials Program
 109 NIST, Statistical Engineering Division
 110 NIST, Surface and Microanalysis Science Division
 111 NIST, Thermophysics Division
 112 Northeastern University
 113 Nova Scientific
 114 Oak Ridge Institute for Science and Education
 115 Oak Ridge National Laboratory
 116 Ohio State University
 117 Ohio University
 118 Olin Conservation Incorporated
 119 Oregon State University
 120 OSMIC, Incorporated
 121 Oxford University, United Kingdom
 122 Paul Scherrer Institute, Switzerland
 123 Pennsylvania State University
 124 Philips Research Laboratories, The Netherlands
 125 Polytechnic University
 126 PPG Industries
 127 Princeton University
 128 Queen's University, Canada
 129 Raychem Corporation
 130 Rice University
 131 Rothe Development, Incorporated
 132 Royal Institute of Technology, Sweden
 133 Royal Institution, UK
 134 Ruhr University, Germany
 135 Rutgers University
 136 SAGE Electrochromics
 137 Sandia National Laboratory
 138 Siemens
 139 Smithsonian Institute,
 140 Stanford Linear Accelerator
 141 Stanford University
 142 State University of New York, Stony Brook
 143 Struck, Incorporated
 144 Sussex
 145 Sydney University, Australia
 146 Tata Institute of Fundamental Research, India
 147 Technical University Darmstadt, Germany
 148 Technical University Delft, The Netherlands
 149 Technical University Munchen, Germany

150 Technical University of Linz, Austria
151 Technobiochip
152 Tel Aviv University, Israel
153 TEC
154 Texaco Research and Development Center
155 Thomas Jefferson High School
156 Tohoku University, Japan
157 Toyo University, Japan
158 Trinity College
159 Tufts University
160 U. S. Department of Transportation
161 U. S. Drug Administration, ARS
162 Universidad de la Republica Argentina
163 Universitat Autònoma de Barcelona, Spain
164 Universität Duisberg, Germany
165 University de Montpellier II, France
166 University des Saarlandes, Germany
167 University di Brescia, Italy
168 University of Aachen, Germany
169 University of Akron
170 University of Antwerp, Belgium
171 University of Brescia, Italy
172 University of California at Berkeley
173 University of California at Davis
174 University of California at Irvine
175 University of California at San Diego
176 University of California at San Francisco
177 University of California at Santa Barbara
178 University of Central Florida
179 University of Chicago
180 University of Cincinnati
181 University of Delaware
182 University of Geneva, Switzerland
183 University of Goettingen, The Netherlands
184 University of Houston
185 University of Illinois
186 University of Innsbruck, Austria
187 University of Iowa
188 University of Maryland at College Park
189 University of Massachusetts
190 University of Michigan
191 University of Minnesota
192 University of Missouri at Columbia
193 University of Missouri-Rolla
194 University of Munich, Germany
195 University of Nebraska
196 University of Notre Dame
197 University of Oklahoma
198 University of Oslo, Norway
199 University of Pennsylvania
200 University of Rhode Island
201 University of South Australia, Australia
202 University of Stuttgart, Germany
203 University of Sydney, Australia
204 University of Tennessee
205 University of Tokyo, Japan
206 University of Toronto, Canada
207 University of Trento, Italy
208 University of Uruguay
209 University of Utah
210 University of Vermont
211 University of Virginia
212 University of Washington
213 University of Waterloo, Canada
214 Uppsala University, Sweden
215 W. R. Grace
216 Walter Reed Army Institute of Research
217 Washington University
218 West Virginia University
219 Worcester Polytechnic Institute
220 X-Ray Optical Systems

NCNR Staff Publications

- Agamalian, M., Christen, D. K., Drews, A. R., Glinka, C. J., Matsouka, H., Wignall, G. D., "Surface-Induced Parasitic Scattering in Bense-Hart Double Crystal Diffractometers", *J. Appl. Crystallogr.* **31**, 235 (1998).
- Agamalian, M., Iolin, E., Rusevich, L., Glinka, C. J., Wignall, G. D., "Back-Face Bragg Diffraction from a Perfect and Ultralightly Deformed Thick Crystal", *Phys. Rev. Lett.* **81**, 602 (1998).
- Allen, A. J., Berk, N. F., "Probing Porous Ceramics Using Small-Angle Neutron Scattering", *Neutron News* **9**, 13 (1998).
- Balbach, J. J., Conradi, M. S., Hoffmann, M. M., Udovic, T. J., Adolphi, N. L., "NMR Evidence of Disorder and Motion in Yttrium Trideuteride", *Phys. Rev. B*, in press.
- Balsara, N. P., Lefebvre, A. A., Lee, J. H., Lin, C. C., Hammouda, B., "The Search for a Model Polymer Blend", *AIChE J.*, in press.
- Bandyopadhyay, S., Klein, M. L., Martyna, G. J., Tarek, M., "Molecular Dynamics Studies of the Hexagonal Mesophase of Sodium Dodecylsulfate in Aqueous Solution", *Mol. Phys.*, in press.
- Bandyopadhyay, S., Shelley, J. C., Tarek, M., Moore, P. B., Klein, M. L., "Surfactant Aggregation at a Hydrophobic Surface", *J. Phys. Chem. B* **102**, 6318 (1998).
- Bao, W., Broholm, C., Aeppli, G., Carter, S. A., Dai, P., Frost, C. D., Honig, J. M., Metcalf, P., "Magnetic Correlations in a Classic Mott System: Pure and Doped V_2O_3 ", *J. Magn. Magn. Mater.* **177-181**, 283 (1998).
- Bao, W., Broholm, C., Aeppli, G., Carter, S. A., Dai, P., Rosenbaum, T. F., Honig, J. M., Metcalf, P., Trevino, S. F., "Magnetic Correlations in All Four Phases of the Mott System V_2O_3 ", *Phys. Rev. B*, in press.
- Barilo, S. N., Shiryayev, S. V., Gatal'skaya, V. I., Lynn, J. W., Baran, M., Szymczak, H., Szymczak, R., Dew-Hughes, D., "Scaling of Magnetization and Some Basic Parameters of $Ba_{1-x}K_xBiO_{3+y}$ Superconductors near T_C ", *Phys. Rev. B*, in press.
- Barilo, S. N., Shiryayev, S. V., Zhigunov, D. I., Pushkarev, A. V., Gatal'skaya, V. I., Fedotova, V. V., Lynn, J. W., Skanthalakumar, S., Rosov, N., Szymczak, H., Szymczak, R., Baran, M., Nabyalek, A., "Investigation of Electrochemical Growth Conditions for $Ba_{1-x}K_xBiO_3$ Single Crystal Superconductor and Its Magnetic Properties", *Proc. Intl. Conf. on Crystal Growth, OBNIS* (1997), in press.
- Bindra, C., Nalimova, V. A., Sklovsky, D. E., Kamitakahara, W. A., Fischer, J. E., "Statics and Dynamics of Interlayer Interactions in Dense High Pressure Graphite Compound LiC_2 ", *Phys. Rev. B* **57**, 5812 (1998).
- Bödeker, P., Hucht, A., Schreyer, A., Borchers, J. A., Guthoff, F., Zabel, H., "Reorientation of Spin Density Waves in Cr(001) Films Induced by Fe(001) Cap Layers", *Phys. Rev. Lett.* **81**, 914 (1998).
- Borchers, J. A., Ijiri, Y., Lee, S.-H., Majkrzak, C. F., Felcher, G. P., Takano, K., Kodama, R. H., Berkowitz, A. E., "Spin-Flop Tendencies in Exchange-Biased Co/CoO Thin Films", *J. Appl. Phys.* **83**, 7219 (1998).
- Borchers, J. A., Ijiri, Y., Lind, D. M., Ivanov, P. G., Erwin, R. W., Lee, S.-H., Majkrzak, C. F., "Polarized Neutron Diffraction Studies of Exchange-Coupled Fe_3O_4/NiO Superlattices", *J. Appl. Phys.*, in press.
- Borchers, J. A., Majkrzak, C. F., "Magnetic Epitaxial Layers", in *Encyclopedia of Electronics and Electrical Engineering*, edited by John G. Webster (Wiley and Sons), in press.
- Brand, P. C., Prask, H. J., Gnäupel-Herold, T., "Residual Stress Measurements at the NIST Reactor", *Physica B* **241-243**, 1244 (1998).
- Brand, P. C., Prask, H. J., Goff, J., Hutchings, M. T., "Residual Stresses in Bent Steel Tubes", *The 5th Intl. Conf. on Residual Stress*, edited by T. Ericsson, M. Oden, and A. Anderson (Linkopings Univ. Press, 1998), p. 622.
- Broholm, C., Reich, D. H., Aeppli, G., Lee, S.-H., Dender, D. C., Hammar, P., Xu, G., Ditusa, J. F., Ramirez, A. P., "Neutron Scattering Studies of Non-Metallic Low-Dimensional Quantum Antiferromagnets", in *Dynamical Properties of Unconventional Magnetic Systems* edited by A. T. Skjeltorp and D. Sherrington, NATO ASI Series, Series E: Applied Sciences **349**, (Kluwer Academic Publishers, Boston, 1998), p. 77.
- Brown, D. W., Sokol, P. E., FitzGerald, S. A., "Inelastic Neutron Scattering Study of H_2 Adsorbed in Porous Vycor Glass", *Phys. Rev. B*, in press.
- Butler, P. D., Hamilton, W. A., Magid, L. J., Slawewski, T. M., Han, Z., Hayter, J. B., "Effect of a Solid/Liquid Interface on Bulk Solution Structures Under Flow", *Physica B* **241**, 1074 (1997).
- Cava, R. J., Ramirez, A. P., Huang, Q., Krajewski, J. J., "Frustrated Magnetism and Spin-Glass Behavior in Compounds with $YbFe_2O_4$ Structure and Type", *J. Solid State Chem.*, in press.
- Clutter, L. K., ed., "MSEL Materials Science and Engineering Laboratory, NIST Center for Neutron Research—Technical Activities 1997", NISTIR 6067.
- Clutter, L. K., ed., "NIST Center for Neutron Research—Annual Report—October 1996 through September 1997", NISTIR 6112.
- Copić, V., Tomita, Y., Akiyama, S. K., Aota, S., Yamada, K. M., Venable, R. M., Pastor, R. W., Krueger, S., Torchia, D. A., "Solution Structure and Dynamics of Linked Cell Attachment Modules of Mouse Fibronectin Containing the RGD and Synergy Regions: Comparison with the Human Fibronectin Crystal Structure", *J. Mol. Biol.* **277**, 663 (1998).
- Copley, J. R. D., "The Conceptual Design of a Disk Chopper Spectrometer", *Proceedings of a Workshop on Methods for Neutron Scattering Instrument Design*, edited by R. P. Hjelm, E. O. Lawrence Berkeley National Laboratory Report 9609353 (1997).
- Copley, J. R. D., "Neutron Powder Diffraction", *Proceedings of a Workshop on Cold Neutrons in Contemporary Materials Research* (Taiwan, December 15-17, 1997).
- Copley, J. R. D., "Neutron Powder Diffraction", NISTIR 6204.
- Copley, J. R. D., "Neutron Time-of-Flight Spectroscopy", *Proc. Workshop on Cold Neutrons in Contemporary Materials Research*, (Taiwan, December 15-17, 1997).
- Copley, J. R. D., "Neutron Time-of-Flight Spectroscopy", NISTIR 6205.
- Copley, J. R. D., Michel, K. H., "Multiple Orientational Order Parameters in Solid C_{60} ", *Physica B* **241-243**, 454 (1998).
- Cowley, R. A., Gehring, P. M., Gibbs, D., Goff, J. P., Majkrzak, C. F., Lake, B., Vigliante, A., Ward, R. C. C., Wells, M. R., "The Magnetic Phase Transition of a Lattice-Matched Holmium Thin Film", *J. Phys. Condens. Matt.* **10**, 6803 (1998).
- Crawford, M. K., Dobbs, K. D., Smalley, R. J., Corbin, D. R., Maliszewskyj, N. C., Udovic, T. J., Cavanagh, R. R., Rush, J. J., Grey, C. P., "A Raman Spectroscopy Study of the Separation of Hydrofluorocarbons Using Zeolites", *J. Phys. Chem.*, in press.

- Drews, A. R., Barker, J. G., Glinka, C. G., Agamalian, M., "Development of a Thermal-Neutron Double-Crystal Diffractometer for USANS at NIST", *Physica B* **241-243**, 189 (1998).
- Drews, A. R., Cline, J. P., Vanderah, T. A., Salazar, K., "High-Temperature X-Ray Diffraction Studies of a Precursor Mixture for Pb-substituted Bi-2223 Superconducting Wires", *J. Mater. Res.* **13**, 574 (1998).
- Dura, J. A., Richter, C. A., Majkrzak, C. F., Nguyen, N. V., "Neutron Reflectometry, X-ray Reflectometry, and Spectroscopic Ellipsometry Characterization of Thin SiO₂ on Si", *Appl. Phys. Lett.* **73**, 2131 (1998).
- Edler, K. J., Reynolds, P. A., Brown, A. S., Slaweki, T. M., White, J. W., "Shear and Salt Effects on the Structure of MCM-41 Synthesis Gels", *Faraday Commun.* **94**, 1287 (1998).
- Ernst, G., Broholm, C., Kowach, G., Ramirez, A. P., "Phonon Density of States and Negative Thermal Expansion in ZrW₂O₈", *Nature* **396**, 147 (1998).
- FitzGerald, S. A., Neumann, D. A., Rush, J. J., Bentz, D. P., Livingston, R. A., "In Situ Quasi-elastic Neutron Scattering Study of the Hydration of Tricalcium Silicate", *Chem. Mater.* **10**, 397 (1998).
- FitzGerald, S. A., Neumann, D. A., Rush, J. J., Kirkpatrick, R. J., Cong, X., Livingston, R. A., "Inelastic Neutron Scattering Study of the Hydration of Tricalcium Silicate", *J. Mater. Res.*, in press.
- Flanagan, T. B., Clewley, J. D., Noh, H., Barker, J. G., Sakamoto, Y., "Hydrogen-Induced Lattice Migration in Pd-Pt Alloys", *Acta Mater.* **46**, 2173 (1998).
- Flanagan, T. B., Noh, H., Clewley, J. D., Barker, J. G., "Evidence for H-Enhanced Metal Atom Diffusion in Pd-Ni Alloys from SANS and H₂ Solubilities", *Scripta Materiala*, in press.
- Fong, H. F., Keimer, B., Lynn, J. W., Hayashi, A., Cava, R. J., "Spin Structure of the Dopable Quasi-One Dimensional Copper Oxide Ca₂Y₂Cu₃O₁₀", *Phys. Rev. B*, in press.
- Gehring, P. M., Neumann, D. A., "Backscattering Spectroscopy at the NIST Center for Neutron Research", *Physica B* **241-243**, 64 (1998).
- Gibaud, A., Sella, C., Maaza, M., Sung, L., Dura, J., Satija, S. K., "Neutron and X-Ray Reflectivity Analysis of Ceramic-Metal Materials", *Thin Solid Films*, in press.
- Glinka, C. J., Barker, J. G., Hammouda, B., Krueger, S., Moyer, J. J., Orts, W. J., "The 30-Meter Small Angle Neutron Scattering Instruments at the National Institute of Standards and Technology", *J. Appl. Crystallogr.* **31**, 430 (1998).
- Gnäupel-Herold, T., Brand, P. C., Prask, H. J., "Accessing the Elastic Properties of Cubic Materials with Diffraction Methods", *Advances in X-ray Analysis*.
- Gnäupel-Herold, T., Brand, P. C., Prask, H. J., "The Calculation of Single Crystal Elastic Constants for Cubic Crystal Symmetry from Powder Diffraction Data", *J. Appl. Crystallogr.*, in press.
- Godart, C., Alleno, E., Tominez, E., Gupta, L. C., Nagarajan, R., Hossain, Z., Lynn, J., Sanchez, J. P., "Some Chemical and Physical Properties of Quaternary Borocarbides", *J. Solid State Chem.* **133**, 169 (1997).
- Goldman, K. I., Giebultowicz, T. M., Kepa, H., Sinha, S. K., "Numerical Simulation of Neutron Diffraction from Correlated/Uncorrelated Magnetic Multilayers", *Physica B* **241**, 717 (1997).
- Goldman, K. I., Springholz, G., Kepa, H., Giebultowicz, T. M., Majkrzak, C. F., Bauer, G., "Interlayer Correlations in Antiferromagnetic Semiconductor Superlattices EuTe/PbTe", *Physica B* **241**, 710 (1997).
- Green, M. A., Dalton, M., Prassides, K., Day, P., Neumann, D. A., "Lattice Vibrations of the Superconducting Oxide Spinels (Li, Mg)_{1+x}Ti_{2-x}O₄", *J. Phys. Condens. Matt.* **9**, 10855 (1997).
- Green, M. A., Prassides, K., Stalick, J. K., Day, P., "The Crystal Structure of SrSnO₃", *Inorg. Chem.*, in press. *
- Guerrero, H. M., Cappelletti, R. L., Neumann, D. A., Yildirim, T., "Structure and Lattice Dynamics of K₁C₆₀ in the Orthorhombic Phase: A Neutron Scattering Study", *Chem. Phys. Lett.*, in press.
- Hammar, P. R., Reich, D. H., Broholm, C., Trouw, F., "Spin Gap in a Quasi-One-Dimensional S=1/2 Antiferromagnet: Cu₂(1,4-Diazacycloheptane)₂Cl₄", *Phys. Rev. B* **57**, 7846 (1998).
- Hammar, P. R., Stone, M. B., Reich, D. H., Broholm, C., Gibson, P. J., Turnbull, M. M., Landee, C. P., Oshikawa, M., "Characterization of a Quasi-One-Dimensional Spin-1/2 Magnet which is Gapless and Paramagnetic for $g\mu_B H \leq J$ and $k_B T \ll J$ ", *Phys. Rev. B*, in press.
- Hanada, T., Izumi, F., Nakamura, Y., Nittono, O., Huang, Q., Santoro, A., "Neutron and Electron Diffraction Studies of ZnGa₂Se₄", *Physica B* **241-243**, 373 (1998).
- Harris, V. G., Fatemi, D. J., Hathaway, K. B., Huang, Q., Mohan, A., Long, G. J., "Atomic Structure and Magnetism of Ordered and Disordered Al_{0.5}Fe_{0.5-x}Mn_x Alloys", *J. Appl. Phys.*, in press.
- Hauer, B., Hempelmann, R., Udovic, T. J., Rush, J. J., Jansen, E., Kockelmann, W., Schäfer, W., Richter, D., "Neutron-Scattering Studies on the Vibrational Excitations and the Structure of Ordered Niobium Hydrides: The ϵ Phase", *Phys. Rev. B* **57**, 1115 (1998).
- Hayes, C., Alefeld, B., Copley, J. R. D., Lartigue, C., Mezei, F., "On the Use of a Toroidal Mirror to Focus Neutrons at the ILL Neutron Spin Echo Spectrometer IN15", *Proc. Workshop on Methods for Neutron Scattering Instrument Design*, edited by R. P. Hjelm, E.O. Lawrence Berkeley National Laboratory Report 9609353 (1997).
- Heiney, P. A., Gidalevitz, D., Maliszewskij, N. C., Satija, S. K., Vaknin, D., Pan, Y., Ford, W. T., "Multilayer Formation in an Azacrown [18]N₆ Langmuir Film", *Chem. Commun.* **14**, 1483 (1998).
- Huang, Q., Lynn, J. W., Erwin, R. W., Jarupatrakorn, J., Cava, R. J., "Oxygen Displacements and Search for Magnetic Order in Sr₃Ru₂O₇", *Phys. Rev. B* **58**, 8515 (1998).
- Huang, Q., Santoro, A., Lynn, J. W., Erwin, R. W., Borchers, J. A., Peng, J. L., Greene, R. L., "Structure and Magnetic Order in La_{1-x}Ca_xMnO₃ (0 < x ≤ 0.33)", *Phys. Rev. B* **58**, 2684 (1998).
- Idemoto, Y., Izumi, F., Huang, Q., Santoro, A., Matsuzawa, M., Koura, N., "Effects of Sr Substitution on the T_c and Crystal Structure of T₁₂(Ba_{1-x}Sr_x)₂Ca₂Cu₃O_y", in *Chemistry and Technology of High-Temperature Superconductors (HTSC) and Related Advanced Materials*, edited by G. van Tendeloo (Kluwer, Dordrecht), in press.
- Ijiri, Y., Borchers, J. A., Erwin, R. W., Lee, S.-H., van der Zaag, P. J., Wolf, R. M., "Perpendicular Coupling in Exchange-biased Fe₃O₄/CoO Superlattices", *Phys. Rev. Lett.* **80**, 608 (1998).
- Ijiri, Y., Borchers, J. A., Erwin, R. W., Lee, S.-H., van der Zaag, P. J., Wolf, R. M., "Role of the Antiferromagnet in Exchange-Biased Fe₃O₄/CoO Superlattices", *J. Appl. Phys.* **83**, 6882 (1998).
- Ikeda, T., Miyazawa, K., Izumi, F., Huang, Q., Santoro, A., "Structural Study of the Aluminophosphate AlPO_{4.5} by Neutron Powder Diffraction", *J. Phys. Chem. Solids*, in press.

- Ilavsky, J., Stalick, J. K., "Phase Composition of Plasma-Sprayed Yttria Stabilized Zirconia", in *Thermal Spray: A United Forum for Scientific and Technological Advances*, Proc. 1st United Thermal Spray Conference (ASM International, Materials Park, OH, 1998), p. 691.
- Irvine, D. J., Mayes, A. M., Satija, S. K., Barker, J. G., Sofia-Allgor, S. J., Griffith, L. G., "Comparison of Tethered Star and Linear Poly(Ethylene Oxide) for Control of Biomaterials Surface Properties", *J. Biomed. Mater. Res.* **40**, 498 (1998).
- Kaduk, J. A., Toby, B., Wong-Ng, W., Greenwood, W., "Crystal Structure and Standard X-Ray Pattern of $\text{Ba}_4\text{Ti}_{10}\text{Al}_2\text{O}_{27}$ ", *Powder Diffr.* **13**, 178 (1998).
- Karen, P., Kjekshus, A., Huang, Q., Lynn, J. W., Rosov, N., Natali-Sora, I., Karen, V. L., Mighell, A. D., Santoro A., "Neutron and X-ray Powder Diffraction Study of $\text{YBa}_2\text{Fe}_3\text{O}_{6+w}$ Phases", *J. Solid State Chem.* **136**, 21 (1998).
- Karim, A., Slaweki, T. M., Kumar, S. K., Douglas, J. F., Satija, S. K., Han, C. C., Russell, T. P., Liu, Y., Overney, R., Sokolov, J., Rafailovich, M. H., "Phase-Separation-Induced Surface Pattern in Thin Polymer Blend Films", *Macromol.* **31**, 857 (1997).
- Karmonik, C., Huang, Q., Udovic, T. J., Rush, J. J., Andersson, Y., Flanagan, T. B., "Localized Diffusional Motion of Hydrogen and Deuterium in Crystalline Pd_9Si_2 ", *Mat. Res. Soc. Symp. Proc.* **527**, 75 (1998).
- Karmonik, C., Udovic, T. J., Huang, Q., Rush, J. J., Andersson, Y., Flanagan, T. B., "Neutron Scattering Study of the Dynamics of Hydrogen and Deuterium Solved in Crystalline Pd_9Si_2 ", *Physica B* **241-243**, 332 (1998).
- Karmonik, C., Udovic, T. J., Paul, R. L., Rush, J. J., Lind, K., Hempelmann, R., "Observation of Dopant Effects on Hydrogen Modes in $\text{SrCe}_{0.95}\text{M}_{0.05}\text{H}_x\text{O}_{3.6}$ by Neutron Vibrational Spectroscopy", *Solid State Ionics* **109**, 207 (1998).
- Karmonik, C., Udovic, T. J., Rush, J. J., "Hydrogen Motion in Lanthanum Hydrides by Means of Quasielastic Neutron Scattering", *Mat. Res. Soc. Symp. Proc.* **513**, 149 (1998).
- Karmonik, C., Yildirim, T., Udovic, T. J., Rush, J. J., Hempelmann, R., "Dynamics of the Perovskite-Based High-Temperature Proton-Conducting Oxides: Theory and Experiment", *Mat. Res. Soc. Symp. Proc.* **496**, 199 (1998).
- Kent, M. S., Majewski, J., Smith, G. S., Lee, L. T., Satija, S. K., "Tethered Chains in Poor Solvent Conditions: An Experimental Study Involving Langmuir Diblock Copolymer Monolayers", *J. Chem. Phys.*, in press.
- Kent, M. S., Smith, G. S., Majewski, J., Lee, L. T., Satija, S. K., "Tethered Chains in Theta Solvent Conditions: An Experimental Study Involving Langmuir Diblock Copolymer Monolayers", *J. Chem. Phys.* **108**, 5635 (1998).
- Kepa, H., Giebultowicz, T. M., Goldman, K. I., Nunez, V., Majkrzak, C. F., Springholz, G., Bauer, G., "Polarized Neutron Diffraction Studies of Antiferromagnetic EuTe/PbTe Superlattices", *J. Appl. Phys.* **81**, 5373 (1997).
- Kepa, H., Kleinwaks, L. J., Berk, N. F., Majkrzak, C. F., Berzina, T. S., Troitsky, V. I., Antolini, R., "Neutron and X-Ray Reflectometry Studies of Rough Interfaces in a Langmuir-Blodgett Film", *Physica B* **241**, 1048 (1997).
- Kesler, O., Matejcek, J., Sampath, S., Suresh, S., Gnaepel-Herold, T., Brand, P. C., Prask, H. J., "Measurement of Residual Stress in Plasma-Sprayed Metallic, Ceramic and Composite Coatings", *J. Mater. Sci. Eng.*, in press.
- Kimura, H., Hirota, K., Matsushita, H., Yamada, K., Endoh, Y., Lee, S.-H., Majkrzak, C. F., Erwin, R. W., Shirane, G., Greven, M., Lee, Y. S., Kastner, M. A., Birgeneau, R. J., "Neutron Scattering Study of Static Antiferromagnetic Correlations in $\text{La}_{2-x}\text{Sr}_x\text{Cu}_1\text{Zn}_y\text{O}_4$ ", *Phys. Rev. B*, in press.
- Kline, S. R., Kaler, E. W., "Interactions in Colloidal Mixtures: Partial Structure Factors in Mixtures of Colloidal Silica and an Anionic Oil-in-Water Microemulsion", *J. Colloids Interface Sci.* **203**, 392 (1998).
- Klosowski, P., Koennecke, M., Tischler, J. Z., Osborn, R., "NeXus: A Common Format for the Exchange of Neutron and Synchrotron Data", *Physica B* **241-243**, 151 (1998).
- Koneripalli, N., Levicky, R., Matsen, M., Bates, F. S., Satija, S. K., Ankner, J. F., Kaiser, H., "Ordering in Blends of Diblock Copolymers", *Macromol.* **31**, 3498 (1998).
- Konrad, H., Weissmüller, J., Birringer, R., Karmonik, C., Gleiter, H., "Kinetics of Gallium Films Confined at Grain Boundaries", *Phys. Rev. B* **58**, 2142 (1998).
- Krueger, S., "SANS Provides Unique Information on the Structure and Function of Biological Macromolecules in Solution", *Physica B*, **241-243**, 1131 (1997).
- Krueger, S., Gorshkova, I., Brown, J., Hoskins, J., McKinney, K. H., Schwarz, F. P., "Determination of the Conformations of cAMP Receptor Protein and Its T127,S128A Mutant with and without cAMP from Small Angle Neutron Scattering Measurements", *J. Biol. Chem.* **273**, 20001 (1998).
- Kvardakov, V. V., Somenkov, V. A., Shilstein, S. Sh., Lynn, J. W., Mildner, D. R. R., Chen-Meyer, H., "Laue Focusing Effect and Its Applications", *Physica B* **241-243**, 1210 (1998).
- Lee, C., Gido, S. P., Poulos, Y., Hadjichristidis, N., Tan, N. B., Trevino, S. F., Mays, J. W., "H-Shaped Double Graft Copolymers: Effect of Molecular Architecture on Morphology", *J. Chem. Phys.* **107**, 6460 (1997).
- Lee, C., Gido, S. P., Poulos, Y., Hadjichristidis, N., Tan, N. B., Trevino, S. F., Mays, J. W., "Pi-Shaped Double-Graft Copolymers: Effect of Molecular Architecture on Morphology", *Polymer* **39**, 4631 (1998).
- Lee, S.-H., Broholm, C., Aeppli, G., Cheong, S.-W., "Short-Range Spin Correlations in a Geometrically Frustrated Magnet, $\text{SrCr}_{9p}\text{Ga}_{12-9p}\text{O}_{19}$ ", *Proc. Intl. Workshop on Cold Neutron Utilization*, Korean Atomic Energy Institute, Taejon, South Korea, December 1997.
- Lee, S.-H., Majkrzak, C. F., "A New Technique for Polarized Neutron Diffraction", *Physica B*, in press.
- Lee, S.-H., Majkrzak, C. F., "Polarized Neutron Diffraction with an Area-Sensitive Detector", *J. Neutron Res.*, in press.
- Levicky, R., Heme, T. M., Tarlov, M. J., Satija, S. K., "Using Self-Assembly to Control the Structure of DNA Monolayers on Gold: A Neutron Reflectivity Study", *J. Am. Chem. Soc.* **120**, 9787 (1998).
- Levicky, R., Koneripalli, N., Tirrell, M., Ankner, J. F., Kaiser, H., Satija, S. K., "Selectively Swollen Films of Triblock/Diblock Copolymer Blends: Dependence of Swollen Film Structure on Blend Composition", *Macromol.* **31**, 4908 (1998).
- Levicky, R., Koneripalli, N., Tirrell, M., Satija, S. K., "Concentration Profiles in Densely Tethered Polymer Brushes", *Macromol.* **31**, 3731 (1998).
- Levicky, R., Koneripalli, N., Tirrell, M., Satija, S. K., "Stratification in Bidisperse Polymer Brushes from Neutron Reflectivity", *Macromol.* **31**, 2616 (1998).
- Li, W.-H., Peng, J. C., Lin, Y.-C., Lee, K. C., Lynn, J. W., Chen, Y. Y., "Magnetic Ordering of Ce in the Heavy-Fermion Compound Ce_3Al ", *J.*

- Appl. Phys. **83**, 6426 (1998).
- Li, W.-H., Wu, S. Y., Lee, K. C., Lynn, J. W., Liu, R. S., Wu, J. B., Huang, C. Y., "Magnetic Order and Spin Reorientation in $\text{Nd}_{0.45}\text{Ca}_{0.55}\text{MnO}_3$ ", J. Appl. Phys., in press.
- Li, W.-H., Wu, S. Y., Lee, K. C., Lynn, J. W., Liu, R. S., Wu, J. B., Huang, C. Y., "Noncollinear Magnetic Structure and Spin Reorientation in $\text{Nd}_{0.94}\text{MnO}_3$ ", Phys. Rev. B. (submitted).
- Lin, E. K., Kolb, R., Wu, W.-L., Satija, S. K., "Shear-induced Polymer Melt Desorption from an Attractive Substrate", Phys. Rev. Lett., (submitted).
- Lin, E. K., Pochan, D. J., Kolb, R., Wu, W. L., Satija, S. K., "Neutron Reflectivity for Interfacial Materials Characterization", Proc. 1998 Intl. Conf. on Characterization and Metrology for ULSI Technology, in press.
- Lin, E. K., Wu, W.-L., Satija, S., "Polymer Interdiffusion Near an Attractive Solid Substrate", Macromol. **30**, 7224 (1997).
- Lin, E. K., Wu, W.-L., Satija, S. K., "Polymer Mobility Near the Polymer/Solid Interface", Macromol. (submitted).
- Lin, M. Y., Hanley, H. J. M., Muzny, C. D., Straty, G. C., "Simultaneous Measurements of Viscosity and Structure for Rod-like Micelles", Physica B **241-243**, 990 (1998).
- Lin, Y.-C., Wu, S. Y., Li, W.-H., Lee, K. C., Lynn, J. W., Lin, C. W., Lin, J.-Y., Yang, H. D., "Neutron Diffraction Studies of Pr Ordering in $\text{PrBa}_2\text{Cu}_4\text{O}_8$ ", Physica B **241-243**, 702 (1998).
- Long, G. G., Krueger, S., Allen, A. J., "Multiple Small-Angle Neutron Scattering", in *Neutron Applications to Materials Science*, edited by T. M. Holden (Chalk River, ON), in press.
- Lynn, J. W., "Magnetic Neutron Scattering", Methods in Materials Research, in press.
- Lynn, J. W., "Spin Dynamics of Magnetoresistive Oxides", in *The Physics of Manganites* (Plenum Publishing), in press.
- Lynn, J. W., "Spin Dynamics of the Magnetoresistive Oxides", International Journal of Modern Physics, in press.
- Lynn, J. W., Skanthakumar, S., "Neutron Scattering Studies of Rare Earth Magnetic Ordering", *Handbook on the Physics and Chemistry of Rare Earths* (edited by K. A. Gschneider, Jr., L. Eyring, and M. B. Maple) Elsevier Science, in press.
- Lynn, J. W., Vasiliu-Doloc, L., Subramanian, M. A., "Spin Dynamics of the Magnetoresistive Pyrochlore $\text{Ti}_2\text{Mn}_2\text{O}_7$ ", Phys. Rev. Lett. **80**, 4582 (1998).
- MacFarlane, W. A., Kiefl, R. F., Dunsiger, S., Sonier, J. E., Chakhalian, J., Fischer, J. E., Yildirim, T., Chow, K. H., "Muon-Spin-Relaxation Studies of the Alkali-Fulleride Superconductors", Phys. Rev. B: Cond. Matt. **58**, 1004 (1998).
- Majkrzak, C. F., "Neutron Applications in Materials Science and Engineering", J. Neutron Res., in press.
- Majkrzak, C. F., Berk, N. F., "Exact Determination of the Phase in Neutron Reflectometry by Variation of the Surrounding Media", Phys. Rev. B: Rapid Comm., in press.
- Majkrzak, C. F., Berk, N. F., "Inverting Neutron Reflectivity from Layered Film Structures Using Polarized Beams", Physica B, in press.
- Majkrzak, C. F., Berk, N. F., Dura, J., Satija, S. K., Karim, A., Pedulla, J., Deslattes, R. D., "Direct Inversion of Specular Reflectivity", Physica B **241**, 1101 (1997).
- Majkrzak, C. F., Berk, N. F., Dura, J., Satija, S. K., Karim, A., Pedulla, J., Deslattes, R. D., "Phase Determination and Inversion in Specular Neutron Reflectometry", Physica B **248**, 338 (1998).
- Manson, J. L., Kmety, C. R., Huang, Q. Z., Lynn, J. W., Bendele, G. M., Pagola, S., Stephens, P. W., Liable-Sands, L. M., Rheingold, A. L., Epstein, A. J., Miller, J. S., "Structure and Magnetic Ordering of $\text{M}^{\text{II}}[\text{N}(\text{CN})_2]_2$ ($\text{M} = \text{Co}, \text{Ni}$)", Chem. Mater. **10**, 2552 (1998).
- Margadonna, S., Prassides, K., Neumann, D. A., Shimoda, H., Iwasa, Y., "Rotational Dynamics of C_{60} in $(\text{ND}_3)_3\text{K}_3\text{C}_{60}$ ", Phys. Rev. B, in press.
- Matejcek, J., Brand, P. C., Prask, H. J., Herman, H., "Neutron Diffraction Residual Stress Measurement on Thermally Sprayed Coatings", Proc. United Thermal Spray Conference, (Indianapolis, IN, 1997), p. 861.
- Matejcek, J., Sampath, S., Brand, P. C., Prask, H. J., "Quenching, Thermal, and Residual Stress in Plasma Sprayed Deposits: NiCrAlY and YSZ Coatings", Acta Mater., in press.
- Merfeld, G. D., Karim, A., Majumdar, B., Satija, S. K., Paul, D. R., "Interfacial Thickness between Immiscible Bilayers of Poly(phenylene oxide) and Styrenic Copolymers", J. Poly. Sci. Part B, in press.
- Merzbacher, C. I., Barker, J. G., Long, J. W., Rolison, D. R., "The Morphology of Nanoscale Deposits of Ruthenium Oxide in Silica Aerogels", Nanostructured Mater., in press.
- Merzbacher, C. I., Barker, J. G., Swider, K. E., Rolison, D. R., "Effect of Re-Wetting on Silica Aerogel Structure: A SANS Study", J. Non-Cryst. Solids **224**, 92 (1998).
- Merzbacher, C. I., Barker, J. G., Swider, K. E., Rolison, D. R., "Structure of Ru-Ti Oxide Aerogels: A SANS Study", Adv. Colloid. Interfac. **77**, 57 (1998).
- Merzbacher, C. I., Barker, J. G., Swider, K. E., Ryan, J. V., Bernstein, R. A., Rolison, D. R., "Characterization of Multi-Phase Aerogels by Contrast-Matching SANS", J. Non-Cryst. Solids **225**, 234 (1998).
- Meuse, C. W., Krueger, S., Majkrzak, C. F., Dura, J. A., Fu, J., Connor, J. T., Plant, A. L., "Hybrid Bilayer Membranes in Air and Water: Infrared Spectroscopy and Neutron Reflectivity Studies", Biophys. J. **74**, 1388 (1998).
- Meyer, A., Wuttke, J., Petry, W., "Two-Step Relaxation in a Viscous Metallic Liquid", J. Non-Cryst. Solids, in press.
- Mos, B., Verkerk, P., Bafile, U., Suck, J.-B., Andersen, K., Cook, J., "The Two-Body Collision Term in the Density Expansion of the Dynamical Structure Factor of Argon Determined by Neutron Scattering", Physica B **241-243**, 955 (1997).
- Moudden, A. H., Vasiliu-Doloc, L., Pinsard, L., Revcolevschi, A., "Spin Dynamics in $\text{La}_{1-x}\text{Sr}_x\text{MnO}_3$ ", Physica B **241-243**, 276 (1998).
- Nakatani, A. I., Sung, L., Hobbie, E. K., Han, C. C., "Shear-Induced Ordering in a Homopolymer Blend with Block-Copolymer 'Surfactant'", Phys. Rev. Lett. **79**, 4693 (1997).
- Natali-Sora, I., Huang, Q., Santoro, A., Cava, R. J., Krajewski, J. J., Peck Jr., W. F., "Crystal Structure of $\text{Y}_{0.95}\text{Ca}_{0.05}\text{CuO}_{2.54}$: A New Oxygen Deficient Perovskite Chemically and Structurally Related to '123' Superconductor", Il Nuovo Cimento **19D**, 8 (1997).
- Nikolaev, A. V., Michel, K. H., Copley, J. R. D., "Orientational Disorder and Order in C_{60} -Fullerite and in MC_{60} -Alkali Metal Fullerides", *Cooperative Phenomena in Condensed Matter* edited by D. I. Uzunov, Ple-

- num Publishing Corporation, in press.
- Nunez, V., Majkrzak, C. F., Springholz, G., Bauer, G., Giebultowicz, T. M., Kepa, H., Goldman, K. I., "Interlayer Spin Coherence in Antiferromagnetic EuTe/PbTe Superlattices Observed by Polarized Neutron Diffraction", *Superlattices Microstr.* **23**, 41 (1998).
- Okui, H., Omura, Y., Wada, N., Kamitakahara, W. A., Fujiwara, A., Suematsu, H., Murakami, Y., "Structural, Lattice-Dynamical and Magnetic Properties of Alkali-Metal Intercalated Vermiculite", *Mol. Cryst. Liquid Cryst.* **311**, 339 (1998).
- Osborn, R., Rosenkranz, S., Argyriou, D. N., Vasiliu-Doloc, L., Lynn, J. W., Sinha, S. K., Mitchell, J. F., Gray, K. E., Bader, S. D., "Neutron Scattering Investigation of Magnetic Bilayer Correlations in $\text{La}_{1.25}\text{Sr}_{1.8}\text{Mn}_2\text{O}_7$: Evidence of Canting above T_c ", *Phys. Rev. Lett.*, in press.
- Overholser, R., Wuttig, M., Neumann, D. A., "Chemical Ordering in Ni-Mn-Ga Heusler Alloys", *Scripta Materiala*, in press.
- Papanek, P., Fischer, J. E., Sauvajol, J. L., Dianoux, A. J., McNeill, P. M., Mathis, C., Francois, B., "Low-Frequency Phonons in Pristine and Doped Phases of Polyacetylene: An Inelastic Neutron Scattering Study", *J. Chem. Phys.*, in press.
- Pellegrini, N. N., Sikka, M., Satija, S. K., Winey, K. I., "Segregation of a Random Copolymer from Miscible Blends", *Macromol.* **30**, 6640 (1997).
- Prask, H. J., Choi, C. S., "Nondestructive Determination of Subsurface Residual Stresses by Means of Neutron Diffraction", Chapter III of AE14+: The Society of Automotive Engineers Fatigue, Design and Evaluation Committee Multiaxial Fatigue Program Update, in press.
- Prince, E., "B1.9 Diffraction: X-Ray, Neutron, and Electron" *American Institute of Physics Encyclopedia of Chemical Physics and Physical Chemistry*, Inst. of Physics, in press.
- Rachdi, F., Hajji, L., Dollt, H., Ribet, M., Yildirim, T., Fischer, J. E., Goze, C., Mehning, M., Hirsch, A., Nuber, B., "NMR Investigation of the Azafullerene $(\text{C}_{59}\text{N})_2$ and the Alkali Fullerides NaXC_{60} with $X=2, 4$, and 6 ", *Carbon* **36**, 607 (1998).
- Rachdi, F., Hajji, L., Galtier, M., Yildirim, T., Fischer, J. E., Goze, C., Mehning, M., " C_{13} and Na_{23} NMR Studies of Na_2C_{60} Fullerides", *Phys. Rev. B: Cond. Matt.* **56**, 7831 (1997).
- Rathgeber, S., Willner, L., Richter, D., Appel, M., Fleischer, G., Brulet, A., Farago, B., Schleger, P., "Polymer Dynamics in Bimodal Melts", *PMSE* **79**, 299 (1998).
- Rijssenbeek, J. T., Matl, P., Batlogg, B., Huang, Q., Ong, N. P., Cava, R. J., "Crystal Structure and Physical Properties of a Series of Ternary Barium Metal Ruthenates: $\text{Ba}_3\text{MRu}_2\text{O}_9$, $M = \text{Fe, Co, Ni, and In}$ ", *Phys. Rev. B*, in press.
- Robert, J., Petit, P., Yildirim, T., Fischer, J. E., "Experimental Lattice Dependence of the Density of States in Alkali Fullerides", *Phys. Rev. B: Cond. Matt.* **57**, 1226 (1998).
- Rosenkranz, S., Osborn, R., Mitchell, J. F., Vasiliu-Doloc, L., Lynn, J. W., Sinha, S. K., Argyriou, D. N., "Magnetic Correlations in the Bilayer Manganite $\text{La}_{1.2}\text{Sr}_{1.8}\text{Mn}_2\text{O}_7$ ", *J. Appl. Phys.* **83**, 7348 (1998).
- Rosov, N., Rathgeber, S., Monkenbusch, M., "Neutron Spin Echo Spectroscopy at the NIST Center for Neutron Research", *ACS Polymeric Materials Science and Engineering*, **79** (Fall Meeting, Boston, MA, August 23-27, 1998), p. 328.
- Rush, J. J., "Multilab Partnerships", *Science* **279**, 965 (1998).
- Ruzette, A.-V. G., Banerjee, P., Mayes, A. M., Pollard, M., Russell, T. P., Jerome, R., Slawacki, T., Hjelm, R., Thiyagarajan, P., "Phase Behavior of Diblock Copolymers between Styrene and N-Alkyl Methacrylates" *Macromol.*, in press.
- Santorio, A., Natali Sora, I., Huang, Q., "Bond-Valence Analysis of the Structure of $(\text{Ba}_{0.875}\text{Sr}_{0.125})\text{RuO}_3$ ", *J. Solid State Chem.*, in press.
- Satija, S. K., Gallagher, P. D., Karim, A., "End-Grafted Polystyrene Brushes in a Critical Binary Mixture", *Proc. ACS Div. Poly. Sci. Eng.* **77**, 630 (1997).
- Satija, S. K., Gallagher, P. D., "Neutron Reflectivity Study of a Chemically End-Grafted Polystyrene Brush in a Binary Solvent Mixture", *Physica B* **248**, 204 (1998).
- Schreyer, A., Majkrzak, C. F., Zeidler, Th., Schmitte, T., Bödeker, P., Theis-Brohl, K., Abromeit, A., Dura, J. A., Watanabe, T., "The Magnetic Structure of Cr in Exchange Coupled Fe/Cr(001) Superlattices", *Phys. Rev. Lett.* **79**, 4914 (1997).
- Schulz, J. C., Warr, G. G., Hamilton, W. A., Butler, P. D., "Neutron Reflectometry of Adsorbed Surfactant Aggregates", *European J. Phys. E*, in press.
- Seehra, M. S., Babu, V. S., Lynn, J. W., "Magnetism of Ferrihydrite Nanoparticles Studied by Neutron Scattering and Magnetometry", *Phys. Rev. Lett.* (submitted).
- Skanthakumar, S., Lynn, J. W., "Rare Earth Magnetic Order in $\text{RNi}_2\text{B}_2\text{C}$ and RNiBC ", *Physica B*, in press.
- Skanthakumar, S., Lynn, J. W., Mazumdar, C., Nagarajan, R., Gupta, L. C., "Magnetic Phase Transitions in $\text{R}_2\text{Ni}_3\text{Si}_3$ ", *Physica B* **241-243**, 693 (1998).
- Skripov, A. V., Cook, J. C., Sibirtsev, D. S., Karmonik, C., Hempelmann, R., "Quasielastic Neutron Scattering Study of Hydrogen Motion in C15-type TaV_2H_x ", *J. Phys. Condens. Matt.* **10**, 1787 (1998).
- Slawacki, T. M., Glinka, C. J., Hammouda, B., "Shear-Induced Micellar Crystal Structures in an Aqueous Triblock Copolymer Solution", *Phys. Rev. E* **58**, R4084 (1998).
- Sokol, P. E., Brown, D. W., FitzGerald, S. A., "An Inelastic Neutron Scattering Study of H_2 in Yycor Glass", *J. Low Temp. Phys.* **113**, 717 (1998).
- Sokol, P. E., Dimeo, R. M., Brown, D. W., Anderson, C. R., Stirling, W. G., Adams, M. A., Lee, S.-H., Rustiser, C., Komarneni, S., "Confinement Effects on the Roton in Helium", *Physica B* **241-243**, 929 (1998).
- Straty, G. C., Munzy, C. D., Butler, B. D., Lin, M. Y., Slawacki, T., Glinka, C. J., Hanley, H. J. M., "A Rheometric Shearing Apparatus at the NIST Center for Neutron Research (NCNR)", *Nucl. Instrum. Meth. A* **408**, 511 (1998).
- Straty, G. C., Munzy, C. D., Butler, B. D., Lin, M. Y., Slawacki, T., Glinka, C. J., Hanley, H. J. M., "An In-Situ Rheometric Shearing Apparatus for SANS", *Physica B* **241-243**, 74 (1998).
- Sung, L., Nakatani, A. I., Han, C. C., Karim, A., Douglas, J. F., Satija, S. K., "The Role of the Copolymer Additives on Phase Behavior of a Polymer Blend", *Physica B* **241-243**, 1013 (1998).
- Thirtle, P. N., Li, Z. X., Thomas, R. K., Rennie, A. R., Satija, S. K., Sung, L. P., "Structure of Non-Ionic Surfactant Layers Adsorbed at the Solid/Liquid Interface on Self-Assembled Monolayers with Different Surface Functionality: A Neutron Reflection Study", *Langmuir* **13**, 5451 (1997).
- Toby, B., Purnell, S., Hu, R., Peters, A., Olson, D. H., "An Attempt to

- Locate Protons in the ZSM-5 Structure by Combined Synchrotron and Neutron Diffraction", Proc. 12th Intl. Zeolite Conference (MRS publishers), in press.
- Toby, B. H., "Diffraction Analysis and Crystallographic Structure Determination", *Handbook of Ceramic Engineering*, ed. M. N. Rahaman, in press.
- Trevino, S. F., Joubran, R., Parris, N., Berk, N. F., "Structure of a Triglyceride Microemulsion: A Small-Angle Neutron Scattering Study", *J. Phys. Chem. B* **102**, 953 (1998).
- Troyanchuk, I. O., Khalyavin, D. D., Solovykh, T. K., Szymczak, H., Huang, Q., Lynn, J. W., "Magnetic and Crystal Structure Phase Transitions in $R_{1-x}Ba_xCoO_{3-y}$ (R=Nd, Gd)", *J. European Phys. B* (submitted).
- Tu, K., Klein, M. L., Tobias, D. J., "Constant Pressure Molecular Dynamics Investigation of Cholesterol Effects in a DPPC Bilayer", *Biophys. J.* **75** (1998).
- Tu, K., Tarek, M., Klein, M. L., Scharf, D., "Effects of Anesthetics on the Structure of a Phospholipid Bilayer: Molecular Dynamics Investigation of Halothane in the Hydrated Liquid Crystal Phase of Dipalmitoylphosphatidylcholine", *Biophys. Journal* **75** (1998).
- Udovic, T. J., Huang, Q., Karmonik, C., Rush, J. J., "Structural Ordering and Dynamics of LaH_{3-x} ", *J. Alloys Compounds*, in press.
- Udovic, T. J., Huang, Q., Lynn, J. W., Erwin, R. W., Rush, J. J., "Neutron Scattering Study of the Nuclear and Magnetic Structure of DyD_3 and Associated Vibrational and Magnetic Excitations", *Phys. Rev. B*, in press.
- Udovic, T. J., Huang, Q., Rush, J. J., "Comment on 'Theoretical Prediction of the Structure of Insulating YH_3 '", *Phys. Rev. Lett.* **79**, 2920 (1997).
- Udovic, T. J., Huang, Q., Rush, J. J., "Neutron Scattering Studies of the Structures and Vibrational Dynamics of the HCP Rare-Earth Trihydrides", *Mat. Res. Soc. Symp. Proc.* **513**, 197 (1998).
- Uma, S., Schnelle, W., Gmelin, E., Rangarajan, G., Skanthakumar, S., Lynn, J. W., Walter, R., Lorenz, T., Buchner, B., Walker, E., Erb, A., "Magnetic Ordering in Single Crystals of $PrBa_2Cu_3O_{7.8}$ ", *J. Phys. Condens. Matt.* **10**, L33 (1998).
- Vanderah, T. A., Wong-Ng, W., Huang, Q., Roth, R. S., Geyer, R. G., Goldfarb, R. B., "Crystal Structures and Properties of $Ba_4Fe_2Ti_{10}O_{27}$ and $Ba_3Fe_{10}TiO_{20}$ ", *J. Phys. Chem. Solid* **58**, 1403 (1997).
- Vasiliiu-Doloc, L., Lynn, J. W., Moudren, A. H., de Leon-Guevara, A. M., Revcolevschi, A., "Anomalous Spin-Wave Damping in the Ground State of $La_{0.85}Sr_{0.15}MnO_3$ ", *Phys. Rev. B*, in press.
- Vasiliiu-Doloc, L., Lynn, J. W., Moudren, A. H., de Leon-Guevara, A. M., Revcolevschi, A., "Structure and Spin Dynamics of $La_{0.85}Sr_{0.15}Mn_2O_7$ ", *Phys. Rev. Lett.*, in press.
- Vasiliiu-Doloc, L., Lynn, J. W., Mukovskii, Y. M., Arsenov, A. A., Shulyatev, D. A., "Spin Dynamics of Strongly-Doped $La_{1-x}Sr_xMnO_3$ ", *J. Appl. Phys.* **83**, 7342 (1998).
- Wakimoto, S., Birgeneau, R. J., Endoh, Y., Gehring, P. M., Hirota, K., Kastner, M. A., Lee, S.-H., Lee, Y. S., Shirane, G., Ueki, S., Yamada, "Observation of New Incommensurate Magnetic Correlations at the Lower Critical Concentration for Superconductivity ($x = 0.05$) in $La_{2-x}Sr_xCuO_4$ ", *Phys. Rev. Lett.*, in press.
- Wakimoto, S., Yamada, K., Ueki, S., Shirane, G., Lee, Y. S., Lee, S.-H., Kastner, M. A., Hirota, K., Gehring, P. M., Endoh, Y., Birgeneau, R. J., "Neutron Scattering Study of Elastic Magnetic Signals in Superconducting $La_{1.94}Sr_{0.06}CuO_4$ ", *J. Phys. Chem. Solids*, in press.
- Wallace, W. E., Beck Tan, N. C., Wu, W. L., Satija, S. K., "Mass Density of Polystyrene Thin Films Measured by Twin Neutron Reflectivity", *J. Chem. Phys.* **108**, 3798 (1998).
- Walton, D. G., Soo, P. P., Mayes, A. M., Allgor, S. J. S., Fujii, J. T., Griffith, L. G., Ankner, J. F., Kaiser, H., Johansson, J., Smith, G. D., Barker, J. G., Satija, S. K., "Creation of Stable Poly(Ethylene Oxide) Surfaces on Poly(Methyl Methacrylate) Using Blends of Branched and Linear Polymers", *Macromol.* **30**, 6947 (1997).
- Wang, H., Newstein, M. C., Krishnan, A., Balsara, N. P., Garetz, B. A., Hammouda, B., Krishnamoorti, R., "Ordering Kinetics and Alignment of Block Copolymer Lamellae Under Shear Flow", *Macromol.*, in press.
- Welp, K. A., Wool, R. P., Agrawal, G., Satija, S. K., Pispas, S., Mays, J., "Direct Observation of Polymer Dynamics: Mobility Comparison Between Central and End Section Monomers", *Macromol.*, in press.
- Welp, K. A., Wool, R. P., Satija, S. K., Mays, J., "Dynamics of Polymer Interdiffusion: The Ripple Experiment", *Macromol.* **31**, 4915 (1998).
- Williams, R. E., Rowe, J. M. and Blau, M., "Benchmark of the Nuclear Heat Deposition in the NIST Liquid Hydrogen Cold Source", Proc. 9th Intl. Symp. on Reactor Dosimetry, edited by H. A. Abderrahim, P. D'hondt, and B. Osmera (World Scientific Publishing, 1998), p. 584.
- Wischniewski, A., Buchenau, U., Dianoux, A. J., Kamitakahara, W. A., Zarestky, J. L., "Neutron Scattering Analysis of Low Frequency Modes in Silica", *Philos. Mag. B* **77**, 579 (1998).
- Wischniewski, A., Buchenau, U., Dianoux, A. J., Kamitakahara, W. A., Zarestky, C., "Sound Wave Scattering in Silica", *Phys. Rev. B* **57**, 2663 (1998).
- Wong-Ng, W., Toby, B. H., Greenwood, W., "Crystallographic Studies of Bar_2ZnO_5 (R = La, Nd, Dy, Ho, Er and Y)", *Powder Diffr.* **13**, 144 (1998).
- Worcester, D., Hammouda, B., "Hydrocarbon Chain Interdigitation by Hydrostatic Pressure in C_{16} - C_{22} Phosphatidicholines", *Biophys. J.* **A28**, Part 2 (1998).
- Worcester, D., Hammouda, B., "Interdigitated Hydrocarbon Chains in C_{20} and C_{22} Phosphatidylcholines Induced by Hydrostatic Pressure", *Physica B* **241**, 1175 (1997).
- Wu, S. Y., Li, W.-H., Lee, K. C., Lynn, J. W., Liu, R. S., Wu, J. B., Huang, C. Y., "Titled Antiferromagnetic Ordering of Mn in $Nd_{0.62}Ca_{0.38}MnO_3$ ", *J. Appl. Phys.* **83**, 7345 (1998).
- Ye, X., Narayanan, T., Tong, P., Huang, J. S., Lin, M. Y., Carvalho, B. L., Fetter, L. J., "Depletion Interactions in Colloid-Polymer Mixtures", *Phys. Rev. E* **54**, 6500 (1996).
- Yildirim, T., "Current Issues in Fullerene-based Superconductors", in *Recent Advances in the Chemistry and Physics of Fullerenes and Related Materials*, edited by K. M. Kadish and R. S. Ruoff, **6**, 360 (1998).
- Yildirim, T., "Ordering Due to Disorder in Frustrated Quantum Magnetic Systems", *Turkish J. Phys.*, in press.*
- Yildirim, T., Gehring, P. M., Neumann, D. A., Eaton, P. E., Emrick, T., "Solid Cubane: A Brief Review", *Carbon* **36**, 809 (1998).
- Yildirim, T., Harris, A. B., Shender, E. F., "Frustrations and Quantum Fluctuations in Heisenberg FCC Antiferromagnets", *Phys. Rev. B* **58**, 3144 (1998).
- Yokoo, T., Raymond, S., Zheludev, A., Maslov, S., Ressouche, E., Zaliznyak, I., Erwin, R. W., Nakamura, M., Akimitsu, J., "Magnetic Ordering

- Spin Waves, and Haldane Gap Excitations in $(\text{Nd}_x\text{Y}_{1-x})_2\text{BaNiO}_5$ Linear-Chain Mixed-Spin Antiferromagnets”, *Phys. Rev. B* **58**, 14424 (1998).
- Zaliznyak, I. A., Dender, D. C., Broholm, C., Reich, D. H., “Tuning the Spin Hamiltonian of $\text{Ni}(\text{C}_2\text{H}_8\text{N}_4)_2\text{NO}_2\text{ClO}_4$ by External Pressure: A Neutron Scattering Study”, *Phys. Rev. B* **57**, 5200 (1998).
- Zhao, J., Glazounov, A. E., Zhang, Q. M., Toby, B. H., “Neutron Diffraction Study of Electrostrictive Coefficients of Prototype Cubic Phase of Relaxor Ferroelectric $\text{PbMg}_{1/3}\text{Nb}_{2/3}\text{O}_3$ ”, *Appl. Phys. Lett.* **72**, 1048 (1998).
- Zheludev, A., Maslov, S., Shirane, G., Tsukada, I., Masuda, T., Uchinokura, K., Zaliznyak, I., Erwin, R. W., Regnault, L. P., “Magnetic Anisotropy and Low-Energy Spin Waves in the Dzyaloshinskii-Moriya Spiral Magnet $\text{Ba}_2\text{CuGe}_2\text{O}_7$ ”, *Phys. Rev. B: Cond. Matt.* 9810122 (submitted).
- Zheludev, A., Maslov, S., Zaliznyak, I., Regnault, L. P., Masuda, T., Uchinokura, K., Erwin, R., Shirane, G., “Experimental Evidence for Shekhtman-Entin-Wohlman-Aharony (SEA) Interactions in $\text{Ba}_2\text{CuGe}_2\text{O}_7$ ”, *Cond. Matt.* 9805236 (1998).
- Zhou, C. L., Hobbie, E. K., Bauer, B. J., Sung, L., Jiang, M., Han, C. C., “Control of Interaction Strength in Hydrogen-Bonded Polymer Blends via the Density of Hydroxyl Group”, *Macromol.* **31**, 1937 (1998).
- Zhou, P., Papanek, P., Bindra, C., Lee, R., Fischer, J. E., “High Capacity Carbon Anode Materials: Structure, Hydrogen Effect, and Stability”, *J. Power Resources* **68**, 296 (1997).

Independent Publications

- Adams, J. M., Catchen, G. L., Loubychev, D., Fu, J., Miller, D. L., "A Novel Apparatus for Performing Perturbed Angular Correlation Spectroscopy Measurements on Epitaxially-Grown III-V Surfaces", Nucl. Instrum. Meth. B, in press.
- Adams, J. M., McGarry, E. D., Hawari, A. I., Venkataraman, R., "The Materials Dosimetry Reference Facility Round Robin Tests of ^{237}Np and ^{238}U Fissionable Dosimeters", in *Reactor Dosimetry*, edited by H. A. Abderrahim, et al. (World Scientific Publishing, 1998), p. 124.
- Agnew, S. R., Elliott, B. R., Youngdahl, C. J., Hernker, K. J., Weertman, J. R., "Structure and Mechanical Properties of Nanocrystalline Metals— with Opportunities for Modeling", 19th Risø International Symposium on Materials Science, Risø National Laboratory, Roskilde, Denmark, in press.
- Alexandridis, P., "Poly(ethylene oxide) Poly(propylene oxide) Block Copolymer Surfactants", *Curr. Opin. Colloid In* **2**, 478 (1997).
- Allen, A. J., Livingston, R. A., "The Relationship Between Differences in Silica Fume Additives and the Fine Scale Microstructural Evolution in Cement Based Materials", *Adv. Cem. Based Mater.* **8**, 118 (1998).
- Allman, B. E., Jacobson, D. L., Lee, W.-T., Littrell, K. C., Werner, S. A., "Neutron Interferometry Instrumentation at MURR", *Nucl. Instrum. Meth. A* **412**, 392 (1998).
- Amos, T. G., Yokochi, A., Sleight, A. W., "Phase Transition and Negative Thermal Expansion in Tetragonal NbOPO_4 ", *J. Solid State Chem.*, in press.
- Anderson, M. L., Morris, C. A., Stroud, R. M., Merzbacher, C. I., Rolison, D. R., "Colloidal Gold Aerogels: Preparation, Properties, and Characterization", *Langmuir*, in press.
- Becker, D. A., "Characterization and Use of the New NIST Rapid Pneumatic Tube Irradiation Facility", *J. Radioanal. Nucl. Chem.* **233**, 155 (1998).
- Becker, D. A., "Accurate Determination of Trace Elements in Sediment CRMs by Instrumental Neutron Activation Analysis", *Proc. Czech. J. Phys.*, in press.
- Bellows, R. J., Lin, M. Y., Arif, M., Thompson, A. K., Jacobson, D., "Neutron Imaging Technique for In-Situ Measurement of Water Transport Gradients Within Nafion in Polymer Electrolyte Fuel Cells", *J. Electrochem. Soc.*, in press.
- Bennett, K., Wenk, H.-R., Durham, W. B., Stern, L. A., Kirby, S. H., "Preferred Crystallographic Orientation in the Ice I-II Transformation and the flow of Ice II", *Phil. Mag. A* **76**, 413 (1997).
- Bindra, C., Nalimova, V. A., Sklovsky, D. E., Benes, Z., Fischer, J. E., "Superdense LiC_2 as a High Capacity Li Intercalation Anode", *J. Electrochem. Soc.* **145**, 2377 (1998).
- Blackman, M. J., Badaljan, R. S., Kikodze, Z. K., Kohl, P. L., "Chemical Characterization of Caucasian Obsidian: Geological Sources", in *Synthese Sur l'Obsidienne au Proche-Orient: Du Volcan a l'Outil*, (BAR Publication, London), in press.
- Blackman, M. J., Redford, S., "Northern Syrian Luster and Fritware: Petrographic and Chemical Implications for Productions and Distribution", *Antiquity*, in press.
- Borsali, R., Nguyen, H., Pecora, R., "Small Angle Neutron Scattering Dynamic Light Scattering from a Polyelectrolyte Solution: DNA", *Macromol.* **31**, 1548 (1998).
- Butler, B. D., Muzny, C. D., Hanley, H. J. M., "Scaling of Small-Angle Neutron Scattering Intensities from Gelling Colloidal Silica", *Int. J. Thermophys.*, Jan. 1999, in press.
- Caffrey, P. F., Ondov, J. M., "Determination of Particle Dry Deposition Velocities Over Southern Lake Michigan Using Elemental Compositions Determined by Instrumental Neutron Activation Analysis", *Trans. Amer. Nuc. Soc.* **77**, 490 (1997).
- Caffrey, P. F., Ondov, J. M., Zufall, M. J., Davidson, C. I., "Determination of Size-Dependent Dry-Particle Deposition Velocities with Multiple Intrinsic Elemental Tracers", *Environ. Sci. Technol.* **32**, 1615 (1998).
- Calpin-Davies, S., Clifton, B. J., Cosgrove, T., Richardson, R. M., Zarkash, A., Booth, C., Yu, G., "The Structure of Block Copolymers of Ethylene Oxide and Butylene Oxide at Fluid/Fluid Interfaces", in *Modern Aspects of Colloidal Dispersions*, edited by R. H. Ottewill and A. R. Rennie, (Kluwer Academic Publishers, 1998), p. 159.
- Carlson, A. D., "Status of the NEANSC Subgroup Working on Improving the $^{10}\text{B}(n, \alpha)$ Standard Cross Sections", *Proc. 9th Intl. Symp. on Reactor Dosimetry*, edited by H. A. Abderrahim, P. D'hondt, B. Osmera, (World Scientific Publishing, Singapore, 1998), p. 632.
- Carlson, A. D., Chiba, S., Hamsch, F.-J., Olsson, N., Smirnov, A. N., "Update to Nuclear Data Standards for Nuclear Measurements", *Proc. Intl. Conf. on Nuclear Data for Science and Technology*, (Trieste, Italy, May 19-24, 1997), p. 1223.
- Chapman, B. R., Hamersky, M. W., Milhaupt, J. M., Kostecky, C., Lodge, T. P., von Meerwall, E. D., Smith, S. D., "Structure and Dynamics of Disordered Tetrablock Copolymers: Composition and Temperature Dependence of Local Friction", *Macromol.* **31**, 4562 (1998).
- Chen, S.-H., Choi, S.-M., "Measurement and Interpretation of Curvatures of the Oil-Water Interface in Isometric Bicontinuous Microemulsions", *J. Appl. Crystallogr.* **30**, 755 (1997).
- Chen-Mayer, H. H., Mildner, D. F. R., Lamaze, G. P., Lindstrom, R. M., Paul, R. L., Kvardakov, V. V., Richards, W. J., "Concentration of Hydrogen in Titanium Measured by Neutron Incoherent Scattering", *Proc. Mat. Res. Soc.* **513**, 191 (1998).
- Chen-Mayer, H. H., Mildner, D. F. R., Lamaze, G. P., Paul, R. L., Lindstrom, R. M., "Neutron Focusing using Capillary Optics and Its Applications to Elemental Analysis", *Proc. 15th Intl. Conf. on Applications of Accelerators in Research and Industry*, in press.
- Chen-Mayer, H. H., Mildner, D. F. R., Sharov, V. A., Xiao, Q. F., Cheng, Y. T., Lindstrom, R. M., Paul, R. L., "A Polycapillary Bending and Focusing Lens for Neutrons", *Rev. Sci. Instrum.* **68**, 3744 (1997).
- Choi, S.-M., Chen, S.-H., "The Relationship between the Interfacial Curvatures and Phase Behavior in Bicontinuous Microemulsions—A SANS Study", *Progr. Colloid Poly. Sci.* **106**, 14 (1997).
- Choi, S.-M., Chen, S.-H., Sottman, T., Strey, R., "Measurement of Interfacial Curvatures in Microemulsions Using Small-Angle Neutron Scattering", *Physica B* **241-243**, 976 (1997).

- Co, C. C., Kaler, E. W., "Particle Size and Monomer Partitioning in Microemulsion Polymerization. 2. On line Small Angle Neutron Scattering Studies", *Macromol.* **31**, 3203 (1998).
- Dadmun, M. D., Clingman, S., Ober, C. K., Nakatani, A. I., "The Flow Induced Structure in a Thermotropic Liquid Crystalline Polymer as Studied by SANS", *J. Poly. Sci.: Poly. Phys.* (submitted).
- Diallo, M. S., Yu, D., Fréchet, J. M. J., Milkis, P., Goddard III, W. A., "Small Angle Neutron Scattering Investigations and Molecular Dynamics Simulations of Hybrid Linear Dendritic Star Copolymers in Polar and Nonpolar Solvents", *Polym. Mat. Sci. Eng.* **79**, 343 (1998).
- Dimeo, R. M., Sokol, Azuah, R. T., Bennington, S. M., Stirling, W. G., Guckelsberger, K., "The Momentum Distribution of ^3He ", *Physica B* **241-243**, 952 (1998).
- Downing, R.G., Lamaze, G.P., "Nondestructive Characterization of Semiconductor Materials Using Neutron Depth Profiling", *Proceedings International Workshop on Semiconductor Characterization: Present Status and Future Needs*, edited by W.M.Bullis, D.G.Seiler, and A.C.Diebold, (AIP Press, 1996), p. 346.
- Downing, R. G., Strong, P. L., "A Round-Robin Determination of Boron in Botanical and Biological Samples", *Biological Trace Element Research*, in press.
- Dulloo, A. R., Ruddy, F. H., Seidel, J. G., Adams, J. M., Nico, J. S., Gilliam, D. M., "The Neutron Response of Miniature Silicon Carbide Semiconductor Detectors", *Nucl. Instrum. Meth.*, in press.
- Effey, B., Cappelletti, R. L., "An Inelastic Neutron Scattering Study of Se-As-Ge Glasses: A Test of the Vibrational Isocoordinate Rule", *Phys. Rev. B*, in press.
- En, Z., Brenizer, J.S., Hostica, B., Gao, J., Becker, D.A., "Nitrogen Distribution Measurements by Neutron Induced Autoradiography", *J. Radioanal. Nucl. Chem.*, in press.*
- Ermi, B. D., Amis, E. J., "Influence of Backbone Solvation on Small Angle Neutron Scattering from Polyelectrolyte Solutions", *Macromol.* **30**, 6937 (1997).
- Fajgelj, A., Zeisler, R., "Particle Size Determination of Some IAEA and NIST Environmental and Biological Reference Materials", *Fresen. J. Anal. Chem.* **360**, 442 (1998).
- Feng, Y., Karim, A., Weiss, R. A., Douglas, J. F., Han, C. C., "Control of Polystyrene Film Dewetting through Sulfonation and Metal Complexation", *Macromol.* **31**, 484 (1998).
- Fernandez-Baca, J. A., Dai, P., Hwang, H. Y., Cheong, S.-W., Kloc, C., "Evolution of the Low-frequency Spin Dynamics in Ferromagnetic Magnetites", *Phys Rev. Lett.* **80**, 4012 (1998).
- Feuerstein, M., Lobo, R. F., "Characterization of Li Cations in Zeolite LiX by Solid-State NMR Spectroscopy and Neutron Diffraction", *Chem. Mater.* **10**, 2197 (1998).
- Fodor, J. S., Briber, R. M., Russell, T. P., Carter, K. R., Hedrick, J. L., Miller, R. D., "Non-Uniform Composition Profiles in Thin Film Polymeric Nanofoams", *Polymer*, in press.
- Fokin, V.S., Chen-Mayer, H. H., Sharov, V.A., Mildner, D.F.R., "Neutron Transmission Through Curved Nickel Capillaries", *Nucl. Instrum. Meth. A* **401**, 355 (1997).
- Foster, M. D., Greenberg, C. C., Teale, D. M., Cloutet, E., Turner, C. M., Quirk, R. P., "Quantifying Surface Segregation in Blends of Linear and Star Branched Molecules", *ACS Preprint* (submitted).
- Glazounov, A. E., Zhao, J., Zhang, Q. M., "Effect of Nanopolar Regions on Electrostrictive Coefficients of a Relaxor Ferroelectric", *Proc. 5th Williamsburg Workshop on First-Principles Calculations for Ferroelectrics*, *AIP Conf. Proc.* **436**, 118 (1998).
- Goessler, W., Rudorfer, A., Mackey, E. A., Becker, P. R., Irgolic, K. H., "Determination of Arsenic Compounds in Marine Mammals with High Performance Liquid Chromatography and Indirectly Coupled Plasma Mass Spectrometry as Element Specific Detector", *J. Appl. Organometal. Chem.* **12**, 491 (1998).
- Gora, L., Streletsky, K., Thompson, R. W., Phillies, G. D. J., "Study of the Crystallization of Zeolite NaA by Quasi-Elastic Light-Scattering Spectroscopy and Electron Microscopy", *Zeolites* **18**, 119 (1997).
- Greenberg, R. R., "The Role of Neutron Activation Analysis in the Development and Certification of NIST Environmental Standard Reference Materials", *Proc. Intl. Symp. on Harmonization of Health Related Environmental Measurements Using Nuclear and Isotopic Techniques* (Vienna, Austria, 1997), p. 137.
- Greenberg, R. R., "Unique Quality Assurance Aspects of Neutron Activation Analysis", *Proc. 9th Intl. Symp. on Trace Elements in Man and Animals* (NRC Research Press, 1997), p. 410.
- Gu, W., Lu, L., Chapman, G. B., Weiss, R. G., "Polymerized Gels and 'Reverse Aerogels' from Methyl Methacrylate or Styrene and Tetraoctadecylammonium Bromide as Gelator", *Chem. Commun.* **6**, 543 (1997).
- Han, C. C., Zhou, C., Hobbie, E. K., "Cross-Link Density and the Strength of the Binding Interaction in Hydrogen-Bonded Polymer Blends", *ACS PMSE preprint*, 141 (1998).
- Hanley, H. J. M., "Structure of Macromolecular Systems under Shear; Application of Neutron Scattering", *Curr. Opin. Colloid In.* **2**, 635 (1997).
- Hanley, H. J. M., Muzny, C. D., Butler, B. D., "Simultaneous SANS and Rheometric Measurements on a Dense Colloidal Silica Gel", *Proc. 16th Symp. on Energy Engineering Sciences (CONF-980571)* 105 (1998).
- Hanley, H. J. M., Muzny, C. D., Butler, B. D., "Surface Adsorption in a Surfactant/Clay Mineral Solution", *Int. J. Thermophys.* **19**, 1155 (1998).
- Hanley, H. J. M., Muzny, C. D., Butler, B. D., Straty, G. C., Bartlett, J., Drabarek, E., "Shear-Induced Restructuring of Concentrated Colloidal Silica Gels", *J. Phys. Condens. Matt.*, in press.
- Hedrick, J. L., Hawker, C. J., Russell, T. P., Sanchez, M., Briber, R. M., "Nanoporous Polyimides", *Rev. Macromol. Chem. Phys.*, in press.
- Heller-Zeisler, S. F., Donais, M. K., Zeisler, R., "Instrumental Neutron Activation Analysis for Quality Assurance of a Hair Reference Material for Mercury", *J. Radioanal. Nucl. Chem.* **233**, 55 (1998).
- Henderson, S. J., "The Second Virial Coefficient of C_{60} in CS_2 Measured by Small-Angle Neutron Scattering", *Langmuir* **13**, 6139 (1997).
- Henrickson, R. C., Blackman, M. J., "Hellenistic Production of Terra Cotta Roof Tiles Among the Ceramic Industries at Gordian", *Oxford J. Archaeology* **18**, in press.
- Heuser, B. J., King, J. S., "Effect of Dislocation Trapping on Deuterium Diffusion in Deformed, Single Crystal Pd", *Metallurgical and Materials Transactions A* **29A**, 1593 (1998).
- Heuser, B. J., King, J. S., "SANS Measurements of Deuterium-Dislocation Trapping in Deformed Single Crystal Pd", *J. Alloy. Compd.* **261**, 225 (1997).

- Hirai, M., Arai, S., Iwase, H., Takizawa, T., "Small-Angle X-ray Scattering and Calorimetric Studies of Thermal Conformational Change of Lysozyme Depending on Ph", *J. Phys. Chem. B* **102**, 1308 (1998).
- Hjelm, R. P., "The Structure of Fillers, Polymers, and Their Interfaces in Polymer Composites Using Neutron Scattering Methods", *Proc. 1998 Meeting on Neutron Scattering*, (1998), p. 11.
- Ho, D. L., Briber, R. M., Jones, R. L., Kumar, S. K., Russell, T. P., "Small Angle Neutron Scattering Studies on Thin Films of Isotopic Polystyrene Blends", *Macromol.* (submitted).
- Hoff, J., Borgouli, P., Ondov, J. M., Kelly, W. R., Chen, L. T., "Feasibility of Applying a New Tracer for Direct Determination of Dry Particulate Deposition to Soybean Plants", *J. Air Waste Manage.* **48**, 721 (1998).
- Huang, E., Russell, T. P., Harrison, C., Chaikin, P. M., Register, R. A., Hawker, C. J., Mays, J., "Using Surface Active Random Copolymers to Control the Domain Orientation in Diblock Copolymer Thin Films", *Macromol.* **31**, 7641 (1998).
- Huffman, P. R., Brome, C. R., Butterworth, J. S., Coakley, K. J., Dewey, M. S., Dzhosyuk, S. N., Gilliam, D. M., Golub, R., Greene, G. L., Habicht, K., Jones, G. L., Lamoreaux, K. S., Mattoni, C. E., McKinsey, D. N., Wietfeldt, F. E., Doyle, J. M., "Progress Towards Magnetic Trapping of Ultracold Neutrons", *Nucl. Instrum. Meth. A*, in press.
- Hummer, G., Garde, S., Garcia, A. E., Paulaitis, M. E., Pratt, L. R., "The Pressure Dependence of Hydrophobic Interactions Is Consistent with the Observed Pressure Denaturation of Proteins", *P. Natl. Acad. Sci. USA* **95**, 1552 (1998).
- Hwang, H. Y., Dai, P., Cheong, S.-W., Aeppli, G., Tennant, D. A., Mook, H. A., "Softening and Broadening of the Zone Boundary Magnons in $\text{Pr}_{0.63}\text{Sr}_{0.37}\text{MnO}_3$ ", *Phys. Rev. Lett.* **80**, 1316 (1998).
- Iampietro, D. J., Brasher, L. L., Stradner, A., Glatter, O., Kaler, E. W., "Direct Analysis of SANS and SAXS Measurements of Catanionic Surfactant Mixtures by Fourier Transformation", *J. Phys. Chem. B* **102**, 3105 (1998).
- Ikkai, F., Shibayama, M., Nomura, S., Han, C. C., "Effect of Degree of Cross-linking on Spatial Inhomogeneity in Charged Gels: 2. Small Angle Neutron Scattering Study", *Macromol.* **31**, 3275 (1998).
- Ilavsky, J., Long, G. G., Allen, A. J., "Evolution of the Microstructure of Plasma Sprayed Deposits During Heating", in *Thermal Spray: Meeting the Challenge of the 21st Century*, edited by C. Coddet (ASM International, Materials Park, OH), p. 1641 (1998).
- Ilavsky, J., Long, G. G., Allen, A. J., Berndt, C. C., Herman, H., "Changes in the Microstructure of Plasma-Sprayed Yttria-Stabilized Zirconia Deposits During Simulated Operating Conditions", in *Thermal Spray: A United Forum for Scientific and Technological Advances*, edited by C. C. Berndt (ASM International, Materials Park, OH, 1997), p. 697.
- Ilavsky, J., Long, G. G., Allen, A. J., Herman, H., Berndt, C. C., "Use of Small Angle Neutron Scattering for the Characterization of Anisotropic Structures Produced by Thermal Spraying", *Ceramics-Silikaty*, in press.
- Ilavsky, J., Long, G. G., Allen, A. J., Prystay, M., Moreau, C., "Anisotropic Microstructure of Plasma-Sprayed Deposits", in *Thermal Spray: Meeting the Challenge of the 21st Century*, edited by C. Coddet (ASM International, Materials Park, OH, 1998), p. 1577.
- Ioffe, A., Jacobson, D., Arif, M., Vrana, M., Werner, S. A., Fischer, P., Greene, G., Mezei, F., "A New Neutron Interferometric Method Used to Measure the Scattering Length of Silicon", *Physica B* **241**, 130 (1998).
- Ioffe, A., Jacobson, D., Arif, M., Vrana, M., Werner, S. A., Fischer, P., Greene, G., Mezei, F., "The Precision Neutron Interferometric Measurement of the Coherent Neutron Scattering Length in Silicon", *Phys. Rev. A* **58**, 1475 (1998).
- Ivkov, R., Forbes, J. G., Greer, S. C., "The Polymerization of Rabbit Muscle Actin: Study by Small Angle Neutron Scattering", *J. Chem. Phys.* **108**, 5599 (1998).
- Izumi, F., Ikeda, T., "A Rietveld-Analysis Program RIETAN-98 and Its Applications to Zeolites", *Proc. 6th Eur. Conf. Powder Diffraction*, Mater. Sci. Forum, in press.
- Jeon, H. S., Lee, J. H., Balsara, N. P., "Intramolecular and Intermolecular Signatures of Incipient Ordering in a Multicomponent Polymer Blend", *Macromol.* **30**, 5572 (1997).
- Jeon, H. S., Lee, J. H., Balsara, N. P., "Predicting the Thermodynamics of Multicomponent Polymer Blends from Measurements on Two-Component Systems", *Phys. Rev. Lett.* **79**, 3274 (1997).
- Jeon, H. S., Lee, J. H., Balsara, N. P., Newstein, M. C., "An Experimental Study of the Thermodynamics of Multicomponent Polyolefin Blends with Ordered and Disordered Phases", *Macromol.*, in press.
- Johnson, D. W., Ottewill, R. H., Rennie, A. R., "Characterization of Particle Packing", in *Modern Aspects of Colloidal Dispersions*, edited by R. H. Ottewill and A. R. Rennie (Dordrecht, Kluwer Academic Publishers, 1998), p. 89.
- Jones, G. L., Gentile, T. R., Thompson, A. K., Chowdhuri, Z., Dewey, M. S., Snow, W. M., Wietfeldt, F. E., "Test of ^3He -based Neutron Polarizers at NIST", *Nucl. Instrum. Meth.*, in press.
- Keith, C. D., Black, T. C., Fei, X., Flamini, M., Gentile, T. R., Jones, G. L., Rich, D. R., Snow, W. M., Thompson, A. K., and Wietfeldt, F. E., "Neutron Polarizers Based on Polarized ^3He ", *Nucl. Inst. Meth. A* **402**, 236 (1998).
- Kent, M. S., McNamara, W. F., Baca, Wriought, Domeier, Wong, Wu, "Water Adsorption in Interfacial Silane Layers by Neutron Reflection: II. Epoxy + Silane on Silicon Wafers", *J. Adhesion* (submitted).
- Kidwell, C. B., Ondov, J. M., Sioutas, C., Koutrakis, P., "Ambient Aerosol Concentration by Condensation and Virtual Impaction for Collection and Chemical Analysis", *J. Aerosol Sci.* **29**, S1039 (1998).
- Kossuth, M. B., Morse, D. C., Bates, F. S., "Viscoelastic Behavior of Cubic Phases in Block Copolymer Melts", *J. Rheology*, in press.
- Kvardakov, V. V., Chen-Mayer, H. H., Mildner, D. F. R., Somenkov, V. A., "Cold Neutron Incoherent Scattering for Hydrogen Detection in Industrial Materials", *J. Appl. Phys.* **83**, 3876 (1998).
- Lamaze, G. P., Chen-Mayer, H. H., "Nitrogen Analysis in Thin Films Using Cold Neutron Depth Profiling", *Proc. 9th Intl. Conf. on Modern Materials and Technologies*, in press.
- Lamaze, G. P., Chen-Mayer, H. H., Badding, M., Laby, L., "In Situ Measurements of Lithium Movement in Thin Film Electrochromic Coatings Using Cold Neutron Depth Profiling", *J. Surf. Interface Anal.*, in press.
- Lamaze, G. P., Chen-Mayer, H. H., Langland, J. K., "Recent Developments in Neutron Depth Profiling at NIST", *Proc. 1998 Intl. Conf. Characterization and Metrology for Ultra Large Scale Integration Technology*, in press.
- Landry, M. R., "Scaling Behavior of Swollen Chains in Bimodal Molecular Weight Blends", *Macromol.* **30**, 7500 (1997).
- Lee, J. H., Jeon, H. S., Balsara, N. P., Newstein, M. C., "Kinetics of Microemulsion Formation in Polymer Mixtures", *J. Chem. Phys.* **108**, 5173

- (1998).
- Lesemann, M., Thirumorthy, K., Kim, Y., Jonas, J., Paulaitis, M. E., "Pressure dependence of the critical micelle concentration of a nonionic surfactant in water studied by H-1-NMR", *Langmuir* **14**, 5339 (1998).
- Lindstrom, R. M., "Neutron Beam Methods in the Analysis of Reference Materials", Proc. IAEA Intl. Symp. on Harmonization of Health Related Environmental Measurements Using Nuclear and Isotopic Techniques, edited by G. V. Ramesh, (Vienna, Austria, 1997), p. 241.
- Lindstrom, R. M., "Prompt Gamma Neutron Activation Analysis", Proc. Korea Atomic Energy Research Institute Cold Neutron Workshop **119**, 205 (1998).
- Lindstrom, R. M., "Reference Material Certification by Prompt-Gamma Activation Analysis", *Fresen. J. Anal. Chem.* **360**, 322 (1998).
- Lindstrom, R. M., Anderson, D. L., Paul, R. L., "Analytical Applications of Neutron Capture Gamma Rays", Proc. 9th Intl. Symp. on Neutron-Capture Gamma-Ray Spectroscopy and Related Topics, edited by G. L. Molnar, T. Belgva, and Z. Revay (Springer, Budapest, Hungary, 1997), p. 693.
- Lindstrom, R. M., Asvavijnijkulchai, C., "Ensuring Accuracy in Spreadsheet Calculations", *Fresen. J. Anal. Chem.* **360**, 374 (1998).
- Lindstrom, R. M., Paul, R. L., "Standards for Hydrogen in Titanium Alloy", Proc. Mat. Res. Soc. Symp. **513**, 283 (1998).
- Liu, Y., Chen, S.-H., Huang, J. S., "Small-Angle Neutron Scattering Analysis of the Structure and Interaction of Tri-Block Copolymer Micelles in Aqueous Solution", *Macromol.*, in press.
- Mackey, E. A., Becker, D. A., "Determination of Methylmercury in Two Mussel Tissue Standard Reference Materials by Pre-Irradiation Separation and Neutron Activation Analysis", *The Analyst* **123**, 779 (1998).
- Mackey, E. A., Demiralp, R., Fitzpatrick, K. A., Porter, B. J., Wise, S. A., Greenberg, R. R., "Quality Assurance in Analysis of Cryogenically Stored Specimens from the NIST National Biomonitoring Specimen Bank", *Sci. Total Environ.*, in press.
- Mang, J. T., Hjelm, R. P., "SANS Investigation of the Pressure and Temperature-Dependent Structure of the Bile Salt Lecithin System", *Molecular Crystals Liquid Crystals* **299**, 439 (1997).
- Mang, J. T., Hjelm, R. P., "Small Angle Neutron Scattering Studies of Vesicle Stability", *Intl. J. of Thermophysics*, in press.
- Mang, J. T., Kumar, S., "A Small Angle Neutron Scattering Investigation of the Effects of Simple and Oscillatory Shear on the CsPFO/H₂O System", in *Phase Transitions in Complex Fluids* (World Scientific Publishing, London, 1998), Ch. 11.3.
- Mansky, P., DeRouchey, J., Russell, T. P., Mays, J., Pitsikalis, M., Morkved, T., Jaeger, H., "Large-Area Domain Alignment in Block Copolymer Thin Films Using Electric Fields", *Macromol.* **31**, 4399 (1998).
- Mansky, P., Russell, T. P., Hawker, C. J., Pitsikalis, M., Mays, J., "Ordered Diblock Copolymer Films on Random Copolymer Brushes", *Macromol.* **30**, 6810 (1997).
- Maurer, W. W., Bates, F. S., Lodge, T. P., Almdal, K., Mortensen, K., Fredrickson, G. H., "Can a Single Function for χ Account for Block Copolymer and Homopolymer Blend Phase Behavior?", *J. Chem. Phys.* **108**, 2989 (1998).
- Migler, K. B., Han, C. C., "Pressure Effects on Diblock Copolymers: Optical Birefringence and Neutron Scattering", *Macromol.*, in press.
- Migler, K. B., Han, C. C., "Static and Kinetic Study of a Pressure Induced Order-Disorder Transition: Birefringence and Neutron Scattering", *Macromol.* **31**, 360 (1998).
- Mildner, D. F. R., "Polycapillary Neutron Lenses", IAEA Technical Document: IAEA-TECDOC-974, in *Trends and Techniques on Neutron Beam Research for Medium and Low Flux Research Reactors* (Vienna, Austria, 1997), p. 63.
- Mildner, D. F. R., Chen-Mayer, H. H., "Neutron Absorption Measurements Using Converging Beams—Increased Reaction Rate", *Nucl. Instrum. Meth. A*, in press.
- Mildner, D. F. R., Chen-Mayer, H. H., Lamaze, G. P., Sharov, V. A., "Characterization of a Cold Neutron Beam from a Curved Guide", *Nucl. Instrum. Meth. A* **413**, 341 (1998).
- Mildner, D. F. R., Chen-Mayer, H. H., Sharov, V. A., "Neutron Focusing Lens Using Capillary Optics", Proc. 9th Intl. Symp. on Capture Gamma Spectroscopy and Related Topics, edited by G. L. Molnar, T. Belgva, and Z. Revay (Springer, Budapest, Hungary, 1997), p. 838.
- Mildner, D. F. R., Lamaze, G. P., "Neutron Transmission of Simple Crystal Sapphire", *J. Appl. Crystallogr.*, in press.
- Mildner, D. F. R., Sharov, V. A., Chen-Mayer, H. H., "Neutron Transmission Through Tapered Channels", *J. Appl. Crystallogr.* **30**, 932 (1997).
- Molnár, G. L., Lindstrom, R. M., "Nuclear Reaction Prompt Gamma-Ray Analysis", Chapter XI in *Nuclear Techniques in Mineral Analysis*, edited by A. Vertes, S. Nagy, and K. Suvegh, (Plenum, New York, 1998), p. 145.
- Molnár, G. L., Révay, Zs., Paul, R. L., Lindstrom, R. M., "Prompt-Gamma Activation Analysis Using the k_0 Approach", *J. Radioanal. Nucl. Chem.* **234**, 21 (1998).
- Morkved, T. L., Chapman, B. R., Bates, F. S., Lodge, T. P., Stepanek, P., Almdal, K., "Dynamics of Ternary Polymer Blends: Disordered, Ordered, and Bicontinuous Microemulsion Phases", *Faraday Discuss.* **112** (submitted).
- Murthy, N. S., Akkepeddi, M. K., Orts, W. J., "Analysis of Lamellar Structure in Semicrystalline Polymers by Studying the Absorption of Water and Ethylene Glycol in Nylons Using Small-Angle Neutron Scattering", *Macromol.* **31**, 142 (1998).
- Nakatani, A. I., Chen, W., Schmidt, R. G., Gordon, G. V., Han, C. C., "Chain Dimensions in Polysilicate-Filled Poly(Dimethylsiloxane)", *ACS PMSE Div. Preprints* **79**, 297 (1998).
- Nakatani, A. I., Han, C. C., "Shear Dependence of the Equilibrium and Kinetic Behavior of Multicomponent Systems", in *Structures and Properties of Multi-Phase Polymeric Materials*, edited by T. Araki, M. Shibayama, and Q. Tran-Cong (Marcel Dekker, Inc., New York, NY, 1998), p. 233.
- Nico, J. S., Adams, J. M., Eisenhauer, C., Gilliam, D. M., Grundl, J. A., "252Cf Fission Neutron Transport Through an Iron Sphere", 9th Intl. Symp. on Reactor Dosimetry, edited by H. A. Abderrahim, P. D'hondt, and B. Osmera (World Scientific Publishing, 1998), p. 714.
- Nisato, G., Ivkov, R., Bauer, B. J., Amis, E. J., "Characterization of Charged PAMAM Dendrimer Interactions in Solutions by Small Angle Neutron Scattering", *ACS Polym. Mat. Sci. Eng.* **79**, 338 (1998).
- Norman, B. R., Igengar, G. V., "Further Applications of Pre-irradiation Combustion and Neutron Activation Analysis Technique for the Determination of Iodine in Food and Environmental Reference Materials:

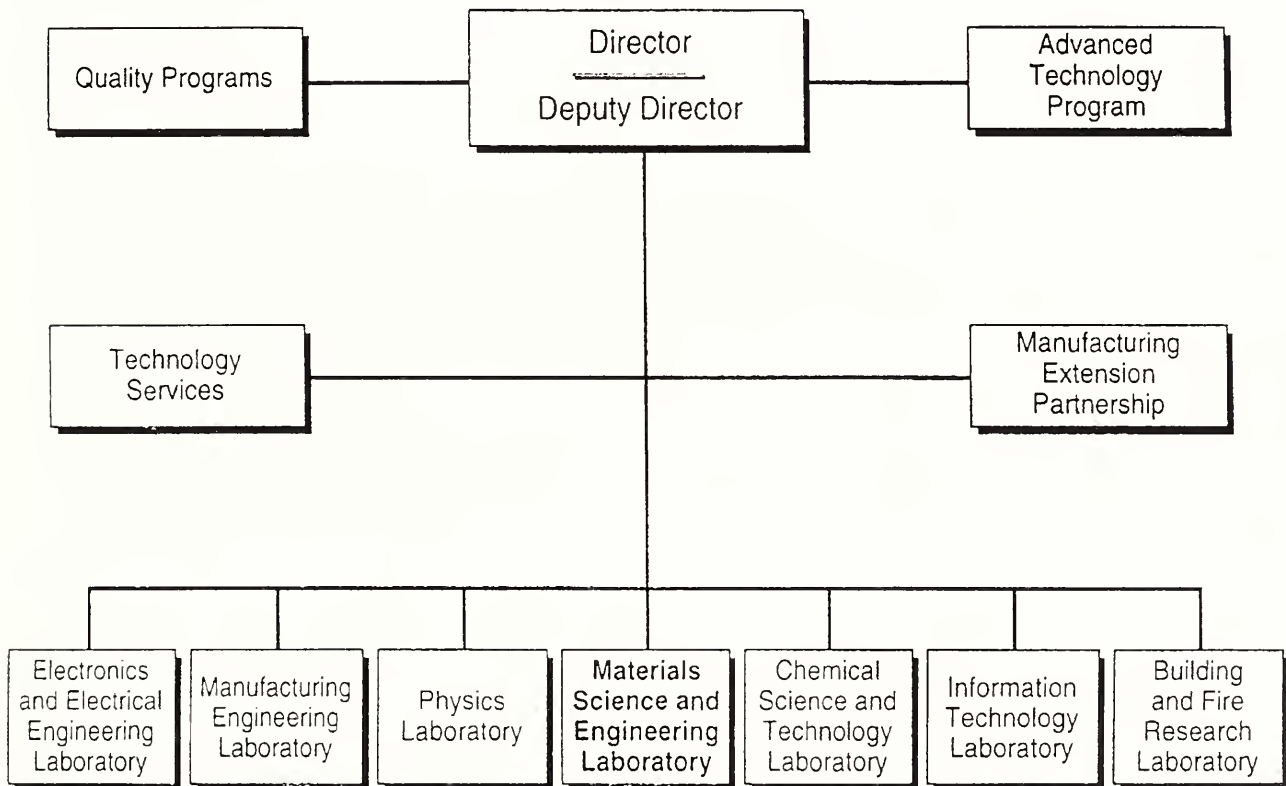
- Merits and Demerits", *Fresen. J. Anal. Chem.*, in press.
- Norman, B. R., Mackey, E.A., "Concentrations of Iodine Determined by Pre-Irradiation Combustion and Neutron Activation Analysis in Powdered Grass as a Function of Particle Size", *Sci. Total Environ.* **205**, 151 (1997).
- Norman, E. B., Browne, E., Chan, Y. D., Goldman, I. D., Larimer, R. M., Lesko, K. T., Nelson, M., Wietfeldt, F. E., Zlimer, I., "Half-Life of ^{44}Ti ", *Phys. Rev. C* **57**, 2010 (1998).
- Nunes, A. C., Yang, L., "Calculated Ferrite Nanocrystal Relaxation and Its Magnetic Implications", *Surface Sci.* **399**, 225 (1998).
- O'Connor, A. J., Hatton, T. A. Bose. A., "The Dynamics of Micelle-Vesicle Transitions in Aqueous Cationic/Anionic Surfactant Mixtures", *Langmuir* **13**, 6931 (1997).
- Ondov, D. J., Ondov, J. M., "Data Management and Acquisition System for INAA", *Trans. Amer. Nuc. Soc.* **78**, in press.
- Ondov, J. M., Wexler, A. S., "Where Do Particulate Toxins Reside? An Improved Paradigm for the Structure and Dynamics of the Urban Mid-Atlantic Aerosol", *Environ. Sci. Technol.* **32**, 2547 (1998).
- Ondov, J. M., Wu, C., Lin, Z.-B., Kidwell, C. B., "Neutron Activation Analysis of an Ir Tracer to Determine Soot Exposure to Students Commuting on Baltimore Public Buses", *Trans. Amer. Nuc. Soc.* **77**, 17 (1998).
- Orts, W. J., Glenn, G. M., "Reducing Soil Erosion Losses with Small Applications of Biopolymers", in *Biopolymers: Utilizing Nature's Advanced Materials*, edited by R. V. Greene and S. H. Imam (ACS Symposium Series, Washington, DC, 1998), in press.
- Orts, W. J., Godbout, L., Marchessault, R. H., Revol, J.-F., "Enhanced Ordering of Liquid Crystalline Suspensions of Cellulose Microfibrils: A Small Angle Neutron Scattering Study", *Macromol.* **31**, 5717 (1998).
- Parr, R. M., Stone, S. F., Bel-Amaketch, T., Zeisler, R., "Survey of Reference Materials for Trace Elements, Nuclides, and Organic Microcontaminants", *Fresen. J. Anal. Chem.* **360**, 350 (1998).
- Paul, R.L., "Determination of Phosphorus in Steels by Radiochemical Neutron Activation Analysis", *J. Radioanal. Nucl. Chem.* **234**, 55 (1998).
- Paul, R. L., Lindstrom, R. M., "Cold Neutron Prompt Gamma-Ray Activation Analysis at NIST—Current Status", *Proc. 9th Intl. Symp. Capture Gamma-Ray Spectroscopy and Related Topics*, (Springer, Budapest, Hungary, 1998), p. 779.
- Paul, R. L., Lindstrom, R. M., "Determination of Hydrogen in Metals, Semiconductors, and Other Materials by Cold Neutron Prompt Gamma-Ray Activation Analysis", *Mat. Res. Soc. Proc.* **513**, 185 (1998).
- Paul, R. L., Lindstrom, R. M., "Applications of Cold Neutron Prompt Gamma Activation Analysis to Characterization of Semiconductors", in *Semiconductor Characterization: Present Status and Future Needs*, edited by W. M. Bullis, D. G. Seiler, and A. C. Diebold, (AIP Press, Woodbury, NY, 1995), p. 342.
- Podurets, K. M., Mildner, D. F., R., Sharov, V. A., "Application of Capillary Optics to Neutron Radiography", *Rev. Sci. Instrum.*, in press.
- Podurets, K. M., Sharov, V. A., Mildner, D. F. R., "Spatial Distribution of Neutrons Guided Through a Monolithic Tapered Lens", *Appl. Phys. Lett.* **71**, 3168 (1997).
- Pollard, M., Russell, T. P., Ruzette, A. V., Mayes, A. M., Gallot, Y., "The Effect of Hydrostatic Pressure on the Lower Critical Ordering Transition in Diblock Copolymers", *Macromol.* **31**, 6493 (1998).
- Quinn, T. L., Ondov, J. M., "Influence of Temporal Changes in Relative Humidity on Dry Deposition Velocities and Fluxes of Aerosol Particles Bearing Trace Elements", *Atmos. Environ.* **32**, 3467 (1998).
- Redford, S., Blackman, M. J., "Luster and Fritware Production and Distribution in Medieval Syria", *J. Field Archaeology* **24**, 233 (1997).
- Reeder, P. L., Peurrung, A. J., Richey, W. C., Chen-Mayer, H. H., Sharov, V. A., Fokin, V. S., Mildner, D. F. R., "Imaging Neutron Beams with Scintillating Fiber Faceplates", *Nucl. Instrum. Meth. A* **402**, 155 (1998).
- Reeder, P. L., Peurrung, A. J., Sunberg, D. S., Stoffels, J. J., Chen-Mayer, H. H., Mildner, D. F. R., Sharov, V. A., Fokin, V. S., "Metal Capillaries for Neutron Lenses", *Nucl. Instrum. Meth. A* **399**, 101 (1997).
- Rhyne, J. J., Kaiser, H., Luo, H., Xiao, G., Gardel, M. L., "Long Wavelength Spin Dynamics in $\text{La}_{0.53}\text{Ca}_{0.47}\text{MnO}_3$ ", *J. Appl. Phys.*, **83**, 7339 (1998).
- Rizi, R. R., Dimitov, I. E., Thompson, A. K., Jones, G. L., Gentile, T. R., Ishii, M., Reddy, R., Schnall, M. D., Leigh, J. S., "NMR Imaging of Hyperpolarized ^3He Gas in Human Paranasal Sinuses", *Magn. Reson. Med.* **39**, 865 (1998).
- Ryan, L. D., Kaler, E. W., "Effect of Alkyl Sulfates on Alkyl Polyglucoside Phase Behavior and Microstructure", *J. Phys. Chem. B* **102**, 7549 (1998).
- Ryan, L. D., Kaler, E. W., "Microstructure Properties of Alkyl Polyglucoside Microemulsions", *Langmuir*, in press.
- Sanders, P. G., Eastman, J. A., Weertman, J. R., "Pore Distributions in Nanocrystalline Metals from Small-Angle Neutron Scattering", *Acta Materialia*, in press.
- Sayer, E. V., Yener, K. A., Joel, E. C., Blackman, M. J., Özbal, "Stable Lead Isotope Studies of Black Sea Anatolian Ore Sources and Related Bronze Age and Phrygian Artifacts from Nearby Archaeological Sites. Appendix: New Central Taurus Ore Data", *Archaeometry*, in press.
- Schoeman, B. J., "A High Temperature In-situ Laser Light-Scattering Study of the Initial Stage in the Crystallization of TPA-Silicalite-1", *Zeolites* **18**, 97 (1997).
- Serebrov, A. P., Kuznetsov, I. A., Stepanenko, I. V., Aldushchenkov, A. V., Lasakov, M. S., Mostovoi, Y. A., Erozolinskii, B. G., Dewey, M.S., Wietfeldt, F.E., Zimmer, O., Boerner, H., "Measurements of the Antineutrino Escape Asymmetry of Antineutrino Escape with Respect to the Spin of Decaying Neutron", *J. Exp. Theor. Phys.* **86**, 1074 (1998).
- Sharpless, K.E., Welch, M.J., Greenberg, R.R., Iyengar, G.V., Colbert, J.C., "Recent SRMs for Organic and Inorganic Nutrients in Food Matrices", *Fresen. J. Anal. Chem.* **360**, 456 (1998).
- Sokolov, M. A., Spooner, S. E., Odette, G. R., Wirth, B. D., Lucas, G. E., "SANS Study of High-Copper RPV Welds in Irradiated and Annealed Conditions", in *Effects of Radiation on Materials: 18th International Symposium*, ASTM STP 1325, edited by R. K. Nanstad, M. L. Hamilton, F. A. Garner, and A. S. Kumar (West Conshohocken, PA, 1999), in press.
- Stone, S. F., Donais, M. K., Zeisler, R., "Instrumental Neutron Activation Analysis for Quality Assurance of a Hair Reference Material for Mercury Speciation", *J. Radioanal. Nucl. Chem.* **233**, 55 (1998).
- Stone, S. F., Fajgelj, A., Bernasconi, G., Tajani, A., Zeisler, R., "Examination of a Procedure for the Production of a Filter-Based Air Particulate Matter Reference Material", *Fresen. J. Anal. Chem.* **360**, 435 (1998).

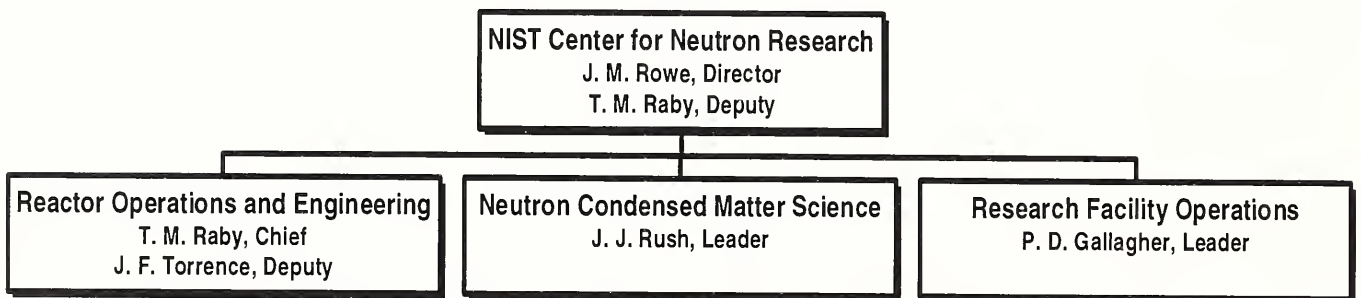
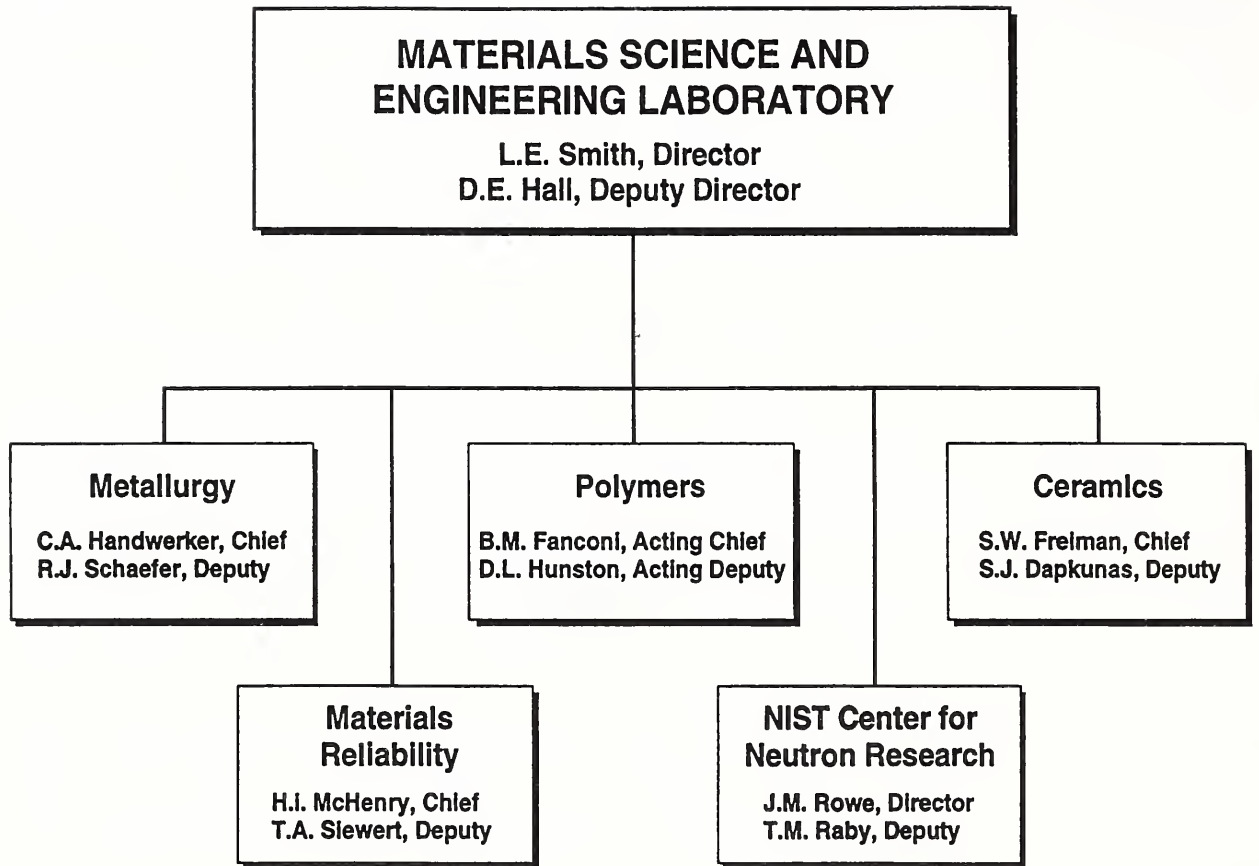
- Stone, S. F., Parr, R. M., Zeisler, R., "Certification of Two Human Hair Reference Materials Issued by the International Atomic Energy Agency", *Fresen. J. Anal. Chem.* **360**, 419 (1998).
- Suarez, A. E., Caffrey, P. F., Ondov, J. M., Divita, Jr. F., "Use of an Ir Tracer to Determine the Size Distribution of Aerosol from Diesel Sanitation Trucks", *Environ. Sci. Technology* **32**, 1522 (1998).
- Takahashi, Y., Kitade, S., Ochiai, N., Noda, I., Matsushita, Y., Imai, M., Nakatani, A. I., Kim, H., Han, C. C., "Order-Disorder Transition of Symmetric Styrene-2-Vinylpyridine Diblock Copolymers in Melts and Solutions", *Polymer (Japan)* **30**, 388 (1998).
- Thiyagarajan, P., Crawford, R. K., Mildner, D. F. R., "Neutron Transmission of Single Crystal MgO Filter", *J. Appl. Crystallogr.*, in press.
- Thomas, J. J., Jennings, H. M., Allen, A. J., "Determination of the Neutron Scattering Contrast of Hydrated Portland Cement Paste Suing H₂O/D₂O Exchange", *Adv. Cem. Based Mater.* **7**, 119 (1998).
- Thomas, J. J., Jennings, H. M., Allen, A. J., "The Surface Area of Cement Paste as Measured by Neutron Scattering—Evidence for Two C-S-H Morphologies", *Cem. Concr. Res.* **28**, 897 (1998).
- Thompson, A. K., Gentile, T. R., Jones, G. L., "Polarized ³He Program", Web address: <http://physics.nist.gov/Divisions/Div846/Gp3/Helium/contents.html>.
- Tranchitella, L. J., Fettinger, J. C., Heller-Zeisler, S. F., Eichhorn, B. W., "La_{8+x}Ti_{8+y}S₂₄O₄ Compounds Where x + y ≤ 2: A Series of Phases with Mixed-Valent Titanium", *Chem. Mater.* **10**, 2078 (1998).
- Trehwella, J., "Conformational Flexibility in the Regulation of Target Proteins by Calmodulin and Troponin C", *Biophys. J.* **74**, A9 (1998).
- Urakawa, O., Yano, O., Tran-Cong, Q., Nakatani, A. I., Han, C. C., "Small-Angle Neutron Scattering Studies on the Phase Behavior of Binary Polymer Blends Driven by Photoisomerization", *Macromol.* **31**, 7962 (1998).
- Velev, O. D., Kaler, E. W., Lenhoff, A. M., "Protein Interactions in Solution Characterized by Light and Neutron Scattering: Comparison of Lysozyme and Chymotrypsinogen", *Biophys. J.*, in press.
- Walker, L. M., Kernick III, W. A., Wagner, N. J., "In Situ Analysis of the Defect Texture in Liquid Crystal Polymer Solutions", *Macromol.* **30**, 508 (1997).
- Wallace, W. E., Jacobson, D. L., Arif, M., Ioffe, A., "Application of Neutron Interferometry to the Measurement of Thin Film Density", *Appl. Phys. Lett.*, in press.
- Watanabe, H., Yao, M. L., Osaki, K., Shikata, T., Niwa, H., Morishima, Y., Balsara, N. P., Wang, H., "Nonlinear Rheology and Flow-Induced Structure in a Concentrated Spherical Silica Suspension", *Rheologica Acta* **37**, 1 (1998).
- Welp, K. A., Co, C., Wool, R. P., "Improved Reflectivity Fitting Using SERF: Spreadsheet Environment Reflectivity Fitting", *J. Neutron Res.*, in press.
- Wietfeldt, F. E., Schima, F. J., Coursey, B. M., Hoppes, D. D., "Long-term Measurement of the Half-Life of ⁴⁴Ti", *Phys. Rev. C*, in press.
- Wirth, B. D., Odette, G. R., Pavinich, W. A., Lucas, G. E., Spooner, S. E., "Small Angle Neutron Scattering Study of Linde 80 RPV Welds", in *Effects of Radiation on Materials: 18th International Symposium*, ASTM STP 1325, edited by R. K. Nanstad, M. L. Hamilton, F. A. Garner, and A. S. Kumar (West Conshohocken, PA, 1999), in press.
- Wu, C. C., Suarez, A. E., Lin, Z.-B., Kidwell, C. B., Borgoul, P. V., Caffrey, P. F., Ondov, J. M., Sattler, B., "Application of an Ir Tracer to Determine Soot Exposure to Students Commuting to School on Baltimore Public Buses", *Atmos. Environ.* **32**, 1911 (1998).
- Wu, W.-L., Wallace, W. E., van Zanten, J. H., Bauer, B. J., Liu, D.-W., Wong, A., "Diffusion of Linear Polystyrene into Crosslinked Polystyrene", *Polymer* **38**, 2583 (1997).
- Yang, L., Harroun, T. A., Heller, W. T., Weiss, T. M., Huang, H. W., "Neutron Off-Plane Scattering of Aligned Membranes: I. Method of Measurement", *Biophys. J.* **75**, 641 (1998).
- Yang, L., Weiss, T. M., Harroun, T. A., Heller, W. T., Huang, H. W., "Supermolecular Structures in Membranes by Neutron Off-Plane Scattering: Method of Analysis", *Biophys. J.* (submitted).
- Zeisler, R., "Reference Materials for Small Sample Analysis", *Fresen. J. Anal. Chem.* **360**, 376 (1998).
- Zeisler, R., Dekner, R., Zeiller, E., Doucha, J., Mader, P., Kucera, J., "Single Cell Green Algae Reference Materials with Managed Levels of Heavy Metals", *Fresen. J. Anal. Chem.* **360**, 429 (1998).
- Zeisler, R., Stone, S. F., Fajgelj, A., "Quality Assurance for Nuclear Techniques Employed in Air Pollution Studies", *J. Radioanal. Nucl. Chem.* **233**, 15 (1998).
- Zeissler, C. J., Wight, S. A., Lindstrom, R. M., "Detection and Characterization of Radioactive Particles", *Appl. Radiat. Isotop.* **49**, 1091 (1998).
- Zhao, J., Hoyer, E., Boylan, S., Walsh, D., Trehwella, J., "Quaternary Structure of the CAMP-Dependent Protein Kinase by Neutron Scattering", *Biophys. J.* **74**, A255 (1998).
- Zhou, C., Hobbie, E. K., Bauer, B. J., Han, C. C., "Equilibrium Structure of Hydrogen-Bonded Polymer Blends", *J. Polym. Sci., Part B, Polym. Phys. Ed.* **36**, 2745 (1998).
- Zufall, M. J., Davidson, C. I., Caffrey, P. F., Ondov, J. M., "Airborne Concentrations and Dry Deposition Fluxes of Particulate Chemical Species to Southern Lake Michigan", *Environ. Sci. Technol.* **32**, 1623 (1998).

Organizational Charts and Staff Roster

National Institute of Standards and Technology

Organizational Chart





NCNR/NIST Resident Staff and Visiting Scientists

CENTER OFFICE - (856)

Rowe, J. M., Director
Sullivan, D. A., Admin. Off.
Neal, S. L., Admin. Asst.
Hill, J. M., Secretary
Prask, H. J., Sci. Asst.
Barker, J. G., Matls. Sci.

REACTOR OPERATIONS & ENGINEERING

Raby, T. M., Chief
Torrence, J. F., Deputy
Poole, L. M., Secretary

Operations

Beasley, R.D.
Bickford, N. A.
Bobik, P. A.
Cassells, M. G.
Clark, F. C.
Dilks, H. W.
Flynn, D. J.
Guarin, E. L.
Lindstrom, L. T.
McDonald, M. J.
Mueller, W. W.
Myers, T. J.
Pierce, S. C.
Ring, J. H.
Slaughter, S. S.
Sprow, R. P.
Stiber, R. F.
Thompson, R. G.
Toth, A. L.
Wilkison, D. P.
Wright, K. D.

Engineering

Suthar, M. A., Chief
Poole, L. M., Secretary
Beatty, J. A.
Boyd, J. M.
Brady, D. E., Inst. Supv.
Hall, K. D.
Liposky, P. J.
Reilly, G. D.
Shuman, L.A.

Guest Researchers

Anderson, D. A.
Dahan, S.
Cunningham, W. C.
Heine, C. J.*
Olin, J.
Yee, K.

NEUTRON CONDENSED MATTER SCIENCE GROUP

Rush, J. J., Leader
Runkles, C. L., Secretary
Spillman, A. R., Office Automat. Asst.
Berk, N. F.
Yildirim, T.

Chemical Physics of Materials

Copley, J. R. D.
Forstner, K. T.
FitzGerald, S. A.*
Gehring, P. M.
Neumann, D. A., Team Leader
Udovic, T. J.

Crystallography

Karen, V. L.
Santoro, A.
Stalick, J. K.
Toby B. H., Team Leader

Magnetism and Superconductivity

Borchers, J. A.
Erwin, R. W.
Ijiri, Y.*
Lynn, J. W., Team Leader
Santodonato, L.

Macromolecular and Microstructure

Butler, P. D.
Glinka, C. J., Team Leader
Hammouda, B.
Kline, S. R.
Readon, J. P.
Rosov, N.
Slawecki, T. M.*

Surfaces and Interfaces

Dura, J. A.
Krueger, S. T.
Ivkov, R.
Majkrzak, C. F., Team Leader
Satija, S. K.

Guest Researchers

Altorfer, F. B.*
Adams, C.
Bourdarot, F.
Broholm, C.
Choi, S.
Cook, J.
Dender, D.
Doloc, L.

Gnaupel-Herold, T.
 Huang, Q. Z.
 Kepa, H.*
 Karmonik, C.*
 Khosrovani, N.*
 Lee, S.-H.
 Lin, M. Y.
 Meyer, A.
 Mighell, A. D.
 Mrose, M.
 Nieh, M.
 Papanek, P.
 Prince, E.
 Raebiger, J.
 Rathgeber, S.
 Schreyer, A.
 Senesi, R.
 Sung
 Tarek, M.
 Trevino, S. F.
 Tsai, A.
 Wilgruber, U.
 Zaliznyak, I.

RESEARCH FACILITY OPERATIONS

Gallagher, P. D., Leader
 Clutter, L. K., User Coord.
 Hill, J. M., Secretary
 Ruhl, K. J., Clerk Typist
 Baltic, G. M., Tech. Suprv.
 Bostian, C. D.
 Brand, P.
 Clarkson, A.
 Clem, D. L.
 Clow, W. R.
 Dickerson, W. E.
 Fravel, D. H.
 Fulford, D.
 Gallagher, P. D.
 Green, T. A.
 Greene, G. C.
 Heald, A. E.
 Kamitakahara, W. A.
 Klosowski, P.
 Knill, W. C.
 Kopetka, P. H.
 Kulp, D. L.
 Maliszewskyj, N. C.
 LaRock, J. G.
 Layer, H. P.
 Pierce, D. J.
 Rinehart, M. J.
 Schroder, I. G.
 Thai, T. T.
 Tobin, P. J.
 Williams, R. E.

Guest Engineers

Brocker, C. W.
 Christman, R.
 Moyer, J. J.
 Murbach, M.
 Wrenn, C. W.

OTHER NIST GROUPS

NEUTRON INTERACTIONS & DOSIMETRY GROUP- (846)

Gilliam, D. M., Leader
 Dunham, C., Secretary
 Adams, J. M.
 Arif, M.
 Carlson, A. D.
 Dewey, M. S.
 Gentile, T. R.
 Huffman, P. R.
 Jacobson, D. L.
 Nico, J. S.
 Thompson, A. K.

Guest Researchers

Brome, C. R.
 Butterworth, J. S.*
 Chowdhuri, S. Z.
 Doyle, J.
 Eisenhauer, C. M.
 Fei, X.*
 Grundl, J. A.*
 Hwang, S.-R.*
 Ioffe, A.
 Jones, G.
 Mattoni, C. E. H.
 Schwartz, R. B.
 Steiger, T.*
 Wietfeldt, F.

NUCLEAR METHODS GROUP-(839)

Greenberg, R. R., Leader
 Wilson, J. M., Secretary
 Becker, D. A.
 Chen-Mayer, H. H.
 Demiralp, R.
 Fitzpatrick, K. A.
 Iyengar, V.
 Lamaze, G. P.
 Langland, J. K.
 Lindstrom, R. M.
 Mackey, E. A.
 Mildner, D.F.R.
 Paul, R. L.
 Porter, B. J.
 Zeisler, R. L.

Guest Researchers

Bishop, R. L.
Blackman, M. J.

HEALTH PHYSICS - Div. 354

Slaback, L. A., Leader
Thomas, C. L., Secretary
Brown, D. R.
Campbell, C. D.
Cassells, L. H.
Clark, J. S.
Deardorff, G. E.
Fink, L. E.
Mengers, T. F.
Shubiak, J. J.

*left during fiscal year

Research and Engineering Staff

J. G. Barker	SANS instrumentation and research Microstructure of materials
N. F. Berk	Condensed matter theory Scattering theory for microstructure analysis Computer software for graphics and data analysis
N. A. Bickford	Reactor operations Reactor irradiations Reactor utilization
J. A. Borchers	Thin-film analysis Artificially modulated materials Magnetism
D. E. Brady	Electrical/electronic engineering Nuclear reactor instrumentation NDE diffraction methods
P. C. Brand	Materials engineering Neutron residual stress measurements Engineering physics
J. M. Boyd	Electrical/electronic engineering Nuclear reactor instrumentation
J. R. D. Copley	Time-of-flight spectrometer development Neutron instrumentation conceptual design Condensed matter physics
W. E. Dickerson	Neutron scattering instrumentation Microcomputer interfacing

J. A. Dura	Nuclear and engineering physics Combined molecular beam epitaxy and neutron reflectivity Instrumentation Surface, interfacial, and epitaxial physics
R. W. Erwin	Magnetic materials Phase transformations Cryogenics
S. A. FitzGerald	Neutron and optical spectroscopy Condensed matter physics Fullerenes and cements
K. T. Forstner	Instrumentation Monochromator development
D. B. Fulford	Mechanical engineering
P. D. Gallagher	Neutron instrumentation Interfacial phenomena in polymer systems and complex fluids Phase transitions and critical phenomena
P. M. Gehring	Neutron backscattering instrumentation Magnetic and structural phase transitions in disordered systems Dynamics of high T _c materials
C. J. Glinka	SANS microstructure of metals and porous media CHRNS project director Cold neutron instrument development
G. C. Greene	System and user software for cold neutron instrumentation Spectrometer and data acquisition systems interfaces
B. Hammouda	SANS from polymers, liquid crystals, and colloids Dynamics of polymers in solution Scattering from sheared fluids
A. E. Heald	Design engineering Neutron instrumentation Shielding
Y. Ijiri	Condensed matter physics Thin films and multilayers Magnetism
W. A. Kamitakahara	Dynamics of disordered solids Condensed matter physics The NCNR guest researcher program
V. L. Karen	Crystallographic database development Theory of lattices and symmetry Neutron and x-ray diffraction
S. R. Kline	Microstructure of colloids and microemulsions Novel surfactant systems SANS instrumentation

P. Klosowski	Scientific data visualization Numerical computer modeling Data acquisition software and hardware
P. A. Kopetka	Mechanical engineering Cold source design Electro-mechanical systems
S. T. Krueger	Structure of biological materials SANS and neutron reflectometry methods Computer software development
J. G. LaRock	Mechanical engineering Neutron instrumentation design
H. P. Layer	Electronics and data processing Advanced instrumentation Fundamental physics
P. J. Liposky	Design engineering Nuclear systems and components
J. W. Lynn	Condensed matter physics Magnetic and superconducting materials Neutron scattering methods
C. F. Majkrzak	Condensed matter physics Polarized neutron scattering and instrumentation development Neutron reflectivity measurements
N. C. Maliszewskyj	Computer software development Time-of-flight instrumentation Condensed matter physics
T. J. Myers	Reactor operations Safety analysis
D. A. Neumann	Molecular and layered materials Condensed matter physics Neutron and x-ray scattering instrumentation
D. J. Pierce	Mechanical engineering Neutron instrumentation design
H. J. Prask	Residual stress measurement methodology Neutron NDE applications Neutron NDE instrumentation
T. M. Raby	Reactor operations and standards Nuclear engineering Nuclear systems and components
G. D. Reilly	Design engineering Nuclear systems and components
N. Rosov	Spin echo techniques Phase transformations

	Magnetic materials
J. M. Rowe	Orientationally disordered solids Cold source development Cold neutron research and instrumentation
J. J. Rush	Catalysts and molecular materials Hydrogen in metals Inelastic scattering methods
L. Santodonato	Condensed matter physics Cryogenics
A. Santoro	Structure of electronic and structured ceramics Theory of crystal lattices Powder diffraction methods
S. K. Satija	Low-dimensional molecular systems Fractal aspects of microporous media Neutron reflectometry
I. G. Schröder	Cold neutron instrumentation development Nuclear and engineering physics Optical devices for neutron transport
T. M. Slawacki	SANS and reflectometry from polymers Complex fluid microstructure SANS instrumentation
J. K. Stalick	Neutron and x-ray diffraction Inorganic chemistry Crystal database development
M. A. Suthar	Design engineering Nuclear systems and components
B. H. Toby	Neutron and synchrotron diffraction Zeolite crystallography Structure determination methods
J. F. Torrence	Reactor supervision Reactor maintenance Nuclear engineering
T. J. Udovic	Neutron time-of-flight instrumentation Properties of catalysts and adsorbates Hydrogen in metals
R. E. Williams	Cold neutron source development Nuclear engineering Reactor physics simulations

